Title: Temporal and Spatial Evolution of Cerebral Injury in the Piglet Asphyxia Model: a Comparative Study of Serial Magnetic Resonance Biomarkers and Histopathology

Osuke Iwata
Institute for Women's Health
University College London
PhD Thesis

Student registration number: 59069869087046

Supervisors:
Profs Nicola J Robertson and Gennadij Raivich, University College London.

Address for Correspondence: Centre for Developmental & Cognitive Neuroscience, Kurume University School of Medicine, 67 Asahimachi, Kurume, Fukuoka, 830-0011 Japan
E-mail: o.iwata@ucl.ac.uk
Tel: +81-942-31-7565
Fax: +81-942-38-1792

Thesis ~58,000 words.

Declaration

I, Osuke Iwata, confirm that the work presented in this thesis is my own. Where information has been derived from other sources, I confirm that this has been indicated in the thesis.

For all studies described in this thesis, I performed the histo-pathological analysis of the brain, data analysis, and interpretation of findings with aids of my collaborators and the supervisor. For the second and the third part of three studies, which are “Energy metabolism during the latent phase and early evolutional period or secondary energy failure” and “Temporal and spatial evolution of secondary energy failure and cerebral Injury”, I also designed the study protocol, and performed the surgical preparation and intensive life support of the experimental model.

Abstract

Background:

After hypoxia-ischaemia and successful resuscitation, cerebral energy metabolism transiently recovers to the normal level (latent phase); after a variable period of time this phase is followed by secondary energy failure (SEF) in those subjects with an adverse outcome. A better understanding of the regional evolution of SEF may enhance the application of future neuroprotective strategies.

Aims:

The aim of this thesis was to determine associations between the insult severity, regional SEF evolution, and subsequent histo-pathological brain injury using magnetic resonance biomarkers.

Methods:

An established piglet model of neonatal encephalopathy was used.

1. Twenty-nine piglets were studied either normothermic or hypothermic (35°C or 33°C during 2-26 hours after hypoxia-ischaemia). 31-phosphorus magnetic resonance spectroscopy (^{31}P MRS) was serially acquired; the brain was assessed with histology after 48 hours.
2. Global ^{31}P MRS, and maps of apparent diffusion coefficient (ADC) and transverse relaxation time (T2) were serially obtained in 3 control and 18 asphyxiated piglets. Histo-pathological brain injury and MR biomarkers were compared at time periods of 16-48 hours after hypoxia-ischaemia.

Results:

1. Severe acute insult, short latent phase, severe SEF, and profound histo-pathological brain injury were associated between each other.
2. Transient recovery in phosphocreatine (PCr) higher than its baseline level was indicative of absent subsequent evolution of SEF, whereas sub-baseline

PCr recovery was suggestive of severe SEF.

3. Global ^{31}P MRS biomarkers and regional ADC obtained just prior to termination and up to 18-24 hours before termination predicted histo-pathological brain injury; the predictive value was optimal for global PCr/inorganic phosphate (Pi), followed by global PCr/exchangeable high-energy phosphate pool (EPP), Pi/EPP and regional ADC. PCr/Pi, PCr/EPP, Pi/EPP and ADC obtained after 6 hours of hypoxia-ischaemia predicted later neuronal death. Analysis with time-series data after resuscitation showed modest predictive values of ^{31}P MRS and ADC for the end point brain injury as early as 3 to 6 hours after hypoxia-ischaemia.

Conclusions:

Although ^{31}P MRS was more accurate, regional ADC predicted subsequent brain injury up to 18 hours in advance of termination. Regional ADC can be used as a sensitive early marker for subsequent tissue injury when ^{31}P MRS is not available.

Acknowledgments

First and foremost, I would like to express my deepest gratitude to Prof Nikki Robertson for her mentorship with continuous encouragement and enthusiastic support to the entire research project. I would have never reached any of the peaks without her expertise, insight and strong belief in science and the research team. I would like to thank Prof John Wyatt for inspiring me and for investing on my projects during my first years in the UK, which was indispensable for the revival of our multidisciplinary research team. My further gratitude goes to Profs Donald Peebles, Gennadij Raivich, Ray Noble and Francesco Scaravilli for their supports as expert scientists, who helped improve my ability in refining experimental design and analytical approach.

I would like to thank Drs Ernest Cady, Alan Bainbridge, Enrico De Vita, David Carmichael, John Thornton, Andrew Priest and Sahan Thalayasingam for their tremendous support as medical physicists in developing and standardising magnetic resonance biomarkers; especially, my career at UCL owes Drs Ernest Cady and Alan Bainbridge, who shared all good days and bad days together. I am grateful to Drs Shanthi Shanmugalingam, Jeanie Cheong, Takenori Kato, Giles Kendall and Andrew Kapetanakis for their support in experiments, and to Dr Linda Herbert for her excellent technique in immune-histochemical staining.
I would also like to express my gratitude to Dr Angela Poulter for her assistance in the inter-Atlantic collaborations after I moved back to Japan. I would also like to thank Profs Toyojiro Matsuishi, Yasuki Maeno and Sachio Takashima, who helped facilitate the research environment in Japan.

Lastly, I would like to thank my family. I am grateful to Dr George Iwata and Mrs Michiko Iwata, who brought me up with love and humour, and helped me nurse justice, curiosity and imagination within myself; and to Dr Yoshito Kadowaki, my father in law, who warmly supported the completion of my project in the UK despite his incurable illness. Above all, I would like to thank my wife Dr Sachiko

Iwata, who shared interests and excitements in every little finding both at work and home, subsequently turning my ordinal life into an endless fete of neuroscience; although Sachiko and I might not always be good parents for our children Shinano, Soshi and Yushin, because of our extreme life style as intensivists and investigators, I still feel proud that, since your births, we have shared all defeats and triumphs in our long exploratory journey.

Abbreviations

ADC, apparent diffusion coefficient
ATP, adenosine triphosphate
aEEG, amplitude-integrated electroencephalogram
DWI, diffusion weighted imaging
EPP, exchangeable high-energy phosphate pool
FA, fractional anisotropy
FiO_2, inspired oxygen fraction
GFAP, glial fibrillary acidic protein
H & E, haematoxylin and eosin
LFB/Nissl, Luxol-fast blue-cresyl violet
MRS, magnetic resonance spectroscopy
NAA, N-acetyl aspartate
NTP, nucleotide triphosphates
PCr, phosphocreatine
Pi, inorganic phosphate
^{31}P, 31-phosphorus
RoI, region of interest
T1, longitudinal relaxation time
T2, transverse relaxation time
TUNEL, terminal deoxynucleotide transferase nick end labelling

Contents

Declaration ……..2
Abstract …… 3
Acknowledgements …… 5
Abbreviations …… 7
Contents …… 8
Index of Figures ……15
Index of Tables ……18

Chapter 1: Introduction……19
1.1 Epidemiology of perinatal hypoxia-ischaemia and neurological Impairments ……19
1.2 Clinical features and diagnosis of neonatal encephalopathy…….. 21
1.2.1 Algorithm of diagnosis of neonatal encephalopathy…… 21
1.2.2 Evidence of systemic hypoxia-ischaemia…….. 22
1.2.3 Clinical findings of encephalopathy…… 23
1.2.4 Diagnostic tools: electroencephalogram…….. 26
1.2.5 Diagnostic tools: conventional MRI…… 29
1.3 Mechanisms of cerebral injury in the newborn infant……30
1.3.1 Primary energy failure and acute phase injury cascade…….. 30
1.3.2 Latent phase and secondary energy failure……31
1.4 Piglet model of neonatal encephalopathy……..33
1.5 Quantitative magnetic resonance biomarkers of cerebral injury……34
1.5.1 ^{31}P MRS ……34
1.5.2 ^{1}H MRS ……37
1.5.3 Diffusion weighted imaging……38
1.5.4 Maps of longitudinal and transverse relaxation times……..42
1.5.5 Monitoring of secondary energy failure and therapeutic time window ……43

1.5. 6 Regional variation of energy metabolism following hypoxia-ischaemia…… 44
1.6 Treatment of neonatal encephalopathy…….. 47
1.6. 1 Therapeutic hypothermia: mechanism…….47
1.6. 2 Therapeutic hypothermia: current clinical evidence……48
1.6. 3 Key factors potentially associated with further improvement of the treatment……49

Chapter 2: Aim and Hypothesis……..51
Aim ……51
Hypotheses ……51
Specific hypotheses……51

Chapter 3: General Materials and Methods……..52
3.1 Preparation of the piglet model of asphyxial encephalopathy……52
3.1. 1 Surgical procedures…… 52
3.1. 2 Magnetic resonance biomarkers……54
3.1. 3 ^{31}P MRS ……54
3.1. 4 Maps of ADC and FA……...55
3.1. 5 T2 maps ……56
3.1. 6 Transient cerebral hypoxia-ischaemia, resuscitation and quantification of acute energy depletion……56
3.1. 7 Temperature control and hypothermia……..58
3.1. 8 Monitoring and treatment of seizure…… 58
3.1. 9 Quantification of latent phase and secondary energy failure…… 58
3.1.10 Histopathology…… 59
3.2 Associations between insult severity and therapeutic time window duration ……..…… 62
3.2. 1 Subjects and study groups…… 62
3.2. 2 Acquisition of magnetic resonance data…….. 62
3.2. 3 Histopathology…….. 63
3.2. 4 Statistical analysis…… 64

3.3 Energy metabolism during the latent phase and early evolutional period of secondary energy failure…… 65
3.3.1 Subjects and procedures…….. 65
3.3.2 Hypoxic-ischaemic insult……65
3.3.3 Acquisition of magnetic resonance biomarkers…… 65
3.3.4 Time course…….. 66
3.3.5 Statistical analysis…….. 66
3.3.5.1 Sham-operated control animals…… 66
3.3.5.2 Animals in the study group…… 66
3.3.5.3 Serial metabolite ratios and rates of metabolic change..... 66
3.3.5.4 Secondary energy failure severity groups…… 67
3.3.5.5 Baseline metabolism, insult severity and PCr recovery…. 67
3.3.5.6 Statistical probability correction……..68
3.4 Temporal and spatial evolution of secondary energy failure and cerebral injury ……69
3.4.1 Subjects and procedures……... 69
3.4.2 Magnetic resonance data processing…….. 69
3.4.3 Histo-pathological assessment…… 70
3.4.4 Statistical analysis……71
3.4.4.1 Sham-operated control animals…… 71
3.4.4.2 Animals in the study group…… 71
3.4.4.3 Statistical probability correction…… 72

Chapter 4: Results…….. 73
4.1 Associations between insult severity and therapeutic time window duration ……73
4.1.1 Summary ……75
4.1.2 Experimental courses and general findings……75
4.1.3 Severity of hypoxia-ischaemia, duration of latent phase and subsequent injury indices in each temperature group……75
4.1.4 Association between the insult severity and the latent phase duration ……76

4.1.5 Association between the insult severity and the severity of secondary energy failure…… 77
4.1.6 Association between the insult severity and neuronal death……78
4.1.7 Association between the latent phase duration and the severity of secondary energy failure…… 78
4.1.8 Association between the latent phase duration and neuronal death ……...79
4.1.9 Association between the severity of secondary energy failure and neuronal death…… 80
4.2 Energy metabolism during the latent phase and early evolutional period or secondary energy failure…….. 81
4.2.1 Summary ……... 81
4.2.2 Temporal changes in energy metabolites after hypoxia-ischaemia…….. 81
4.2.2.1 Sham-operated animals……...81
4.2.2.2 Acute insult, recovery and secondary energy failure……82
4.2.3 Energy metabolism at 2-8 hours after hypoxia-ischaemia and the severity of secondary energy failure……84
4.2.4 Baseline metabolism, insult severity, and PCr at 2-8 hours after hypoxia-ischaemia……...86
4.3 Temporal and spatial evolution of secondary energy failure and cerebral injury ……88
4.3.1 Summary ……..... 88
4.3.2 Sham-operated control subjects……88
4.3.3 Temporal changes in magnetic resonance biomarkers up to 24 hours after resuscitation…… 88
4.3.3.1 ^{31}P MRS biomarkers…….. 88
4.3.3.2 Maps of ADC……...90
4.3.3.3 T2 maps…….. 94
4.3.3.4 Histopathological brain injury……96
4.3.4 Serial magnetic resonance biomarkers obtained 1 to 24 hours after resuscitation and histo-pathological brain injury……99

4.3.4.1 Insult severity, experimental duration, magnetic resonance biomarkers, and histo-pathological brain injury..... 99
4.3.4.2 ^{31}P MRS biomarkers and brain injury……..100
4.3.4.3 Maps of ADC and brain injury……..103
4.3.4.4 T2 maps and brain injury……..104
4.3.5 Serial magnetic resonance biomarkers obtained shortly before to 24 hours before termination and histo-pathological brain injury…..105
4.3.5.1 ^{31}P MRS biomarkers and brain injury……..105
4.3.5.2 Maps of ADC and brain injury……..108
4.3.5.3 T2 maps and brain injury……..109

Chapter 5: Discussion…… 110
5.1 Associations between insult severity and therapeutic time window duration …… 110
5.1.1 Summary ……..... 110
5.1.2 Key findings from the study……110
5.1.3 Acute energy depletion and evolution of secondary energy failure 110
5.1.4 Level of acute energy depletion and the effect of hypothermic neuroprotection…… 111
5.1.5 Evolution of secondary energy failure and neuroprotective treatments …… 112
5.1.6 Clinical implications……113
5.1.7 Strengths and limitations of the study…….. 113
5.1.8 Conclusions ……..114
5.2 Energy metabolism during the latent phase and early evolutional period or secondary energy failure……115
5.2.1 Summary ……..115
5.2.2 Key findings from the study……115
5.2.3 Changes in high energy phosphates during transient hypoxia-ischaemia, latent phase and secondary energy failure…..115

5.2.4 Cerebral stress response after the commencement of resuscitation and PCr recovery overshoot……..116
5.2.5 Clinical implications……118
5.2.6 Limitations and advantages of the study……118
5.2.7 Future studies ……..118
5.2.8 Conclusions ……..119
5.3 Temporal and spatial evolution of secondary energy failure and cerebral injury ……..120
5.3.1 Summary ……..120
5.3.2 Key findings from the study……..120
5.3.3 Diagnostic value of global and regional magnetic resonance biomarkers for histo-pathological brain injury……120
5.3.4 Spatial changes of ADC and transverse relaxation time during the evolutional process of secondary energy failure……122
5.3.5 T2 maps during acute phase after perinatal hypoxia-ischaemia…123
5.3.6 Clinical implications……123
5.3.7 Limitations of the study……124
5.3.8 Future studies……125
5.3.9 Conclusions ……..125

Chapter 6: Overall conclusion and implication of the findings from this thesis ……..126
6.1 Conclusions ……..126
6.2 Latent phase, secondary energy failure and tissue homeostasis…… 127
6.3 Magnetic resonance biomarkers and histo-pathological findings…… 128
6.4 Monitoring of secondary energy failure…… 129
6.5 Secondary energy failure and cerebral protection…… 130
6.6 Strength and limitation……131
6.7 Future studies ……..132
6.8 Implication of the findings from this thesis……133

Bibliography 134

Supplementary Material and Appendix.....144

List of Abstracts and Presented at Meetings from this analysed data..... 145

List of Publications related to this work..... 149

List of Publications derived from this work..... 151

Appendix 152

Index of Figures

Fig. 1.1-1: Neonatal encephalopathy and related outcomes…….. 20

Fig. 1.2-1: Classification of aEEG traces after perinatal hypoxia-ischaemia by Hellstrom-Westas and colleagues…….. 28

Fig. 1.2-2: Mild MRI lesions in the deep grey matter and internal capsule ……29

Fig. 1.3-1: Primary energy depletion and acute phase injury cascade……...30

Fig. 1.3-2: Evolution of energy failure after the latent phase in a severely asphyxiated newborn infant…….... 31

Fig. 1.3-3: Evolution of secondary brain injury……32

Fig. 1.4-1: Evolution of secondary energy failure in the piglet model of neonatal asphyxial encephalopathy…….. 33

Fig. 1.5-1: High resolution ^{31}P MRS spectra from the brain of the piglet model ……34

Fig. 1.5-2: Temporal changes in PCr/Pi and NTP/EPP in the piglet model of asphyxial encephalopathy…….....35

Fig. 1.5-3: Cerebral tissue covered by the surface coil in the acquisition of ^{31}P MRS spectra from the piglet brain…….. 36

Fig. 1.5-4: ^{1}H MRS spectra, lactate/NAA and outcome of asphyxiated infants …….. 38

Fig. 1.5-5: Conventional MRI and DWI after perinatal hypoxia-ischaemia ……40

Fig. 1.5-6: Correlation between PCr/Pi and ADC……...41

Fig. 1.5-7: Transverse relaxation time in the thalamus and basal ganglia …….. 42

Fig. 1.5-8: Evolution of secondary energy failure in a rodent model of transient hypoxia-ischaemia……44

Fig. 1.5-9: Diagram of normal basal ganglia motor control circuit and areas damaged by near-total asphyxia……..... 45

Fig. 1.5-10: Pattern of brain injury after perinatal hypoxia-ischaemia and neurodevelopmental outcome at 30 months of age…… 46
Fig. 1.6-1: Systemic hypothermia and therapeutic time window in the piglet model of asphyxial encephalopathy…….. 47
Fig. 1.6-2: Cooling level and region-specific brain protection…… 50
Fig. 3.1-1: Piglet model after surgical procedures…… 52
Fig. 3.1-2: Piglet positioned within the plastic cylinder pod…….. 53
Fig. 3.1-3: Representative ^{31}P spectra from the piglet brain before hypoxia-ischaemia…… 54
Fig. 3.1-4: Regions of interest on a schema and maps of ADC and FA……. 56
Fig. 3.1-5: Schematic diagram summarising the quantification of the acute insult severity…… 57
Fig. 3.1-6: Region of interest for histo-pathological assessment in the cortical grey matter……..60
Fig. 3.2-1: NTP/EPP changes of representative piglets over 48 hours…….. 63
Fig. 3.2-2: Schematic diagram depicting the histo-pathological regions of interest in a coronal slice of the piglet brain…… 64
Fig. 3.4-1: Brain regions of interest for histo-pathological assessment……. 69
Fig. 4.1-1: Cerebral high-energy phosphates before, during and after hypoxia-ischaemia…… 74
Fig. 4.1-2: Correlation between the latent phase duration and the insult severity ……..77
Fig. 4.1-3: Association between the severity of acute insult and secondary energy failure…… 77
Fig. 4.1-4: Correlation between the insult severity and neuronal death in the cortical grey matter…… 78
Fig. 4.1-5: Correlation between the latent phase duration and the severity of secondary energy failure…… 78
Fig. 4.1-6: Dependences of neuronal death on the latent phase duration …… 79
Fig. 4.1-7: Dependence of neuronal death on the severity of secondary energy failure…… 80

Fig. 4.2-1: Trajectories of NTP, PCr and Pi over time relative to EPP……. 83
Fig. 4.2-2: Metabolite ratios 2-8 hours after hypoxia-ischaemia relative to individual baselines…….. 85
Fig. 4.2-3: Representative ^{31}P MRS spectra from three outcome groups…. 85
Fig. 4.2-4: PCr/EPP 2-8 hours after hypoxia-ischaemia…….. 86
Fig. 4.2-5: Baseline and early ^{31}P MRS biomarkers and PCr recovery……. 87
Fig. 4.2-6: Baseline metabolism and recovery PCr/EPP…….. 87
Fig. 4.3-1: Temporal changes in global ^{31}P MRS biomarkers…….. 89
Fig. 4.3-2: Two distinct patterns of ADC changes with time following hypoxia-ischaemia…….. 90
Fig. 4.3-3: Temporal changes of ADC in representative regions…….. 92
Fig. 4.3-4: Temporal changes of T2 maps…….. 94
Fig. 4.3-5: Temporal changes of T2 relaxation time in representative regions ……95
Fig. 4.3-6: Representative histo-pathological findings-1..……. 97
Fig. 4.3-7: Representative histo-pathological findings-2..……....98
Fig. 4.3-8: Associations between ^{31}P MRS biomarkers obtained 1-24 hours after resuscitation and histo-pathological brain injury……101
Fig. 4.3-9: Associations between maps of ADC obtained 1-24 hours after resuscitation and histo-pathological brain injury…….. 103
Fig. 4.3-10: Associations between T2 maps obtained 1-24 hours after resuscitation and histo-pathological brain injury……104
Fig. 4.3-11: Associations between ^{31}P MRS biomarkers obtained 1-24 hours before termination and histo-pathological brain injury…...106
Fig. 4.3-12: Associations between maps of ADC obtained 1-24 hours before termination and histo-pathological brain injury……..108
Fig. 4.3-13: Associations between T2 maps obtained 1-24 hours before termination and histo-pathological brain injury…….. 109

Index of Tables

Table 1.2-1: Outline of diagnostic algorithm for neonatal encephalopathy used in clinical trials of therapeutic hypothermia…… 21

Table 1.2-2: Predictive value of arterial cord blood gas for cerebral palsy... 23

Table 1.2-3: Encephalopathy grading system by Sarnat and Sarnat…….25

Table 1.2-4: Encephalopathy scoring system by Thompson and colleagues……26

Table 1.6-1: Therapeutic hypothermia and outcomes at 18 months of age ……48

Table 3.1-1: Definition of pathological scoring for neuronal damages…….. 61

Table 3.4-1: Injury scales for histo-pathological assessment in the white Matter ……70

Table 4.1-1: Magnetic resonance and histo-pathological injury indices in each temperature group……..76

Table 4.2-1: Temporal changes in ^{31}P MRS biomarkers in sham operated animals ……81

Table 4.2-2: Rates of change in metabolite ratios during and following hypoxia-ischaemia……...82

Table 4.2-3: Metabolite ratios before, during, and after hypoxia-ischaemia ……84

Chapter 1: Introduction

1.1 Epidemiology of perinatal hypoxia-ischaemia and neurological impairments

Perinatal hypoxia–ischaemia and subsequent neonatal encephalopathy remain major causes of neonatal death and permanent neurological impairments worldwide, which are responsible for ~23% of annual neonatal deaths (1). Even in the developed world, some form of resuscitation is required for ~10% of all newborn infants before spontaneous breathing and circulation are established (2). Although the majority of these infants are stabilised without further need for intensive medical care, moderate to severe neonatal encephalopathy develops, in approximately 1-3 per 1000 live births (3), resulting in up to 60% of mortality and at least 25% of survivors with long term neurodevelopmental sequelae (Fig. 1.1-1) (4). Perinatal hypoxia-ischaemia also affects the long term outcome of infants who were resuscitated at birth but were asymptomatic for encephalopathy and had no further neonatal care; these infants are at increased risks of having low intelligence quotients at school age compared to their peers who did not require resuscitative procedures (5). The incidence of probable intrapartum-related respiratory depression, neonatal encephalopathy and subsequent death is much higher in developing countries and low resource settings (6).

Until recently there was no efficient treatment for the devastating consequences of perinatal asphyxia and neonatal encephalopathy. However, recent experimental and clinical evidence has led to the establishment of therapeutic hypothermia, which has now been recognised as the first clinically effective neuroprotective treatment for infants with neonatal encephalopathy (7-9). Currently, however therapeutic hypothermia is offered only to a limited number of infants with neonatal encephalopathy worldwide as clinical trials have only shown its safety and efficacy in the developed world setting under intensive care conditions (10). In addition some infants reach tertiary care centres too late - there is a relatively short therapeutic time window of hypothermia of up to ~6 hours (11). Furthermore, the number of infants who respond to the treatment is still limited, with the number of patients needed to treat to improve outcome remaining around 9 for the reduction of death or severe neurodevelopmental impairments at 18 months of age (12). Many gaps remain in our knowledge of the best treatment for

individual babies with neonatal encephalopathy. Despite a consistent presentation, neonatal encephalopathy may have diverse aetiologies. The infant's maturity, inflammatory, nutrition, development of seizures, hormonal status and combination of these factors may influence the response to an acute hypoxic-ischaemic insult. Further work is needed to determine the optimal application of hypothermia for different infants. Establishment of early diagnostic biomarkers, such as magnetic resonance imaging (MRI) and magnetic resonance spectroscopy (MRS), may facilitate tailored neuroprotective treatments.

Figure 1.1-1: Neonatal encephalopathy and related outcomes

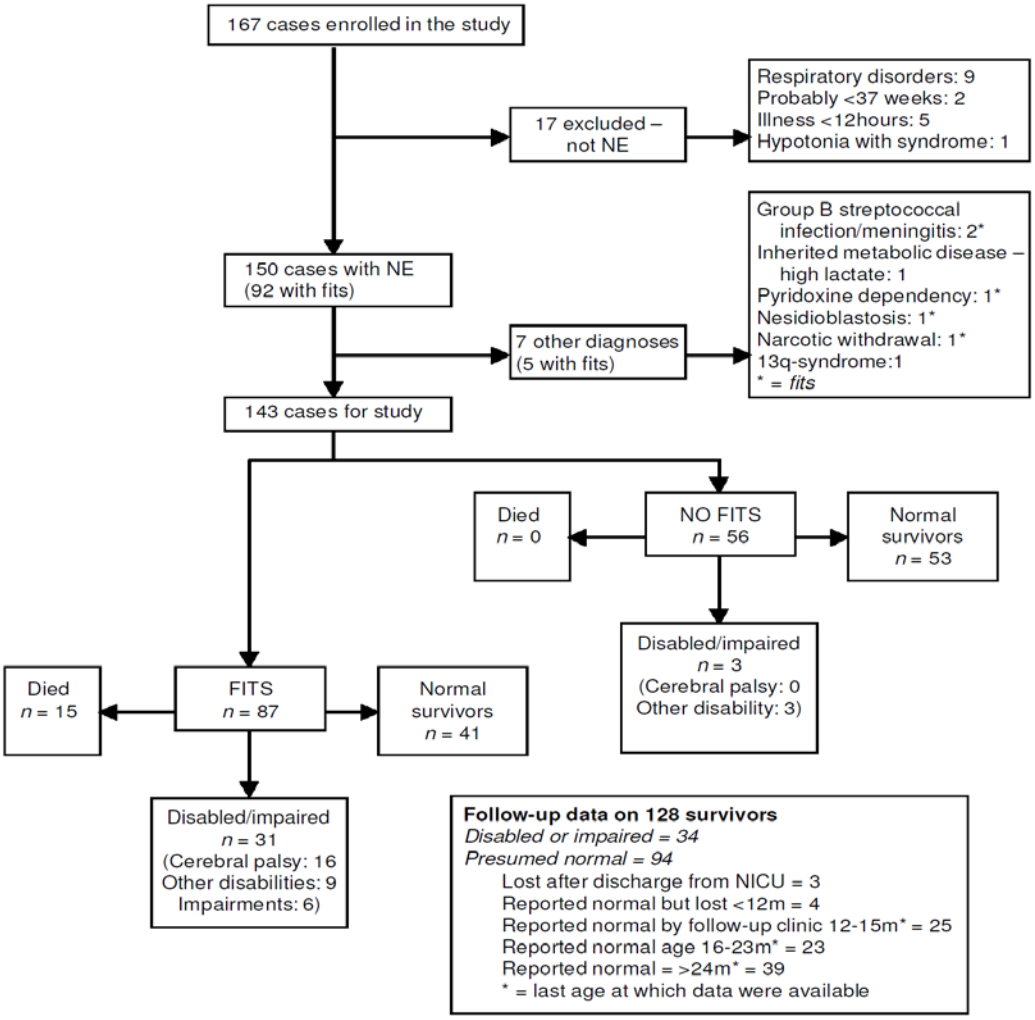

In a cohort study which enrolled 57,259 births, 150 cases of neonatal encephalopathy (NE) were identified, with the incidence of 2·62 per 1000 births (95% CI: 2·20–3·04). Sixteen infants with NE subsequently had definite or probable cerebral palsy, a rate of one in 3572 births. From "The relationships between neonatal encephalopathy and cerebral palsy: a cohort study." by Evans K, Rigby AS, Hamilton P, Titchiner N, Hall DM. J Obstet Gynaecol. 2001 Mar;21(2):114-20.

1.2 Clinical features and diagnosis of neonatal encephalopathy

1.2.1 Algorithm of diagnosis of neonatal encephalopathy

Impaired cerebral functions characterised by clinical findings, such as abnormal motion, muscle tone, reflexes, and seizures are key features that constitute the diagnosis of neonatal encephalopathy (2). However, early recognition of neurological manifestations indicative of neonatal encephalopathy requires special expertise, because early clinical signs, especially of mild to moderate neonatal encephalopathy, are subjective, affected by sleep sates, and difficult to be distinguished from normal conditions. In addition, the primary screening of neonatal encephalopathy is generally performed by midwives and physicians with limited expertise in neonatal neurology, resulting in the requirement for reliable, objective markers for the global stress. Hence, recent large scale clinical trials which enrolled infants with neonatal encephalopathy employed a two- or three-step diagnostic algorithm (Table 1.2-1) (7-9).

Table 1.2-1: Outline of diagnostic algorithm for neonatal encephalopathy used in clinical trials of therapeutic hypothermia

	CoolCap Trial	NICHD Trial	TOBY Trial
Apgar score	≤ 5 at 10min.	≤ 5 at 10min.	≤ 5 at 10min.
Resuscitation	≥ 10min.	≥ 10min.	≥ 10min.
Blood gas			
pH	<7	<7	<7
BD	≥ 16	≥ 16	≥ 16
Sarnat score	II or III	II or III	II or III
aEEG	≥ Moderate abnormality	Did not use	≥ Moderate abnormality

Three major randomised controlled trials of selective head cooling (CoolCap Trial) and whole body cooling (NICHD Trial and TOBY Trial) used similar entry criteria to identify infants with moderate to severe neonatal encephalopathy. Terms and abbreviations: aEEG, amplitude-integrated electroencepharogram. Apgar score, a 10-point scale assigned to assesses the early transition of newborn infants. BD, base deficit. Sarnat score, a 3-level clinical grading system to assess the severity and development of neonatal encephalopathy from mild (I) to severe (III).

The first stage of diagnosis involves objective clinical evidence of global hypoxia-ischaemia, as represented by abnormal cord blood gas analysis and Apgar

scores, which also assure that hypoxic-ischaemic stress occurred shortly before or around the timing of delivery. To confirm the influence of global hypoxia-ischaemia to the cerebral function, the next step of the diagnosis assesses the presence and lack of primitive reflexes and pathological neurological findings (13). Electrophysiological findings may further confirm the impaired cortical activity in a more objective method. Because neonatal encephalopathy is an evolving syndrome commencing at resuscitation, physiological and neurological assessments need to be repeated to monitor the process and to allow interventions appropriate to the severity of encephalopathy and the systemic condition.

1.2.2 Evidence of systemic hypoxia-ischaemia

Because the systemic condition of asphyxiated infants alters dynamically with time before and after the commencement of resuscitative interventions, physiological information obtained at or shortly after birth may suggest inconsistent views on the severity of global asphyxia between each other. Hence it is important to obtain comprehensive information about the patient including clinical findings using alternative diagnostic scales and detailed clinical histories. To improve the accuracy and reliability of the initial screening scale, diagnostic tools at this stage should be simple, objective and reproducible, while obtained scores or information are still associated with the natural outcome of the infant.

Of several biomarkers of intrapartum hypoxia-ischaemia, evidence of severe acidosis on the cord blood sample is most frequently used as a handy and objective surrogate for the foetal condition (Table 1.2-2) (14). The presence of lactic acidosis with increased base deficits is indicative of prolonged anaerobic metabolism. Foetal acidosis defined by umbilical cord blood pH of <7.00 and a base deficit of ≥12 mmol/L is known to be associated with an increased risk of cerebral palsy (15). A preliminary meta-analysis based on nine clinical studies suggested the association between foetal acidosis, neonatal death and cerebral palsy (16). Previous observational studies, however, provided inconsistent views in the detailed association between cord blood pH and outcomes, in part because of various thresholds of abnormal blood gas and end points for the outcome of the infant (17, 18). A recent meta-analysis based on the data from more than fifty studies confirmed that low arterial cord pH was a strong and consistent predictor of the outcome for asphyxiated infants even after adjustments for the study design, sample size, cut off level and the clinical endpoint (19), justifying the use of cord

blood gas analysis to screen infants at increased risks of mortality and permanent neurological impairments.

Table 1.2-2: Predictive value of arterial cord blood gas for cerebral palsy

Study	Definition	No of true positives or true negatives/ No with or without cerebral palsy: Cerebral palsy	No cerebral palsy	No of children	pH threshold	Odds ratio (random effects) (95% CI)	Odds ratio (random effects) (95% CI); EPI
Ingemarrson et al 1997[68]	NS	0/2	139/200	202	7.00		0.5 (0.02 to 9.6)
Socol 1994[81]	NS	5/6	3/6	12	7.00		5.0 (0.3 to 72.8)
Gaudier et al 1994[49]	Abnormal movements/posture	3/30	182/189	219	7.05		2.9 (0.7 to 11.9)
Beeby et al 1994[4]	NS	1/20	219/235	255	7.10		0.7 (0.1 to 5.7)
Murphy et al 1995[75]	Permanent movement disorder	6/24	112/128	152	7.10		2.3 (0.8 to 6.8)
Kato et al 1996[5]	NS	3/8	98/113	121	7.20		3.9 (0.9 to 18.1)
Luthy et al 1987[74]	NS	3/19	126/137	156	7.20		2.2 (0.5 to 8.5)
Overall (7 studies)				1117			2.3 (1.3 to 4.2); 1.1-5.0

Test for heterogeneity: I^2=0.0%, P=0.777

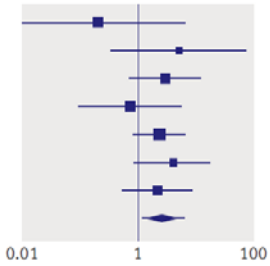

A meta-analysis confirmed that low arterial cord pH was associated with the incidence of cerebral palsy. From "Strength of association between umbilical cord pH and perinatal and long term outcomes: systematic review and meta-analysis." by Malin GL, Morris RK, Khan KS. BMJ. 2010 May 13;340:c1471.

The Apgar score is another universal scale assigned for almost all newborn infants born in developed countries. The score can be assigned using readily available clinical observations without requiring for burdensome data collection (20). Although the Apgar score is assigned subjectively for components other than the heart rate, the inter-rater agreement of the scores is generally high. The Apgar score can be assessed by nurses, midwives and trainee doctors without requiring for special skills and intensive training sessions. Negative relationships have been confirmed between the 1 and 5 minutes Apgar scores and neonatal mortality in large cohorts of newborn infants (21, 22). While the predictive value of the 5 minute Apgar score has been accepted as a simple, reliable predictor of neonatal mortality for singleton premature and term newborn infants (15), the Apgar score at 10 minutes is likely to provide even more useful prognostic information following perinatal hypoxia-ischaemia (20).

1.2.3 Clinical findings of encephalopathy

The type and severity of neonatal encephalopathy need to be determined by comprehensive neurological assessments, which help predict likely neurological outcomes and appropriate therapeutic options. Since the clinical features of neonatal encephalopathy evolve over a period of days, neurological examinations have to be

performed repeatedly. Of scales used for the classification of neonatal encephalopathy, the grading developed by Sarnat and Sarnat is most universally used in the neonatal intensive care (Table 1.2-3) (13); this grading system assigns one of three categories of grade I (mild), II (moderate) and III (severe) encephalopathy to the affected infant based on subjective clinical observations. The maximum benefit of this system is yielded when it is used serially to record the temporal alteration of neurological findings. Infants who were never diagnosed as severe encephalopathy and who were not assigned into moderate encephalopathy for more than four days were suggested to have normal medium-term outcomes, whereas persistent moderate encephalopathy for longer than seven days was suggestive of mortality or neurological impairments. However, in the clinical practice, this grading system is frequently used to assess the severity of and to estimate the outcome of encephalopathy shortly after birth, occasionally before making clinical decisions whether invasive treatments are required to improve the neurodevelopmental outcome of affected infants. While this grading system provides reliable estimation of the outcome for grade I and grade III encephalopathy, which are associated with favourable and poor outcomes respectively, the outcome associated with the grade II encephalopathy is various, ranging between intact survival to death or severe neurodevelopmental impairments. In addition, the assignment of this grading system is time consuming, and the final decision as to whether an infant falls into the moderate or severe category is at times difficult, requiring substantial expertise in neonatal neurology (23).

Several other groups also proposed scoring systems for neonatal encephalopathy to improve the quality and utility of early diagnosis and outcome prediction (23-26). Of these, a scoring system developed by Thompson and colleagues has an outstanding advantage in its simplified numeric assignment system (Table 1.2-4).

Table 1.2-3: Encephalopathy grading system by Sarnat and Sarnat

Table 2.—Distinguishing Features of the Three Clinical Stages of Postanoxic Encephalopathy in the Full-Term Newborn Infant

	Stage 1	Stage 2	Stage 3
Level of consciousness	Hyperalert	Lethargic or obtunded	Stuporous
Neuromuscular control			
Muscle tone	Normal	Mild hypotonia	Flaccid
Posture	Mild distal flexion	Strong distal flexion	Intermittent decerebration
Stretch reflexes	Overactive	Overactive	Decreased or absent
Segmental myoclonus	Present	Present	Absent
Complex reflexes			
Suck	Weak	Weak or absent	Absent
Moro	Strong; low threshold	Weak; incomplete; high threshold	Absent
Oculovestibular	Normal	Overactive	Weak or absent
Tonic neck	Slight	Strong	Absent
Autonomic function	Generalized sympathetic	Generalized parasympathetic	Both systems depressed
Pupils	Mydriasis	Miosis	Variable; often unequal; poor light reflex
Heart rate	Tachycardia	Bradycardia	Variable
Bronchial and salivary secretions	Sparse	Profuse	Variable
Gastrointestinal motility	Normal or decreased	Increased; diarrhea	Variable
Seizures	None	Common; focal or multifocal	Uncommon (excluding decerebration)
Electroencephalogram findings	Normal (awake)	Early: low-voltage continuous delta and theta. Later: periodic pattern (awake). Seizures: focal 1-to 1½-Hz spike-and-wave	Early: periodic pattern with isopotential phases. Later: totally isopotential
Duration	Less than 24 hr	Two to 14 days	Hours to weeks

An encephalopathy grading system proposed by Sarnat and Sarnat in 1976. A 3-scale encephalopathy grade is assigned for the affected infant using a checklist, which comprises physiological and neurological signs. Although this grading is currently used to evaluate the severity of neonatal encephalopathy, the original concept was to monitor the temporal development of encephalopathy from grade I to II and III. From "Neonatal encephalopathy following fetal distress. A clinical and electroencephalographic study." by Sarnat HB, Sarnat MS. Arch Neurol. 1976 Oct;33(10):696-705.

Table 1.2-4: Encephalopathy scoring system by Thompson and colleagues

Sign	Score 0	1	2	3	Day 1	Day 2	Day 3
Tone	Normal	Hyper	Hypo	Flaccid			
LOC	Normal	Hyper alert, stare	Lethargic	Comatose			
Fits	None	Infreq < 3 d^{-1}	Frequent>2/day				
Posture	Normal	Fisting, cycling	Strong, distal flexion	Decerebrate			
Moro	Normal	Partial	Absent				
Grasp	Normal	Poor	Absent				
Suck	Normal	Poor	Absent ± bites				
Resp.	Normal	Hypervent	Brief apnoea	IPPV (apnoea)			
Font'l	Normal	Full, not tense	Tense				
				Total score per day			

A simple scoring system for neonatal encephalopathy developed by Thompson and colleagues. One may simply check the item which most precisely reflects the patient's state, and add the scores to quantify the severity of encephalopathy. From "The value of a scoring system for hypoxic ischaemic encephalopathy in predicting neurodevelopmental outcome." by Thompson CM, Puterman AS, Linley LL, Hann FM, van der Elst CW, Molteno CD, Malan AF. Acta Paediatr. 1997 Jul;86(7):757-61.

This system, based on that of Sarnat and Sarnat, employs only nine categories of clinical signs, where scores of 0 (normal) to 3 (highly abnormal) are given for each item to give total scores between 0 and 22. Total scores of 0 to 9, 10 to 14, and 15 to 22 correspond to mild, moderate and severe neonatal encephalopathy diagnosed using Sarnat's grading system (23). In addition to its agreement to the previous system, this scoring system showed excellent predictive values of neurodevelopmental outcomes for asphyxiated newborn infants at 1 year old. For example, the peak score of 15 or higher was highly suggestive of abnormal outcomes, with the positive predictive value of 92%, negative predictive value of 82%, sensitivity of 71%, and the specificity of 96%.

1.2.4 Diagnostic tools: electroencephalogram

Studies which used standard electroencephalogram and amplitude-integrated electroencephalogram (aEEG) demonstrated that perinatal hypoxia-ischaemia attenuates electrocortical activities as a dose dependent manner, reflecting the depth of the stress (13, 27). However, electrographic findings are generally normal or of minimum suppression for infants with mild encephalopathy. For infants with moderate encephalopathy, high frequency domains such as alpha and a part of theta activities disappear, and low frequency domains such as delta and a part of theta activities are attenuated in their voltage. Such a mildly suppressed electrographic pattern is often followed by a burst and suppression pattern, which is highly suppressed and occasionally deformed compared to the normal alternating trace of the newborn infant.

Electrocortical activities are further attenuated for severe encephalopathy. As well as the suppression in voltage, the interval between bursts is significantly prolonged, which evolves into a flat trace. The background activity of standard electroencephalogram in asphyxiated newborn infants is known to be associated with neurodevelopmental outcomes at 2 years old (28). Moderate to severe suppression with or without alternating burst suppression pattern is indicative of abnormal neurodevelopmental outcomes, whereas normal traces and immature patterns relative to the gestational age of the infant are suggestive of normal development. A more recent study which serially obtained standard electroencephalogram following perinatal hypoxia-ischaemia demonstrated that electroencephalogram obtained after six hours of birth was more indicative of the neurodevelopmental outcome compared to twelve, twenty-four and forty-eight hours after birth (29).

Despite the substantial information derived from standard electroencephalogram in asphyxiated newborn infants, only a limited number of hospitals can currently provide the examination 24 hours a day. In addition, interpretation of electroencephalogram traces requires expertise in neonatal neurology. To improve the utility of electrographic assessment of the brain function, aEEG has been proposed by clinicians who care for high risk newborn infants as a simple and handy alternative for standard electroencephalogram (Fig. 1.2-1) (30). This device was developed and initially applied for adult patients who underwent cardiac surgeries to monitor the trend of electrocortical activity in the 1960s (31). Waveforms of electroencephalogram obtained using two or four recording electrodes are filtered and compressed to reconstruct aEEG output. Because of its time compressed trend view, one can evaluate a long term recording instantly by simple pattern recognition with the minimum instruction and training. Despite its simplicity, aEEG obtained within 6 hours of birth from asphyxiated term newborn infants has been recognised as a reliable predictor for the outcome of affected infants (32, 33). More recent studies suggested that the timing in recovery for the amplitude and the sleep wake cycle of the aEEG trace is useful to predict the outcome of infants (34).

Figure 1.2-1: Classification of aEEG traces after perinatal hypoxia-ischaemia by Hellstrom-Westas and colleagues

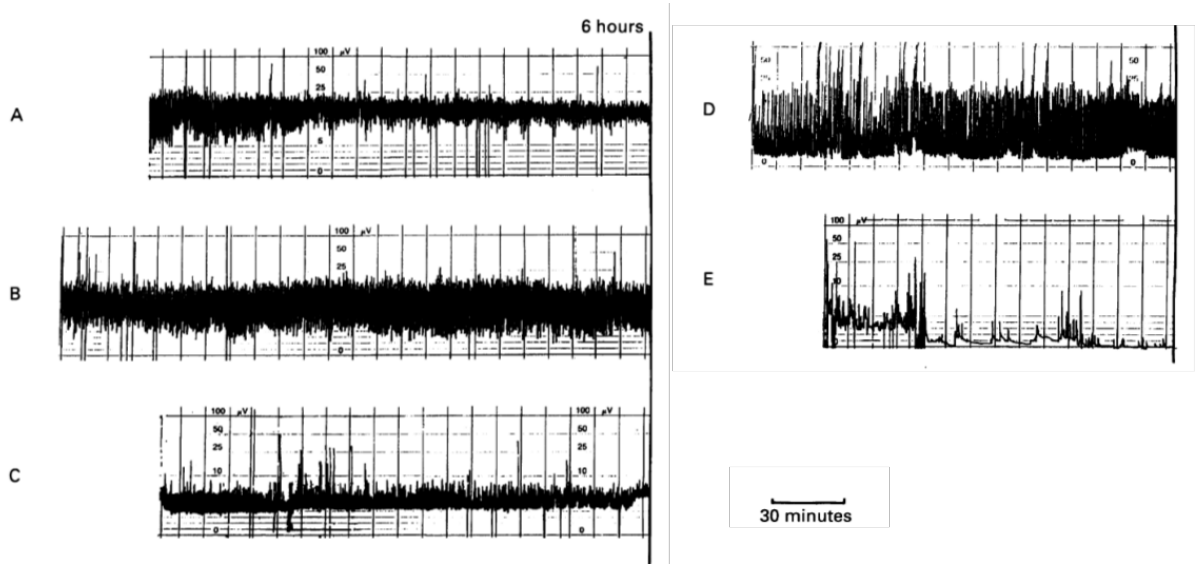

Four types of background patterns recorded from full term asphyxiated new born infants during the first six hours of life are shown. (A) Continuous normal voltage with sleep-wake cycles. (B) Continuous normal voltage with absent sleep-wake cycles following phenobarbital administration. (C) Continuous extremely low voltage pattern with suspected seizure pattern. (D) Suppression-burst pattern. (E) Flat tracing, mainly isoelectric. From "Predictive value of early continuous amplitude integrated EEG recordings on outcome after severe birth asphyxia in full term infants." by Hellström-Westas L, Rosén I, Svenningsen NW. Arch Dis Child Fetal Neonatal Ed. 1995 Jan;72(1):F34-8.

Although aEEG obtained within 6 hours of life has been recognised as the best single outcome predictor in asphyxiated newborn infants who were cared for under normothermia (35), the predictive value is known to be altered or even lost by therapeutic interventions such as therapeutic hypothermia (36), suggesting that further improvement of the diagnostic algorithm is required potentially by combining with additional acute phase biomarkers.

1.2.5 Diagnostic tools: Conventional MRI

Conventional MRI provides detailed information about types and depths of hypoxic-ischaemic injury with spatial resolution (Fig. 1.2-2) (37). Following severe perinatal hypoxia-ischaemia, abnormal MRI signal intensities in the deep grey matter and the posterior limb of the internal capsule are some of the most common findings, which predict abnormal neurodevelopmental outcomes in term infants with neonatal encephalopathy (38).

Figure 1.2-2: Mild MRI lesions in the deep grey matter and internal capsule

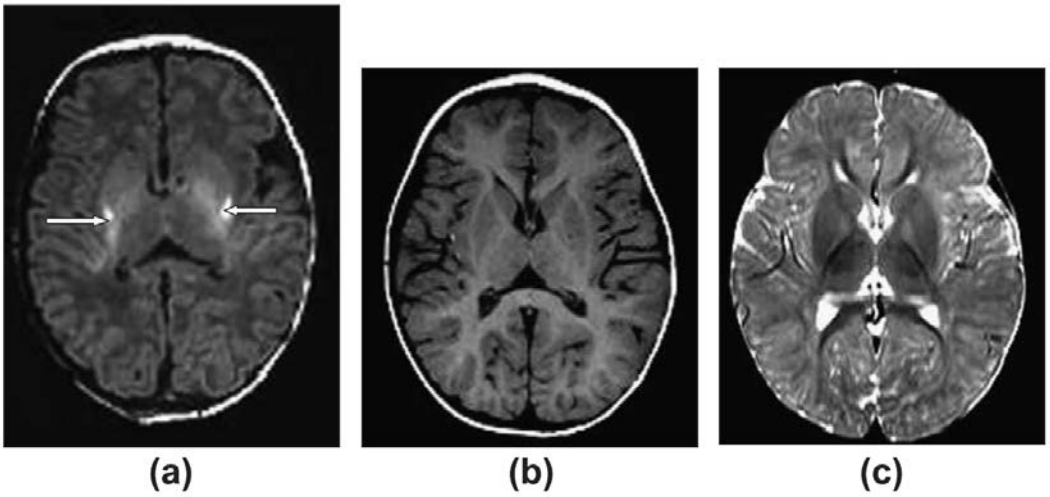

(a) T1-weighted imaging of an asphyxiated newborn infant showing abnormal high signal intensities (arrows) within the lentiform nuclei with intact posterior limb of the internal capsule. Follow up T1-weighted (b) and T2-weighted (c) imaging at 12 months shows normal appearances. From "Magnetic resonance imaging in neonatal encephalopathy." by Rutherford M, Ward P, Allsop J, Malamatentiou C, Counsell S. Early Hum Dev. 2005 Jan;81(1):13-25.

Deep grey matter lesions are often accompanied by injury in the cerebral cortex and subcortical white matter around the central sulcus, which become most obvious after the first week from injury (37, 38); extensive white matter abnormalities are observed in approximately 50% of infants with deep grey matter lesions. Although MRI is useful to predict the motor and cognitive outcomes during the early infancy, these abnormal signs are not obvious within the first week of life (37, 39), suggesting the requirement to incorporate either advanced, quantitative magnetic resonance techniques (e.g. maps of transverse relaxation time (T2) and apparent diffusion coefficient (ADC)), or alternative biomarkers such as electroencephalogram (40) for early and precise diagnosis of neonatal encephalopathy.

1.3 Mechanisms of cerebral injury in the newborn infant

1.3.1 Primary energy failure and acute phase injury cascade

Cerebral injury secondary to hypoxia-ischaemia is an evolving process, which takes place over days and weeks. Severe hypoxic–ischaemic events disable mitochondrial synthesis of adenosine triphosphate, resulting in the loss of energy-dependent functions to maintain cellular homeostasis (41). When severe shortage in energy substrates is prolonged, neuronal cells become unable to maintain the cellular membrane potential, resulting in neuronal depolarisation and subsequent release of excitatory neurotransmitters such as glutamates (Fig. 1.3-1). Persistent excitation of the cerebral tissue causes unregulated influx of calcium into the cytoplasmic space, further leading to the activation of nitric oxide synthase and the production of reactive oxygen species.

Figure 1.3-1: Primary energy depletion and acute phase injury cascade

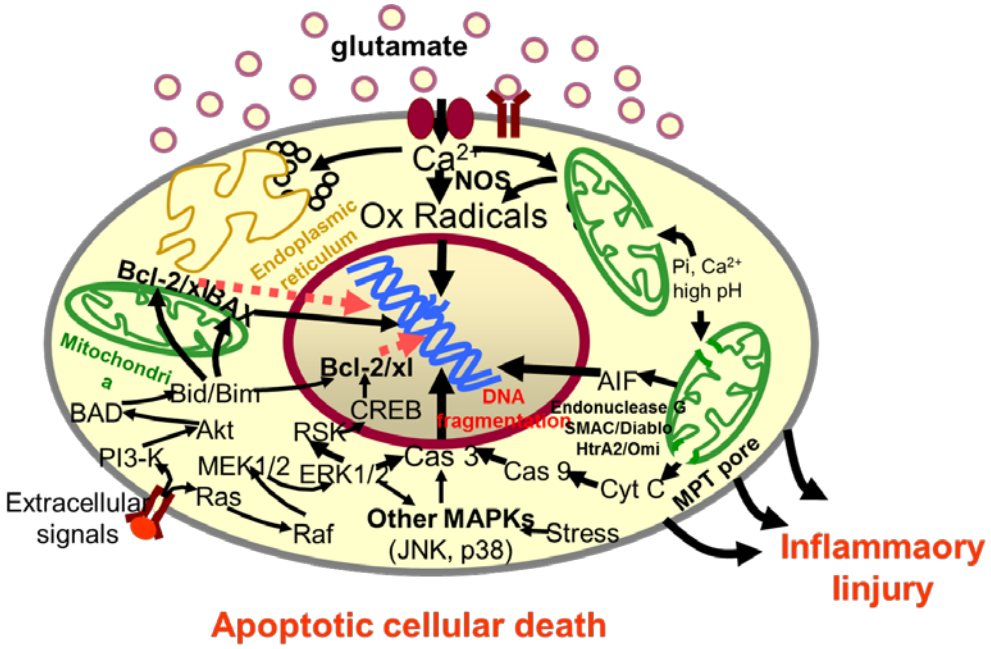

Cartoon depicting the acute phase injury cascade following acute hypoxia-ischaemia and subsequent primary energy depletion. Prolonged energy depletion results in the accumulation of excitatory neurotransmitters, which triggers the influx and deposition of calcium to cytoplasmic organellae, generation of oxygen free radicals, mitochondrial dysfunction and prolonged cellular death induced by the activation of pro-apoptotic proteins. Such a complex and persistent evolutional process of cerebral injury causes acute cellular loss mainly via necrosis and subacute to chronic cellular loss via apoptosis and autophagy.

1.3.2 Latent phase and secondary energy failure

Although severe hypoxia-ischaemia exhausts cerebral tissue energy substrates, efficient resuscitation may temporary reverse the tissue energy metabolism to normal levels (42). Indeed, in asphyxiated newborn infants, phosphorus (^{31}P) magnetic resonance spectroscopy (MRS) revealed “at a glance normal” cerebral metabolism shortly after delivery (Fig. 1.3-2) (43, 44). This transient period with near-normal energy metabolism, or the “latent-phase”, is followed by a secondary phase of impaired cerebral energy generation ensued 8 to 24 hours after hypoxia-ischaemia despite adequate oxygenation and circulation (42). Secondary energy failure is characterised by progressive declines in phosphocreatine (PCr) and nucleotide triphosphates (NTP; mainly adenosine triphosphate (ATP)) and increased inorganic phosphate (Pi) (43).

Figure 1.3-2: Evolution of energy failure after the latent phase in a severely asphyxiated newborn infant

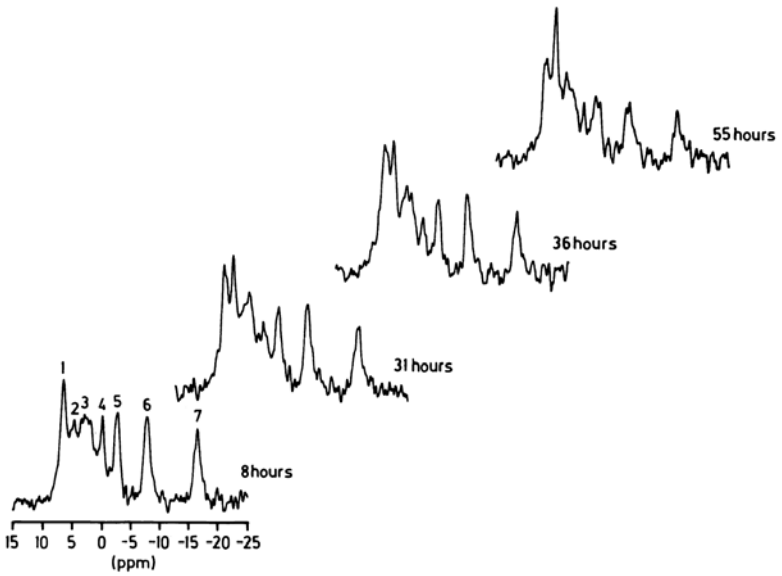

Brain tissue energetic metabolites were observed using ^{31}P MRS from a baby born at 37 weeks gestation who had sustained severe birth asphyxia. The peaks (1-7) are attributable to phosphomonoesters, inorganic phosphate, phosphodiesters, phosphocreatine, and three phosphorus nuclei of adenosine triphosphate, respectively. In contrast to the baseline spectrum at 8 hours, where relative concentrations of phosphocreatine and adenosine triphosphate were still maintained at subnormal levels, high energy phosphate peaks fell with time while inorganic phosphate increased. The infant died at 60 hours after birth. From “Prognosis of newborn infants with hypoxic-ischemic brain injury assessed by phosphorus magnetic resonance spectroscopy.” Azzopardi D, Wyatt JS, Cady EB, Delpy DT, Baudin J, Stewart AL, Hope PL, Hamilton PA, Reynolds EO. Pediatr Res. 1989 May;25(5):445-51.

The severity of secondary energy failure and subsequent neurodevelopmental impairments are closely correlated been each other (43, 45, 46). The importance of the latent phase is increasingly recognised (47), as this period is likely to constitute a "therapeutic window" for neuroprotective treatments such as therapeutic hypothermia (7-9, 48, 49). Despite the “normal” high energy phosphate concentrations within the brain tissue during the latent phase, evidence of cellular injury at this time has been reported, which includes raised lactate dehydrogenase and propidium iodide fluorescence (50); abnormal white-matter nerve fibres and increased white-matter apoptosis (51); increased β-amyloid precursor protein (52); and calcium accumulation, mitochondrial swelling with nuclear chromatin condensation accompanying maximal mitochondrial enlargement, and apoptosis and necrosis features (Fig. 1.3-3) (53). It is hence important to understand the subtle change in cerebral high-energy phosphates during the latent phase in developing early diagnostic biomarkers. However, few studies have thus far scrutinised temporal changes in brain energy metabolites in detail.

Figure 1.3-3: Evolution of secondary brain injury

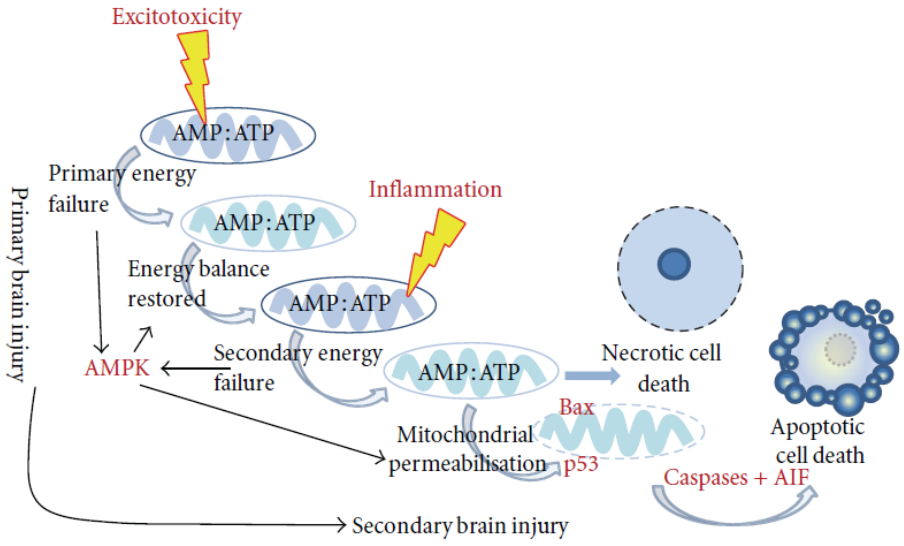

Energy depletion culminating in Bax-dependent mitochondrial permeabilisation represents an irreversible commitment to cell death in neonatal brain injury. Adenosine monophosphate-activated protein kinase (AMPK) is activated in response to stresses which change either intracellular calcium levels or deplete intracellular adenosine triphosphate concentrations. Although AMPK works to return energy levels to baseline, prolonged activation results in upregulation of the proapoptotic protein, Bim. From “Molecular mechanisms of neonatal brain injury. Thornton C, Rousset CI, Kichev A, Miyakuni Y, Vontell R, Baburamani AA, Fleiss B, Gressens P, Hagberg H. Neurol Res Int. 2012;2012:506320.

1.4 Piglet model of neonatal encephalopathy

Over the past 20 years, our group has used a newborn piglet model of transient hypoxia-ischaemia induced by reversible occlusion of the common carotid arteries by remotely controlled balloon vascular occluders and simultaneous reduction in the inspired oxygen fraction to 0.12 (42). The use of large animal models benefits from intensive care settings, which mimics the clinical situation in detail, using mechanical ventilation, continuous fluid and drug infusion, and continuous physiological monitoring throughout the experiment. Piglets are cared for within the bore of the magnetic resonance spectrometer, before, during and after hypoxia-ischaemia, for up to 60 hours at a time to serially monitor cerebral energy metabolism. Thus, quantitative measures of acute hypoxic-ischaemic insult, latent phase and secondary energy failure are obtained non-invasively (Fig. 1.4-1). In addition to the similarity in the experimental setting to the clinical practice, there is another outstanding benefit in using this model, because piglets have much larger brain compared to rodents, which allows the assessment of the regional impact of hypoxia-ischaemia and therapeutic interventions (49).

Figure 1.4-1: Evolution of secondary energy failure in the piglet model of neonatal encephalopathy

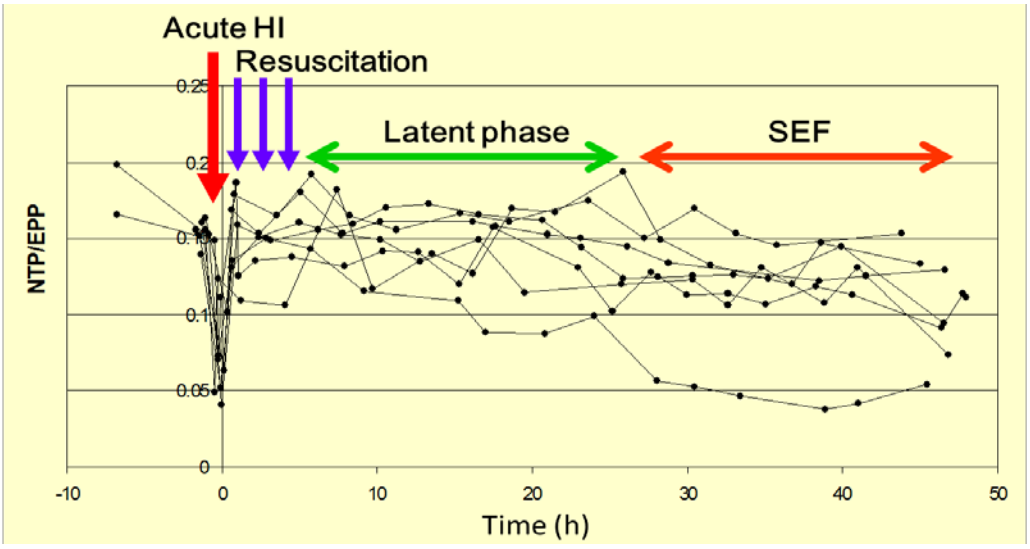

Temporal changes in cerebral nucleotide triphosphate (mainly adenosine triphosphate) concentration relative to exchangeable high-energy phosphate pool is shown before, during and after hypoxia-ischaemia. Resuscitation transiently reversed cerebral high energy phosphate to the normal level (the latent phase), which is followed by secondary energy failure after 8-24 h of resuscitation.

1.5 Quantitative magnetic resonance biomarkers of cerebral injury

1.5.1 ^{31}P MRS

As described in the previous section, ^{31}P MRS has been utilised as a unique biomarker, with which cerebral tissue energy metabolites are directly observed without invasive procedures (42-44). Using ^{31}P MRS, temporal changes in high energy phosphates, including the transient decline during acute hypoxia-ischaemia, recovery following the commencement of resuscitation, latent phase, and the delayed decline due to the progress of secondary energy failure, can be monitored continuously (42, 47). Metabolites observed using ^{31}P MRS include high energy phosphates such as nucleotide triphosphate (NTP), which is mainly adenosine triphosphate (ATP), and phosphocreatine (PCr), which serves as a stable high energy phosphate pool, whereas inorganic phosphate (Pi), which is virtually the ashes of high energy phosphates, can also be monitored simultaneously (Fig. 1.5-1) (54).

Figure 1.5-1: High resolution ^{31}P MRS spectra from the brain of the piglet model

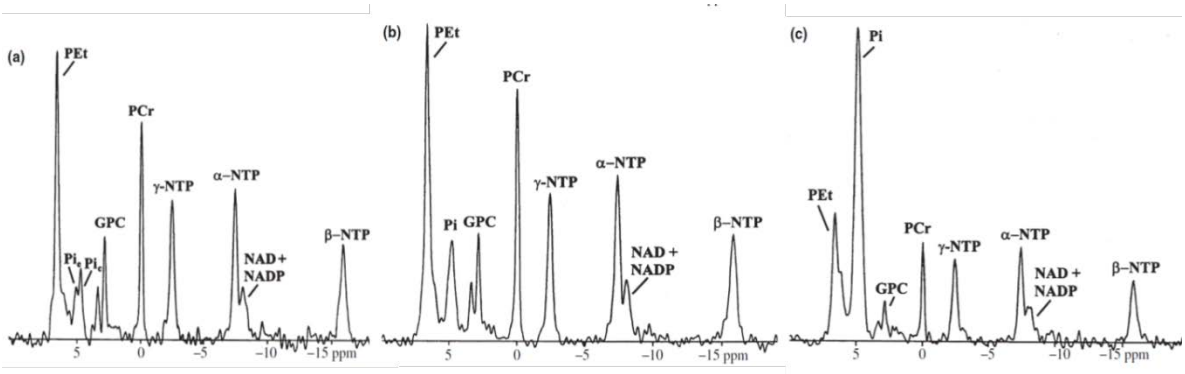

Representative spectra from a piglet which developed severe secondary energy failure. (a) before hypoxic-ischaemic insult; (b) 1.6 hours after hypoxia-ischaemia; and (c) during secondary energy failure 23.4 hours after the commencement of resuscitation. Although no apparent decline is observed for PCr and NTP, Pi is slightly increased 1.6 hours after hypoxia-ischaemia (b) versus baseline (a). In (c) Pi is further increased, with overt reduction in PCr and NTP, which is characteristic of secondary energy failure. From "Phosphorus magnetic resonance spectroscopy 2 h after perinatal cerebral hypoxia-ischemia prognosticates outcome in the newborn piglet." by Cady EB, Iwata O, Bainbridge A, Wyatt JS, Robertson NJ. J Neurochem. 2008 Nov;107(4):1027-35.

Although the MRS signal obtained along different frequencies corresponds to the concentration of each metabolite, it is technically difficult to give the absolute concentration of these molecules precisely. Hence, currently, ratios of concentrations between metabolites have widely been used. PCr/Pi is considered to give sensitive stress marker, because PCr serves to maintain the concentration of ATP, thus starting declining before the overt change in ATP; in addition, because Pi increases with the acceleration of ATP consumption, PCr/Pi is supposed to change dynamically even when the shortage in energy substrates is still tolerated by the cerebral tissue (Fig. 1.5-2) (42). However, PCr/Pi is theoretically influenced by factors including the flux within the mitochondrial electron transport chain, re-phosphorylation of adenosine diphosphate via creatine kinase, and anaerobic glycolysis under unimpaired substrate delivery (11). In our more recent studies, we employed another approach to assess energy metabolites; each metabolite is quantified relative to the total mobile exchangeable phosphate pool (EPP), which is the sum of Pi, PCr and 3 NTPs (54). This method may be inferior in its sensitivity to detect subtle temporal changes in high energy phosphates, however, there is an advantage that the temporal change in each metabolite can be assessed differently by monitoring Pi/EPP, PCr/EPP and NTP/EPP.

Figure 1.5-2: Temporal changes in PCr/Pi and NTP/EPP in the piglet model of asphyxial encephalopathy

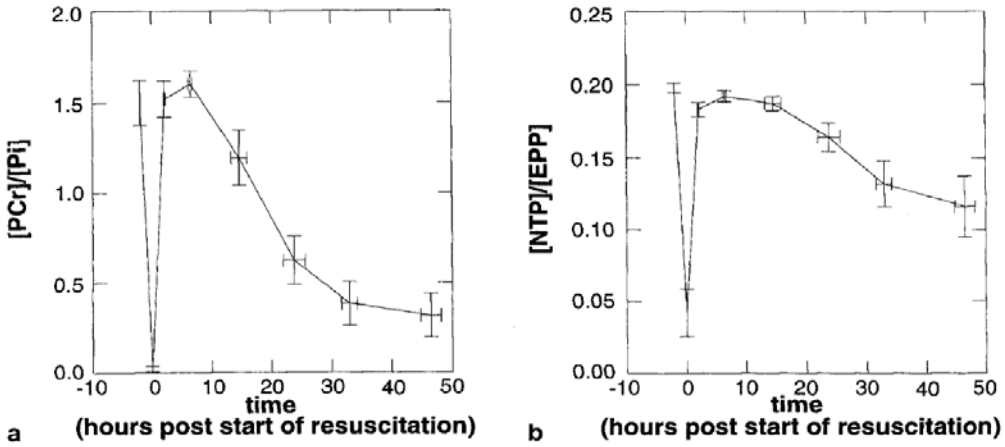

Secondary energy failure is identified much earlier in the trend of PCr/Pi compared to NTP/EPP because the decline in PCr and the increase in Pi occurs even while ATP levels are maintained within the cerebral tissue. From "Temporal and anatomical variations of brain water apparent diffusion coefficient in perinatal cerebral hypoxic-ischemic injury: relationships to cerebral energy metabolism." by Thornton JS, Ordidge RJ, Penrice J, Cady EB, Amess PN, Punwani S, Clemence M, Wyatt JS. Magn Reson Med. 1998 Jun;39(6):920-7.

Early clinical studies which used ^{31}P MRS in infants with severe neonatal encephalopathy revealed that the MRS spectrum shortly after birth demonstrates 'normal' cerebral energy metabolism (44). Azzopardi and colleagues demonstrated that, after such a latent phase, PCr and NTP decrease and Pi increases despite adequate oxygenation and circulation (43). Low levels of high energy phosphates, decreased PCr/Pi and increased Pi in the first days of life have been associated with neurodevelopmental impairment and increased mortality (43, 45, 46).

Despite the advantage of^{31}P MRS in allowing direct monitoring of brain tissue energy metabolism, the use of ^{31}P MRS is not popular in clinical practice, because of its requirement for expertise and special hardware. In addition, the signal of ^{31}P MRS is usually obtained from the entire brain without specifying the region of interest, mainly because of the weak signal from ^{31}P molecule compared to 1-H (Fig. 1.5-3) (^{1}H).

Figure 1.5-3: Cerebral tissue covered by the surface coil in the acquisition of ^{31}P MRS spectra from the piglet brain

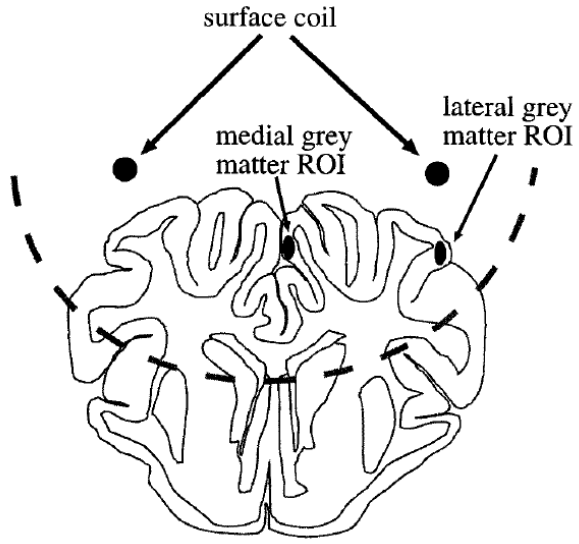

Schematic drawing showing the coronal section of the piglet brain, together with the surface coil position and the approximate extent of the surface coil sensitive volume. From "Temporal and anatomical variations of brain water apparent diffusion coefficient in perinatal cerebral hypoxic-ischemic injury: relationships to cerebral energy metabolism." by Thornton JS, Ordidge RJ, Penrice J, Cady EB, Amess PN, Punwani S, Clemence M, Wyatt JS. Magn Reson Med. 1998 Jun;39(6):920-7.

1.5.2 ^{1}H MRS

Compared to^{31}P MRS, ^{1}H MRS can be performed using most newly built MRI scanners, and has various advantages including the short acquisition time, spatial resolution, and the potential for absolute quantification of the molecules (55). In addition, because ^{1}H is the most common structural element within the human body, a wide range of metabolites, such as lactate, N-acetyl aspartate (NAA), choline, creatine, and alanine, can be identified at their corresponding unique chemical shifts (Fig. 1.5-4). Although the current technique used for the clinical and experimental studies does not allow the isolation of peaks for energy metabolites, such as ATP, PCr and Pi, the level of anaerobic metabolism within the cerebral tissue can be extrapolated using the lactate peak. Following perinatal hypoxia-ischaemia, the concentration of cerebral tissue lactate increases according to the depth of acute insult (56, 57). This increase in lactate is attributable to impaired oxidative metabolism due to mitochondrial damage, however, other mechanisms, such as the alteration of the cellular component, may also be involved, because, following severe perinatal hypoxia-ischaemia, the elevation of lactate sometimes persists for weeks (58). N-acetyl aspartate is another useful marker for intact neurons and axons; a reduction in NAA following perinatal hypoxia-ischaemia is associated with reduced neuronal and axonal viability (59-61). A recent meta-analysis concluded that lactate/NAA peak-area ratio obtained from the deep grey matter during the neonatal period provides the best predictive value of the outcome in infants with neonatal encephalopathy with higher sensitivity (82%, 95% CI: 74%–89%) and specificity (95%, 95% CI: 88%–99%) compared to conventional MRI, diffusion weighted imaging (DWI), and other metabolite ratios of ^{1}H MRS (58).

Figure 1.5-4: ^{1}H MRS spectra, lactate/NAA and outcome of asphyxiated infants

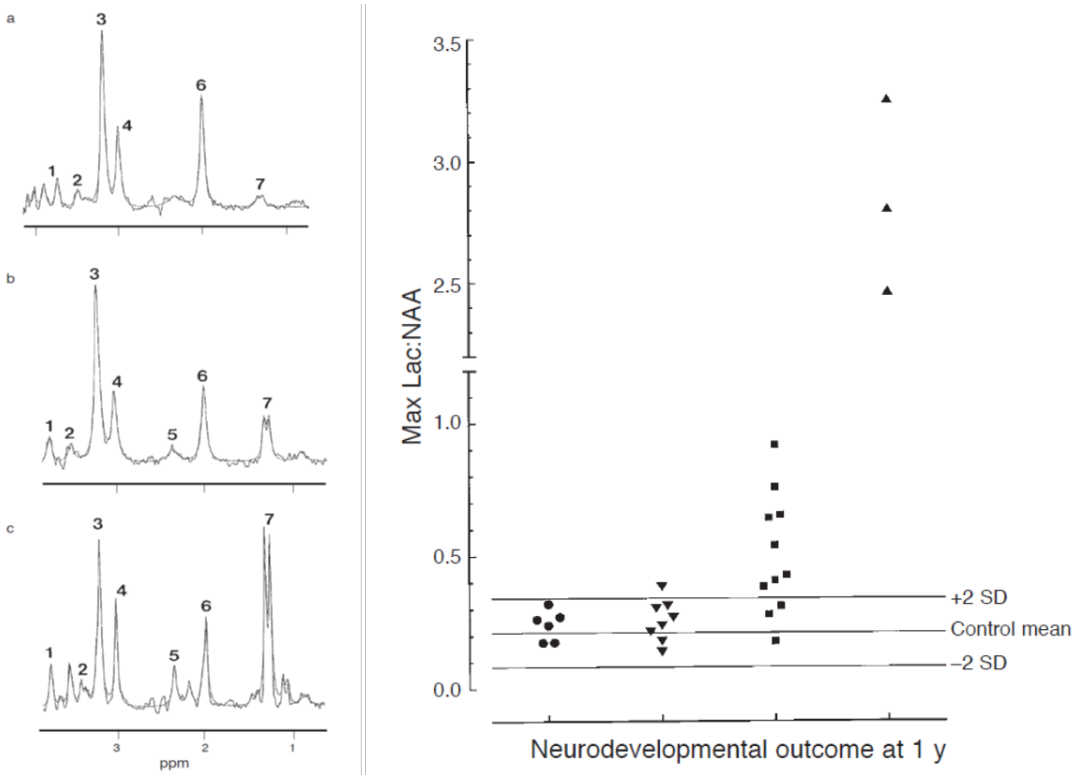

Left panel: ^{1}H MRS spectra obtained from thalamic region of: (a) a control infant aged 84 hours; (b) an infant 19 hours after moderate hypoxia-ischaemia; (c) an infant 17 hours after severe hypoxia-ischaemia. Resonance identifications: (1) glutamate/glutamine; (2) myoinositol/glycine; (3) choline; (4) creatine; (5) glutamate/glutamine; (6) NAA; (7) lactate. Right panel: Maximum lactate/NAA measured at >12 hours (n=28) and neurodevelopmental outcome at 1 year of age (● Normal outcome; ▼ impairment with no disability; ■ impairment with disability; ▲dead). From "Early brain proton magnetic resonance spectroscopy and neonatal neurology related to neurodevelopmental outcome at 1 year in term infants after presumed hypoxic-ischaemic brain injury." by Amess PN, Penrice J, Wylezinska M, Lorek A, Townsend J, Wyatt JS, Amiel-Tison C, Cady EB, Stewart A. Dev Med Child Neurol. 1999 Jul;41(7):436-45.

1.5.3 Diffusion weighted imaging

Diffusion weighted imaging (DWI) is a MRI technique, which is sensitive to acute phase brain injury induced by hypoxia-ischaemia (62). DWI reflects changes in water diffusion due to redistribution of water between cytoplasmic and extra-cellular spaces, cytotoxic oedema and other derangements in cellular homeostasis. After perinatal hypoxia-ischaemia, abnormal MRI findings on conventional sequences remain invisible within several days of the acute event, when important clinical decisions have to be

made to maximise the benefit from neuroprotective interventions (11). In contrast to the limited utility of conventional MRI during the acute period, DWI provides more sensitive marker in assessing tissue integrity and damage from shortly after hypoxia-ischaemia (Fig. 1.5-5). While the assessment of DWI is qualitative, maps of apparent diffusion coefficient (ADC) enable objective assessment and comparison of acute phase brain injury even when the injury pattern is global and little amount of cerebral tissue is spared (63). Following perinatal hypoxia-ischaemia, ADC values are significantly reduced in the first week of birth in the white matter and/or deep grey matter. However, ADC values are reversed to the normal level after approximately a week. After the second week of life, ADC levels of affected regions are either normal or increased (64).

A study which prospectively assessed DWI from infants with neonatal encephalopathy found that infants with poor outcome had lower ADC values at early imaging in the Rolandic cortex, hippocampus, deep grey matter and PLIC. However the authors suggested that the regional ADC values are of limited predictive value for the outcome, while the combined assessment of conventional MRI and the spatial pattern of DWI changes were better predictors of neurological outcomes (65). In agreement with this finding, a meta-analysis which compared the predictive values of magnetic resonance biomarkers during the neonatal period revealed that predictive values of ADC for the neurodevelopmental outcome are generally poor, and are inferior to ^{1}H MRS (58). Because the timing of MRI scans is inconsistent between subjects, it is difficult to define at which phase of the injury evolution (i.e. the latent period, sub-acute phase decline in ADC or pseudo-normalisation) the infant was scanned. However, ADC changes following transient hypoxia-ischaemia in a piglet model has been demonstrated to have tight linear correlations with cerebral high energy phosphate levels, such as PCr and ATP (Fig. 1.5-6) (62). This suggests that ADC can be used as the acute phase maps of tissue energy metabolism although the difference in background variables between clinical and experimental settings, such as the maturational status of the brain, the type, timing and depth of hypoxia-ischaemia and the fixed/unfixed timing for studies, need to be accounted for. With further experimental validations of ADC with histo-pathological assessments at different evolutional stage of neonatal encephalopathy, this technique can be used to evaluate the progress of injury and efficacy of treatments, as well as to predict the precise outcome of the infant.

Figure 1.5-5: Conventional MRI and DWI after perinatal hypoxia-ischaemia

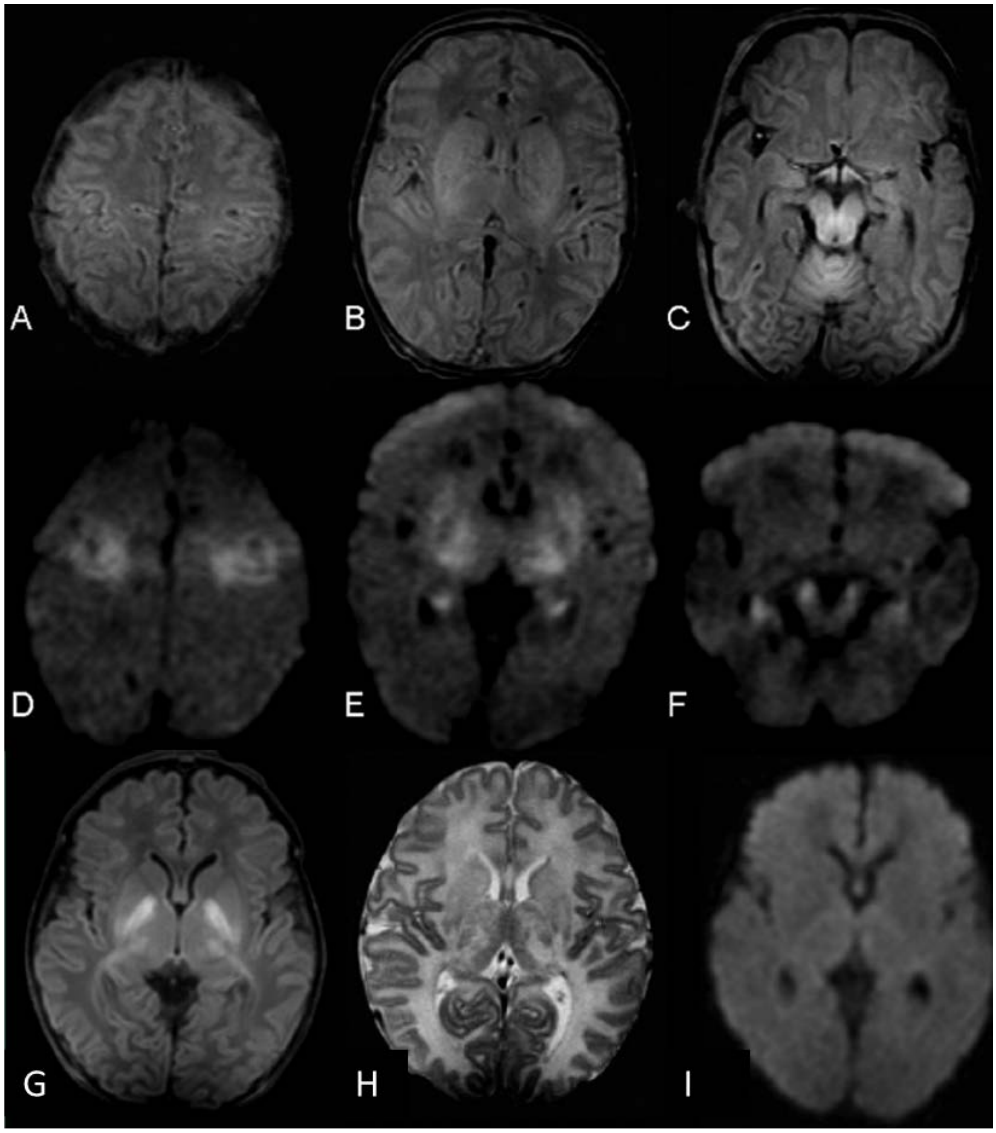

A-F: MRI obtained on the 3rd day of life from an infant with a poor motor outcome. A-C, T1-weighted images with absence of normal signal intensity in the internal capsule. D-F, DWI with hyperintense signal in the Rolandic cortex, basal ganglia, hippocampus, and cerebral peduncle. G-I: MRI at day 9 in an infant with a good motor outcome. G, T1-weighted image with an abnormal high signal intensity in the globus pallidus and thalamus. H, T2-weighted image with an irregular, abnormal high signal intensity in the thalamus and globus pallidus. I, DWI without abnormalities. From "Diffusion-weighted and conventional MR imaging in neonatal hypoxic ischemia: two-year follow-up study." by Vermeulen RJ, van Schie PE, Hendrikx L, Barkhof F, van Weissenbruch M, Knol DL, Pouwels PJ. Radiology. 2008 Nov;249(2):631-9.

Figure 1.5-6: Correlation between PCr/Pi and ADC

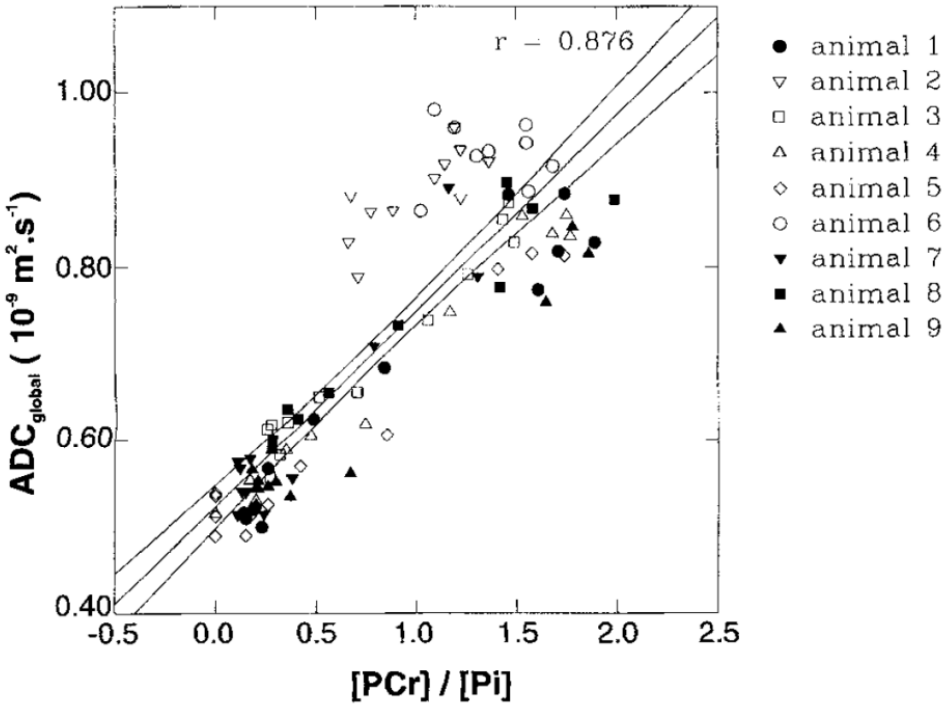

Combined scatter plot of ADC against PCr/Piin a piglet model of perinatal asphyxial encephalopathy. From "Temporal and anatomical variations of brain water apparent diffusion coefficient in perinatal cerebral hypoxic-ischemic injury: relationships to cerebral energy metabolism." by Thornton JS, Ordidge RJ, Penrice J, Cady EB, Amess PN, Punwani S, Clemence M, Wyatt JS. Magn Reson Med. 1998 Jun;39(6):920-7.

Recently, additional use of fractional anisotropy (FA), which is derived from diffusion tensor imaging (DTI), is expected to improve the detection of early microstructural changes after hypoxia-ischaemia. FA has been proposed to quantify the overall directionality of water diffusion. Cerebral regions with cylindrical microstructure (myelinated white matter) have high FA values close to 1 because of anisotropic diffusion, whereas regions with highly isotropic diffusion (e.g. cerebro-spinal fluid and cystic lesions) have low FA values close to 0 (38). In the cerebral tissue, diffusion is greatest parallel to the axonal tract, whereas diffusion is restricted in the perpendicular direction. It has been demonstrated that FA values in the white matter decrease following moderate to severe perinatal hypoxia-ischaemia, and, unlike ADC, abnormal low FA values can be observed persistently after the second week of life, suggesting the benefit of combining ADC and FA values (66).

1.5.4 Maps of longitudinal and transverse relaxation times

Clinical diagnosis of cerebral injury using conventional MRI relies on altered tissue signal intensities, which are caused by the change in longitudinal (T1) or transverse (T2) relaxation times. Although mapping of the longitudinal relaxation time has not widely been used in the clinical diagnosis because of its requirement for expertise and relatively long acquisition time (67, 68), the opportunity to use T2 maps has exponentially increased (Fig. 1.5-7) (69). Most modern MRI scanners can now develop T2 maps with the minimum additional scanning time. T2 relaxation time is known to increase following perinatal hypoxia-ischaemia (70).

Figure 1.5-7: Transverse relaxation time in the thalamus and basal ganglia

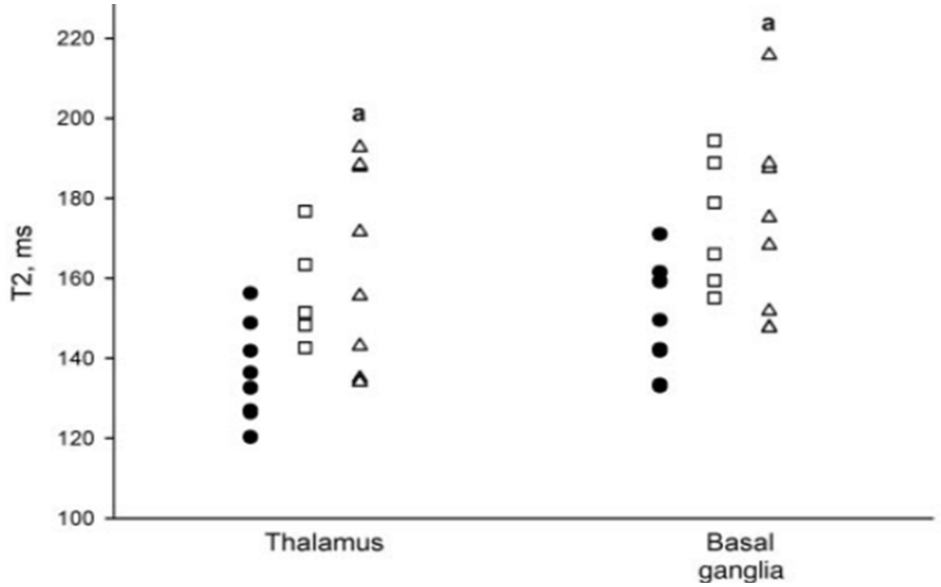

T2-relaxation time of RoIs in the thalamus (left) and basal ganglia (right) by neurodevelopmental outcome at age 1 year. a: P <0.05, analysis of variance and Dunnett test versus normal-outcome group. Closed circle, normal; open square, moderate; open triangle, severe. From "Comparative prognostic utilities of early quantitative magnetic resonance imaging spin-spin relaxometry and proton magnetic resonance spectroscopy in neonatal encephalopathy." By Shanmugalingam S, Thornton JS, Iwata O, Bainbridge A, O'Brien FE, Priest AN, Ordidge RJ, Cady EB, Wyatt JS, Robertson NJ. Pediatrics. 2006 Oct;118(4):1467-77.

Quantitative maps of relaxation times are expected to improve the diagnostic value on MRI by eliminating subjective biases, which were inevitable for the interpretation of conventional MRI (69). Compared to ADC, changes in T2 relaxation time are relatively less dynamic. However, extrapolated from the temporal change in the signal intensity on T2-weighted imaging, temporal changes in T2 relaxation time after perinatal hypoxia

ischaemia is unlikely to involve complex biphasic patterns, potentially providing a simple interpretation of the finding. Although there currently are only a limited number of studies which used T2 maps after perinatal hypoxia-ischaemia, this technique may also be used in future in combination with ADC and other imaging biomarkers.

1.5.5 Monitoring of secondary energy failure and therapeutic time window

Following moderate to severe hypoxia-ischaemia, cerebral metabolism recovers on resuscitation but only to develop secondary energy failure hours after the acute event (42, 43). Adverse biological reactions responsible for the evolution of secondary energy failure include accumulation of excitatory neurotransmitters, intracellular calcium accumulation, generation of oxygen free radicals, and mitochondrial dysfunction (71-75). A range of magnetic resonance biomarkers obtained using ^{31}P MRS and DWI have demonstrated biphasic patterns of metabolic derangement following perinatal hypoxia-ischaemia (43, 45, 62). Severity of secondary energy failure represented by low cerebral PCr/Pi, NTP/EPP, increased brain lactate and an alkaline intracellular pH in the first few days after birth were associated with neurodevelopmental impairment and increased mortality (43, 45, 46, 76). Cerebral injury after perinatal hypoxia-ischaemia is an evolving process with necrosis and apoptosis, which are predominant mode of cellular death during acute phase and thereafter, respectively (73). Neuronal injury at the cellular level can be identified with closer inspection even during the latent phase; increase in lactate dehydrogenase and propidium iodide fluorescence, abnormal nerve fibres and increased apoptotic cells in white matter, increased β-amyloid precursor protein, calcium accumulation, mitochondrial swelling with nuclear chromatin condensation, and apoptotic and necrotic features, can be observed even during the period which corresponds to the latent phase (50-53). Understanding of secondary energy failure is especially important because, in experimental models, significant long term neuroprotection by therapeutic interventions occurs only when the gap between the acute event and the start of treatment remains within ~6 hours; no benefit has been observed when treatments are initiated after the evolution of secondary energy failure and epileptic activity (11, 77). Further investigations in the animal model targeting the mechanism of secondary energy failure, especially detailed energy metabolism during the latent period, when normal energy metabolism is maintained despite activated injury cascades, is required for the future improvement of acute phase diagnosis and treatment.

Figure 1.5-8: Evolution of secondary energy failure in a rodent model of transient hypoxia-ischaemia

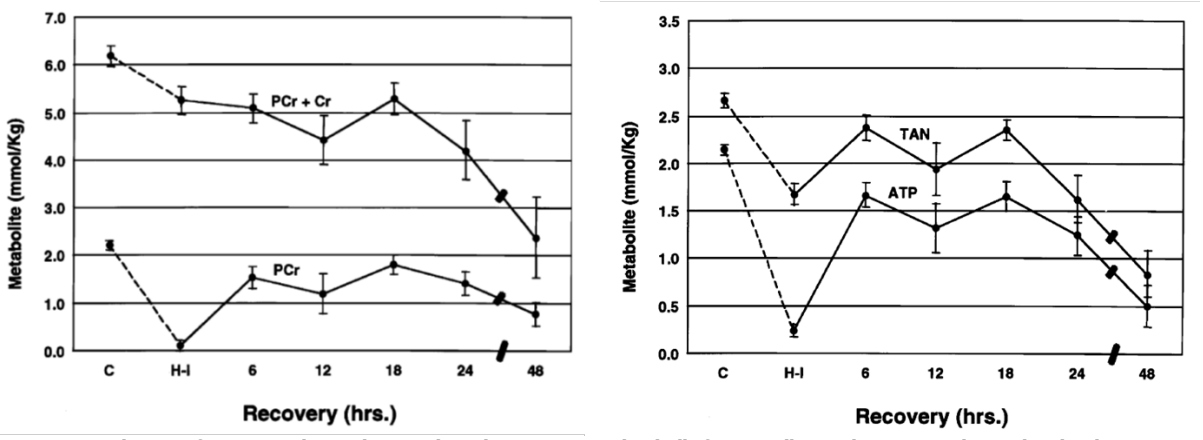

Concentrations of PCr and total creatine (PCr + creatine) (left panel), and ATP and total adenine nucleotides (TAN) (right panel) during and after hypoxia-ischaemia in a newborn rat model of transient hypoxia-ischaemia. C, control; H-I, hypoxia–ischemia. Concentrations of during and after hypoxia–ischaemia in the immature rat. C, control; H-I, hypoxia–ischemia. From "Secondary energy failure after cerebral hypoxia-ischemia in the immature rat." by Vannucci RC, Towfighi J, Vannucci SJ. J Cereb Blood Flow Metab. 2004 Oct;24(10):1090-7.

Quantitative measurements of total mobile phosphate and EPP by MRS, and of total adenine nucleotides and total creatine by biochemical methods have demonstrated falls at similar times to the declines in NTP/EPP and PCr/Pi (45, 78, 79). Using an established rodent model, Vannucci and colleagues demonstrated linear relationships between histo-pathological tissue injury and high energy phosphate concentrations at 6 to 18 hours after hypoxia-ischaemia and with much greater significance at 24 to 48 hours, and concluded that secondary energy failure was the consequence of evolving cellular destruction rather than causal of cellular death in surviving tissue (Fig. 1.5-8) (79). Although secondary energy failure observed using ^{31}P MRS is likely to be a phenomenon directly associated with a delayed, irreversible metabolic crisis, it is unclear whether secondary energy failure directly parallels the temporal evolution of cell death itself.

1.5.6 Regional variation of energy metabolism following hypoxia-ischaemia

Although the global evolution of secondary energy failure following perinatal hypoxia-ischaemia is already complex in its timing and severity, these factors may be spatially different between different cerebral regions and even between cellular

components, because the response to hypoxia-ischaemia, resuscitation and treatment is likely to be dependent on the background characteristics in metabolism, anatomical structure, vascularity and neuronal circuitry (Fig. 1.5-9) (80).

Figure 1.5-9: Diagram of normal basal ganglia motor control circuit and areas damaged by near-total asphyxia

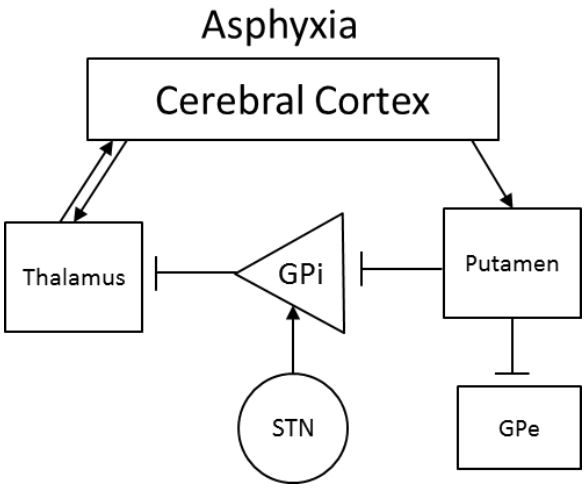

Arrows indicate synapses with excitatory glutamate neurotransmitter; blunted lines indicate inhibitory synapses. GPi, globus pallidus interna; GPe, globus pallidus externa; STN, subthalamic nucleus. If these regions are firing rapidly, the effect on globus pallidus interna and globus pallidus externa is expected to be inhibitory because of inhibitory input from putamen, resulting in increased heterogeneity in spatial injury pattern. From "Possible mechanisms in infants for selective basal ganglia damage from asphyxia, kernicterus, or mitochondrial encephalopathies." by Johnston MV and Hoon AH Jr. J Child Neurol. 2000 Sep;15(9):588-91.

In a primate model of neonatal encephalopathy, different durations and severities of ischemia were associated with specific regional distribution of brain injury; partial asphyxia resulted in white matter injury whereas total asphyxia led to deep grey matter injury (81, 82). In the term newborn infant, cerebral injury following perinatal asphyxia has been identified as two major patterns of (i) the watershed predominant pattern involving the white matter, extending to cortical grey matter when severe, and (ii) the deep grey matter predominant pattern involving the deep grey nuclei and perirolandic cortex, extending to the total cortex when severe (Fig. 1.5-10) (83-86). Understanding of spatial and temporal evolution of cerebral injury would be important to estimate the associated outcome, and also to make important therapeutic decisions which bring the greatest opportunity of intact survival to the affected infant.

Figure 1.5-10: Pattern of brain injury after perinatal hypoxia-ischaemia and neurodevelopmental outcome at 30 months of age

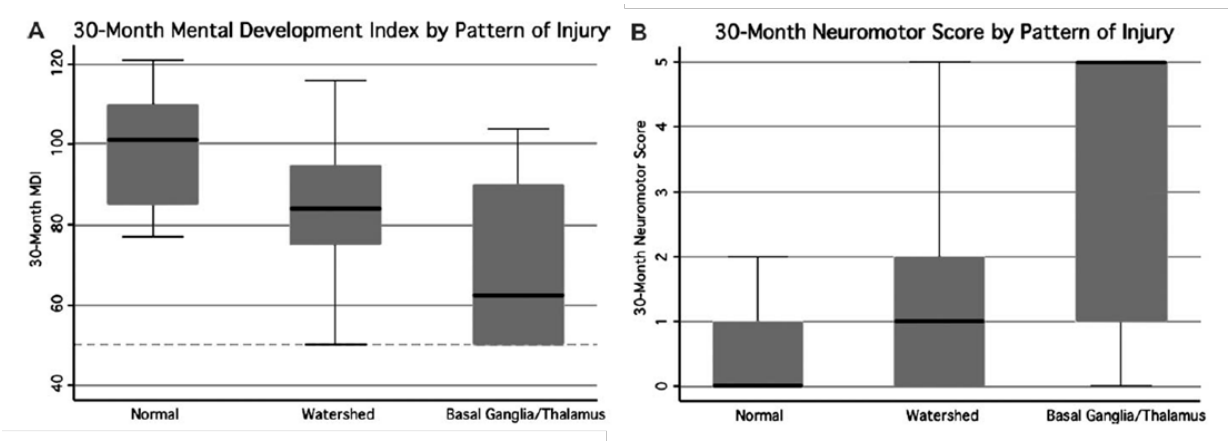

Box plot of the 30-month Mental Development Index (A) and neuromotor score (B) by the pattern of injury. MDI was lowest in the infants with the basal ganglia/thalamus predominant pattern, with intermediate scores in infants with the watershed pattern (p = 0.0007). Neuromotor impairments were most severe in the infant with the basal ganglia/thalamus pattern (p = .0001). From "Patterns of brain injury in term neonatal encephalopathy." by Miller SP, Ramaswamy V, Michelson D, Barkovich AJ, Holshouser B, Wycliffe N, Glidden DV, Deming D, Partridge JC, Wu YW, Ashwal S, Ferriero DM. J Pediatr. 2005 Apr;146(4):453-60.

1.6 Treatment of neonatal encephalopathy

1.6.1 Therapeutic hypothermia: mechanism

A wide range of experimental evidence has been accumulated supporting the effect of mild to moderate cerebral hypothermia (32 to 34°C) applied immediately after transient hypoxia-ischaemia to reduce brain injury and to improves behavioural outcome (87, 88). Hypothermia applied following perinatal hypoxia-ischaemia suppresses numerous chemical reactions on the neurotoxic cascade, which includes the reduction in the metabolic rate by 4 to 7% per 1°C temperature reduction, attenuation of inflammatory reactions, decrease in the glutamate release, attenuation of the activity of N-methyl-D-aspartate receptors, reduction in the production of oxygen free radicals and nitric oxide, contribution to the reduction in intracranial pressure, and the prolongation of the therapeutic time window for other treatments (Fig. 1.6-1) (89-92).

Figure 1.6-1: Systemic hypothermia and therapeutic time window in the piglet model of asphyxial encephalopathy

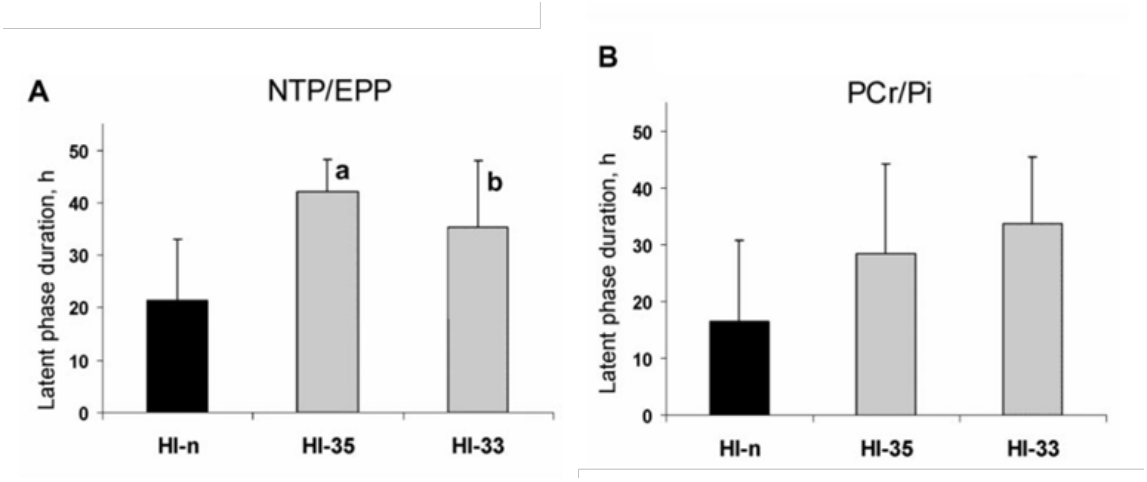

Duration of latent phase measured by (A) NTP/EPP and (B) PCr/Pi in the normothermic (HI-n), hypothermic to 35°C (HI-35) and hypothermia to 33°C (HI-33) groups. Duration of the NTP/EPP latent phase was significantly longer in the cooled groups. There was no significant difference in the PCr/Pi latent-phase duration between the HI groups. a P<0.01; b P<0.05, compared with HI-n. From "Delayed whole-body cooling to 33 or 35 degrees C and the development of impaired energy generation consequential to transient cerebral hypoxia-ischemia in the newborn piglet." by O'Brien FE, Iwata O, Thornton JS, De Vita E, Sellwood MW, Iwata S, Sakata YS, Charman S, Ordidge R, Cady EB, Wyatt JS, Robertson NJ. Pediatrics. 2006 May;117(5):1549-59.

Simultaneously with the beneficial effect of hypothermia for neuroprotection, several deleterious effects of hypothermia are known, including the cardiac suppression, reduction in cerebral blood flow, and increased blood viscosity (11). Thus the overall effect of therapeutic hypothermia is determined by the balance between protective and harmful effects, which may vary according to the type and depth of hypoxia-ischaemia. In addition to the direct neuroprotective effect of therapeutic hypothermia, both mild and moderate systemic hypothermia has been demonstrated to double the duration of the latent phase, or therapeutic time window, thus extending the period when additional neuroprotective interventions may be beneficial (47).

1.6.2 Therapeutic hypothermia: current clinical evidence

The results of the first large scale randomised controlled trials of selective head cooling and whole body cooling in neonatal encephalopathy was released in 2005, both of which showing the improved survival without severe neurodevelopmental impairments at 18 months of age (8, 9). Several more medium to large scale studies consistently demonstrated the beneficial effect of therapeutic hypothermia (7, 93-95).

Table 1.6-1: Therapeutic hypothermia and outcomes at 18 months of age

Table 2 | Effect of moderate hypothermia on neurological outcomes at 18 months compared with controls

	Risk ratio (95% CI)	Risk difference (95% CI)	Number needed to treat (95% CI)	P value
Death or severe disability*	0.81 (0.71 to 0.93)	−0.11 (−0.18 to −0.04)	9 (5 to 25)	0.002
Survival with normal outcome†	1.53 (1.22 to 1.93)	0.12 (0.06 to 0.18)	8 (5 to 17)	‹0.001
Mortality	0.78 (0.66 to 0.93)	−0.07 (−0.12 to −0.02)	14 (8 to 47)	0.005
Severe disability in survivors*	0.71 (0.56 to 0.91)	− 0.11 (−0.20 to −0.03)	9 (5 to 30)	0.006
Cerebral palsy in survivors	0.69 (0.54 to 0.89)	−0.12 (−0.20 to −0.04)	8 (5 to 24)	0.004
Severe neuromotor delay in survivors‡	0.73 (0.56 to 0.95)	−0.10 (−0.18 to −0.02)	10 (6 to 71)	0.02
Severe neurodevelopmental delay in survivors§	0.71 (0.54 to 0.92)	−0.11 (−0.19 to −0.03)	9 (5 to 39)	0.01
Blindness in survivors	0.57 (0.33 to 0.96)	−0.06 (−0.11 to 0.00)	17 (9 to 232)	0.03
Deafness in survivors	0.76 (0.36 to 1.62)	−0.01 (−0.05 to 0.03	NA	0.47

From "Neurological outcomes at 18 months of age after moderate hypothermia for perinatal hypoxic ischaemic encephalopathy: synthesis and meta-analysis of trial data." by Edwards AD, Brocklehurst P, Gunn AJ, Halliday H, Juszczak E, Levene M, Strohm B, Thoresen M, Whitelaw A, Azzopardi D. BMJ. 2010 Feb 9;340:c363.

A recent meta-analysis based on the accumulated clinical evidence from medium to large scale clinical studies confirmed that therapeutic hypothermia of either using selective head cooling or whole body cooling ameliorated the outcome measures, such as mortality, death or severe neurodevelopmental impairment within overall participants

of the studies, and neurodevelopmental impairments in survivors at 18 months of age (Table 1.6-1) (12). Subsequently, in October 2010, the International Liaison Committee on Resuscitation released its revised recommendation for the newborn resuscitation, which strongly recommended the application of therapeutic hypothermia in near term and term infants with moderate to severe neonatal encephalopathy within 6 hours of birth (96).

1.6.3 Key factors potentially associated with further improvement of the treatment

Although clinical trials of therapeutic hypothermia demonstrated consistent neuroprotective effect of cooling, these studies raised important questions about the optimal modality, timing and duration of cooling, which maximise the neuroprotective effect of the treatment (20, 97). Experimental evidence suggested that inter- and intra-subject factors influence the neuroprotective potential of hypothermia; the protective effect of therapeutic hypothermia may be less prominent following very severe hypoxia-ischaemia (8, 98-100); the optimal temperature for neuroprotection may vary between different brain regions (Fig. 1.6-2) (49). If the spatial evolutional pattern of cerebral injury can be serially monitored using advanced imaging technique, it would be easier to identify a group of infants who respond to specific type of cooling before waiting for the assessment of long term outcomes.

Thus far, no pharmacological treatments have been demonstrated to be clinically neuroprotective following perinatal hypoxia-ischaemia in large scale prospective studies (101). Nevertheless, a range of neuroprotective drugs are being assessed as add-on therapies to cooling (10, 102) expecting additive or synergistic effects. In a rodent model, the combination of xenon and hypothermia given 4 hours after hypoxia-ischaemia provided synergistic neuroprotection up to 30 days after birth (103). Because cooling itself can delay the evolution of secondary energy failure (Fig. 1.6-1) (47), the prolonged latent phase may provide sufficient therapeutic time window for additional neuroprotective treatments (104, 105). For example, a single dose of topiramate after hypoxia-ischaemia in the neonatal rat was not protective itself but extended the therapeutic window for brief transient hypothermia of as long as 3 hours (106). A robust biomarker, which reflects the severity and pattern of brain injury during the latent phase, is desirable to target neuroprotective therapies to patients who are most likely to benefit from invasive treatments.

Figure 1.6-2: Cooling level and region-specific brain protection

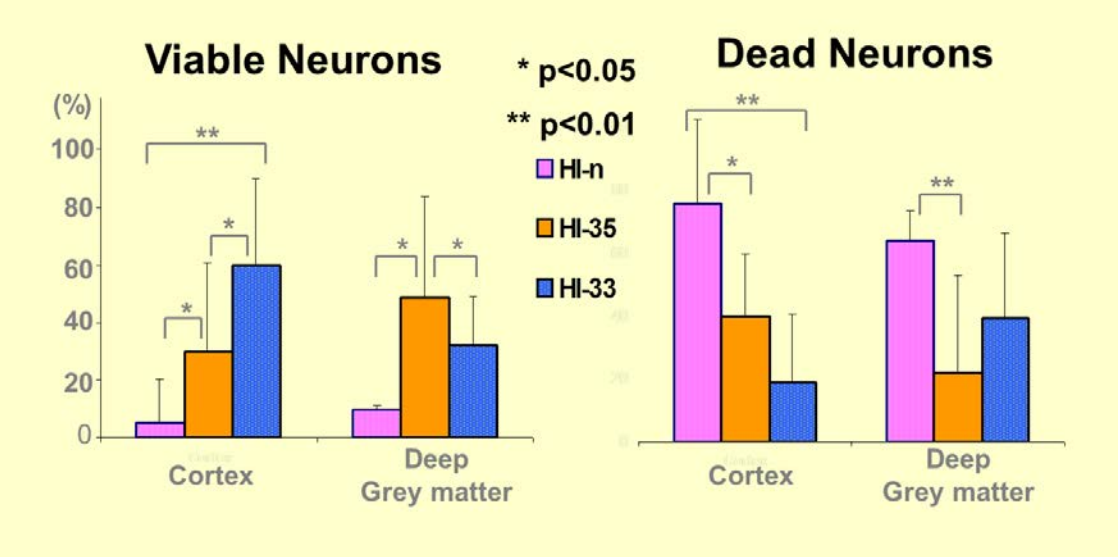

In a piglet model of neonatal asphyxial encephalopathy, whole body cooling to 35°C (HI-35) provided modest tissue protection in both the cerebral cortex and deep grey matter, whereas cooling to 33°C resulted in improved neuroprotection in the cerebral cortex although protection in the deep grey matter was lost. From "Depth of delayed cooling alters neuroprotection pattern after hypoxia-ischemia." by Iwata O, Thornton JS, Sellwood MW, Iwata S, Sakata Y, Noone MA, O'Brien FE, Bainbridge A, De Vita E, Raivich G, Peebles D, Scaravilli F, Cady EB, Ordidge R, Wyatt JS, Robertson NJ. Ann Neurol. 2005 Jul;58(1):75-87.

Chapter 2: Aim and Hypothesis

Aim

To assess temporal and spatial evolution of cerebral injury in the piglet model of asphyxial encephalopathy using serial magnetic resonance biomarkers and histo-pathological assessments

Hypotheses

Regional magnetic resonance biomarkers obtained during the acute phase of perinatal asphyxial encephalopathy predict histo-pathological cerebral injury when the brain is harvested either shortly after or up to 24 hours after the scan.

Specific hypotheses

1. A more severe hypoxic-ischaemic insult leads to a shorter latent phase and more severe secondary energy failure.
2. Variation in energy metabolites is associated with the severity of secondary energy failure even before the overt evolution of secondary energy failure.
3. Evolution of secondary energy failure is spatially heterogeneous when observed using ADC maps.
4. Regional ADC values and global ^{31}P MRS markers have different predictive values of later tissue damage between each other.

Chapter 3: General Materials and Methods

3.1 Preparation of the Piglet model of asphyxial encephalopathy

Experiments were performed under a UK Home Office Licence in accordance with UK guidelines.

3.1.1 Surgical procedures

An established piglet model of neonatal asphyxial encephalopathy was used with modifications in the protocol for each experiment (42, 49). Healthy Large-White piglets of either sex born at term were delivered from a licenced farm in the morning of the experiment within 24 hours of birth. The piglets were initially sedated with intramuscular midazolam (0.2mg/kg). Intensive life support and continuous physiological monitoring were provided throughout experiments, including core body temperature (Arbo N44-91, Kendall, Powell, TN, U.S.A), heart rate, arterial oxygen saturation (5500 Hudson RCI, Temecula, CA, U.S.A.) and the invasive arterial pressure.

Five-percent isoflurane was given to the piglet as the initial concentration through a facial mask during the insertion of the tracheostomy tube. Anaesthesia was maintained by the combination of isoflurane (3% during the surgical procedures and <2% for the rest of the procedures), nitrous oxide, and a continuous infusion of morphine (0.05mg/kg/h). Piglets were mechanically ventilated; ventilator settings were adjusted to maintain normal PaO_2 and $PaCO_2$ levels at 8 - 13 kPa and 4.5 - 6.5 kPa, respectively, allowing for the temperature correction of the arterial blood sample (Fig. 3.1-1).

Figure 3.1-1: Piglet model after surgical procedures

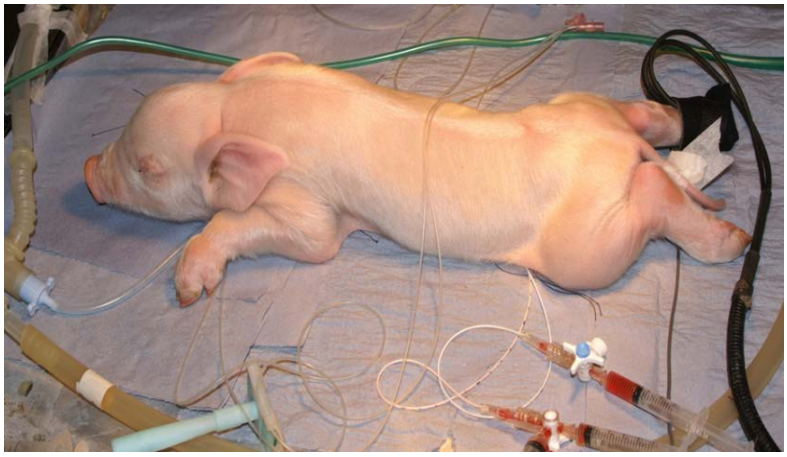

The piglet underwent tracheotomy and was mechanically ventilated under general anaesthesia. Balloon vascular occluders and umbilical arterial/venous catheters were inserted. A pulseoxymeter was attached to the posterior limb of the piglet.

An umbilical venous catheter was inserted for the continuous infusion of maintenance fluids (10% dextrose, 60ml/kg/day), morphine, and intravenous injections of antibiotics (benzylpenicillin 50mg/kg and gentamicin 2.5mg/kg, every 12 hours). An umbilical arterial catheter was also inserted to enable continuous monitoring of the heart rate and arterial blood pressure, and intermittent blood sampling to measure PaO_2, $PaCO_2$, pH, electrolytes, glucose, and lactate. Bolus infusions of colloid (Gelofusin, Braun Medical. Emmenbrucke, Switzerland) and continuous dopamine infusions (5-15µg/kg/minute) were used as required to maintain the mean arterial blood pressure > 40mmHg.

Figure 3.1-2: Piglet positioned within the plastic cylinder pod

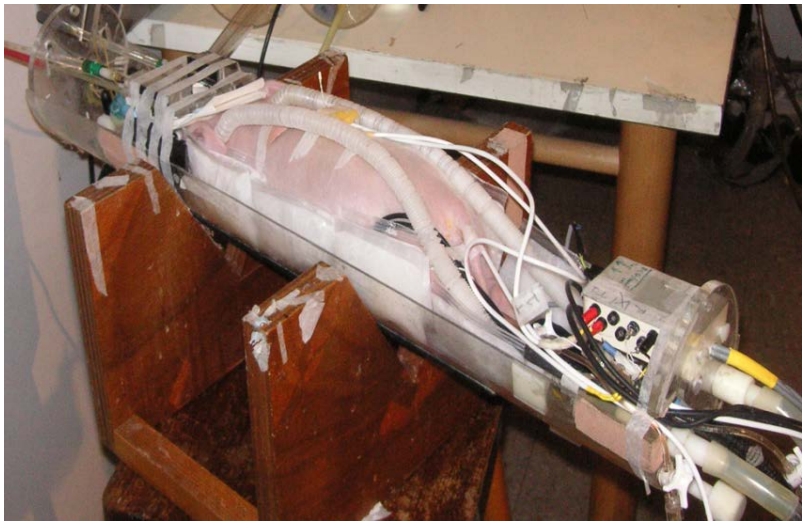

An animal is positioned and immobilised within a plastic pod before insertion into the magnet bore. The piglet is anaesthetised and mechanically ventilated through tubes connected to the right end of the pod.

Both common carotid arteries were surgically isolated at the level of the fourth cervical vertebra and encircled by remotely controlled vascular occluders (OC2A, In Vivo Metric, Healdsburg, CA, U.S.A.). All the surgical procedures were undergone using the aseptic technique, and the incision was closed by sutures. To enable the continuous monitoring of brain metabolism and microstructural changes using the magnetic resonance spectrometer, subjects were sheltered within a specially designed plastic pod following the surgical procedures (Fig. 3.1-2). Within the pod, piglets were positioned prone with the scalp firmly immobilised below the surface coil; the pod was then inserted into the bore of the magnet.

3.1.2 Magnetic resonance biomarkers

All or a part of following magnetic resonance biomarkers were serially obtained before, during and after transient hypoxia-ischaemia approximately every 3 to 5 hours according to the purpose of the study. However, during the insult, only ^{31}P MRS was acquired continuously to closely follow the temporal change in energy metabolites.

3.1.3 ^{31}P MRS

A 7 Tesla Biospec spectrometer (Bruker Medizintechnik, Karlsruhe, Germany) was used for the acquisition of ^{31}P MRS from the whole brain (^{31}P frequency 121.6 MHz) using an elliptical surface coil (6.5 × 5.5 cm) positioned directly on the intact scalp (Fig. 3.1-3). A single-pulse acquire sequence was used with the repetition time (TR): 10 s, quadrature data points: 2048, and the spectral width: 14286 Hz. Spectra were thus acquired effectively fully relaxed and, hence, peak-area ratios were directly related to metabolite concentration ratios (54). Generally 192 (baseline), 24 (during hypoxia-ischaemia and resuscitation), or 384 (thereafter) free induction decays were summed during each acquisition, NTP and EPP, where EPP = Pi + PCr + β- + 2γ- NTP.

Figure 3.1-3: Representative ^{31}P spectra from the piglet brain before hypoxia-ischaemia

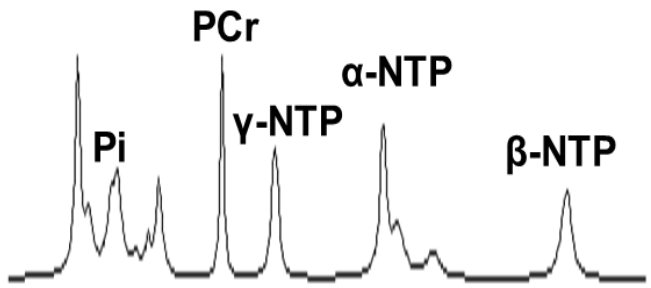

^{31}P MRS spectra acquired from a piglet before hypoxic-ischaemic insult shows peaks of inorganic phosphate (Pi), phosphocreatine (PCr) and three peaks of NTP, which is mainly ATP.

MRS data were analysed using AMARES (107) as implemented in the jMRUI software (108). Prior knowledge of the multiple structures of NTP peaks was used (fitting doublets to α-NTP and γ-NTP and a triplet to β-NTP) but no assumption was made as to their relative sizes. NTP is predominately ATP, comprising approximately 70% of the NTP signal in the rat pup (109). Thus the observed changes in NTP during this experiment predominately reflect changes in ATP. Inorganic phosphate was fitted using

4 separate components. The resonant frequency of the Pi signal is pH dependant (110, 111) and comes from many physically separated brain compartments with different pH. Thus the Pi signal is complex and a single component is not sufficient for analysis. Phosphocreatine was fitted with a single component.

3.1.4 Maps of ADC and FA

The diffusion tensor was measured using single-shot spin-echo diffusion-weighted echo-planar imaging (11 coronal slices, echo time (TE) 76 msec; acquisition bandwidth 200 kHz; slice thickness 2 mm; field of view 4 x 5 cm; image matrix 128 x 128; 10 averages). Diffusion weighting was applied using a Stejskal Tanner gradient scheme. A single image with no diffusion weighting (b = 0 sec mm^{-2}) was acquired along with 6 images with diffusion weighting b = 1155 sec mm^{-2} and diffusion encoding directions uniformly distributed. The diffusion tensor was estimated using analytical expressions (112), and from this, ADC and FA maps were calculated for each pixel (Fig. 3.1-4). To compare regional ADC variations, regions of interest (RoIs) were placed in the cortical and deep grey matter, and peripheral and central white matter, corresponding to the RoIs for the histo-pathological assessment; the actual RoI placement was performed based on maps of ADC and FA using an image processing software (ImageJ, the National Institutes of Health, U.S.A.) (Fig. 3.1-4). ADC values were measured in a coronal plane which dissects the putamen, globus pallidus and thalamus; additional slices were used for the head of the caudate nucleus and hippocampus when necessary.

Figure 3.1-4: Regions of interest on a schema and maps of ADC and FA

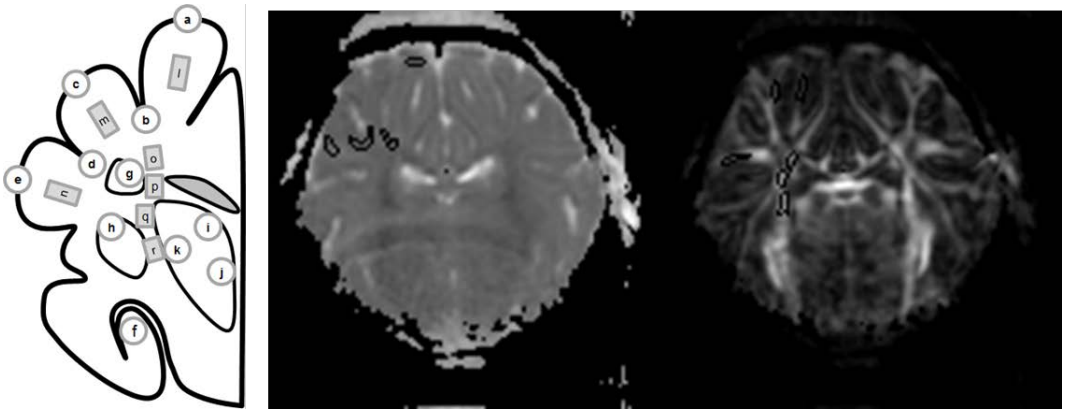

Regions of interest (RoIs) are shown in the cartoon (left) including a, sagittal-top; b, sagittal-bottom; c, parietal-top; d, parietal-bottom; e, temporal-top; f, CA1 region of the hippocampus; g, caudate nucleus, h, putamen; I, anterior thalamus; j, medial thalamus; k, lateral thalamus; l, sagittal white matter, m, parietal white matter; n, temporal white matter; o, superior periventricular white matter; p, periventricular white matter; q, inferior periventricular white matter; and r, posterior limb of the internal capsule. RoIs were placed guided by maps of ADC (middle) and fractional anisotropy (right).

3.1.5 T2 maps

T2 mapping was performed by acquiring two sets of spin-echo echo-planar images with different TEs (TR = 3 s; TE = 66 ms and 110 ms; Bandwidth, 200Hz; 11 coronal sections; 2 mm slice thickness; field of view, 4 x 5 cm; matrix, 128 x 128;10 averages). The T2 relaxation time was calculated using a program developed in a numerical computing software (Matlab, version 6.0, Mathworks, Cambridge, UK) by fitting a decreasing exponential to the signal intensity as a function of TE.

3.1.6 Transient cerebral hypoxia-ischaemia, resuscitation and quantification of acute energy depletion

After the completion of the baseline data acquisition, a transient hypoxic-ischaemic insult was given to the piglet while ^{31}P MRS spectra were acquired every 4 minutes for the real time visual monitoring of the cerebral energy deficit using the β-NTP amplitude. The inspired oxygen fraction (F_iO_2) was reduced to 0.10-0.12 simultaneously with bilateral carotid-artery occluder inflation. When the β-NTP amplitude had decreased to 30% of baseline, this amplitude was maintained for 20 minutes by titrating F_iO_2. After the insult, the animal was resuscitated by deflating the occluder and increasing F_iO_2 to achieve normal oxygen saturation.

Although we aimed to yield similar insult severities between subjects by utilising the feedback from simultaneously obtained ^{31}P MRS spectra, the insult severity and subsequent cerebral damage still differed between subjects, presumably due to technical variations in hypoxia-ischaemia and biological characteristics in the response to the insult. To assess the impact of variations in the insult severity, the cerebral "acute energy depletion" was retrospectively calculated from the difference between the ratio β-NTP/EPP and its baseline, pre-insult level integrated during hypoxia-ischaemia and the first 60 minutes of resuscitation (Fig. 3.1-5) (42).

Figure 3.1-5: Schematic diagram summarising the quantification of the acute insult severity

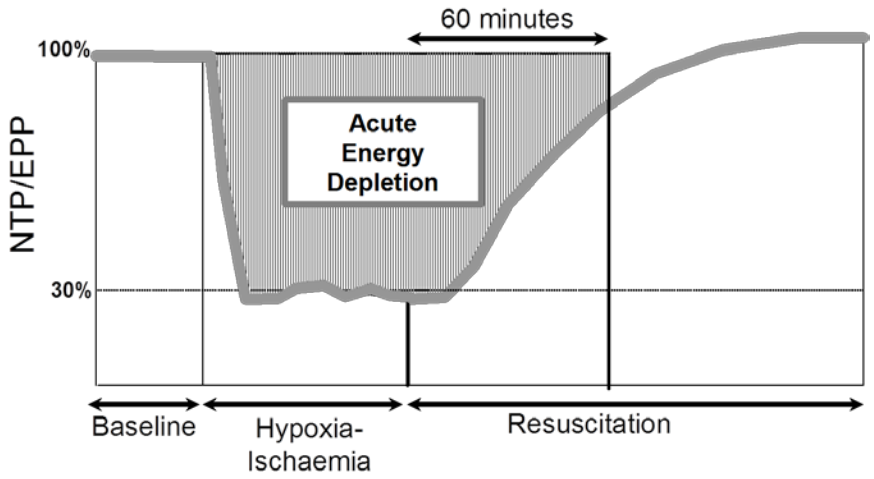

The time integral of the acute energy depletion was calculated during hypoxia-ischaemia and the first 60 minutes of the resuscitation. The energy depletion during the early resuscitation was included because the tissue energy derangement lasts until high-energy phosphates are fully restored by successful resuscitation.

The degree of acute cerebral energy depletion was quantified as the time integral of the fall in β-NTP/EPP relative to mean baseline during transient hypoxia-ischaemia and the first 60 minutes of resuscitation. The early resuscitation period was included on the basis that the degree of cellular injury is related not only to the duration and amount of NTP depletion during transient hypoxia-ischaemia but also to that during resuscitation when energy generation has not yet fully recovered (42).

3.1.7 Temperature control and hypothermia

The rectal temperature of the piglet was continuously monitored throughout the experiment using a thermistor probe (Arbo N44-91, Kendall, Powell, TN, U.S.A.), which was maintained within the normal range (38.5-39.0°C) for piglets using either a heated operating table and an overhead warmer during surgical procedures, or a thin mattress of plastic tubing through which water at a controlled temperature passed was used covering the ventral half of the trunk and the limbs during magnetic resonance studies.

For groups of piglet which underwent delayed therapeutic hypothermia, the mattress temperature was lowered between 2 and 26 hours following the end of hypoxia-ischaemia to induce whole body cooling at the appropriate target rectal temperatures. Animals were then re-warmed slowly at less than 1°C per hour, and the normal core temperature was maintained until the end of the experiment.

3.1.8 Monitoring and treatment of seizure

Continuous monitoring of electroencephalogram was not available for the current study due to technical reasons. Possible seizure activities were suspected if there was a sudden change in the heart rate, arterial blood pressure, SaO_2, breathing pattern and the motion artefact on the magnetic resonance signal. The isoflurane concentration was transiently increased to 2-3% and mechanical causes such as tube obstruction were excluded. If all other possible causes of physiological instability were excluded, the event was recorded as a seizure. An injection of phenobarbital (20mg/kg) was given intravenously, which was followed by additional doses (10mg/kg) up to twice when the initial dose was ineffective or when seizures were recurrent.

3.1.9 Quantification of latent phase and secondary energy failure

The latent-phase was defined as the period between NTP/EPP ascending to within its 99% confidence interval of the baseline value during metabolic recovery after hypoxia-ischaemia and it later falling below again indicating the start of overt secondary energy failure (47). Secondary-energy-failure severity was quantified in each piglet as the minimum NTP/EPP during the period 6 to 48 hours post hypoxia-ischaemia determined by fitting a cubic polynomial to the time-series data in order to avoid systematic bias to lower NTP/EPP due to random error, confirming secondary energy failure when NTP/EPP had fallen to less than 60% of baseline. For the study series which used variable study durations, the severity of secondary energy failure was

defined based on the minimum NRP/EPP during 8 to 24 hours after hypoxia-ischaemia (see section 3.3.5.4 in page 67 for detail).

3.1.10 Histopathology

After the completion of the planned data acquisition and incubation time, animals were humanely sacrificed under terminal anaesthesia by an overdose of pentobarbital injection. Each brain was fixed by perfusion through the heart with 4% cold paraformaldehyde in phosphate saline buffer, dissected out, post-fixed for further 24 hours within 2% paraformaldehyde, cut in 5mm thick coronal slices, and prepared for embedding in paraffin wax. Sections (6μm thick) were stained routinely with haematoxylin and eosin (H & E), Luxol-fast blue-cresyl violet (LFB/Nissl), and immuno-histochemistry using antibodies to glial fibrillary acidic protein (GFAP, 1: 500, Dako Cytomation, Glostrup, Denmark) for the activation of astrocytes, and CD68 (H-255, 1: 200, Santa Cruz Biotechnology, Santa Cruz, CA, U.S.A.) for cells of microglial/macrophage lineage. The terminal deoxynucleotide transferase nick end labelling (TUNEL, Roche Applied Science, Indianapolis, IN) was also used to identify cell death with apoptotic features. Quantitative analyses of the neuronal damage were performed using H & E stained sections from the following regions:

(i) the superior and inferior frontal, superior and inferior parietal, insular, temporal, and parahippocampal cortex and the corresponding white matter
(ii) the CA1-4 regions and the dentate gyrus of the hippocampus
(iii) the putamen, globus pallidus, and anterior, medial, lateral dorsal, and the ventral nuclei of the thalamus
(iv) the periventricular white matter and the posterior limb of the internal capsule
(v) the cerebellar hemisphere

For the analysis, up to four brain sections (generally 1 to 3 sections for regions i, ii, iii and iv; and another section for cerebellum) were carefully chosen to represent afore-mentioned regions. In the neo-cortical regions, observations were taken from both top of the gyrus and the bottom of the sulcus, respectively. The brain stem and hypothalamic nuclei were qualitatively but not quantitatively examined as these regions of the brain appeared to be much less affected in our model (113). The detailed cerebral regions assessed within each study are presented in the sections 3.2 and 3.3.

Figure 3.1-6: Region of interest for histo-pathological assessment in the cortical grey matter

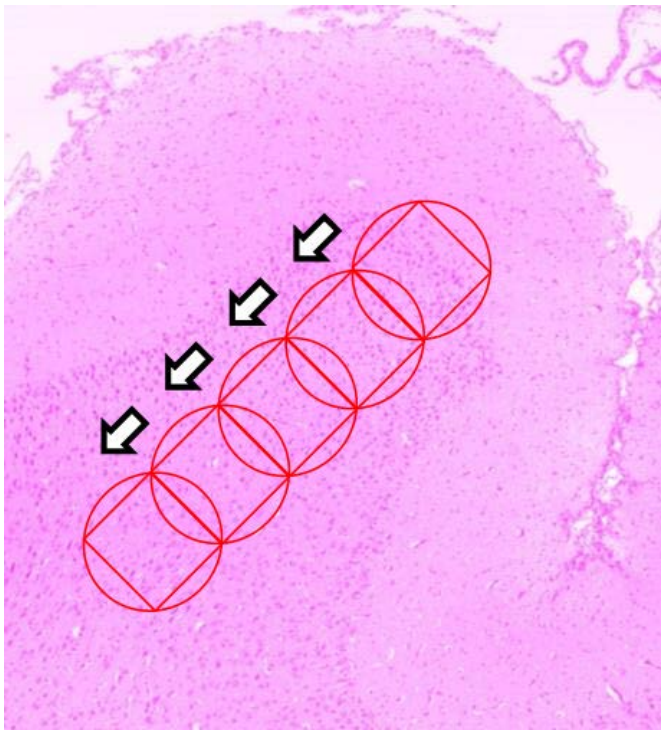

In the neo-cortical grey matter, assessment was performed over multiple views to include all cortical layers except for the molecular layer. Circles are views on the microscope; rectangles are the area where counts for neuronal assessment were performed.

The neuronal changes on H & E stained samples in each region were scored in 6 grades (0-5) of severity according to the morphological changes in staining (nuclear hyperchromasia and cytoplasmic eosinophilia) and shape (cytoplasmic/nuclear shrinkage) as follows: 0 normal, 1 very mild changes in staining, 2 mild neuronal change in staining and shape, 3 moderate neuronal change in staining and shape, 4 acute neuronal death (karyolysis or karyorrhexis), 5 complete neuronal loss (Table 3.1-1). Two experienced investigators examined the brain samples blind to the experimental group. For quantification, at least 250 neurons per region in the neo-cortical grey matter, deep grey matter, and the cerebellar granule cell layers and 100 neurons in the remaining regions were assessed in each animal, using ×200 magnification and paying attention to include each neuronal layer or region equally (typically 2 views for the bottom of sulci and 3 to 5 views for the top of giri; see Fig. 3.1-6). In the cerebellum the neuronal appearance was separately evaluated in Purkinje and granule cells, due to the marked susceptibility of Purkinje cells. For further analysis, neuronal counts which scored 0 or 1, 2 or 3, and 4 or 5 were combined to give percentages of ‘viable’, ‘intermediate’, and ‘dead’ neurons, respectively.

Table 3.1-1: Definition of pathological scoring for neuronal damages

Score	Neuronal Appearance	Neuronal Status
0	no significant changes	Viable
1	mild neuronal change in staining	
2	mild neuronal change in staining and shape	Intermediate
3	moderate neuronal change in staining and shape	
4	acute neuronal death	Dead
5	neuronal death with complete neuronal loss or tissue destruction	

Neuronal changes in staining include nuclear hyper basophilia, condensation of chromatin, and cytoplasmic eosinophilia. Changes in shape include cytoplasmic and nuclear shrinkage and deformation. Percentages of neurons with each score were recorded in each region. For further analysis, scores 0 and 1, 2 and 3, and 4 and 5 were combined to give percentages of 'viable', intermediate, and 'dead' neurons, respectively.

Brain samples stained using LFB/Nissl, immuno-histochemical and TUNEL stains were assessed qualitatively and descriptively for the first study, or "Associations between insult severity and therapeutic time window duration", whereas quantitative or rank-ordinal assessments were performed for the third study, or "Temporal and spatial evolution of secondary energy failure and cerebral injury" (see sections 3.2.3. and 3.4.3. in page 63 and 70 for detail).

3.2 Associations between insult severity and therapeutic time window duration

3.2.1 Subjects and study groups

Forty-two healthy Large-White piglets of either sex born at term (115 (2) days, mean (standard deviation)) weighing 1495 (170) g were studied within 24hours of birth. Baseline data were acquired after stabilization of the animal in the spectrometer. Piglets were then randomised into 5 groups:

(i) sham operation and normothermia (rectal temperature 38.5-39^{o}C; n=10)

(ii) sham operation and transient whole body cooling at rectal temperature 33°C (n=3)

(iii) transient hypoxia-ischaemia and normothermia, (HI-n, n=12)

(iv) transient hypoxia-ischaemia and delayed transient whole body cooling at rectal temperature 35°C (HI-35, n=7)

(v) transient hypoxia-ischaemia and delayed transient whole body cooling at rectal temperature 33°C (HI-33, n=10).

After randomisation, piglets in groups (iii)-(v) were exposed to a hypoxic-ischaemic insult. The groups (ii), (iv) and (v) were cooled to the target rectal temperature between 2 and 26 hours after resuscitation, which was followed by gradual rewarming with the rate of approximately 0.5^{o}C/hour. Experiments were terminated 48 hours after the baseline data acquisition for groups (i) and (ii), or 48 hours after the commencement of resuscitation for groups (iii), (iv) and (v).

3.2.2 Acquisition of magnetic resonance data

The ^{31}P MRS spectra were obtained approximately every 4 hours after the commencement of resuscitation. The final spectra were acquired within 2 hours of termination (Fig. 3.2-1).

Figure 3.2-1: NTP/EPP changes of representative piglets over 48 hours

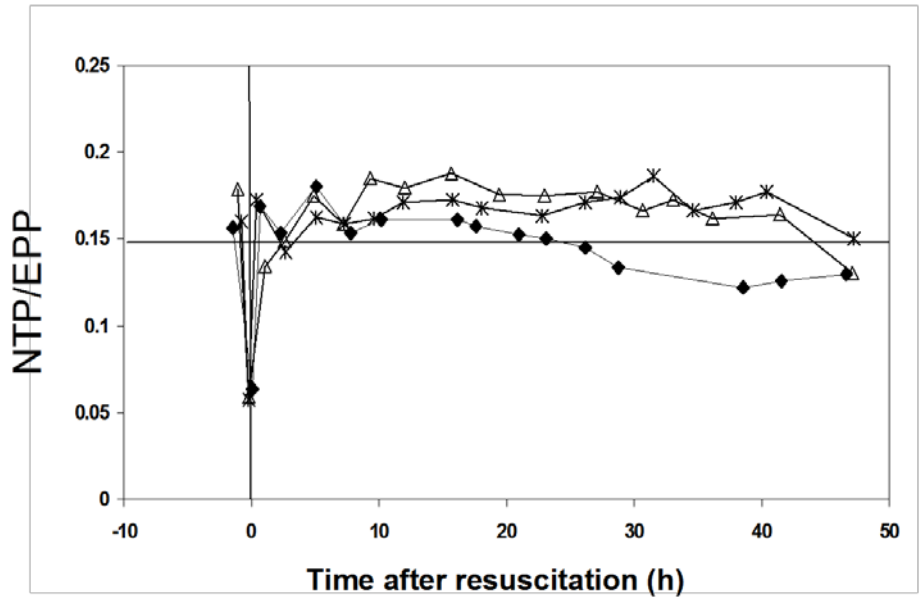

Cerebral NTP/EPP of representative piglets from the HI-n (♦), HI-35 (*) and HI-33 (Δ) groups at baseline, during transient hypoxia-ischaemia, and for 48 h following resuscitation. The vertical line shows the commencement of resuscitation and the horizontal line shows the lower 99% confidence interval of the baseline NTP/EPP.

3.2.3 Histopathology

H & E stained sections were used for the assessment of the neuronal injury. For specific comparison with MRS measures, an observer blind to the experimental piglet group assessed neuronal morphological changes in 10 brain regions in the surface-coil sensitive volume (6 cortical grey matter regions from 3 gyri and 3 sulci in the inferior frontal, superior and inferior parietal cortex, and 4 deep grey matter regions from the putamen and anterior, medial, and lateral dorsal thalamic nuclei) and the average percentages of dead neurons were calculated (Fig. 3.2-2).

Figure 3.2-2: Schematic diagram depicting the histo-pathological regions of interest in a coronal slice of the piglet brain

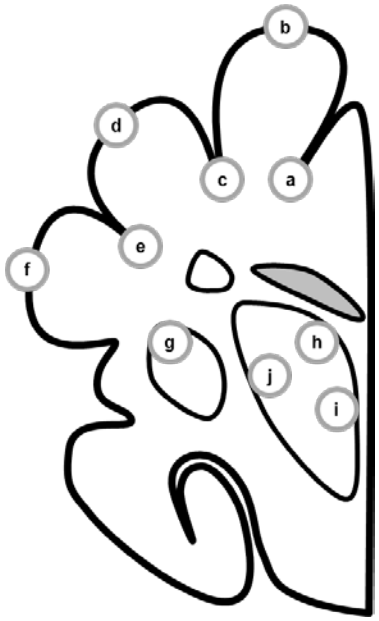

Cartoon depicting regions assessed histo-pathologically, including the inferior frontal (a, b), superior (c, d) and inferior (e, f) parietal cortex, and 4 deep grey-matter from the putamen (g) and anterior (h), medial (i), and lateral dorsal (j) thalamic nuclei.
For this study, unlike our previous studies, temporal cortex, hippocampus and several other regions in the deep brain structure were not considered because of the corresponding brain regions covered by the MRS coil (see Fig. 1.5-3 for detail).

3.2.4 Statistical analysis

Neuroprotective effect of transient whole body cooling to 33°C and 35°C has been reported previously (47, 49). In this current study, we only considered the groups HI-n, HI-35, and HI-33. To examine the dependences of the latent-phase duration, severity of secondary energy failure, and neuronal mortality on acute energy depletion and rectal temperature separately, multivariate analysis (analysis of covariance) and the Bonferroni test were used. In order to avoid the use of independent variables which may co-correlate, relationships between measures after hypoxia-ischaemia (i.e. latent-phase duration, severity of secondary energy failure, and neuronal death) were assessed univariately (analysis of variance) using the combined temperature groups i.e. ignoring the target rectal temperature. Statistical probabilities (p) were presented with corrections for multiple cerebral regions and the target rectal temperatures.

3.3 Energy metabolism during the latent phase and early evolutional period or secondary energy failure

3.3.1 Subjects and procedures

Twenty-three Large-White piglets of either sex (body weight 1640 (220) g, mean (standard deviation)) were surgically prepared within 24 hours after birth under general anaesthesia and received continuous physiological monitoring and intensive life support throughout the experimental procedure as described previously. The animals were then inserted into the bore of the magnet scanner and were subjected to transient hypoxia-ischaemia after the baseline data acquisition. In this study, cooling was not applied and all subjects were kept normothermic throughout the experiment. Three sham-operated piglets were also studied for at least 24 hours without giving the hypoxic-ischaemic insult.

3.3.2 Hypoxic-ischaemic insult

Following baseline ^{31}P MRS acquisition, transient global cerebral hypoxia-ischaemia was induced in 20 piglets by reducing the inspired oxygen fraction (FiO_2) to 12% and simultaneously inflating bilateral carotid artery occluders. During hypoxia-ischaemia,^{31}P spectra were acquired every four minutes. After the β-NTP peak amplitude had fallen to 30% of baseline, FiO_2 was adjusted to maintain this β-NTP level for 0 to 24 minutes to yield a range of insult severities. Resuscitation was then commenced by deflating the occluders and increasing FiO_2.

3.3.3 Acquisition of magnetic resonance biomarkers

During hypoxia-ischaemia and resuscitation, ^{31}P MRS spectra were acquired every 4 minutes. An hour after the commencement of resuscitation, in addition to whole brain ^{31}P MRS spectra, maps of ADC and T2 relaxation time were acquired serially approximately every three to four hours. Because of technical reasons, T2 maps were not available for the first 8 piglets, and both ADC and T2 maps were not obtained in one sham operated animal.

3.3.4 Time course

In order to correlate serially acquired magnetic resonance biomarkers, especially of the ones acquired shortly before termination, with histo-pathological cerebral injury, experiments were terminated at various time points when NTP/EPP had fallen to less than 60% of baseline thus confirming secondary energy failure (n = 11) with the maximum duration of 48 hours after hypoxia-ischaemia. Several subjects were terminated preliminarily because of technical problems or unpredictable clinical consequences (see the Result section for detail).

3.3.5 Statistical analysis

In this study, only ^{31}P MRS data were used (see the next study in the chapter **3.4** for the analyses on ADC and T2 maps).

3.3.5.1 Sham-operated control animals

Because of the small number of control subjects, their MRS measures were presented without statistical analysis.

3.3.5.2 Animals in the study group

Because we applied hypoxia-ischaemia of different durations in this study to yield a range of insult severities, several subjects developed relatively more severe encephalopathy and cardiopulmonary impairments. One experiment was terminated 14 hours after hypoxia-ischaemia because of an extremely short latent phase (in the "severe secondary energy failure" group). The following were excluded from analysis: one animal which experienced extremely severe hypoxia-ischaemia and NTP/EPP remained < 60% of baseline even after 4 hours of hypoxic-ischaemic insult, and 1 animal which developed lethal arrhythmia and required cardiac massage 6 hours after hypoxia-ischaemia.

3.3.5.3 Serial metabolite ratios and rates of metabolic change (over all subjects)

Mixed models with fixed (time and metabolite ratios) and random (subject and time) effects were used to determine the rates of change of NTP/EPP, PCr/EPP and Pi/EPP within the periods (i) first 10 minutes of hypoxia-ischaemia, (ii) rest of hypoxia-ischaemia (excluding first 10 minutes), (iii) 0-2 hours, (iv) 2-8 hours, (v) 8-16 hours and (vi) 16-24

hours after hypoxia-ischaemia. Although we aimed to acquire at least 2 spectra for each of the time intervals (iii) to (vi), in 3, 2, and 4 animals, only a single spectrum was acquired at respectively 2-8, 8-16 and 16-24 hours after the insult. For the mixed model, the missing measurements at 2-8 and 8-16 hours (regarded as "missing completely at random"), but not at 16-24 hours (when the paucity of data resulted from early termination), were estimated by linear interpolation from the existing measurement in that time interval and the next available measurement: the mixed model during 16-24 hours used only the 14 remaining piglets. ^{31}P-MRS measures at baseline and later time intervals were compared using repeated measure analysis of variance: for this analysis, only 17 piglets were included during the period 16-24 hours due to one early termination.

3.3.5.4 Secondary energy failure severity groups

A surrogate for eventual cerebral injury, the severity of secondary energy failure was quantified in each piglet as the minimum NTP/EPP 8-24 hours after hypoxia-ischaemia determined by fitting a cubic polynomial to the NTP/EPP time-series in order to avoid bias to lower NTP/EPP by random error. Using this severity index for secondary energy failure, piglets were classified into 3 groups: (a) "no secondary energy failure" (n = 5, minimum NTP/EPP ≥ 85% of individual baseline), (b) "moderate secondary energy failure" (n = 8, 60% ≤ minimum NTP/EPP < 85%) and (c) "severe secondary energy failure" (n = 5, minimum NTP/EPP < 60%). Metabolite ratios were compared with baseline values in each group and between groups using the analysis of variance.

3.3.5.5 Baseline metabolism, insult severity and PCr recovery (over all subjects)

In our analysis, a positive relationship was observed between PCr/EPP 2 to 8 hours after hypoxia-ischaemia and secondary energy failure severity. To identify possible determinants of this relationship, both simple and multiple linear regression models were used with the index of acute energy depletion (insult severity) and/or baseline ^{31}P-MRS measures as independent variables. Due to the variation in the head size of the piglet, we anticipated inconsistent ^{31}P MRS coverage of the brain; if cerebral metabolite ratios varied regionally, this might result in dependences of baseline metabolite ratios on body weight: this possibility was investigated using a simple linear regression model.

3.3.5.6 Statistical probability correction

Statistical results from comparisons in high energy phosphates between groups defined by the severity of secondary energy failure were corrected for multiple comparisons between different time intervals and between different groups using Bonferroni test.

3.4 Temporal and spatial evolution of secondary energy failure and cerebral injury

3.4.1 Subjects and procedures

The same subjects and magnetic resonance data with the second study “Energy metabolism during the latent phase and early evolutional period or secondary energy failure” were used (see the chapter **3.3** for detail).

3.4.2 Magnetic resonance data processing

RoIs on the maps of ADC were placed guided by both maps of ADC and fractional anisotropy using the ImageJ software (see Figure 3.1-5 for the representative maps with RoIs). In the cortical grey matter, three gyri (sagittal, parietal and temporal) and two sulci (sagittal and parietal) were chosen as well as the hippocampus (CA1). The caudate nucleus, putamen, thalami (anterior, medial and lateral) were also assessed. For the white matter, three regions of the peripheral white matter (sagittal, parietal and temporal lobes) and four regions of central white matter (superior and medial periventricular white matter and posterior limb of the internal capsule) were investigated. These RoIs were transferred to T2 maps after inspections for motion artefacts and accuracy of positions for RoIs.

Figure 3.4-1: Brain regions of interest for histo-pathological assessment

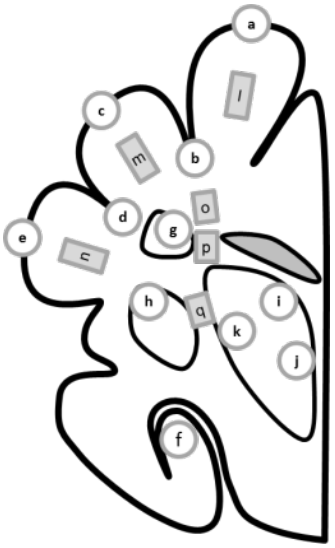

Diagram depicting the regions placed on the ADC and T2 maps, and histo-pathological samples. a sagittal-top, b sagittal-bottom, c parietal-top, d parietal-bottom, e temporal-top, f CA1 region of the hippocampus, g caudate nucleus, h putamen, i anterior thalamus, j medial thalamus, k lateral thalamus, l sagittal white matter, m parietal white matter, n temporal white matter, o superior periventricular white matter, p periventricular white matter, and q posterior limb of the internal capsule. See Figure 3.1-5 for the representative maps of ADC and fractional anisotropy with RoIs.

3.4.3 Histo-pathological assessment

Paraffinised coronal brain samples were carefully assessed and the ones closest to the MRI slices used for quantitative analysis were chosen. Six μm thick coronal brain sections were prepared for stains such as H & E, LFB/Nissl, GFAP, CD68, TUNEL and β-APP. RoIs on ADC and T2 maps were then transferred to the brain sections on the slide glass by marking the corresponding region using a fibre tipped pen (Fig. 3.4-1). Neuronal damage was assessed for each RoI using H & E stained samples based on the scale indicated in the Table 3.1-1, page 61, which gave percentages of neuronal death. The damage in the white matter was assessed using H & E and LFB/Nissl stains, which were classified into four grades of 0 to 3 (Table 3.4-1). On GFAP stained samples, the activation of astrocytes within the cortical grey matter and white matter was assessed respectively, and scores of 0 to 3 were assigned for each region. CD68 positive microglia and vessels were counted respectively, and the numbers per a view at the x400 magnification were recorded. Similarly, TUNEL positive cells with fragmentation of nuclei were counted to give the number of apoptotic cell death per a view at the x400 magnification. For the assessment of grey matter regions, each neuronal layer or region was equally examined by typically including 2 to 5 views for the cerebral cortex and 1 to 3 regions for the deep grey matter; Fig. 3.1-6, page 60), whereas 1 to 2 representative views were assessed for the white matter regions.

Table 3.4-1: Injury scales for histo-pathological assessment in the white matter

Stains	Scores			
	0	1	2	3
H & E and LFB/Nissl*	No damage	Focal injury without destruction in axonal integration	Up to moderate destruction with substantial disintegration in axon and myelin	Severe destruction with total loss of structural integration
GFAP	Mild expression in the process and plasma membrane of astrocytes	Moderate expression	Strong expression	Marked expression
β-APP*	No positive fibres	Solitary/scattered positive fibres	Grouped positive fibres with mild to moderate density	Profound fibres with strong stains

***Evaluation on LFB/Nissl and β -APP stains focused on axonal injury. Evaluation of neuronal injury on H & E, CD68 expressions on microglia and vessels, and TUNEL positive cells with morphological features of apoptosis were performed numerically by counting affected cells.**

3.4.4 Statistical analysis

3.4.4.1 Sham-operated control animals

Because of the small number of control subjects, findings in magnetic resonance biomarkers were presented without statistical analysis.

3.4.4.2 Animals in the study group

Magnetic resonance biomarkers were sorted along the time line either (i) prospectively starting from the pre-insult baseline, 60 minutes to <3 hours, 3 to < 6 hours, 6 to < 12 hours, 12 to < 18 hours, 18 to < 24 hours, 24 to < 30 hours, 30 to < 36 hours, 36 to < 42 hours and 42 to 48 hours after the commencement of resuscitation, or (ii) retrospectively starting from 0 to < 3 hours, 3 to < 6 hours, 6 to < 12 hours,12 to < 18 hours,18 to < 24 hours, 24 to < 30 hours, 30 to < 36 hours,36 to < 42 hours, and 42 to 48 hours before termination. When there were multiple data within the same time period, the average of these were used; missing values were estimated by linear interpolation from existing measurements only when there were valid data in both the previous (excluding the baseline) and the following time intervals.

To investigate the variation in ADC and T2 maps within region groups of the cortical grey matter (excluding the hippocampus), deep grey matter, peripheral white matter, and the central white matter, and also between these region groups (mean values within groups were used), the baseline and serial data were assessed using the analysis of variance. Because experiments were terminated at different time intervals after hypoxia-ischaemia (and hence before termination), the number of subjects considered at each time interval differed; to minimise the influence of the sample size to the statistical result, analysis was performed on magnetic resonance biomarkers obtained (i) equal to or less than 24 hours after hypoxia-ischaemia and (ii) equal to or shorter than 24 hours before termination. Associations between global (^{31}P MRS) and regional (ADC and T2 maps) magnetic resonance biomarkers obtained at each time interval after hypoxia-ischaemia and regional histo-pathological damages were assessed using general linear models for either numeric or rank ordinal data with adjustment for the insult severity (acute energy depletion) and the experimental duration. The predictive value of magnetic resonance biomarkers analysed according to (i) the time after resuscitation and (ii) the time before termination were assessed using either the Pearson product moment correlation coefficient or the Spearman rank correlation coefficient.

3.4.4.3 Statistical probability correction

P-values from comparisons in magnetic resonance biomarkers between different time intervals (vs. baseline) were corrected for multiple comparisons using the Dunnett test. Results from comparisons in ADC and T2 relaxation time within and between region groups at each time interval after resuscitation were corrected using the Bonferroni test. For comparisons between magnetic resonance biomarkers and regional histo-pathological brain injury, which involved six magnetic resonance biomarkers and eight histo-pathological assessments in over seventeen cerebral regions, p-values were shown without correction to avoid type-II errors.

Chapter 4: Results

Values are shown as mean (standard deviation) unless stated otherwise.

4.1 Associations between insult severity and therapeutic time window duration

Results from comparisons between temperature groups in the severity of secondary energy failure and histo-pathological outcome have been reported elsewhere (47, 49). Briefly, therapeutic hypothermia to 35^{o}C and 33^{o}C prolonged the latent phase duration (Fig. 1.6-1 in page 47), ameliorated the severity of secondary energy failure (Fig. 4.1-1), and reduced the neuronal death in both cortical grey and deep grey matter (47); the pattern of cerebral protection differed between 35^{o}C and 33^{o}C, with the former protecting the deep grey matter predominantly while the latter preserving the cortical grey matter better (Figure 1.6-2 in page 50) (49).

Figure 4.1-1: Cerebral high-energy phosphates before, during and after hypoxia-ischaemia

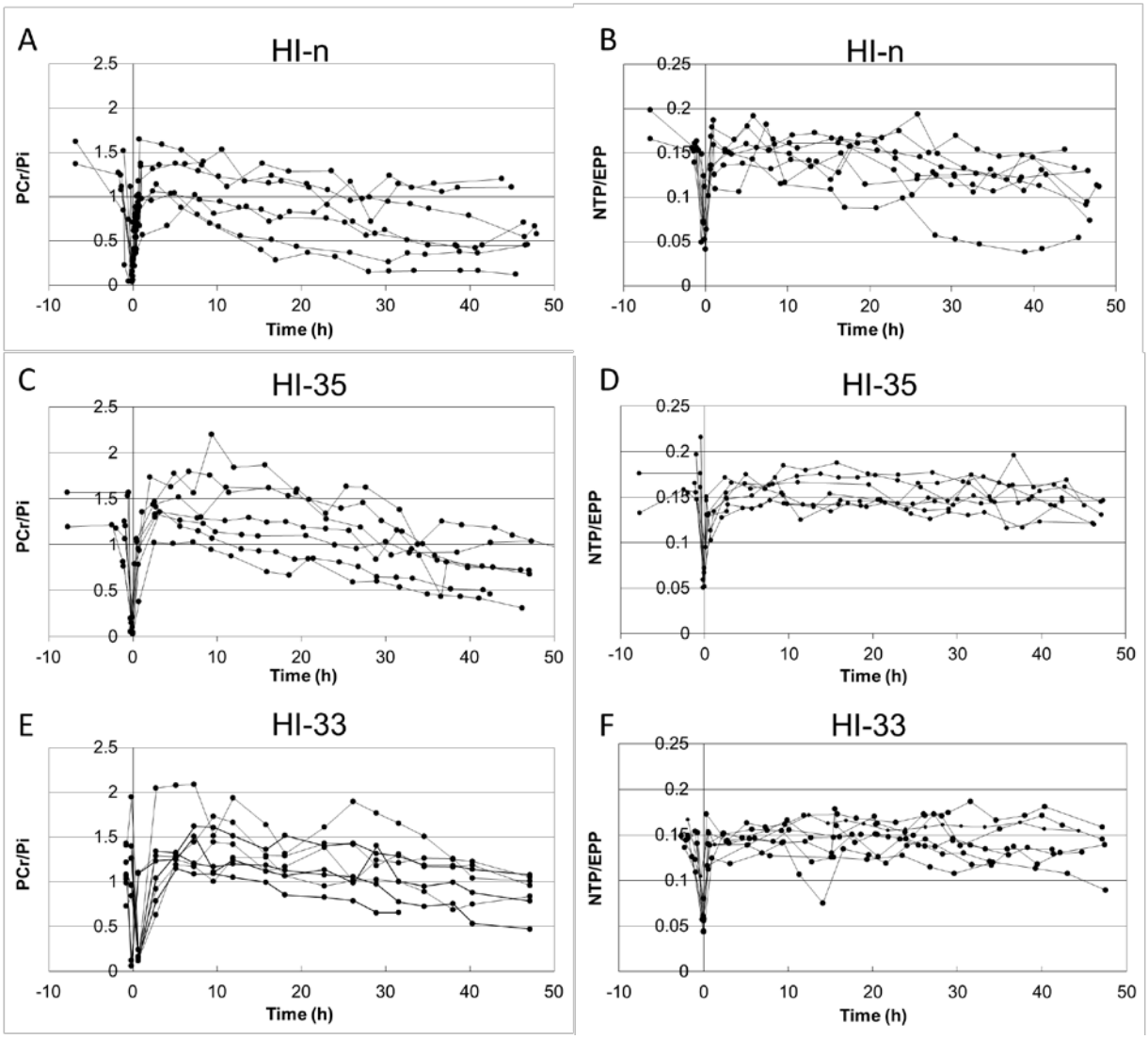

Cerebral PCr/Pi (A, C, and E) and NTP/EPP (B, D, and F) for each piglet at baseline, during transient HI, and for 48 hours after resuscitation in the HI-n (A and B), HI-35 (C and D), and HI-33 (E and F) groups. In 1 HI-33 piglet, no data were acquired beyond 36 hours because of spectrometer failure. Graphs demonstrate significant intrinsic biological variability despite similar HI insult severities. PCr/Pi tended to be preserved in cooled piglets. A significant decline in NTP/EPP was only seen in the HI-n group. Abbreviations: HI, hypoxia-ischaemia. HI-n, HI and normothermia. HI-35, HI and delayed whole body cooling to 33°C. HI-33, HI and delayed whole body cooling to 35°C. From "Delayed whole-body cooling to 33 or 35°C and the development of impaired energy generation consequential to transient cerebral hypoxia-ischemia in the newborn piglet" by O'Brien FE, Iwata O, Thornton JS, De Vita E, Sellwood MW, Iwata S, Sakata YS, Charman S, Ordidge R, Cady EB, Wyatt JS, Robertson NJ. Pediatrics. 2006 May;117(5)1549-59.

4.1.1 Summary

In this chapter, results of the first part of the study, “Associations between insult severity and therapeutic time window duration” are presented. A more severe hypoxic-ischaemic insult was associated with a shorter latent-phase ($p = 0.002$), worse secondary energy failure ($p = 0.023$), and more neuronal death in the cortical grey matter ($p = 0.016$). The latent phase duration was inversely related to insult severity, suggesting the brevity of the therapeutic time window following severe cerebral hypoxia-ischaemia.

4.1.2 Experimental courses and general findings

In seven animals, experimentation terminated early: 2 due to NTP depletion persisting more than 2 hours after hypoxia-ischaemia (1 HI-n and 1 HI-33); 2 due to equipment problems (2 HI-n); and 3 piglets died as a direct consequence of hypoxia-ischaemia (2 HI-n at 18 and 28 hours and 1 HI-33 at 20 hours after the insult). All other piglets survived to 48 hours after hypoxia-ischaemia. Two brains were damaged during removal or histological processing (1 HI-n and 1 HI-33). Results from all these animals were not included in the analysis. Consequently the numbers of piglets analysed were: 6 HI-n; 7 HI-35; and 7 HI-33; in one HI-33 piglet MRS data were only available up to 36 hours due to spectrometer failure. There were no significant differences in the body weight, age, heart rate, blood pressure, or other variables between study groups before hypoxia-ischaemia.

4.1.3 Severity of hypoxia-ischaemia, duration of latent phase and subsequent injury indices in each temperature group

We aimed for hypoxic-ischaemic insults of similar severity between subjects. However, amongst the piglets, acute energy depletion ranged widely due to variations in the biological responses to both transient hypoxia-ischaemia and resuscitation. The mean acute energy depletion was 0.048 (0.021) hours for HI-n; 0.070 (0.024) hours for HI-35; and 0.086 (0.032) hours for HI-33 but statistically invariant ($p = 0.116$). When the magnetic resonance biomarkers were compared between temperature groups with the acute energy depletion as a covariate, HI-35 had a longer latent-phase ($p < 0.001$), less severe secondary energy failure ($p = 0.032$), and less neuronal death (cortical grey matter $p = 0.001$, deep grey matter $p = 0.020$); and HI-33 had a longer latent phase ($p = 0.014$), less severe secondary energy failure, and less neuronal death only in cortical grey matter ($p < 0.001$), compared to HI-n (Table 4.1-1). There was less neuronal death

in the cortical grey matter in HI-33 compared to HI-35 (p = 0.022), however, the duration of the latent phase, severity of secondary energy failure, and the neuronal death in the deep grey matter were similar in both cooled groups.

Table 4.1-1: Magnetic resonance and histo-pathological injury indices in each temperature group

		HI-n	HI-35	HI-33
Latent phase duration in hours		17.5 (10.0, 24.9)	41.4 (35.1, 47.7)***	34.3 (27.5, 41.1)*
Minimum NTP/EPP (6 – 48 hours)		0.106 (0.090, 0.122)	0.136 (0.122, 0.150)*	0.135 (0.120, 0.151)
Neuronal death (%)	Cortical grey matter	85.7 (69.6, 101.8)	39.6 (26.1, 53.1)**	10.8 (-3.8, 25.4)***†
	Deep grey matter	66.5 (44.4, 89.6)	22.1 (2.8, 41.5)*	37.4 (16.4, 58.3)

Values are mean (upper and lower 95% confidence interval) corrected for the mean acute energy depletion = 0.069 hours.

***, ** and ***: HI-n vs. HI-35 or HI-33, p < 0.05, 0.005 and 0.001 respectively;**

†: HI-35 vs. HI-33, p < 0.05; p values were corrected for multiple comparisons using Bonferroni test.

4.1.4 Association between the insult severity and the latent phase duration

A more severe hypoxic-ischaemic insult (greater acute energy depletion) was associated with a shorter latent phase (Fig. 4.1-2) (r^2 = 0.55, p = 0.002, corrected for temperature groups).

Figure 4.1-2: Correlation between the latent phase duration and the insult severity

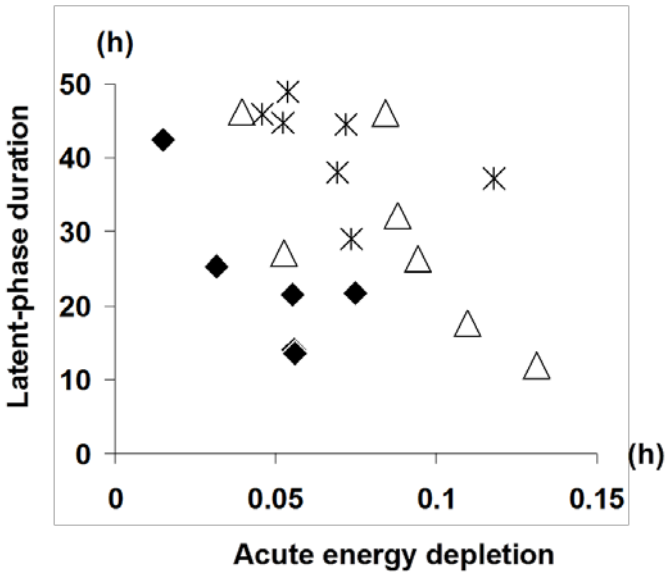

Acute insult severity represented by the acute energy depletion index was inversely correlated with the duration of the latent phase. Symbols: HI-n (♦), HI-35 (*), HI-33 (Δ). r^2 = 0.55, p = 0.002, analysis of covariance. Regression line not indicated because the analysis was performed with correction for temperature groups.

4.1.5 Association between the insult severity and the severity of secondary energy failure

The severity of secondary energy failure represented by lower NTP/EPP was correlated with the insult severity (Fig. 4.1-3) (r^2 = 0.44, p = 0.023, corrected for temperature groups).

Figure 4.1-3: Association between the severity of acute insult and secondary energy failure

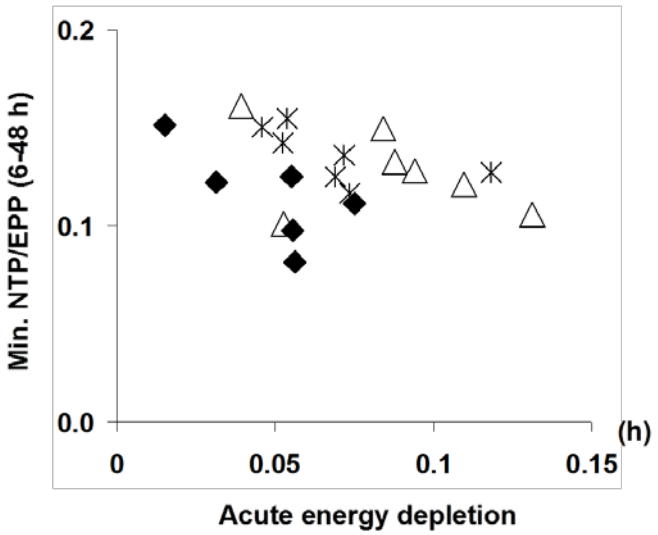

Severity of secondary energy failure was dependent on the severity of acute insult represented by the acute energy depletion. Symbols: HI-n (♦), HI-35 (*), HI-33 (Δ). r^2 = 0.44, p = 0.023, analysis of covariance. Regression line not indicated because the analysis was performed with correction for temperature groups.

4.1.6 Association between the insult severity and neuronal death

Neuronal death in the cortical grey matter, but not in the deep grey matter, depended on the insult severity (Fig. 4.1-4) ($r^2 = 0.75$, $p = 0.016$, corrected for temperature groups).

Figure 4.1-4: Correlation between the insult severity and neuronal death in the cortical grey matter

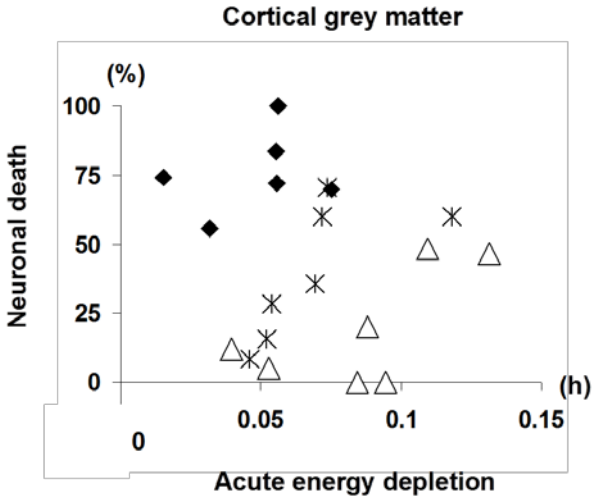

Histo-pathologically assessed neuronal death in the cortical grey matter was dependent on the acute insult severity. Symbols: HI-n (♦), HI-35 (*), HI-33 (Δ). $r^2 = 0.75$, $p = 0.016$, analysis of covariance. Regression line not indicated because the analysis was performed with correction for temperature groups.

4.1.7 Association between the latent phase duration and the severity of secondary energy failure

A longer latent phase duration was associated with a less severe secondary energy failure (Fig. 4.1-5) ($r^2 = 0.78$, $p < 0.001$).

Figure 4.1-5: Correlation between the latent phase duration and the severity of secondary energy failure

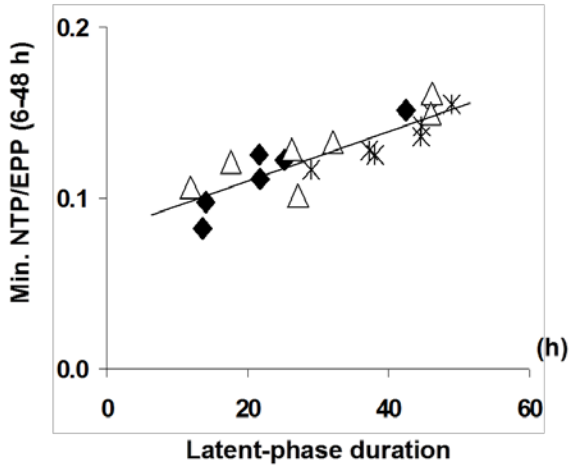

The latent phase duration was linearly correlated with the severity of secondary energy failure.
Symbols: HI-n (♦), HI-35 (*), HI-33 (Δ). $r^2 = 0.78$, $p < 0.001$.Regression line is from combined temperature groups.

4.1.8 Association between the latent phase duration and neuronal death

A longer latent phase was associated with fewer neuronal death in the cortical grey matter ($r^2 = 0.26$, $p = 0.023$) and deep grey matter ($r^2 = 0.43$, $p = 0.002$) (Fig. 4.1-6).

Figure 4.1-6: Dependences of neuronal death on the latent phase duration

(A) Cortical grey matter

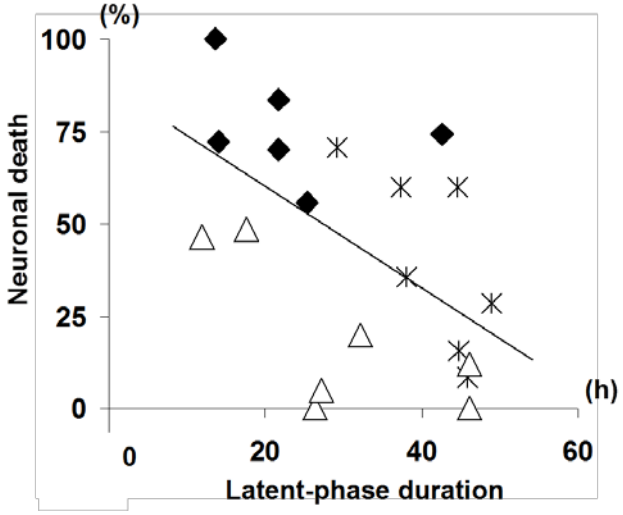

The latent phase duration was linearly correlated with the neuronal death in the cortical grey matter. Symbols: HI-n (♦), HI-35 (*), HI-33 (Δ). r^2 = 0.26, p=0.023. Regression line is from combined temperature groups.

(B) Deep grey matter

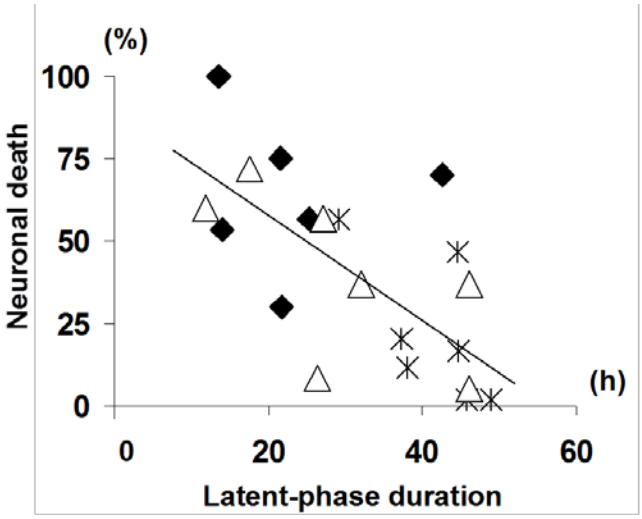

The latent phase duration was linearly correlated with the neuronal death in the deep grey matter. Symbols: HI-n (♦), HI-35 (*), HI-33 (Δ). r^2 = 0.43, p = 0.002. Regression line is from combined temperature groups.

4.1.9 Association between the severity of secondary energy failure and neuronal death

More severe secondary energy failure was associated with greater neuronal death in both cortical grey matter (r^2 = 0.27, p = 0.020) and deep grey matter (r^2 = 0.36, p = 0.005) (Fig. 4.1-7).

Figure 4.1-7: Dependence of neuronal death on the severity of secondary energy failure

(A) Cortical grey matter

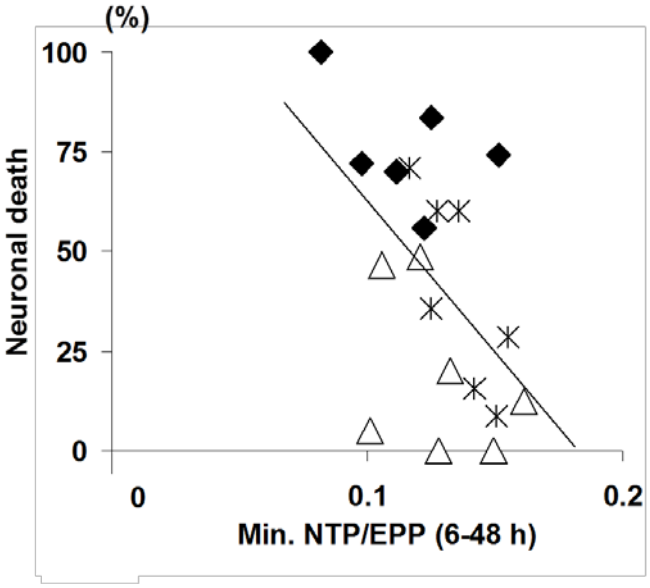

The severity of secondary energy failure was linearly correlated with neuronal death in the cortical grey matter. Symbols: HI-n (♦), HI-35 (*), HI-33 (Δ). r^2=0.27, p=0.020.Regression line is from combined temperature groups.

(B) Deep grey matter

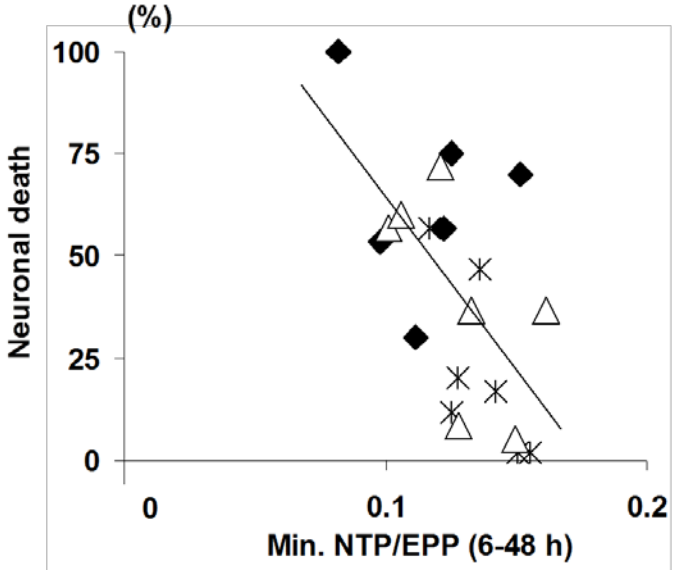

The severity of secondary energy failure was linearly correlated with neuronal death in the deep grey matter. Symbols: HI-n (♦), HI-35 (*), HI-33 (Δ). r^2 = 0.36, p = 0.005, corrected for temperature groups. Regressions are from combined temperature groups.

4.2 Energy metabolism during the latent phase and early evolutional period or secondary energy failure

4.2.1 Summary

In this chapter, results of the second part of this study are presented. Following resuscitation, in subjects with favourable outcome, PCr recovered to higher than its baseline level (overshoot). In subjects with unfavourable outcome, maximum PCr recovery was lower than baseline and lower than in subjects with favourable and intermediate outcomes. Recovery PCr correlated linearly and negatively with acute insult severity, suggesting that recovery metabolism 2 to 8 hours after hypoxia-ischaemia may provide an early biomarker of injury severity.

4.2.2 Temporal changes in energy metabolites after hypoxia-ischaemia

4.2.2.1 Sham-operated animals

Sham operated animals showed no apparent temporal change in NTP/EPP, PCr/EPP and Pi/EPP (Table 4.2-1).

Table 4.2-1: Temporal changes in ^{31}P MRS biomarkers in sham operated animals

		Baseline	Time from baseline (h)			
	Piglet		0-2	2-8	8-16	16-24
NTP/EPP	1	0.26	0.25	0.23	0.25	0.23
	2	0.21	0.21	0.21	0.20	0.20
	3	0.20	0.20	0.20	0.21	0.19
PCr/EPP	1	0.18	0.18	0.18	0.18	0.17
	2	0.22	0.21	0.21	0.22	0.22
	3	0.23	0.23	0.23	0.24	0.24
Pi/EPP	1	0.13	0.14	0.17	0.17	0.19
	2	0.18	0.20	0.22	0.20	0.19
	3	0.17	0.17	0.17	0.17	0.20

4.2.2.2 Acute insult, recovery and secondary energy failure

Significant rates of change of NTP/EPP (falling) and Pi/EPP (increasing) were observed during both the first 10 minutes ($p = 0.006$ and $p < 0.005$ respectively) and the remainder of hypoxia-ischaemia ($p < 0.005$ and $p = 0.006$ respectively); falling PCr/EPP was observed only during the first 10 minutes of hypoxia-ischaemia (Table 3.2-2 and Fig. 4.2-1) ($p < 0.005$). Compared with baseline, mean PCr/EPP was lower during both the first 10 minutes and the remainder of hypoxia-ischaemia, whereas mean Pi/EPP was higher and mean NTP/EPP lower only during the later period of hypoxia-ischaemia (all $p < 0.001$).

Table 4.2-2: Rates of change in metabolite ratios during and following hypoxia-ischaemia

			During hypoxia-ischaemia		Time after hypoxia-ischaemia (h)			
			First 10 minutes	Remainder	0-2	2-8	8-16	16-24
NTP/EPP	Slope	(x 10^{-3}/h)	-174.8	-153.5	52.4	1.6	-2.7	-3.2
	SE	(x 10^{-3}/h)	47.6	31.5	7.7	1.17	1.01	1.11
	p		0.006	<0.005	<0.005	NS	NS	0.042
PCr/EPP	Slope	(x 10^{-3}/h)	-670.0	-15.3	136.9	-0.6	-4.2	-4.7
	SE	(x 10^{-3}/h)	115.3	40.2	17.0	0.9	1.2	0.9
	p		<0.005	NS	<0.005	NS	0.006	<0.005
Pi/EPP	Slope	(x 10^{-3}/h)	1118.4	520.3	-323.2	-3.9	15.6	12.3
	SE	(x 10^{-3}/h)	255.1	116.9	36.5	2.3	2.8	3.1
	p		<0.005	0.006	<0.005	NS	<0.005	0.006

Abbreviations: SE, standard error. NS, not significant.

Figure 4.2-1: Trajectories of NTP, PCr and Pi over time relative to EPP

(A) PCr/EPP

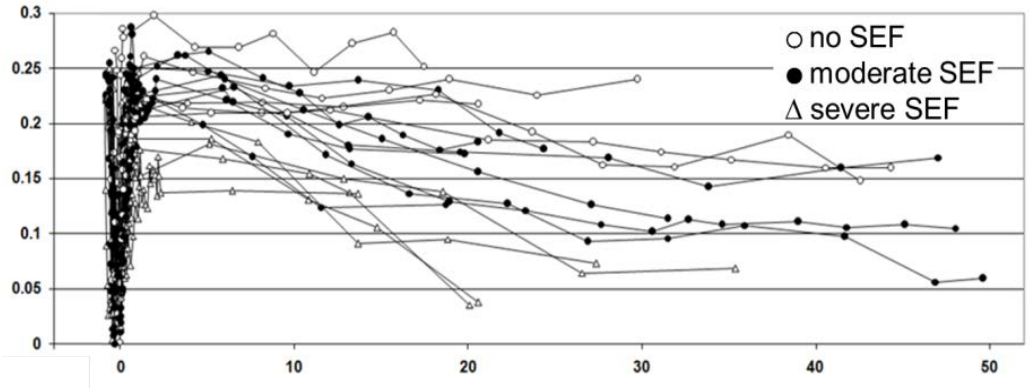

(B) NTP/EPP

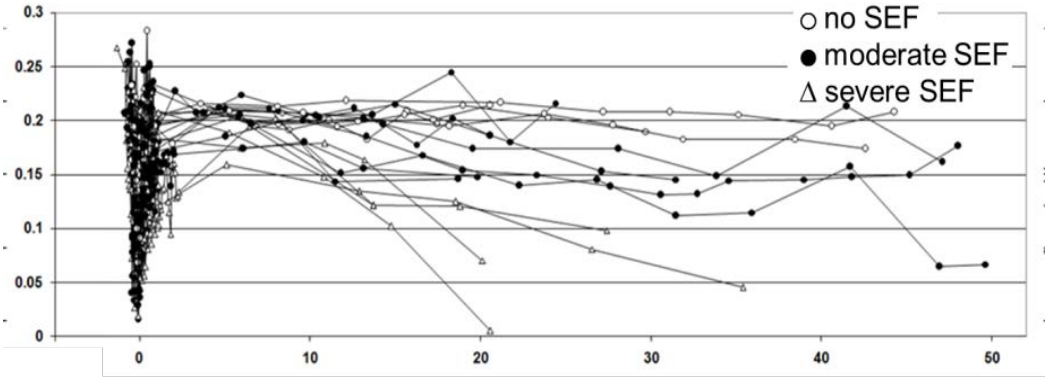

(C) Pi/EPP

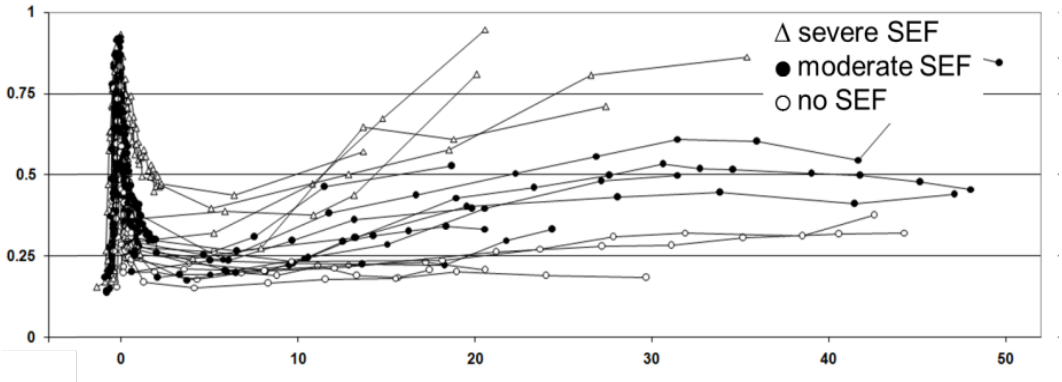

Data are shown for only representative time points during and shortly after hypoxia-ischaemia. Variation in the recovery phosphates is evident despite overall incomplete recovery in NTP and Pi and complete recovery in PCr. X-axes are the time interval in hours after hypoxia-ischaemia.

After commencing resuscitation, significant rates of change of PCr/EPP and NTP/EPP (both increasing) and Pi/EPP (falling) were observed during the period 0-2 hours after hypoxia-ischaemia (all $p < 0.005$). Metabolite ratios had recovered closest to their baseline values during the period 2-8 hours after hypoxia-ischaemia when mean PCr/EPP was similar to baseline but mean NTP/EPP was slightly smaller ($p = 0.012$) and mean Pi/EPP greater (Table 4.2-3) ($p = 0.027$). The earliest time interval displaying overt secondary energy failure was 8-16 hours after hypoxia-ischaemia when there were significant rates of change for PCr/EPP (falling, $p = 0.006$) and Pi/EPP (rising, $p < 0.005$): a significant NTP/EPP rate of change during secondary energy failure (falling, $p = 0.042$) was first seen at 16-24 hours. During 8-16 hours and 16-24 hours after hypoxia-ischaemia, mean PCr/EPP and NTP/EPP were lower and mean Pi/EPP higher compared with the baseline (all $p < 0.001$).

Table 4.2-3: Metabolite ratios before, during and after hypoxia-ischaemia

		Baseline	During hypoxia-ischaemia		Time after hypoxia-ischaemia (h)			
			First 10minutes	Remainder	0-2	2-8	8-16	16-24
NTP/EPP	Mean	0.22	0.21	0.12	0.17	0.19	0.18	0.16
	Standard deviation	0.02	0.02	0.04	0.03	0.02	0.03	0.05
	p:vs. baseline		NS	<0.001	<0.001	0.012	<0.001	<0.001
PCr/EPP	Mean	0.23	0.18	0.064	0.18	0.22	0.19	0.16
	Standard deviation	0.02	0.04	0.029	0.04	0.03	0.04	0.06
	p:vs. baseline		<0.001	<0.001	<0.001	NS	<0.001	<0.001
Pi/EPP	Mean	0.19	0.26	0.65	0.40	0.27	0.33	0.43
	Standard deviation	0.03	0.07	0.13	0.12	0.09	0.13	0.21
	p:vs. baseline		NS	<0.001	<0.001	0.027	<0.001	<0.001

NS, not significant.

4.2.3 Energy metabolism at 2-8 hours after hypoxia-ischaemia and the severity of secondary energy failure

Compared with baseline, recovery PCr/EPP 2-8 hours after hypoxia-ischaemia was higher (overshoot) for subjects with "no" secondary energy failure and was lower for subjects with "severe" secondary energy failure (Figs. 4.2-2 and 4.2-3) ($p = 0.043$ and 0.008 respectively). In the same time interval, Pi/EPP was higher for subjects with both "moderate" and "severe" secondary energy failure compared to baseline ($p = 0.006$ and 0.013 respectively), however, NTP/EPP was similar to baseline in each group.

Figure 4.2-2: Metabolite ratios 2-8 hours after hypoxia-ischaemia relative to individual baselines

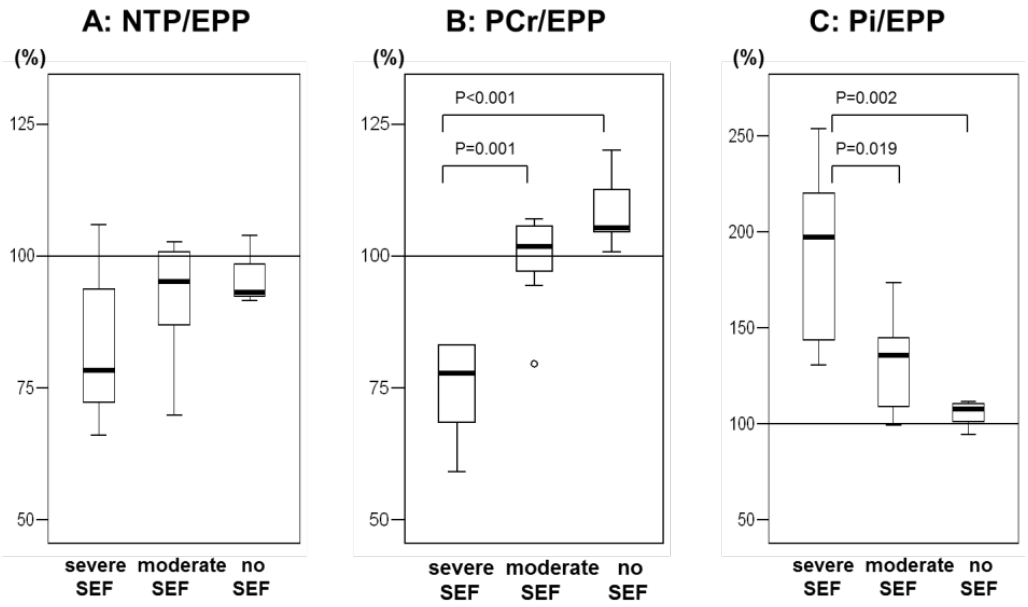

PCr/EPP in subjects which never developed secondary energy failure showed overshoot compared to the baseline level. Metabolite ratios differed between three outcome groups for PCr/EPP and Pi/EPP but the trend did not reach statistical significance for NTP/EPP. Symbols: box - first and third quartiles, bold line - median, perpendicular line - range without outliers, open circle - extreme outlier less than 1.5 times the interquartile range from the first quartile.

Figure 4.2-3: Representative ^{31}P MRS spectra from three outcome groups

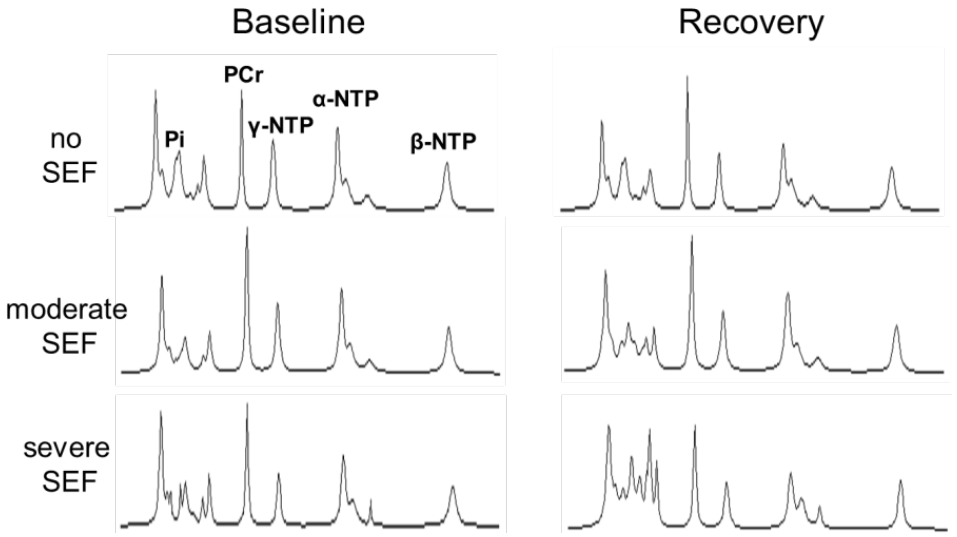

Subtle PCr recovery overshoot relative to NTP peaks is notable in subjects which did not develop secondary energy failure (SEF).

Subjects with "no" or “moderate" secondary energy failure had higher PCr/EPP ($p < 0.001$ and $p = 0.001$ respectively) and lower Pi/EPP ($p = 0.002$ and 0.019 respectively) compared with subjects with “severe" secondary energy failure; NTP/EPP showed no intergroup differences (Fig. 4.2-4).

Figure 4.2-4: PCr/EPP 2-8 hours after hypoxia-ischaemia

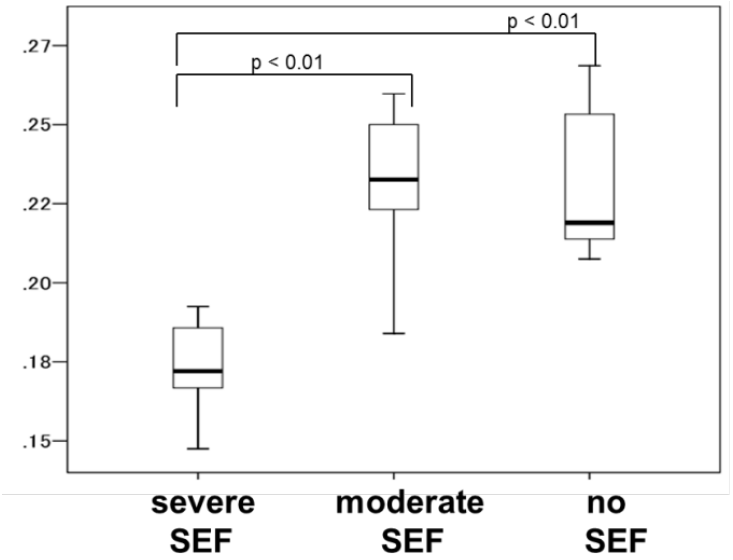

PCr/EPP 2-8 hours after hypoxia-ischaemia for “no secondary energy failure (SEF)”, “moderate SEF”, and “severe SEF”. The groups with no or moderate SEF consistently showed higher PCr/EPP compared with the severe SEF group. Symbols: box - first and third quartiles, bold line - median, perpendicular line - range.

4.2.4 Baseline metabolism, insult severity, and PCr at 2-8 hours after hypoxia-ischaemia

PCr/EPP 2-8 hours after hypoxia-ischaemia correlated linearly with both the acute energy depletion index and baseline PCr/NTP with simple linear regression analysis ($p = 0.024$ and 0.049 respectively): correlation significance was higher with multivariate analysis which incorporated the interaction between the acute energy depletion index and baseline PCr/NTP ($p = 0.008$ and 0.015 respectively). Baseline PCr/NTP was not associated with the body weight (Figs. 4.2-5 and 4.2-6).

Figure 4.2-5: Baseline and early ^{31}P MRS biomarkers and PCr recovery

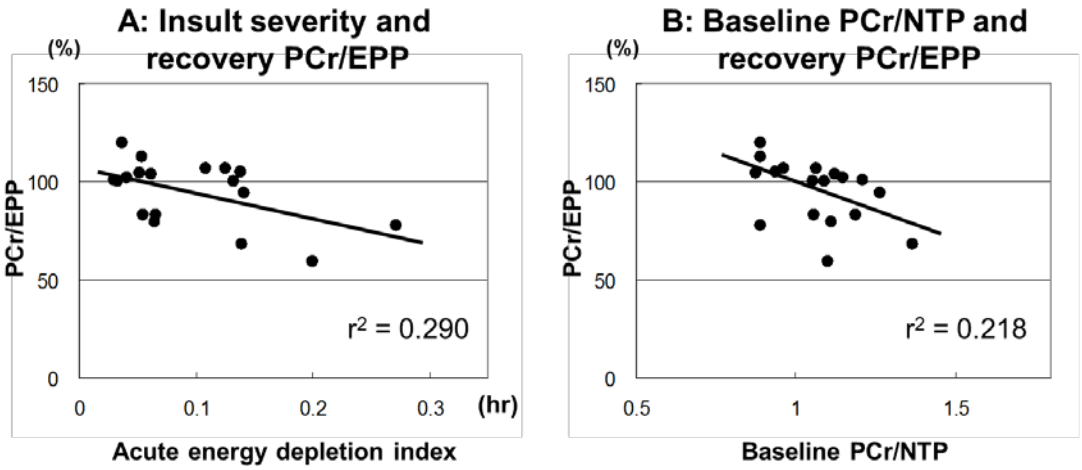

PCr/EPP 2 to 8 hours after hypoxia-ischaemia and (A) the acute energy depletion index (insult severity) and (B) baseline PCr/NTP, both demonstrating significant linear relationships.

Figure 4.2-6: Baseline metabolism and recovery PCr/EPP

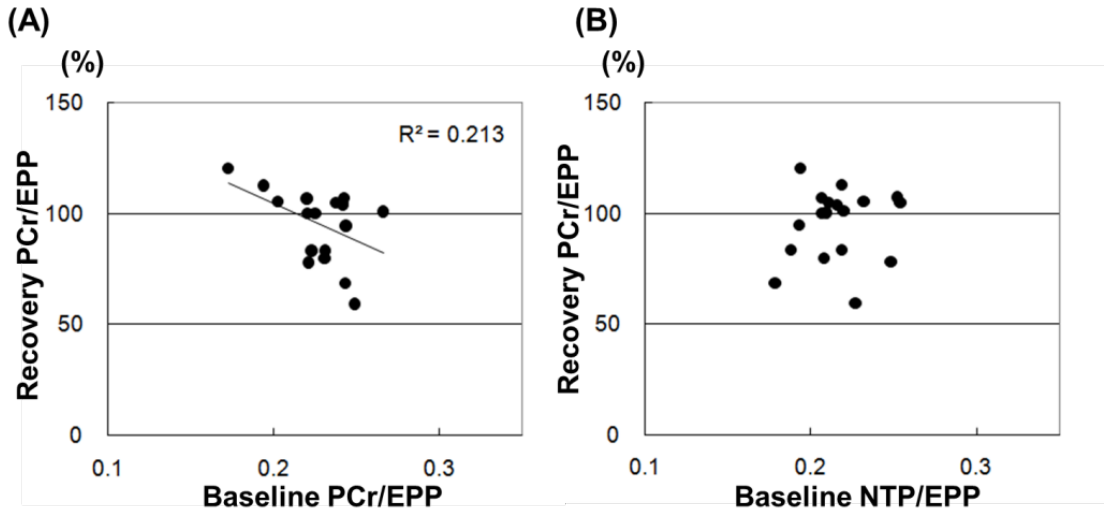

Baseline PCr/EPP (A, $p < 0.05$) but not NTP/EPP (B) showed linear correlation with recovery PCr/EPP 2 to 8 hours after hypoxia-ischaemia.

4.3 Temporal and spatial evolution of secondary energy failure and cerebral injury

4.3.1 Summary

In this chapter, results of the third part of this study are presented. When regional maps of ADC were analysed, substantial reductions in ADC values were present in susceptible regions, such as parietal watershed cortex, peripheral white matter and deep grey matter, as early as 6 hours, correlating with subsequent histo-pathological brain injury. Although global PCr/Pi was the most accurate early biomarker for histo-pathological brain injury, ADC values also predicted l cerebral injury up to 18 hours in advance of termination, which would be useful to optimise neuroprotective treatments when ^{31}P MRS biomarkers are not available.

4.3.2 Sham-operated control subjects

For sham-operated control subjects, no significant temporal changes were observed in ^{31}P MRS biomarkers and maps of ADC and T2 (see Chapter **4.2.2.1** and Table **4.2-1** for temporal changes in ^{31}P MRS biomarkers).

4.3.3 Temporal changes in magnetic resonance biomarkers up to 24 hours after resuscitation

4.3.3.1 ^{31}P MRS biomarkers

^{31}P MRS metabolites at the baseline were similar to those of sham control subjects. Compared to the baseline, lower NTP/EPP and PCr/Pi, and higher Pi/EPP were observed between 1 and 24 hours after the commencement of resuscitation, whereas the reduction in PCr/EPP was noted between 6 and 24 hours after resuscitation, reflecting the gradual decline in PCr/Pi and PCr/EPP and increase in Pi/EPP with time (Fig. 4.3-1 and Supplemental Table 1 in page 157).

Figure 4.3-1: Temporal changes in global ^{31}P MRS biomarkers

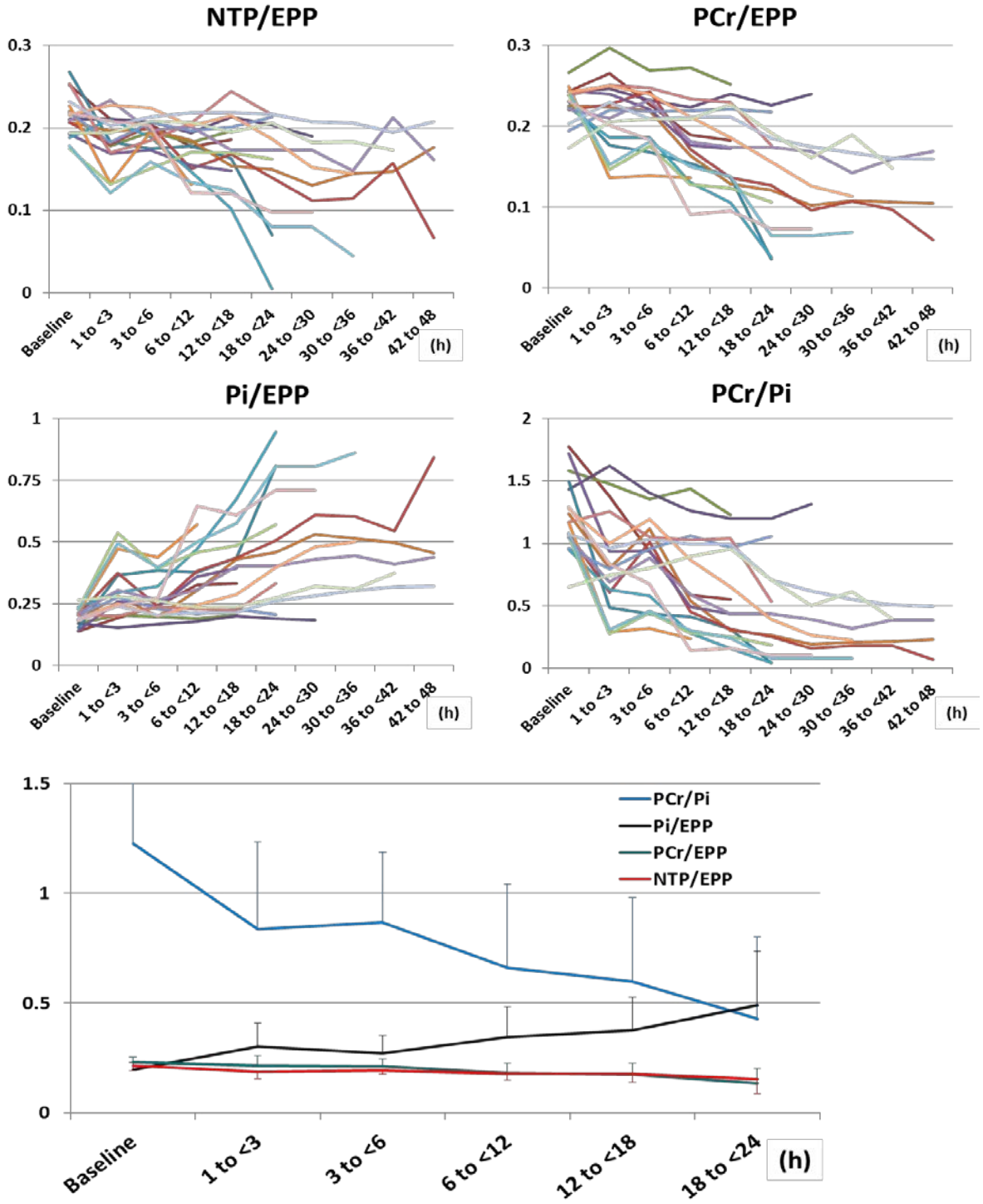

Upper panel: Trajectories of NTP/EPP, PCr/EPP, Pi/EPP and PCr/Pi at baseline and after resuscitation showing the rapid and dynamic change in PCr/Pi, followed by PCr/EPP and Pi/EPP, and then, by NTP/EPP. Lower panel: Temporal change in the mean (standard deviation) ^{31}P MRS markers up to 24 hours after resuscitation. Data after 24 hours are not shown because of the smaller number of subjects thereafter.

4.3.3.2 Maps of ADC

Reductions in regional ADC values were already apparent during the period of 1 to < 3 hours after the commencement of resuscitation in all cortical grey matter regions, putamen, sagittal white matter, parietal white matter, and posterior limb of internal capsule, reflecting a rapid decline in regional ADC values following hypoxia-ischaemia (Fig. 4.3-2 and 4.3-3; Supplemental Table 2 in page 158). Significant reductions in ADC for the lateral thalamus, temporal white matter, superior periventricular white matter, and periventricular white matter were first noted during the period of 6 to12 hours of resuscitation. A decline in ADC was also observed in the anterior and medial thalami, which did not lead to statistical significance until 12 to 18 hours after resuscitation due to wide inter-subject variations.

Figure 4.3-2: Two distinct patterns of ADC changes with time following hypoxia-ischaemia

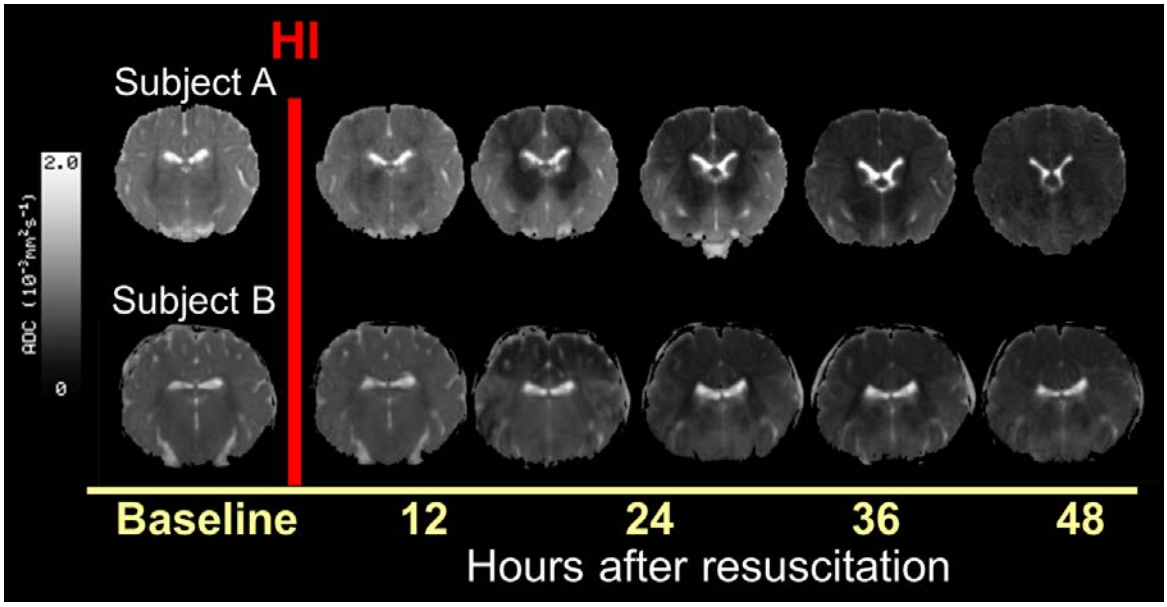

In subject A (upper panel), ADC reduction was initially observed in the striatum spreading to the parasagittal cortex/white matter. In subject B (lower panel), initial ADC reduction was prominent in the sagittal and parasagittal cortex/white matter. Despite the difference in the progress of brain injury, both subjects showed profound ADC changes to 30-50% of the baseline level throughout the brain by the time of termination.

Abbreviation: HI, hypoxia-ischaemia.

At baseline, ADC values were similar between regions within the cortical grey matter; in the deep grey matter, the lateral thalamus had lower ADC values compared to other regions of the caudate nucleus, putamen and medial thalamus, whereas the medial thalamus showed lower ADC levels compared to the caudate nucleus and lateral thalamus; in the peripheral white matter, ADC was lower in the sagittal and temporal regions compared to the parietal region; in the central white matter, the posterior limb of the internal capsule had higher ADC values compared to the superior periventricular white matter and periventricular white matter. When mean baseline ADC values for the region groups of the cortical grey matter, hippocampus, deep grey matter, peripheral white matter and the central white matter were compared, the central white matter had higher ADC values compared to the cortical grey matter, hippocampus and the peripheral white matter, whereas the cortical grey matter and hippocampus had higher ADC values than the deep grey matter. During the period of 1 to 6 hours after hypoxia-ischaemia and the commencement of resuscitation, ADC levels in the sagittal cortex was lower than in the temporal cortex, however, no other difference in ADC values within the region groups was observed up to 24 hours after resuscitation. The mean ADC values for each region group observed at the baseline disappeared after hypoxia-ischaemia and resuscitation.

Figure 4.3-3: Temporal changes of ADC in representative regions

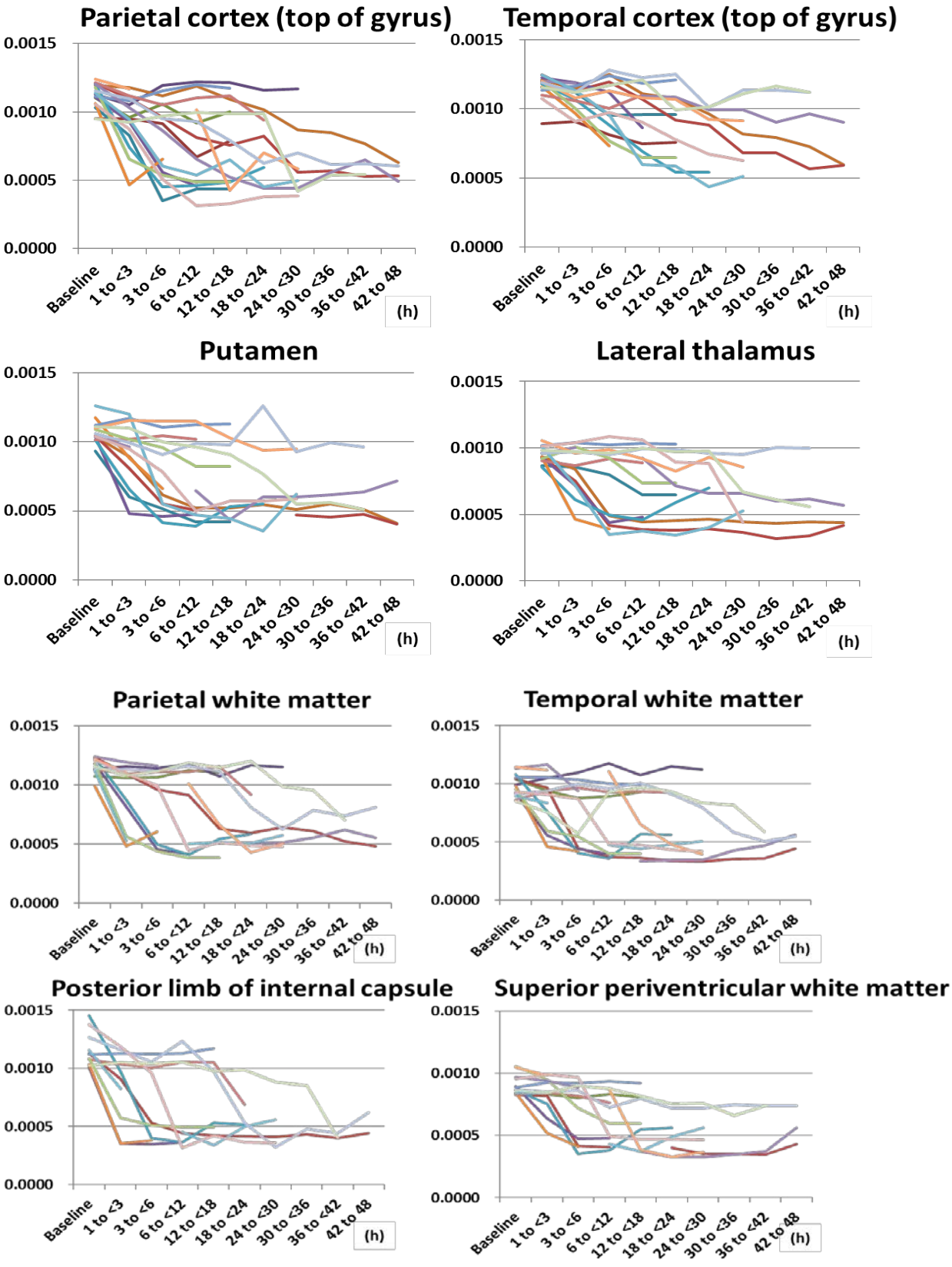

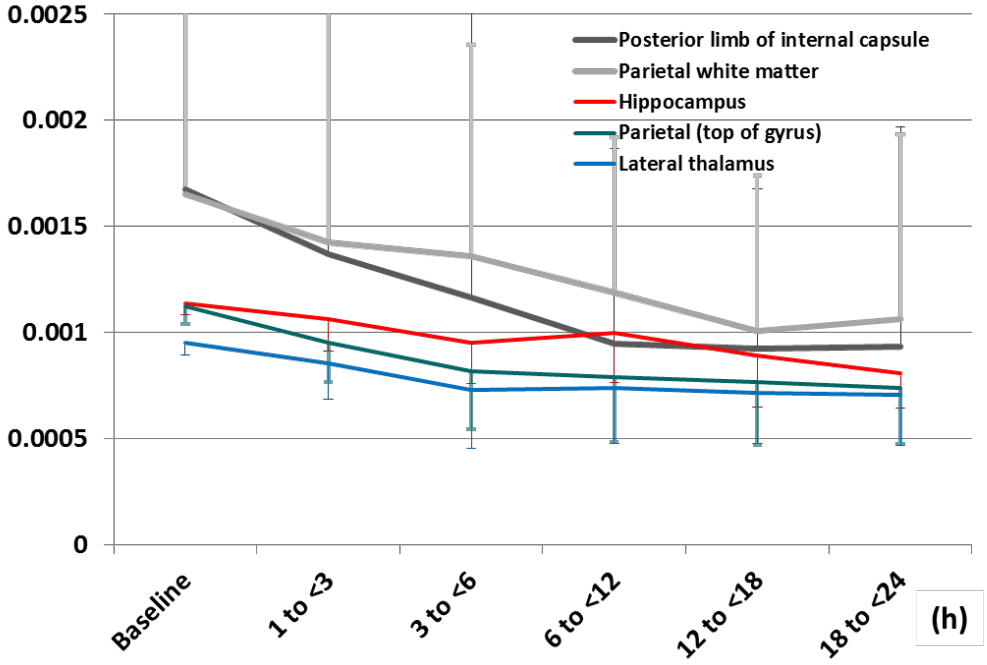

Left panel: Trajectories showing inter-regional variation in the timing of ADC decline from all subjects with valid ADC data. Rapid decrease in ADC was observed in the parietal cortex and white matter, putamen, and the posterior limb of the internal capsule whereas the change was slow in the temporal grey and white matters and the superior periventricular white matter. Right panel: Temporal change in the mean (standard deviation) ADC values up to 24 hours after resuscitation in representative regions. Data after 24 hours are not shown because of the smaller number of subjects thereafter.

4.3.3.3 T2 maps

The T2 relaxation time showed overall trends to increase after resuscitation, however, statistically significant increase relative to the baseline value was noted in limited regions of the cortical grey matter (mainly in the bottom of the sulci), hippocampus, lateral thalamus and the parietal white matter (Fig. 4.3-4 and Supplemental Table 3 in page 162).

Figure 4.3-4: Temporal changes of T2 maps

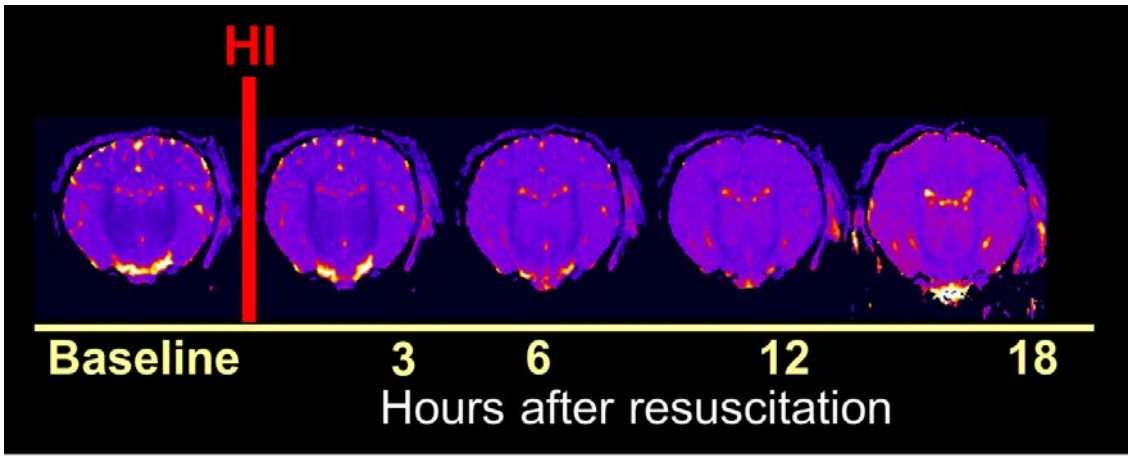

Spatial and temporal change in T2 relaxation time following most severe HI, showing progressive increase in T2 involving the whole brain. Short T2 and prolonged T2 are shown in dark purple and lighter purple, respectively, whereas extremely long T2 from cerebrospinal fluid is shown in red and yellow.
Abbreviation: HI, hypoxia-ischaemia.

At baseline, the T2 relaxation time was similar within the region groups of the cortical grey matter and the deep grey matter; in the peripheral white matter, the T2 relaxation time was shorter in the temporal white matter compared to the sagittal and parietal white matter; in the central white matter, the periventricular white matter had the longest T2 relaxation time, which was followed by the superior periventricular white matter and then, by the posterior limb of the internal capsule. When the mean baseline T2 relaxation time was compared between the region groups, the cortical grey matter and the hippocampus both had longer T2 relaxation times compared to the peripheral white matter and the central white matter; the T2 relaxation time was longer for the deep grey matter compared to the central white matter. After resuscitation, despite the overall temporal increase in the T2 relaxation time, the regional pattern of the T2 relaxation time remained unchanged in most regions.

Figure 4.3-5: Temporal changes of T2 relaxation time in representative regions

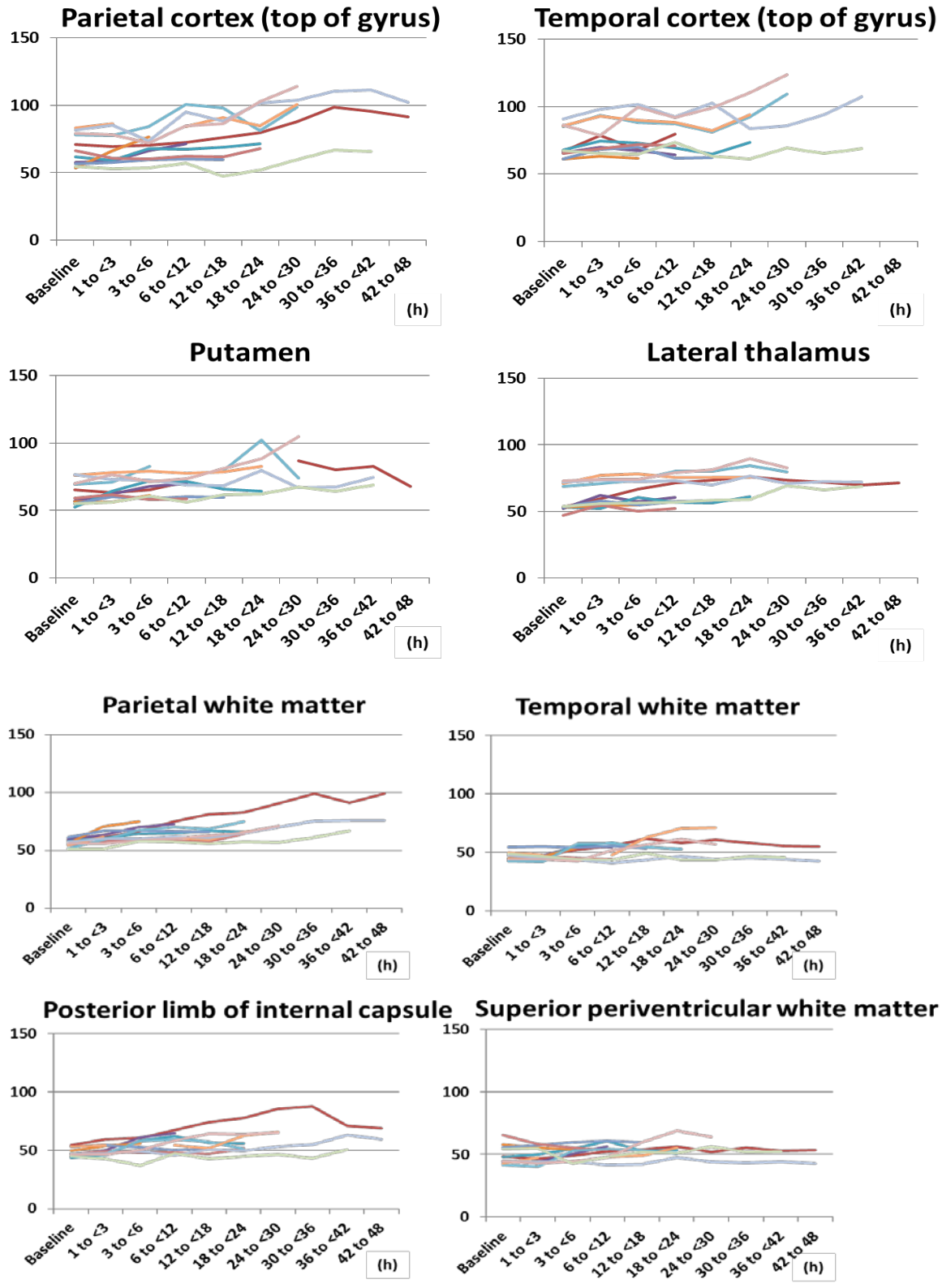

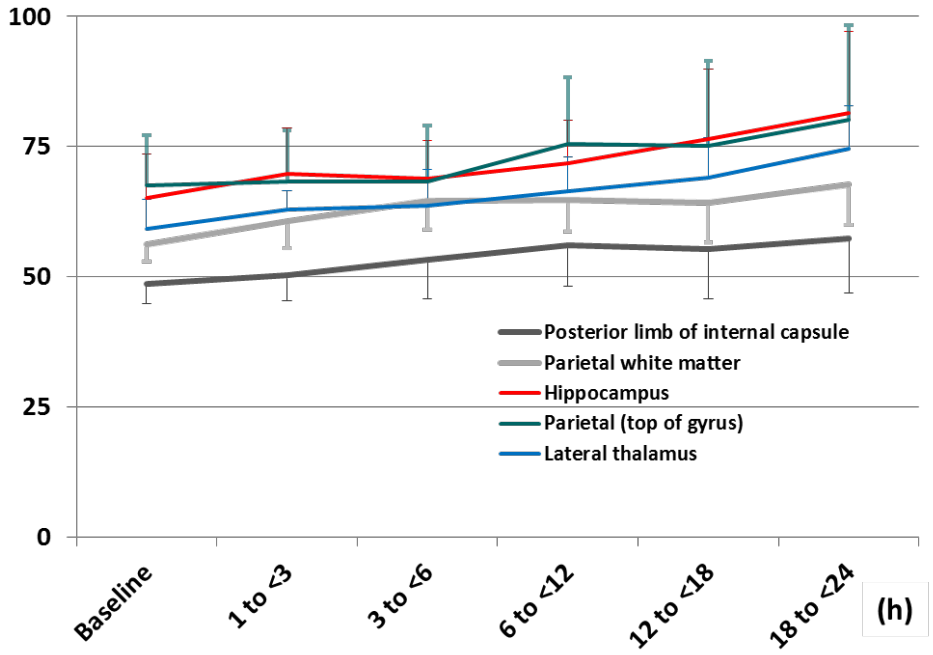

Left panel: Trajectories of regional T2 relaxation time from all subjects with valid T2 data, showing trends towards gradual increase in T2 with time although the dynamic range appears to be smaller compared to ^{31}P MRS markers and ADC. Right panel: Temporal change in the mean (standard deviation) T2 relaxation time up to 24 hours after resuscitation. Data after 24 hours are not shown because of the smaller number of subjects thereafter.

4.3.3.4 Histopathological brain injury

For sham-operated control animals, no significant damage was noted for brain samples stained using H & E stains, LFB/Nissl stain and β-APP immuno-histochemical stain (Figs. 4.3-5 and 4.3-6); a small number of TUNEL-positive neurons were observed in the cerebral cortex and hippocampus with nuclear shrinkage, condensation, or fragmentation suggestive of apoptotic cell death; CD68-positive vessels and microglial cells were occasionally observed in the white matter and cortical/deep grey matter.

A wide range of histo-pathological brain injury and immuno-histochemical reactions were observed for brain samples of subjects which experienced transient hypoxia-ischaemia. The most extensive damage on H & E-stained samples was observed in the watershed zones in the para-sagittal and parietal cortex, and the hippocampus; extension of the damage towards the deep grey matter was highly heterogeneous between subjects. Generally, severe grey matter injury observed on H & E-stained samples was accompanied by a greater number of TUNEL-positive neurons

and CD68-positive endothelial/microglial cells. Similarly, more severe white matter injury was associated with relatively more profound changes in β-APP espression. GFAP immuno-histochemical stain showed high level of expression in both sham-operated control and study groups unassociated with the insult severity and experimental duration, which were not considered further in the current analysis.

Figure 4.3-6: Representative histo-pathological findings-1

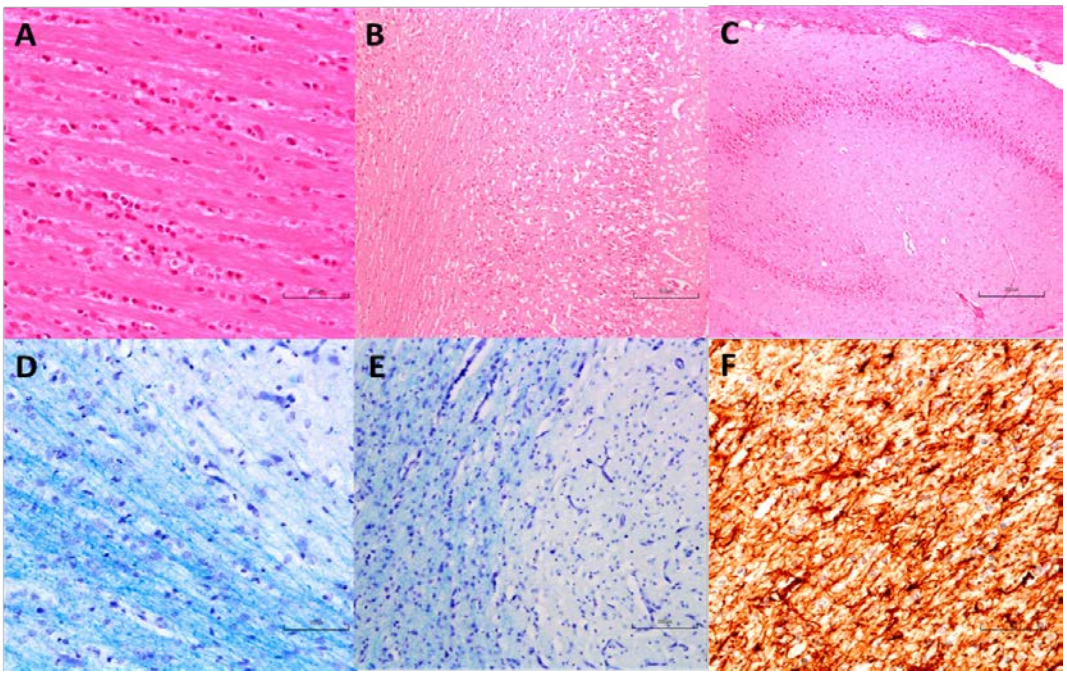

Representative brain samples stained using H & E stains (A-C), LFB/Nissl stain (D-E) and GFAP immuno-histochemical stain (F), showing normal white matter structure (A); severe destruction in microanatomical architecture in both the white matter and cortical grey matter (B); moderate pyramidal cell damage in the hippocampus (C); mild (D) and moderate (E) axonal injury; and increased GFAP expression in the white matter (F).

Figure 4.3-7: Representative histo-pathological findings-2

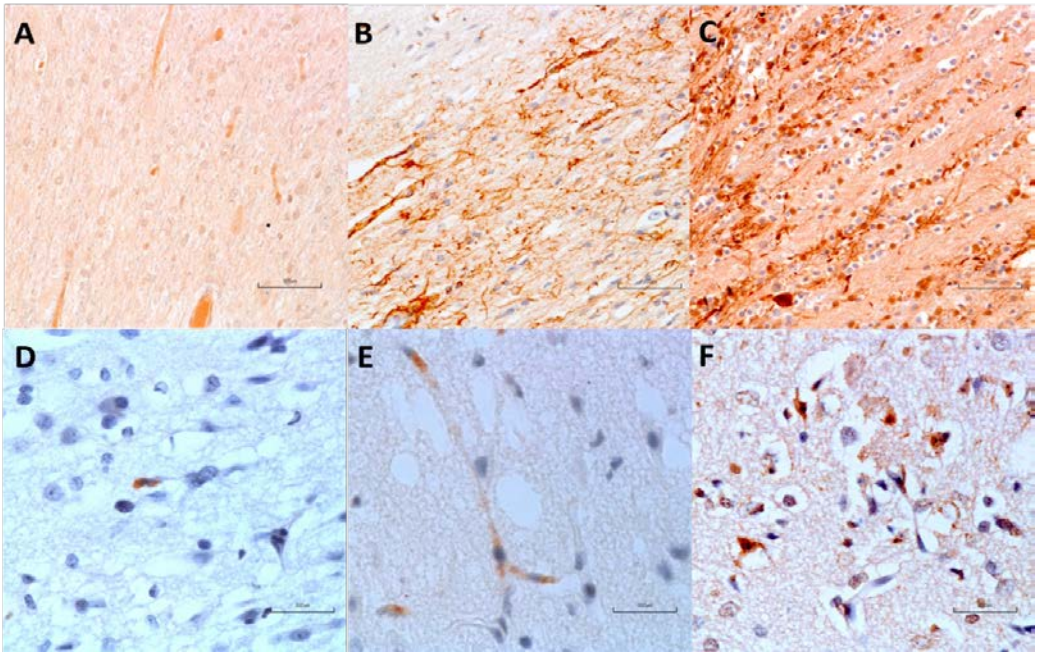

Representative brain samples stained using β-APP (A-C), CD68 immuno-histochemical stain (D-E) and TUNEL stain (F) with mild (A), moderate (B) and strong (C) expression of β-APP in the white matter; CD68 positive microglia (D) and vessel (E) in the parietal cortex; and TUNEL positive neurons with nuclear fragmentation (F) in the sagittal cortex.

4.3.4 Serial magnetic resonance biomarkers obtained 1 to 24 hours after resuscitation and histo-pathological brain injury (adjusted for the insult severity and experimental duration)

4.3.4.1 Insult severity, experimental duration, magnetic resonance biomarkers, and histo-pathological brain injury

Greater insult severity represented by the acute energy depletion index was associated with higher Pi/EPP at 3 to < 6 hours after resuscitation and with lower PCr/EPP at 18 to < 24 hours after resuscitation (Supplemental Table 4 A in page 166). Greater insults showed only modest influence on ADC values obtained 1 to < 12 hours after resuscitation in both the grey and white matters. Associations between the insult severity and T2 relaxation times were observed only for limited regions and time intervals. The severity of acute insult showed limited associations with histo-pathological brain injury even when adjusted for the time period between hypoxia-ischaemia and termination; greater insult severity led to greater number of CD68 positive microglia and vessels in the deep grey matter and the central white matter, and the white matter injury assessed on LFB/Nissl (Supplemental Table 4 B and C in pages 168-169).

4.3.4.2 ^{31}P MRS biomarkers (1 to 24 hours after resuscitation) and brain injury

During the periods 1 to < 3 hours and 3 to < 6 hours after resuscitation, only inconsistent correlations between global ^{31}P MRS biomarkers and regional histo-pathological injury were observed except that lower PCr/Pi in the white matter was associated with worse injury on H & E stains and more CD68 positive microglia and vessels in the corresponding regions (Fig. 4.3-7 and Supplemental Table 5 in page 170). During the periods 6 to < 12 hours, 12 to < 18 hours, and 18 to < 24 hours after resuscitation, consistent correlations were observed between global ^{31}P MRS biomarkers and the percentage of neuronal death in the cortical and deep grey matters, and white matter injury assessed on H & E stains and β–APP stain. Only modest correlations were observed between global ^{31}P MRS biomarkers and CD68 positive microglia and vessels. Of global ^{31}P MRS biomarkers, there were trends that NTP/EPP showed less prominent associations with histo-pathological outcomes, whereas PCr/Pi showed most prominent associations. Between the periods of 6 to < 12 hours, 12 to < 18 hours, and 18 to < 24 hours after resuscitation, there was no obvious trend towards specific timing for the optimal prediction of the histo-pathological outcome, however, modest relationships between abnormal ^{31}P MRS biomarkers and percentages of TUNEL positive apoptotic cells were observed only for the period of 6 to < 12 hours after resuscitation.

Figure 4.3-8: Associations between ^{31}P MRS biomarkers obtained 1-24 hours after resuscitation and histo-pathological brain injury

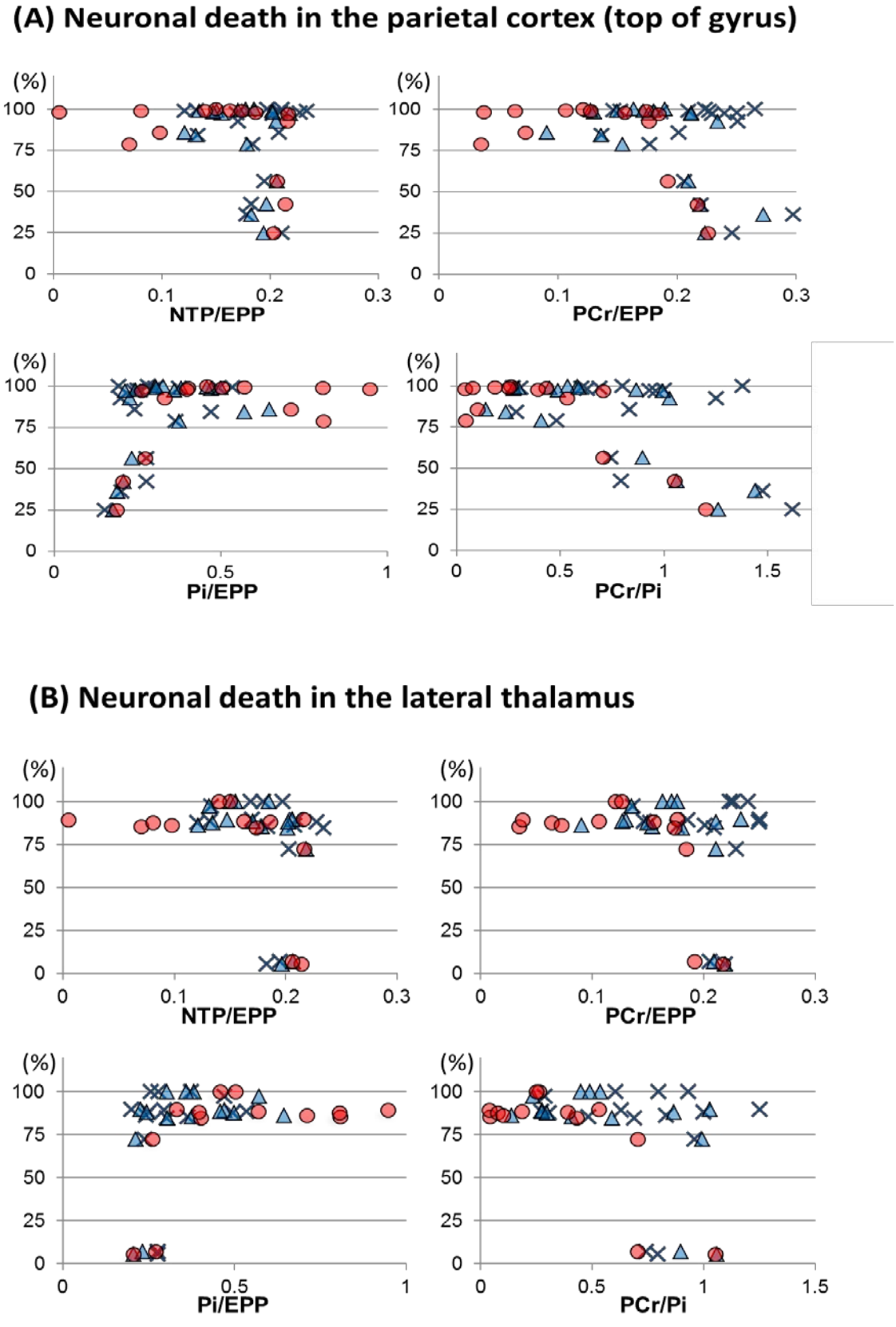

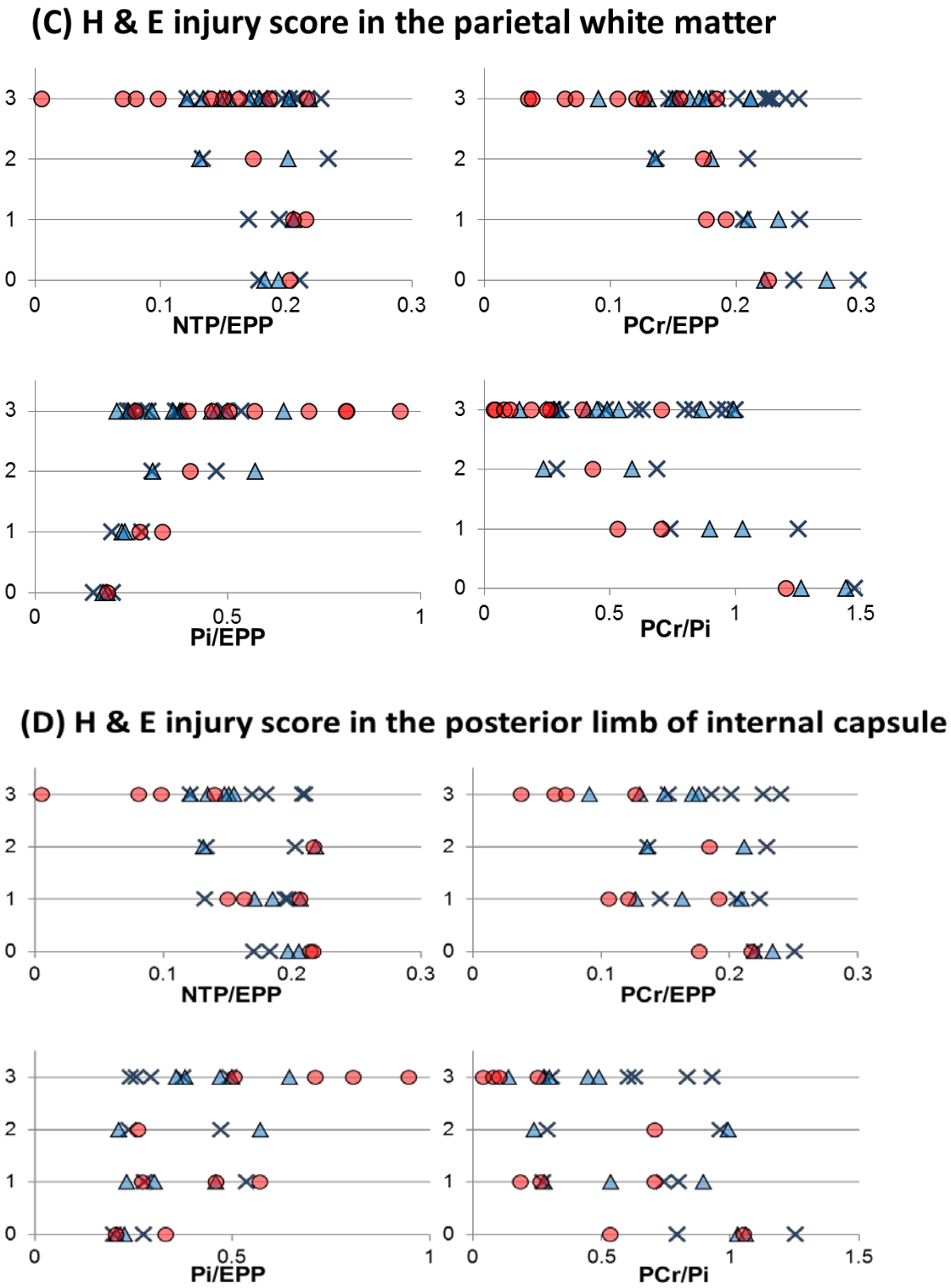

Scatter graphs showing associations between ^{31}P MRS markers obtained 1 to < 3 (x), 6 to < 12 (▲) and 6 to < 24 hours (●) after resuscitation and histo-pathological brain injury assessed using H & E stains in representative regions. There was a trend towards tighter linear relationships between histo-pathological outcomes and ^{31}P MRS biomarkers obtained at later time intervals (see Supplemental Table 5 in page 170 for statistical findings and data at other time intervals).

4.3.4.3 Maps of ADC (1 to 24 hours after resuscitation) and brain injury

During the periods 1 to < 3 hours and 3 to <6 hours after resuscitation, regional ADC values did not show consistent correlations with histo-pathological cerebral injury except that lower ADC levels during these periods were modestly correlated with numbers of CD68 positive microglia and vessels (Fig. 4.3-8 and Supplemental Table 6 in page 183). During the periods 6 to <12 hours, 12 to <18 hours, and 18 to <24 hours after resuscitation, regional ADC reductions showed modest associations with percentages of neuronal death in the cortical and deep grey matters, white matter damage assessed using H & E stains, and CD68 positive microglia and vessels.

Figure 4.3-9: Associations between maps of ADC obtained 1-24 hours after resuscitation and histo-pathological brain injury

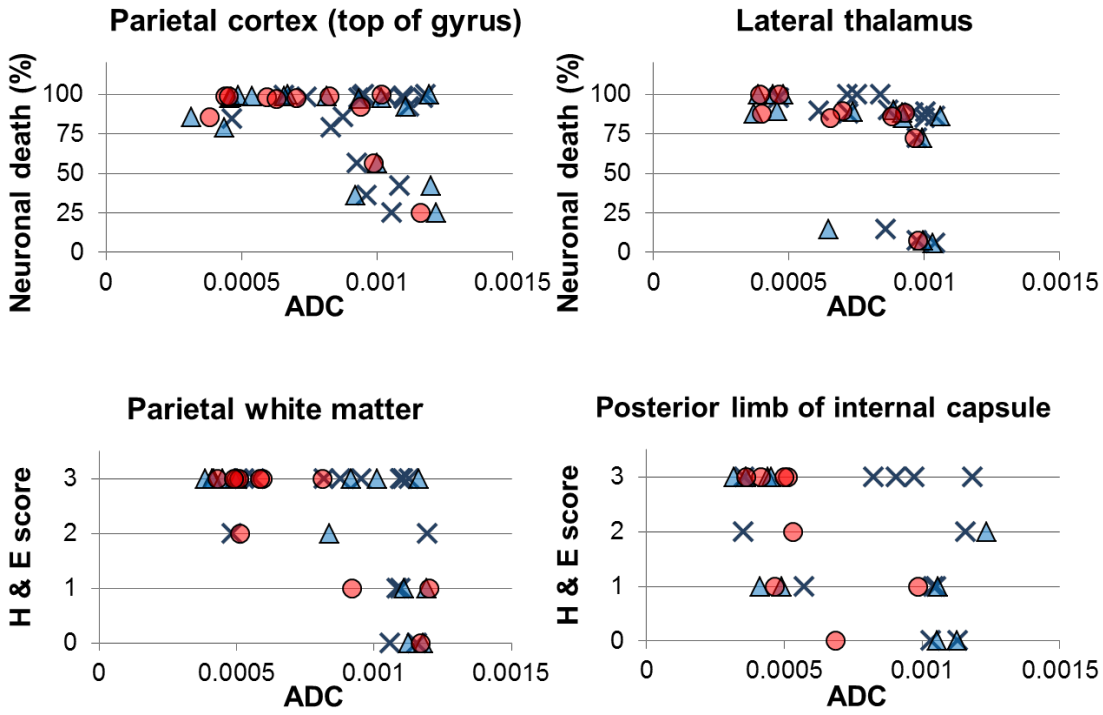

Scatter graphs showing associations between ADC obtained 1 to < 3 (x), 6 to < 12 (▲) and 6 to < 24 hours (●) after resuscitation and histo-pathological brain injury assessed using H & E stains in representative regions. Even subtle reductions in ADC shortly after resuscitation corresponded to a considerable fraction of neuronal death in the grey matter (see Supplemental Table 6 in page 183 for statistical findings and data at other time intervals).

4.3.4.4 T2 maps (1 to 24 hours after resuscitation) and brain injury

Regional T2 relaxation times did not show consistent associations with histo-pathological brain damage regardless of the timing of data acquisition and the type of histo-pathological assessment (Fig. 4.3-9 and Supplemental Table 7 in page 189). However, the longer T2 relaxation time in the cortical grey matter regions showed modest relationship with increased TUNEL positive apoptotic cellular death in the corresponding regions.

Figure 4.3-10: Associations between T2 maps obtained 1-24 hours after resuscitation and histo-pathological brain injury

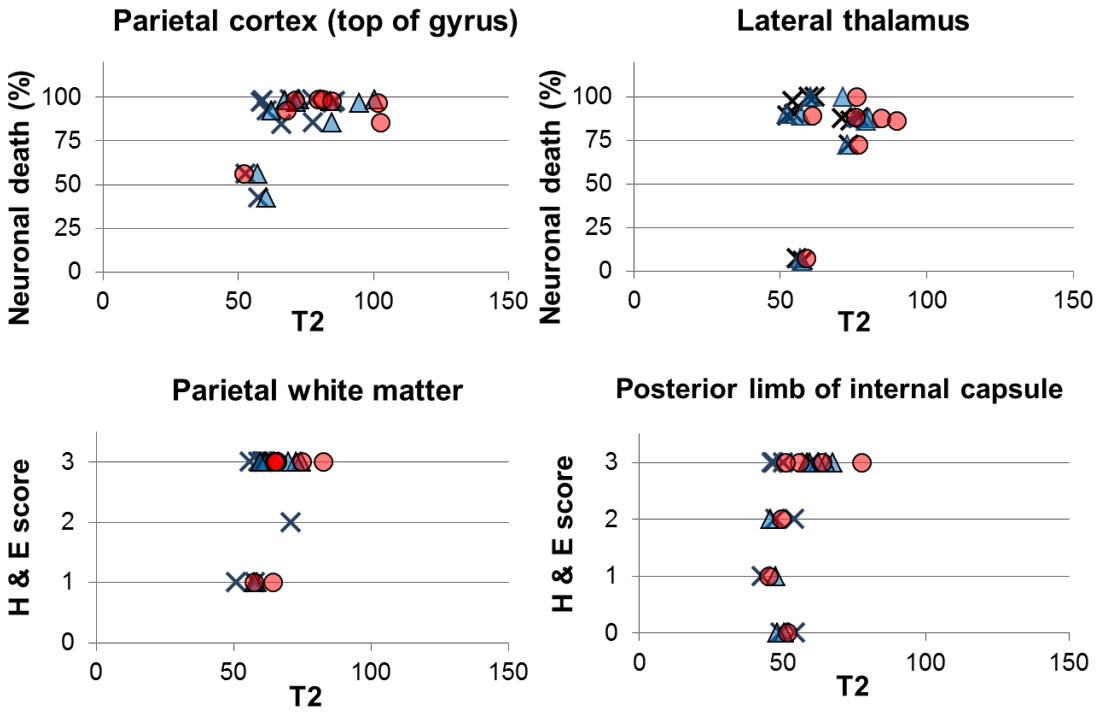

Scatter graphs showing associations between T2 relaxation times obtained 1 to < 3 (x), 6 to < 12 (▲) and 6 to < 24 hours (●) after resuscitation and histo-pathological brain injury assessed using H & E stains in representative regions. Regional T2 relaxation times showed relatively less prominent relationships with histo-pathological outcomes (see Supplemental Table 7 in page 189 for statistical findings and data at other time intervals).

4.3.5 Serial magnetic resonance biomarkers obtained shortly before to 24 hours before termination and histo-pathological brain injury

4.3.5.1 ^{31}P MRS biomarkers (1 to 24 hours before termination) and brain injury

Consistent predictive values of ^{31}P MRS biomarkers for percentages of neuronal death and white matter injury assessed on H & E stains were observed as early as 18 to 24 hours before the termination of the study, which became more consistent and robust in intervals closer to the time of termination; PCr/Pi showed optimal prediction of regional histological damage, whereas the predictive value of NTP/EPP was suboptimal to other ^{31}P MRS biomarkers (Fig. 4.3-10 and Supplemental Table 8 in page 195). During the period 12 to < 18 hours before termination, predictive values of ^{31}P MRS biomarkers were further observed for the TUNEL positive apoptotic cellular death in the cortical grey matter, CD68 positive microglia and vessels in the cortical grey matter and the peripheral white matter, and β-APP positive axonal changes in the white matter. There was a trend towards more precise prediction of histo-pathological outcomes with time intervals closer to termination, except for the TUNEL positive apoptotic cellular death in the cortical grey matter, the optimal prediction of which was observed during the period of 12 to < 18 hours before termination.

Figure 4.3-11: Associations between ^{31}P MRS biomarkers obtained 1-24 hours before termination and histo-pathological brain injury

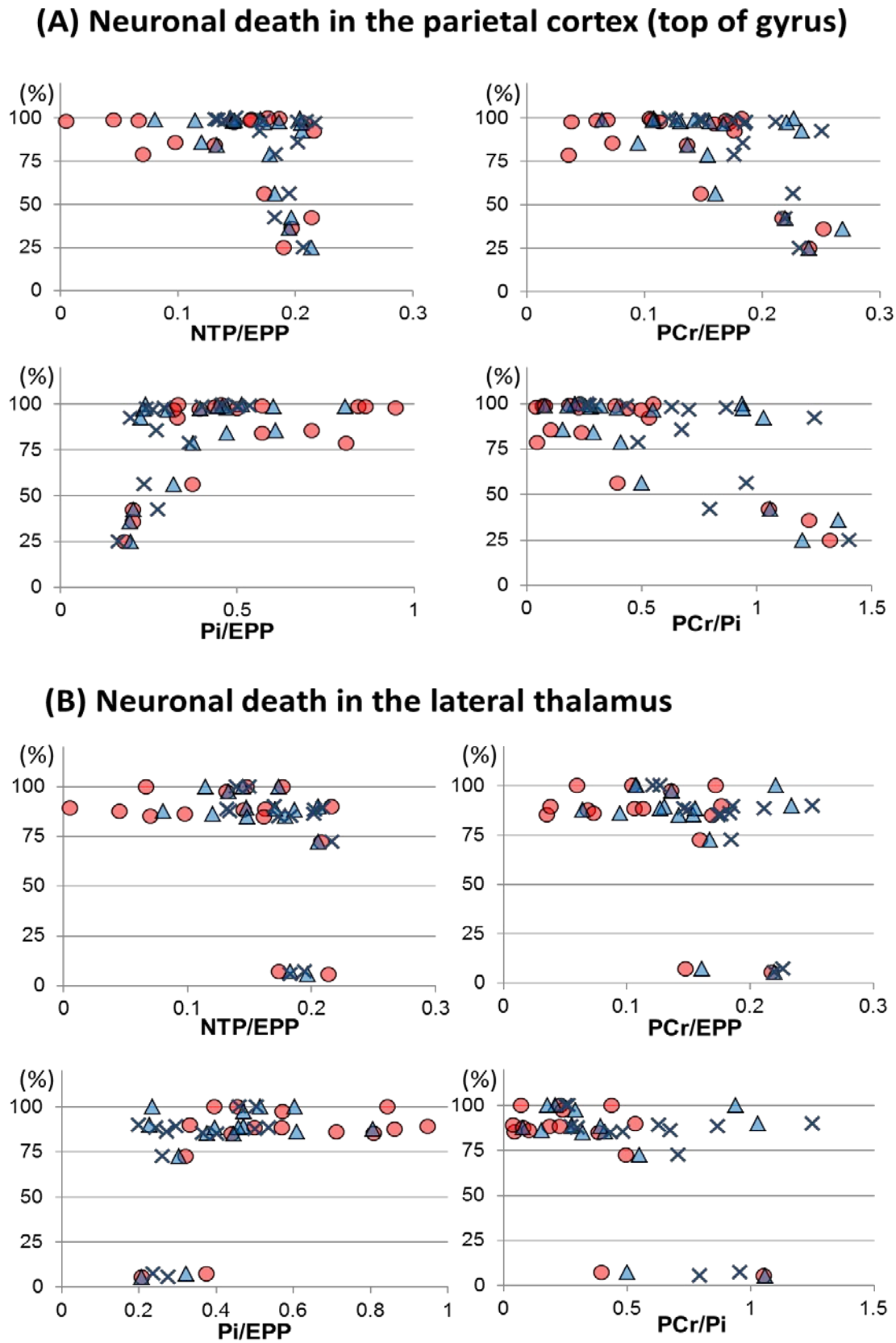

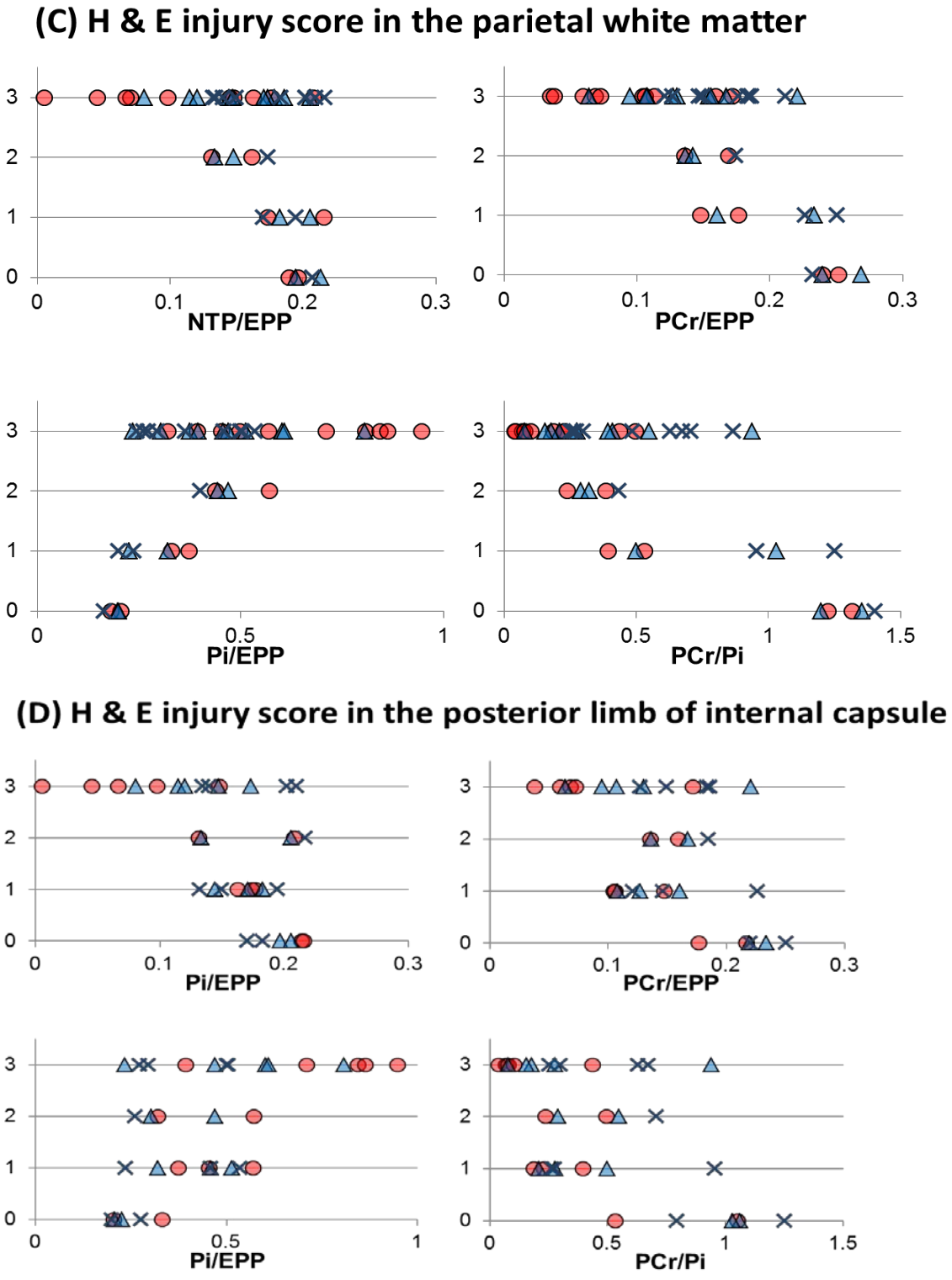

Scatter graphs showing associations between ^{31}P MRS markers obtained 1 to < 3 (●), 6 to < 12 (▲) and 6 to < 24 hours (x) before termination and histo-pathological brain injury assessed using H & E stains in representative regions. Tighter linear relationships with histo-pathological outcomes were observed for biomarkers obtained shortly before termination (see Supplemental Table 8 in page 195 for statistical findings and data at other time intervals).

4.3.5.2 Maps of ADC (1 to 24 hours before termination) and brain injury

Regional ADC values started showing consistent predictive values for the percentage of neuronal death in the cortical and deep grey matters, white matter injury assessed on H & E stains and LFB, and CD68 positive microglia and vessels in the cortical grey matter and the peripheral white matter during the period of 12 to < 18 hours before termination and the time intervals closer to termination (Fig. 4.3-11 and Supplemental Table 9 in page 208). Regional ADC in the white matter also predicted β-APP positive axonal changes after time intervals of 6 to < 12 hours before termination.

Figure 4.3-12: Associations between maps of ADC obtained 1-24 hours before termination and histo-pathological brain injury

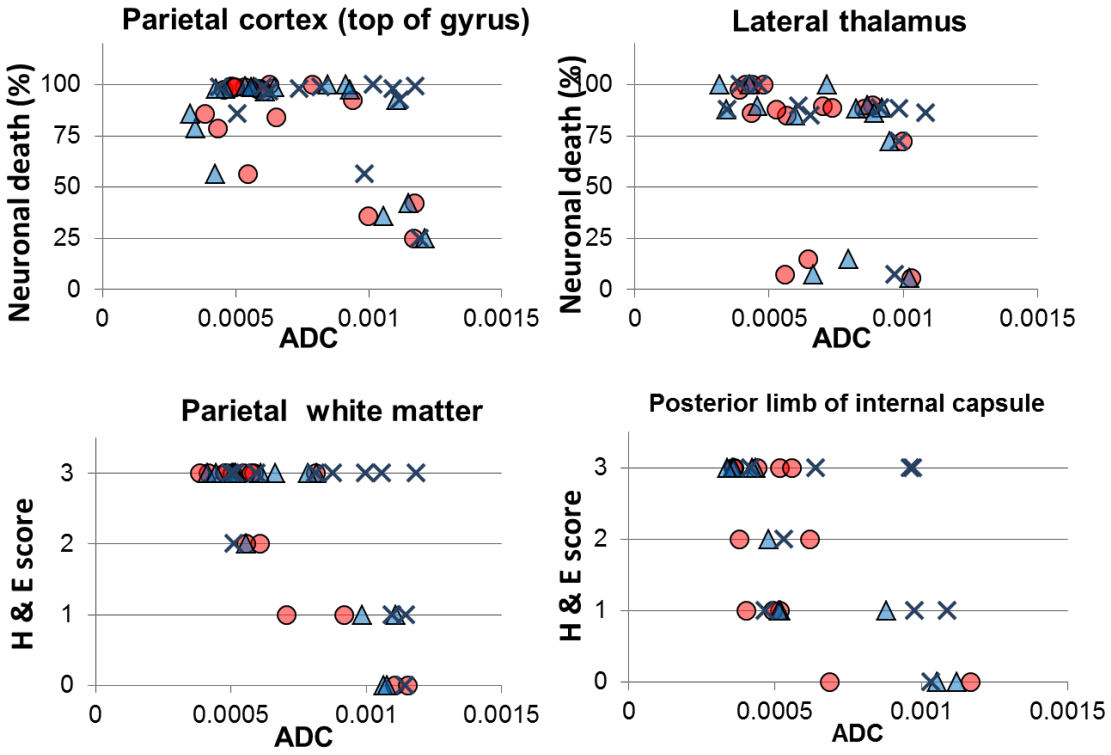

Scatter graphs showing associations between ADC obtained 1 to < 3 (●), 6 to < 12 (▲) and 6 to < 24 hours (x) before termination and histo-pathological brain injury assessed using H & E stains in representative regions. Subtle reduction in ADC just prior to termination corresponded to a considerable fraction of neuronal death in the parietal cortex. Tighter linear relationships were observed between histo-pathological outcomes and ADC obtained closer to termination (see Supplemental Table 9 in page 208 for statistical findings and data at other time intervals).

4.3.5.3 T2 maps (1 to 24 hours before termination) and brain injury

Predictive values of regional T2 relaxation times were limited and inconsistent. However, longer T2 relaxation times in the white matter showed modest predictive value for worse white matter injury assessed on H & E stains during the time intervals of 18 to < 24 hours before and closer to the time of termination (Fig. 4.3-12 and Supplemental Table 10 in page 214). Longer T2 relaxation times were also associated with greater percentages of TUNEL positive apoptotic cellular death in the cortical grey matter during the period 18 to < 24 hours before termination and time intervals closer to termination.

Figure 4.3-13: Associations between T2 maps obtained 1-24 hours before termination and histo-pathological brain injury

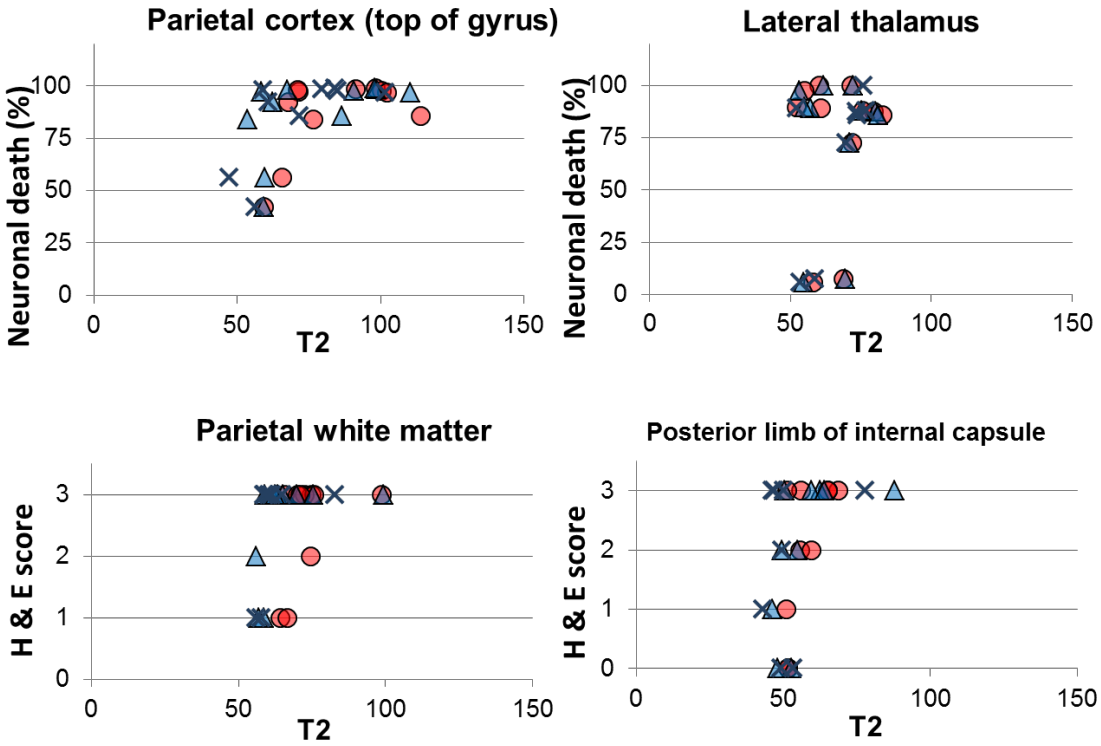

Scatter graphs showing associations between T2 relaxation times obtained 1 to < 3 (●), 6 to < 12 (▲) and 6 to < 24 hours (x) before termination and histo-pathological brain injury assessed using H & E stains in representative regions. Regional T2 relaxation times showed relatively less prominent relationships with histo-pathological outcomes (see Supplemental Table 10 in page 214 for statistical findings and data at other time intervals).

Chapter 5: Discussion

5.1 Associations between insult severity and therapeutic time window duration

5.1.1 Summary

We have proved the hypotheses that a more severe hypoxic-ischaemic insult leads to a shorter latent phase, more severe secondary energy failure and greater neuronal death. The findings of this study are discussed in this chapter.

5.1.2 Key findings from the study

In a newborn piglet model of asphyxial encephalopathy, we have demonstrated that the more severe the cerebral energy depletion during transient hypoxia-ischaemia was, the shorter the subsequent latent-phase was, the worse the severity of secondary energy failure was, and the more extensive neuronal death in the cortical grey matter was. The duration of the latent phase itself showed significant relationships with the severity of secondary energy failure and the eventual extent of neuronal injury in both the cortical grey matter and the deep grey matter. Further, we confirmed that a higher neuronal mortality was associated with more severe secondary energy failure. Previously the association between the duration of therapeutic time window and the severity of acute hypoxia-ischaemia had been deduced indirectly on the basis of faster development in the histo-pathological injury with more severe hypoxia-ischaemia (114, 115). However, using quantitative measures and multivariate analysis, we have demonstrated here that the duration of the latent phase was shorter following more severe insults, and that this period, which is likely to include the therapeutic time window, can be lengthened by therapeutic hypothermia.

5.1.3 Acute energy depletion and evolution of secondary energy failure

Secondary energy failure has been observed in several different species at various maturational stages as reduced high energy phosphates (e.g. PCr and NTP). Our group has mainly used NTP/EPP and PCr/Pi as indices of high-energy phosphate reserves. In this current analysis, we used NTP/EPP as a robust index of the severity for secondary energy failure, because PCr/Pi would be affected by factors including the flux within the

mitochondrial electron transport chain and re-phosphorylation of adenosine diphosphate via creatine kinase; furthermore, PCr/Pi can fall before ATP because, with unimpaired substrate delivery, anaerobic glycolysis can maintain ATP (47).

Using MRS and biochemical methods, previous studies quantified the absolute concentrations of high energy phosphates (45, 78) and of total adenine nucleotides and total creatine (79) respectively. These studies have demonstrated falls in total mobile phosphates, EPP, total adenine nucleotides and total creatine at the similar timing to the reduction in NTP/EPP and PCr/Pi. Although energy metabolism apparently recovers within approximately an hour after the primary insult, injury cascades have already been activated at the cellular level even at this stage (50-54). Vannucci and colleagues observed linear relationships between histological tissue injury and high energy phosphate concentrations at 6 to 18 hours after resuscitation, with greater significance at 24 to 48 hours, suggesting that secondary energy failure was consequential to evolving cellular destruction rather than causal of cellular death in so far surviving tissue (79). Although it is agreeable that secondary energy failure as observed by ^{31}P MRS is likely to be a phenomenon directly associated with a delayed, irreversible metabolic crisis, it may not closely match the temporal evolution of cell death itself. Our present study in a piglet model suggests that considerable histological cell death may already be present during the latent phase (i.e. before overt secondary energy failure). This suggests that, during the early phase of secondary energy failure, co-existing earlier and progressing histological damage may not relate directly to the surviving exchangeable phosphate pool, and that the latent phase may simply represent damaged but surviving tissue maintaining normal high energy phosphate levels via salvage systems, because ^{31}P MRS is likely to be "blind" to dead cells, from where all mobile phosphate has leaked out. Hence we believe that the latent phase represents normal high energy phosphate levels in surviving tissue; it is during the latent phase that therapeutic interventions are most likely to preserve tissue vitality - but only that of tissue which has survived to this stage.

5.1.4 Level of acute energy depletion and the effect of hypothermic neuroprotection

There is some evidence suggesting that hypothermia is less neuroprotective in the most severely asphyxiated subjects. In a study of adult traumatic brain injury, moderate systemic hypothermia improved the outcome of patients with an initial Glasgow Coma

Scale of 5-7 but not for those with 3-4 (116). A study of selective head cooling for infants with neonatal encephalopathy showed improved survival with lessened severe disability only in infants whose aEEG demonstrated moderate (but not most severe) background abnormalities before cooling (8). In our current study, a more severe acute insult (greater acute energy depletion) led to a shorter latent phase. If therapy is only effective during the latent phase, then the brevity of that stage in the most severely injured patients may explain the reduced hypothermic neuroprotection.

5.1.5 Evolution of secondary energy failure and neuroprotective treatments

The therapeutic time window for potentially neuroprotective interventions may vary depending on the treatment, as particular neuroprotective agents ameliorate different cytotoxic stages (11, 101, 117). Hence the latent phase duration may not directly correspond with the window of opportunity for neuroprotection following hypoxia-ischaemia. However, once secondary energy failure is established, therapeutic interventions may provide no or minimal benefit, because deleterious reactions expands rapidly to the downstream cascades of cerebral injury by the end of the latent phase, suggesting that the earlier the intervention is, the greater the benefit of neuroprotective treatments are.

Diffusion-weighted imaging of hypoxic-ischaemic cerebral injury has demonstrated temporal and anatomical variations in brain water ADC which correlated with NTP/EPP (62). Albeit slightly biased towards cortical grey matter, we used effectively whole brain ^{31}P MRS to monitor the latent phase and the evolution of secondary energy failure: hence, we could not discern regional differences in the latent phase. However, the regional ADC differences suggest that the therapeutic time window may also vary between regions. Our study was not designed to elucidate the optimal therapeutic time window for hypothermic neuroprotection. Further studies, utilising a wide range of hypothermic delays and durations, are needed to achieve this. Our study was also not designed to address the direct relationship between the insult severity and hypothermic neuroprotection. However, only in both cooled groups was there a suggestion in cortical grey matter that the most severe insults were associated with greater neuronal death and more moderate insults with less: further studies are required to investigate the relationship between the severity of hypoxia-ischaemia and the efficacy of cooling.

5.1.6 Clinical implications

In infants with neonatal encephalopathy consequential to perinatal hypoxia-ischaemia, the exact timing, duration, and magnitude of the intrapartum events are unknown. Using our translational model of perinatal asphyxial encephalopathy, the insult severity of which can be quantified, we have shown that the latent phase shortens as insult severity increases. Thus the time between birth and the onset of secondary energy failure may constitute a retrospective index of the severity in intrapartum hypoxa-ischaemia.

Recently, large scale clinical trials of therapeutic hypothermia following perinatal hypoxia-ischaemia have confirmed that intervention within the first 6 hours after birth reduces death and severe disability at 18 months after birth (12). The possibility of only a brief latent phase in the most severely injured patients, who had very abnormal background activity on the pre-randomisation aEEG, may explain the reduced hypothermic neuroprotection in such infants (8). These trials, whilst results are encouraging, highlight the need to select candidates for intervention, excluding those who are unlikely to benefit, and also to tailor specific treatments to individual infants in order to fully optimise neuroprotection.

Very early ^{31}P MRS may help define the severities of a preceding hypoxic-ischaemic insult and the consequential secondary energy failure (54), however, given the clinical problems associated with very early application of this modality to encephalopathic infants, it is important that experimental research focuses on relationships between quantitative ^{31}P MRS and other magnetic resonance biomarkers, such as ^{1}H MRS and ADC, and cotside tools such as aEEG.

5.1.7 Strengths and limitations of the study

We used acute energy depletion as an index of the insult severity, because our group has reported that this index correlates with the severity of secondary energy failure (42) and neuronal death (118) in this model. Throughout the present study, we aimed for insults of similar severity by using a standardised protocol employing continuous^{31}P MRS to monitor β-NTP in real time during the acute hypoxic-ischaemic insult: however, there were variations in the biological response to both transient hypoxia-ischaemia and resuscitation. Such variability, often encountered in the clinical practice as well, may explain a wide range of outcome severities in infants with neonatal encephalopathy consequential to perinatal hypoxia-ischaemia. It may be important to understand the infant specific biological response to the stress as well as the insult morbidity itself to

improve the diagnostic accuracy and neuroprotective effect of therapies. In the currents study, we were unable to maintain our model for more than 60 hours in total for ethical and practical reasons. Consequentially it is possible that the severity of both secondary energy failure and histological injury may have been worse than that measured. It is also important to note that, unlike in our model, the precise timing of perinatal hypoxia-ischaemia is generally unclear in clinical practice. Further studies in our model may help establish biomarkers, which indicate the timing, type and depth of insults.

Multivariate analysis adjusting for the temperature groups demonstrated correlation between neuronal death and acute energy depletion only in cortical grey matter. On-axis reception sensitivity of a circular MRS surface coil (radius r) decreases with coil distance (d) as $r^2/(r^2 + d^2)^{3/2}$ with comparable behaviour off-axis (119): elliptical surface-coil sensitivity also decreases similarly. Hence, the observed acute energy depletion may have been more representative of the insult experienced by the cortical grey matter rather than the deep grey matter. Characteristic intrinsic factors of the deep grey matter in the developing brain, such as the high metabolic rate and overexpression of glutamate receptors and nitric oxide synthase, may render this region highly susceptible to perinatal hypoxia-ischaemia, potentially yielding different consequences from the cortical grey matter (120-122). In addition, our previous histological analysis on the same experimental subjects demonstrated that the optimal protection for the cortical grey matter was observed at 33ºC, whereas the deep grey matter was most protected at 35ºC (49), suggesting potentially different optimal temperature values for neuroprotection in different cerebral regions; the relationship between the insult severity and the outcome measure might also be affected by cooling.

5.1.8 Conclusions

We have shown that increasing insult severity is associated with shortening of the subsequent latent phase, and more severe secondary energy failure and neuronal damage in the cortical grey matter. The severity of secondary energy failure correlated linearly with neuronal mortality. The brevity of the latent phase in subjects with severe perinatal hypoxia-ischaemia may explain the apparently reduced hypothermic neuroprotection in the most severely asphyxiated newborn infants. Further work is needed to investigate the relationship between the severity of the insult and the efficacy of cooling. It is also important to develop cotside tools providing early measures which correlate with the impairment of brain energy generation.

5.2 Energy metabolism during the latent phase and early evolutional period or secondary energy failure

5.2.1 Summary

We have proved the hypothesis that subtle variation in global energy metabolites during the latent phase is associated with the severity of secondary energy failure even before the overt evolution of secondary energy failure. The findings of this study are discussed in this chapter.

5.2.2 Key findings from the study

Following resuscitation, in subjects with favourable outcome, PCr/EPP recovered to higher than its baseline level (overshoot); in subjects with unfavourable outcome, maximum recovery in PCr/EPP was lower than baseline and lower than in subjects with favourable and intermediate outcomes. Recovery PCr/EPP correlated linearly and negatively with both acute insult severity and baseline PCr/NTP. These results suggest that recovery in energy metabolites shortly after resuscitation may provide an early biomarker for the tissue viability. PCr recovery overshoot may indicate a protective response to hypoxia-ischaemia leading to cell recovery, survival and protection against subsequent stress. In addition, baseline cerebral metabolism (PCr/NTP) may identify vulnerable subjects and cerebral regions prior to invasive surgery.

5.2.3 Changes in high energy phosphates during transient hypoxia-ischaemia, latent phase and secondary energy failure

A range of compensatory systems exist to maintain the tissue metabolism under the shortage or lack in energy substrates. For example, the creatine kinase reaction can generate ATP from PCr and adenosine diphosphate at sites of high energy demand (123) constituting a temporal and spatial buffering system for cellular energy stores (124, 125). In our study, a rapid reduction in PCr/EPP was observed only during the first 10 minutes of hypoxia-ischaemia, whereas NTP/EPP declined slowly throughout the insult, suggesting that NTP was initially maintained at the expense of PCr via the creatine kinase reaction. We observed a similar sequence in the reduction of PCr/EPP and NTP/EPP during secondary energy failure, suggesting that creatine kinase was employed to initially but temporarily maintain the NTP level even during this secondary

phase of metabolic derangement. Studies by our group and others have suggested that secondary energy failure occurs concomitantly with irreversible, terminal stage tissue injury (45, 53, 78, 79). Although this phase may not directly reflect the consequence of on-going cellular death, our current results also suggest that secondary energy failure is a consequence of a substantial tissue fraction, which survived acute hypoxia-ischaemia only to later undergo further metabolic derangement, eventually leading to more cell death and tissue loss. Further studies need to address mitochondrial functions during evolutional phases of secondary energy failure.

5.2.4 Cerebral stress response after the commencement of resuscitation and PCr recovery overshoot

When all experimental subjects were analysed together, resuscitation led to the recovery in PCr/EPP to the baseline level 2-8 hours following transient hypoxia-ischaemia, whereas neither NTP/EPP nor Pi/EPP fully recovered. Group analysis revealed that the “full recovery” of PCr/EPP was due to the combined effects of incomplete recovery in the “severe" secondary energy failure group and recovery beyond baseline levels for “no" secondary energy failure: in the latter piglet group, PCr/EPP 2-8 hours after resuscitation was higher than at the baseline and higher than for subjects with “severe" secondary energy failure. Even during the latent phase, the neurotoxic cascade (the death programme) and the recovery process induced by reperfusion (the rescue programme) compete to determine the extent of the eventual cerebral injury (51-53, 72, 126-128).

Brief PCr recovery overshoot, quantified either as the absolute PCr concentration or measured relative to NTP, is considered to be one of such stress responses widely recognised in skeletal muscle (129, 130) and myocardium (131-136). However, it remains unclear if this phenomenon is beneficial, detrimental, or inconsequential. In skeletal muscle, endurance training up-regulates PCr recovery and improves exercise performance (129), whereas in cardiac muscle, PCr recovery overshoot following ischaemia and reperfusion has been related both to adversities including depressed contractile function (“myocardial stunning”), poor ATP restoration, and worse histological injury (132, 137), and to favourable remote effects such as more efficient energy consumption and tolerance to forthcoming potentially lethal hypoxia-ischaemia (“ischaemic preconditioning”) (133-135). Although cerebral PCr recovery overshoot

following hypoxia-ischaemia has not been described previously, several stimuli such as hypothermia and creatine supplementation, both of which are potent neuroprotective treatments, induce an elevation in cerebral PCr (138-140). In our current study, the recovery in PCr/EPP above the baseline level occurred only in the subject with "no" secondary energy failure, and the PCr/EPP level correlated linearly and negatively with the insult severity, suggesting that PCr recovery overshoot in brain is a welcome response to hypoxia-ischaemia potentially heralding cell recovery and survival. Given that induced high cerebral PCr (e.g. incurred by hypothermia or creatine supplementation) is associated with increased resistance to hypoxia-ischaemia, cerebral PCr recovery overshoot following mild hypoxia-ischaemia might also protect against subsequent potentially lethal stressors.

Our study was not designed to investigate the mechanism of PCr recovery above baseline in the developing brain. However in the skeletal muscle, this stress response is attributed to delayed downgrading of oxidative phosphorylation from the activated high demand status (130). In myocardium, a potential explanation is mitochondrial PCr synthesis proceeds unperturbed but deficiency in creatine kinase specific within cytoplasm due to oxygen radical toxicity reduces PCr utilisation (131, 137). Another possibility is that cardiac function is down regulated either passively due to severe damage or actively as a “hibernation period” for the stressed tissue (141). A transient reduction of intracellular adenine nucleotides by loss into the interstitial and vascular space observed in myocardium following hypoxia-ischaemia could also explain why neither NTP/EPP nor Pi/EPP regained baseline levels after the insult (142, 143). Indeed, in the developing brain, a transient, reversible reduction in total cerebral adenine nucleotides has been observed following hypoxia-ischaemia although the relationship with PCr recovery level was not investigated (79, 128). However given the prolonged PCr recovery above baseline observed in the current study, it is possible that the underlying mechanism may be different from that in the skeletal and cardiac muscle.

We also observed that lower baseline PCr/NTP was associated with higher recovery PCr/EPP. Although we used term born piglets of similar size and maturation, high brain PCr/NTP under normal physiological conditions may imply differences in maturity, metabolic activity and subsequent vulnerability to hypoxia-ischaemia. Interestingly, pre-existing low PCr (relative to NTP or creatine) leads to a greater increase in PCr

following exercise (skeletal muscle) and creatine supplementation (skeletal muscle and brain) (130, 144, 145). Further studies are required to elucidate the relationship between cerebral PCr recovery overshoot and background metabolism.

5.2.5 Clinical implications

Early prediction of the extent of cerebral injury following transient hypoxia-ischaemia is desirable for the refining and appropriate targeting of neuroprotective therapies in the newborn. Our current results suggest that subtle changes in the global brain PCr/EPP and Pi/EPP during the latent phase (2-8 hours after resuscitation) can discriminate subjects which will later develop minimal, moderate and severe secondary energy failure.

5.2.6 Limitations and advantages of the study

The number of subjects (particularly controls) and the interval of serial MRS acquisitions were limited for ethical and practical reasons. Our group has reported previously that PCr remains unchanged relative to the total mobile phosphate over 48 hours in sham operated subjects (42). This mirrors human studies in which PCr, Pi, NTP, and total mobile phosphate concentrations changed only gradually up to the age of 20 months old (146). The duration of our present study was shorter compared to those in our previous reports, which kept the piglet within the bore over 48 hours after resuscitation (42, 47): it is possible that subjects with no or moderate secondary energy failure may have eventually developed severe secondary energy failure with longer observations.

5.2.7 Future studies

We have demonstrated, for the first time, the presence of cerebral PCr recovery overshoot after hypoxia-ischaemia. Although this phenomenon appeared to be a favourable event leading to the optimal metabolic function during the sub-acute phase, detailed associations between injury reactions and energy metabolism need to be delineated (i) to improve understanding of injury cascade, (ii) to develop more precise diagnostic tools, and (iii) to increase the beneficial effect of neuroprotective treatments.

5.2.8 Conclusions

PCr recovery overshoot has been reported elsewhere in skeletal muscle after exercise and in myocardium after reperfusion. The presence of cerebral PCr recovery above baseline in a newborn porcine model of asphyxial encephalopathy was demonstrated using serial ^{31}P MRS: piglets in which secondary energy failure did not develop displayed supra-baseline recovery in PCr/EPP. Our findings give novel insight into the cerebral stress response to hypoxia-ischaemia and suggest that, as well as Pi/EPP, cerebral PCr/EPP might be an early favourable biomarker before the evolution of secondary energy failure following perinatal hypoxia-ischaemia.

5.3 Temporal and spatial evolution of secondary energy failure and cerebral injury

5.3.1 Summary

We have proved the hypothesis that evolution of secondary energy failure observed using ADC maps was spatially heterogeneous, and that early regional ADC values predicted tissue damage up to 18 hours in advance of termination. Although the predictive value of magnetic resonance biomarkers for histo-pathological brain injury appeared to be optimal with global PCr/Pi, regional ADC provided equivalent predictive values to global PCr/EPP and Pi/EPP, and may be clinically useful as an alternative to ^{31}P MRS biomarkers. The findings of this study are discussed in this chapter.

5.3.2 Key findings from the study

Global cerebral energy metabolite levels observed using ^{31}P MRS were confirmed to be a robust biomarker for histo-pathological brain damage, with PCr/Pi providing the optimal estimation of existing and forthcoming brain damage. Although regional ADC values failed to demonstrate superior predictive value to global PCr/Pi, ADC showed significant regional heterogeneity during the evolutional phase of secondary energy failure. Given that global ^{31}P MRS biomarkers predominantly reflected tissue changes in the superficial architecture corresponding to regions covered by the surface coil, maps of ADC may additionally provide spatial information especially in deep brain structures. Maps of T2 relaxation time showed only limited predictive value of brain damage, however, its temporal increase was predominantly associated with apoptotic cellular death. Given that T2 relaxation time is mainly determined by changes in the water-macromolecule ratio within the tissue (69), T2 prolongation may well be observed for tissue injury where other types of cellular death is predominant. Further investigation is required to confirm whether our current finding was caused by chance or by characteristic changes in tissue integrity associated with apoptotic cellular death.

5.3.3 Diagnostic value of global and regional magnetic resonance biomarkers for histo-pathological brain injury

We have confirmed that ADC values can provide precise estimation of histo-pathological brain injury up to 18 hours in advance of termination, the predictive

value of which appeared to be relatively more robust compared to the global NTP/EPP. However, unlike our initial hypothesis, the maps of ADC failed to demonstrate superior predictive values for histo-pathological brain damage to global PCr/Pi despite the advantage in the spatial information. Our group has utilised the ^{31}P MRS variables by quantifying the concentration of energetic metabolites relative to EPP. The reduction in PCr/EPP and the increase in Pi/EPP precede the decline in NTP/EPP, as the ATP concentration is maintained by utilising the PCr pool via the creatine kinase reaction (124, 125). Although the reduction in NTP/EPP is more likely to be linked with the terminal energy derangement of the cerebral tissue (147), this may not provide highly sensitive early marker of delayed tissue injury. Given that PCr/EPP and Pi/EPP have been demonstrated to be more sensitive early markers compared to NTP/EPP (54), the metabolite ratio between PCr and Pi may reasonably provide an even more sensitive biomarker to on-going tissue injury during the acute phase. Further studies are required to compare the predictive value of PCr/Pi, ADC and lactate relative to N-acetylaspartate (Lac/NAA) obtained using ^{1}H MRS, the last of which is currently recognised to be the most sensitive and specific magnetic resonance biomarker for the neurodevelopmental outcome after perinatal hypoxia-ischaemia in the clinical practice (58).

Despite the excellent predictive value of global PCr/Pi for the endpoint brain injury, currently few research and clinical institutions can obtain ^{31}P MRS from the newborn brain because of its high demand for the hardware, expertise and skilled personnel as well as the lack in the spatial information and the relatively long acquisition time. In contrast, ADC maps can be acquired in most clinical MRI scanners, rendering this modality one of most useful early biomarker to support tailored neuroprotective treatments after perinatal hypoxia-ischaemia. Although there remained uncertainty around the optimal timing of the scan and the interpretation into clinical outcome especially because of the pseudo-normalisation of ADC several days after hypoxia-ischaemia, our current study demonstrated that, during the evolutional phase of secondary energy failure, regional ADC values can be used to estimate the histo-pathological brain injury in the corresponding region both at the time of and up to 18 hours after the MRI study. To clinically apply early prediction of cerebral injury following hypoxia-ischaemia using the maps of ADC, further translational studies are required to give ranges in ADC values corresponding to normal and abnormal outcomes for each region, infant's maturational stage, and time after birth. Experimental studies

with longer observational intervals are required to delineate the optimal time window for ADC to predict the associated brain injury.

Our current study was initially designed to assess correlations between histo-pathological brain injury and serially obtained magnetic resonance biomarkers at specific time intervals before termination of each study, so that clinicians may be able to monitor and predict the type and depth of tissue damage both at the moment of and after hours of the magnetic resonance data acquisition. However, we also analysed the time-series data according to the elapsed time after resuscitation, which may provide useful information for clinical assessment of injury severity. When the analysis was performed with adjustment for the insult severity and the survival time after resuscitation, both global ^{31}P MRS biomarkers and regional ADC values showed modest correlation with the end point brain injury, however, the level and pattern of positive findings were less robust compared to the former approach, which was based on the data classified according to specific time intervals before termination. The difference in the findings might be explained by previous studies which have found that brain injury on histopathology increases with longer survival times within the first few days after the acute event (148, 149); other bias might also influence the predictive value of magnetic resonance biomarkers, as, in our study, the dependence of histo-pathological outcomes on the insult severity and the time interval after resuscitation was relatively weak. One limitation of the current study is that, although we intended to correlate serial magnetic resonance biomarkers with histo-pathological samples harvested at different time points with different levels of energy failure, we did not have sufficient numbers at each time point for robust analysis. Future studies need to assign multiple subjects to several predetermined termination points to remove the probable bias in our current study.

5.3.4 Spatial changes of ADC during the evolutional process of secondary energy failure

A previous study from our group demonstrated that, in a similar piglet model of perinatal asphyxial encephalopathy, ADC changes in the superficial cerebral cortex and white matter precisely surrogate the decline in high energy phosphates quantified using ^{31}P MRS (62). Based on this observation, in this current study, we used the maps of ADC to monitor regional evolution of secondary energy failure in the piglet model. Consistent to this assumption, both global NTP/EPP and ADC values in the cortical grey matter and peripheral white matter were lower than baseline from 1 to < 3 hours after resuscitation.

Serial observations in regional ADC values suggested that the evolutional timing of secondary energy failure was spatially heterogeneous, presumably reflecting the inter-subject and inter-regional variations in the reaction to both hypoxia-ischaemia and resuscitation. Rapid reduction in ADC values in the cerebral cortex and peripheral white matter was observed predominantly in the sagittal and parietal watershed regions between anterior and middle cerebral arteries; these changes were followed by gradual ADC declines in the temporal lobe, deep grey matter and central white matter after 6 to <12 hours of resuscitation. ADC values at baseline were highest in the central white matter and lowest in the deep grey matter, the contrast of which was lost shortly after hypoxia-ischaemia, supporting the rapid change in the water diffusion within the susceptible cerebral regions of the watershed cortex, white matter and the posterior limb of the internal capsule. Future studies need to address the relationship between types and depth of insult, and spatial pattern of ADC decline with time.

5.3.5 T2 maps during acute phase after perinatal hypoxia-ischaemia

In contrast to the information obtained from global ^{31}P MRS and ADC, T2 maps showed only weak predictive values of histo-pathological brain injury. At baseline, there was a considerable inter-regional variation in the T2 relaxation time as estimated from the contrast on T2 weighted imaging from the newborn brain. However, such an inter-regional variability was lost shortly after hypoxia-ischaemia and resuscitation. Although we rarely observe marked reductions in T2 contrast within a few days of perinatal hypoxia-ischaemia in clinical cases, quantitative approach may enable to identify subtle reductions in T2 contrast objectively. Relatively small temporal changes of this variable following hypoxia-ischaemia may render this measure suboptimal surrogate biomarker for the tissue injury, however, it was interesting that the T2 relaxation time was predominantly associated with apoptotic cell death. Although further studies are needed to elucidate the exact micro-structural change of apoptotic cell death associated with T2 prolongation, in future, T2 maps may additionally provide specific information about delayed and prolonged tissue damage via apoptosis when it is used in combination with other magnetic resonance biomarkers.

5.3.6 Clinical implications

Monitoring of the regional evolution of secondary energy failure using the maps of ADC may help predict histo-pathological brain injury corresponding to both the same timing of

and up to 18 hours after the imaging acquisition. For example, if regional ADC suggests the survival of considerable fraction of neurons at the time of scan, and the likelihood of profound cerebral injury after 18 hours without efficient treatment, one may be able to introduce invasive but efficient neuroprotective treatments even out of generally accepted window of opportunity for the treatment. Clinically reliable threshold levels of ADC drops need to be established, with which one can predict later brain injury before overt, global drops in ADC are observed reflecting the development of secondary energy failure.

5.3.7 Limitations of the study

The current study used variable experimental durations after resuscitation to investigate the relationship between histo-pathological brain injury and magnetic resonance biomarkers obtained a certain time interval before termination, and hence, we were unable to identify specific biomarkers and timings for acquisition, which provide optimal predictive value for the endpoint histo-pathological brain injury. Because most animals were sacrificed between 24 and 48 hours after the commencement of resuscitation, we were unable to assess the predictive value of magnetic resonance biomarkers both later than 24 hours after resuscitation and earlier than 24 hours before termination. T2 maps were obtained within a limited number of subjects, which may in part be responsible for their lack in predictive values for histo-pathological brain injury using this modality. In addition, we were unable to include temporal and spatial changes in FA for the current analysis, which might provide optimal diagnostic utility in the white matter.
Acquisition intervals for magnetic resonance biomarkers were limited for technical reasons, resulting in uncertainty around the optimal timing in acquiring magnetic resonance biomarkers to predict the outcome. Our assumption that regional variations of ADC following hypoxia-ischaemia reflect local energy metabolism might be wrong given the superior predictive value of global PCr/Pi compared to regional ADC for regional histo-pathological injury. It was of note that the correlation between ADC and histo-pathological injury was relatively weak in small deep structures such as the caudate nucleus and the posterior limb of the internal capsule, which could be attributed to the inaccuracy in calculating ADC values in small RoIs. Further studies are needed using ^{31}P MRS imaging to identify associations between regional energy metabolism, ADC values, long term MRS and histological outcome (150).

5.3.8 Future studies

Clinical studies have to establish the relationship between ADC changes at different time point after resuscitation and eventual patters and depths of injury using both conventional and volumetric MRI as endpoint markers. Although T2 maps provided much less information in predicting the tissue damage, difference in the temporal changes with a range of apoptotic cell death may be worth investigation to see whether these maps are useful to discriminate specific types of cellular death and their early signs especially in conjunction with other magnetic resonance biomarkers.

5.3.9 Conclusions

Findings in the maps of ADC following transient hypoxia-ischaemia, although highly sensitive during the acute phase, have thus far considered as a difficult variable to interpret into clinical information because of their dynamic temporal changes after hypoxia-ischaemia (64). However, our current study highlighted that absolute ADC values obtained during the evolutional phase of secondary energy failure can precisely predict the tissue damage at and up to 18 hours after the data acquisition; analysis with the time-series data after resuscitation showed modest predictive values of ^{31}P MRS and ADC for the end point brain injury as early as 3 to 6 hours after resuscitation. Future studies have to validate the level of ADC change corresponding to mild, moderate and severe tissue damage for each time point after hypoxia-ischaemia, so that the natural course can be predicted with early, subtle changes in regional ADC values.

Chapter 6: Overall conclusion and implication of the findings from this thesis

6.1 Conclusions

A more severe acute insult led to a shorter latent phase duration, more severe secondary energy failure and more deleterious brain damage. Although energy metabolism recovers to the normal level at a glance, subtle increase in PCr and Pi relative to EPP may identify subjects with favourable and unfavourable outcomes in energy metabolism. During the evolutional phase of secondary energy failure, global PCr/Pi was the most sensitive early marker which provided robust prediction of endpoint histo-pathological brain injury up to 24 hours in advance of termination. Regional ADC, although inferior to global PCr/Pi, also demonstrated sufficient predictive values for the endpoint brain injury with spatial resolution. Evolution of secondary energy failure was heterogeneous between subjects and cerebral regions, according to the variations in the severity of hypoxia-ischaemia, susceptibility of specific subjects and regions, and the response to resuscitation.

Maps of ADC have been utilised as a reliable surrogate biomarker for high energy phosphates; in our study, regional ADC obtained up to 18 hours before termination predicted later neuronal, glial and axonal injury. Regional ADC also predicted the endpoint neuronal injury and microglial reaction as early as 12 hours after resuscitation, the period of which is within the latent phase for most subjects when assessed by global NTP/EPP. Thus far, ADC values following hypoxia-ischaemia have been considered to be of limited utility because of their dynamic and multiphasic changes after the acute event (64). However, our current findings suggested that, when obtained during the evolutional phase of secondary energy failure i.e. within up to 48 hours after resuscitation, ADC values may provide highly useful information to predict the pattern and severity of tissue damages. Further evidence is required to establish ADC ranges corresponding to specific outcomes at different stages after hypoxia-ischaemia.

6.2 Latent phase, secondary energy failure and tissue homeostasis

The discovery of secondary energy failure following hypoxia-ischaemia in late 1980s to 1990s (42-44) gave an illusion to clinicians and investigators as if cerebral energy metabolism recovers to the normal function after successful resuscitation. However, despite sufficient supply in oxygen and energy substrates to the brain, the latent phase is followed by an overt loss of high energy phosphate after 8 to 24 hours of resuscitation. Recent experimental and clinical studies which addressed the evolutional period of secondary energy failure suggested the presence of substantial metabolic derangement and tissue destruction has been confirmed even before or during the early evolutional stage of secondary energy failure (45, 53, 78, 79), highlighting the importance of understanding injury reactions which are processed during the latent phase. Given the wide range of deleterious chemical reactions which are activated shortly after reoxygenation and reperfusion (41, 151), it is more likely that, following severe hypoxia-ischaemia but before the evolution of overt secondary energy failure, cerebral tissue is maintaining a normal balance between energetic metabolites only by maximising salvage systems to compensate for damaged cytoplasmic organelle such as mitochondria and endoplasmic reticulum (41, 101). Subtle increase in PCr and Pi, and subnormal ADC levels observed during the latent phase may be the signs suggestive of on-going competitions between deleterious injury program and protection program.

6.3 Magnetic resonance biomarkers and histo-pathological findings

Global ^{31}P MRS biomarkers and regional ADC showed good predictive values for later histo-pathological brain injury over most cerebral regions. However, the association between these biomarkers and CD68 expression was mainly observed within superficial part of the brain, presumably because of the higher incidence of CD68 positive microglia and vessels in the cortical grey matter compared to the deep grey matter. Although the spatial information provided by ADC maps may improve the quality of diagnosis to identify regionally heterogeneous evolution of secondary energy failure, agreements between regional ADC values and histo-pathological injury appeared to be relatively worse in small deep regions such as the caudate nucleus and the posterior limb of the internal capsule, suggesting that the placement of small RoIs for ADC maps (and potentially for T2 maps) is technically unreliable. Our current findings need to be confirmed in future experimental studies using consistent study durations. Although the regional T2 relaxation time was insensitive to most cerebral injury observed during the acute phase, it showed specific sensitivity to apoptotic cell death in the cortical grey matter; these maps may be used to predict prolonged tissue damage via apoptosis when they are combined with other magnetic resonance biomarkers.

6.4 Monitoring of secondary energy failure

Because of spatially highly heterogeneous evolution of secondary energy failure, the maps of ADC appear to be more suitable to monitor the energy metabolism after hypoxia-ischaemia. Thus far, it remains unclear why temporal changes in ADC mimics those in high energy phosphates; it is presumed that the maintenance of the normal spatial distribution for intracellular and extracellular water is of high energy demand, and that, with energy deficit of even short period, significant reductions in water diffusion can be observed (152). In our current study, early absolute ADC values obtained within 48 hours of birth predicted the natural histo-pathological outcome even without referring to the baseline data. Early reductions in regional ADC to subnormal levels are suggestive of later development of substantial cerebral injury.

Although the predictive value of global ^{31}P MRS biomarkers, especially PCr/Pi, was optimal, these markers have significant clinical limitations, because currently, only few institutions have access to a spectrometer which can obtain ^{31}P MRS from the newborn brain. In contrast, ADC maps are available using most existing MRI scanners within a short period. Further experimental studies may help promote ADC maps during the evolutional phase of secondary energy failure into a handy, standard biomarker after perinatal hypoxia-ischaemia. Studies in ^{31}P MRS also need to establish absolute quantification of phosphates from the whole brain to discriminate the tissue loss from reductions in phosphates, and also to give temporal changes in regional ^{31}P MRS measures using MRS imaging.

6.5 Secondary energy failure and cerebral protection

Our current findings suggested that the severity of acute insult is positively correlated with the brevity of the latent phase duration, which is likely to include the therapeutic time window for hypothermia and most other neuroprotective treatments. Neuroprotective interventions should be commenced as early as possible given the evidence to support the process of deleterious chemical reactions even during the latent phase (11). For subjects who experienced the most severe hypoxia-ischaemia, very early interventions such as pre-hospital cooling may increase the opportunity to respond the treatment (153). Maps of ADC, by providing the spatial pattern of metabolic derangement, may help improve the choice of treatments, as we have previously reported that different body temperatures are likely to lead to spatially different protection patterns of the cerebral tissue (49). Similarly, if early evolution of apoptotic cell death is noticed using T2 maps, additional pharmacological treatments targeting pro-apoptotic proteins can be applied as a tailored treatment (41, 154).

6.6 Strength and limitation

We were able to obtain a range of magnetic resonance biomarkers including ^{31}P MRS and maps of ADC and T2 relaxation time. However, because of the limited acquisition cycle, we were unable to include ^{1}H MRS, which has been demonstrated to be the optimal clinical biomarker to predict the neurodevelopmental outcome after perinatal hypoxia-ischaemia (58). For the current study, we were able to use an established piglet model of perinatal asphyxial encephalopathy (42, 47, 49, 155, 156). This model was established as a clinically relevant translational model where intensive life support can be provided mimicking the clinical intensive cares for sick newborn infants. Bridging biomarkers such as near infrared spectroscopy, aEEG, MRS and MRI can be obtained and validated for the potential use in the human newborn infants. In addition, the use of a large animal enabled us to compare magnetic resonance biomarkers and histo-pathological outcomes in different cerebral regions. In contrast, because our model induces terminal anaesthesia, we were unable to assess the neurological functioning associated with spatial injury patterns observed on magnetic resonance biomarkers and histo-pathologically assessed brain injury. In addition, our model still varies from human newborn infants who experienced perinatal hypoxia-ischaemia, where the onset, pattern, repetition and depth of hypoxia-ischaemia are various and difficult to extrapolate. Another limitation is that, for the ethical and practical reason, we were unable to maintain the model longer than 48 hours after the commencement of resuscitation, resulting in the lack of observations on magnetic resonance biomarkers during the period when ADC values are likely to start to pseudo-normalise.

6.7 Future studies

Although our current findings suggested the benefit of using regional ADC as a surrogate biomarker for cerebral tissue energy metabolism and subsequent tissue damage, further validation studies in both preclinical and clinical settings are required (i) to confirm the relationship between regional ADC and phosphate levels assessed using MRS imaging; (ii) to elucidate typical fractional ADC reductions from the institutional standard corresponding to normal, mild, moderate and severe later tissue destructions; and (iii) to confirm the optimal placement of RoIs which provides reproducible measures of ADC in each region. In addition to the standardisation of normal and abnormal ranges of ADC for each maturational stage, it is also of great interest to investigate whether ^{1}H MRS or ^{1}H MRS imaging can provide better surrogate biomarker for tissue energy derangement and ultimate tissue injury. Given that temporal changes in ^{1}H MRS metabolites such as lactate/NAA show monotonic increase after severe hypoxia-ischaemia, this measure can be useful biomarker especially during the period when ADC shows pseudo-normalisation (58).

6.8 Implication of the findings from this thesis

Infants with most severe neonatal encephalopathy may benefit from induction of therapeutic interventions as early as possible because of the extremely short therapeutic time window. Normal energetic metabolites obtained later than 24 hours of hypoxia-ischaemia may be indicative of relatively longer latent phase and optimal metabolic and histo-pathological outcomes. By identifying subtle abnormalities in global cerebral PCr/Pi as well as regional ADC, the severity of secondary energy failure and histo-pathological cerebral injury can be predicted. Future studies need to address the threshold of magnetic resonance biomarkers suggestive of later severe cerebral injury and the timing when the predictive value of ADC is lost due to pseudo-normalisation.

Bibliography

1. Lawn JE, Cousens S, Zupan J. 4 million neonatal deaths: when? Where? Why? Lancet. 2005;365(9462):891-900.
2. Roka A, Azzopardi D. Therapeutic hypothermia for neonatal hypoxic ischaemic encephalopathy. Early Hum Dev. 2010;86(6):361-7. Epub 2010/06/24.
3. Kurinczuk JJ, White-Koning M, Badawi N. Epidemiology of neonatal encephalopathy and hypoxic-ischaemic encephalopathy. Early Hum Dev. 2010;86(6):329-38. Epub 2010/06/18.
4. Vannucci RC. Current and potentially new management strategies for perinatal hypoxic-ischemic encephalopathy. Pediatrics. 1990;85(6):961-8.
5. Odd DE, Lewis G, Whitelaw A, Gunnell D. Resuscitation at birth and cognition at 8 years of age: a cohort study. Lancet. 2009;373(9675):1615-22.
6. Lee AC, Mullany LC, Tielsch JM, Katz J, Khatry SK, LeClerq SC, et al. Incidence of and risk factors for neonatal respiratory depression and encephalopathy in rural Sarlahi, Nepal. Pediatrics. 2011;128(4):e915-24. Epub 2011/09/29.
7. Azzopardi DV, Strohm B, Edwards AD, Dyet L, Halliday HL, Juszczak E, et al. Moderate hypothermia to treat perinatal asphyxial encephalopathy. N Engl J Med. 2009;361(14):1349-58. Epub 2009/10/03.
8. Gluckman PD, Wyatt JS, Azzopardi D, Ballard R, Edwards AD, Ferriero DM, et al. Selective head cooling with mild systemic hypothermia after neonatal encephalopathy: multicentre randomised trial. Lancet. 2005;365(9460):663-70. Epub 2005/02/22.
9. Shankaran S, Laptook AR, Ehrenkranz RA, Tyson JE, McDonald SA, Donovan EF, et al. Whole-body hypothermia for neonates with hypoxic-ischemic encephalopathy. NEnglJMed. 2005;353(15):1574-84.
10. Higgins RD, Raju T, Edwards AD, Azzopardi DV, Bose CL, Clark RH, et al. Hypothermia and other treatment options for neonatal encephalopathy: an executive summary of the Eunice Kennedy Shriver NICHD workshop. J Pediatr. 2011;159(5):851-8 e1. Epub 2011/08/31.
11. Robertson NJ, Iwata O. Bench to bedside strategies for optimizing neuroprotection following perinatal hypoxia-ischaemia in high and low resource settings. Early Hum Dev. 2007;83(12):801-11. Epub 2007/10/30.
12. Edwards AD, Brocklehurst P, Gunn AJ, Halliday H, Juszczak E, Levene M, et al. Neurological outcomes at 18 months of age after moderate hypothermia for perinatal hypoxic ischaemic encephalopathy: synthesis and meta-analysis of trial data. BMJ. 2010;340:c363. Epub 2010/02/11.
13. Sarnat HB, Sarnat MS. Neonatal encephalopathy following fetal distress. A clinical and electroencephalographic study. Arch Neurol. 1976;33(10):696-705. Epub 1976/10/01.
14. Dijxhoorn MJ, Visser GH, Huisjes HJ, Fidler V, Touwen BC. The relation between umbilical pH values and neonatal neurological morbidity in full term appropriate-for-dates infants. Early Hum Dev. 1985;11(1):33-42. Epub 1985/05/01.
15. Fahey J, King TL. Intrauterine asphyxia: clinical implications for providers of intrapartum care. Journal of midwifery & women's health. 2005;50(6):498-506. Epub 2005/11/02.
16. van de Riet JE, Vandenbussche FP, Le Cessie S, Keirse MJ. Newborn assessment and long-term adverse outcome: a systematic review. Am J Obstet Gynecol. 1999;180(4):1024-9. Epub 1999/04/16.

17. Wildschut J, Feron FJ, Hendriksen JG, van Hall M, Gavilanes-Jiminez DW, Hadders-Algra M, et al. Acid-base status at birth, spontaneous motor behaviour at term and 3 months and neurodevelopmental outcome at age 4 years in full-term infants. Early Hum Dev. 2005;81(6):535-44. Epub 2005/06/07.
18. van den Berg PP, Nelen WL, Jongsma HW, Nijland R, Kollee LA, Nijhuis JG, et al. Neonatal complications in newborns with an umbilical artery pH < 7.00. Am J Obstet Gynecol. 1996;175(5):1152-7. Epub 1996/11/01.
19. Malin GL, Morris RK, Khan KS. Strength of association between umbilical cord pH and perinatal and long term outcomes: systematic review and meta-analysis. BMJ. 2010;340:c1471. Epub 2010/05/15.
20. Laptook AR, Shankaran S, Ambalavanan N, Carlo WA, McDonald SA, Higgins RD, et al. Outcome of term infants using apgar scores at 10 minutes following hypoxic-ischemic encephalopathy. Pediatrics. 2009;124(6):1619-26. Epub 2009/12/02.
21. Drage JS, Kennedy C, Schwarz BK. The Apgar Score as an Index of Neonatal Mortality. A Report from the Collaborative Study of Cerebral Palsy. Obstetrics and gynecology. 1964;24:222-30. Epub 1964/08/01.
22. Apgar V, Holaday DA, James LS, Weisbrot IM, Berrien C. Evaluation of the newborn infant; second report. J Am Med Assoc. 1958;168(15):1985-8. Epub 1958/12/13.
23. Thompson CM, Puterman AS, Linley LL, Hann FM, van der Elst CW, Molteno CD, et al. The value of a scoring system for hypoxic ischaemic encephalopathy in predicting neurodevelopmental outcome. Acta Paediatr. 1997;86(7):757-61. Epub 1997/07/01.
24. Bao XL, Yu RJ, Li ZS. 20-item neonatal behavioral neurological assessment used in predicting prognosis of asphyxiated newborn. Chinese medical journal. 1993;106(3):211-5. Epub 1993/03/01.
25. Lipper EG, Voorhies TM, Ross G, Vannucci RC, Auld PA. Early predictors of one-year outcome for infants asphyxiated at birth. Dev Med Child Neurol. 1986;28(3):303-9. Epub 1986/06/01.
26. Portman RJ, Carter BS, Gaylord MS, Murphy MG, Thieme RE, Merenstein GB. Predicting neonatal morbidity after perinatal asphyxia: a scoring system. Am J Obstet Gynecol. 1990;162(1):174-82. Epub 1990/01/01.
27. Tao JD, Mathur AM. Using amplitude-integrated EEG in neonatal intensive care. J Perinatol. 2010;30 Suppl:S73-81. Epub 2010/10/12.
28. Holmes G, Rowe J, Hafford J, Schmidt R, Testa M, Zimmerman A. Prognostic value of the electroencephalogram in neonatal asphyxia. Electroencephalography and clinical neurophysiology. 1982;53(1):60-72. Epub 1982/01/01.
29. Murray DM, Boylan GB, Ryan CA, Connolly S. Early EEG findings in hypoxic-ischemic encephalopathy predict outcomes at 2 years. Pediatrics. 2009;124(3):e459-67. Epub 2009/08/27.
30. Shah DK, de Vries LS, Hellstrom-Westas L, Toet MC, Inder TE. Amplitude-integrated electroencephalography in the newborn: a valuable tool. Pediatrics. 2008;122(4):863-5. Epub 2008/10/03.
31. Maynard D, Prior PF, Scott DF. Device for continuous monitoring of cerebral activity in resuscitated patients. Br Med J. 1969;4(5682):545-6. Epub 1969/11/29.
32. Tich SN, d'Allest AM, Villepin AT, de Belliscize J, Walls-Esquivel E, Salefranque F, et al. Pathological features of neonatal EEG in preterm babies born before 30 weeks of gestationnal age. Neurophysiologie clinique = Clinical neurophysiology. 2007;37(5):325-70. Epub 2007/12/08.

33. Toet MC, Hellstrom-Westas L, Groenendaal F, Eken P, de Vries LS. Amplitude integrated EEG 3 and 6 hours after birth in full term neonates with hypoxic-ischaemic encephalopathy. Arch Dis Child Fetal Neonatal Ed. 1999;81(1):F19-23. Epub 1999/06/22.
34. Takenouchi T, Rubens EO, Yap VL, Ross G, Engel M, Perlman JM. Delayed onset of sleep-wake cycling with favorable outcome in hypothermic-treated neonates with encephalopathy. J Pediatr. 2011;159(2):232-7. Epub 2011/03/01.
35. Hellstrom-Westas L, Rosen I, Svenningsen NW. Predictive value of early continuous amplitude integrated EEG recordings on outcome after severe birth asphyxia in full term infants. Arch Dis Child Fetal Neonatal Ed. 1995;72(1):F34-8. Epub 1995/01/01.
36. Thoresen M. Hypothermia after perinatal asphyxia: selection for treatment and cooling protocol. J Pediatr. 2011;158(2 Suppl):e45-9. Epub 2011/02/02.
37. Rutherford M, Malamateniou C, McGuinness A, Allsop J, Biarge MM, Counsell S. Magnetic resonance imaging in hypoxic-ischaemic encephalopathy. Early Hum Dev. 2010;86(6):351-60. Epub 2010/06/15.
38. Counsell SJ, Tranter SL, Rutherford MA. Magnetic resonance imaging of brain injury in the high-risk term infant. Semin Perinatol. 2010;34(1):67-78. Epub 2010/01/30.
39. Iwata S, Bainbridge A, Nakamura T, Tamura M, Takashima S, Matsuishi T, et al. Subtle white matter injury is common in term-born infants with a wide range of risks. Int J Dev Neurosci. 2010;28(7):573-80. Epub 2010/08/03.
40. Leijser LM, Vein AA, Liauw L, Strauss T, Veen S, Wezel-Meijler G. Prediction of short-term neurological outcome in full-term neonates with hypoxic-ischaemic encephalopathy based on combined use of electroencephalogram and neuro-imaging. Neuropediatrics. 2007;38(5):219-27. Epub 2008/03/12.
41. Thornton C, Rousset CI, Kichev A, Miyakuni Y, Vontell R, Baburamani AA, et al. Molecular mechanisms of neonatal brain injury. Neurology research international. 2012;2012:506320. Epub 2012/03/01.
42. Lorek A, Takei Y, Cady EB, Wyatt JS, Penrice J, Edwards AD, et al. Delayed ("secondary") cerebral energy failure after acute hypoxia-ischemia in the newborn piglet: continuous 48-hour studies by phosphorus magnetic resonance spectroscopy. PediatrRes. 1994;36(6):699-706.
43. Azzopardi D, Wyatt JS, Cady EB, Delpy DT, Baudin J, Stewart AL, et al. Prognosis of newborn infants with hypoxic-ischemic brain injury assessed by phosphorus magnetic resonance spectroscopy. PediatrRes. 1989;25(5):445-51.
44. Hope PL, Costello AM, Cady EB, Delpy DT, Tofts PS, Chu A, et al. Cerebral energy metabolism studied with phosphorus NMR spectroscopy in normal and birth-asphyxiated infants. Lancet. 1984;2(8399):366-70.
45. Martin E, Buchli R, Ritter S, Schmid R, Largo RH, Boltshauser E, et al. Diagnostic and prognostic value of cerebral 31P magnetic resonance spectroscopy in neonates with perinatal asphyxia. PediatrRes. 1996;40(5):749-58.
46. Roth SC, Baudin J, Cady E, Johal K, Townsend JP, Wyatt JS, et al. Relation of deranged neonatal cerebral oxidative metabolism with neurodevelopmental outcome and head circumference at 4 years. DevMedChild Neurol. 1997;39(11):718-25.
47. O'Brien FE, Iwata O, Thornton JS, De Vita E, Sellwood MW, Iwata S, et al. Delayed whole-body cooling to 33 or 35 degrees C and the development of impaired energy generation consequential to transient cerebral hypoxia-ischemia in the newborn piglet. Pediatrics. 2006;117(5):1549-59. Epub 2006/05/03.

48. Gunn AJ, Gunn TR, Gunning MI, Williams CE, Gluckman PD. Neuroprotection with prolonged head cooling started before postischemic seizures in fetal sheep. Pediatrics. 1998;102(5):1098-106.
49. Iwata O, Thornton JS, Sellwood MW, Iwata S, Sakata Y, Noone MA, et al. Depth of delayed cooling alters neuroprotection pattern after hypoxia-ischemia. Ann Neurol. 2005;58(1):75-87. Epub 2005/06/29.
50. Graulich J, Hoffmann U, Maier RF, Ruscher K, Pomper JK, Ko HK, et al. Acute neuronal injury after hypoxia is influenced by the reoxygenation mode in juvenile hippocampal slice cultures. Brain ResDevBrain Res. 2002;137(1):35-42.
51. Meng S, Qiao M, Foniok T, Tuor UI. White matter damage precedes that in gray matter despite similar magnetic resonance imaging changes following cerebral hypoxia-ischemia in neonatal rats. ExpBrain Res. 2005;166(1):56-60.
52. Baiden-Amissah K, Joashi U, Blumberg R, Mehmet H, Edwards AD, Cox PM. Expression of amyloid precursor protein (beta-APP) in the neonatal brain following hypoxic ischaemic injury. NeuropatholApplNeurobiol. 1998;24(5):346-52.
53. Puka-Sundvall M, Gajkowska B, Cholewinski M, Blomgren K, Lazarewicz JW, Hagberg H. Subcellular distribution of calcium and ultrastructural changes after cerebral hypoxia-ischemia in immature rats. Brain ResDevBrain Res. 2000;125(1-2):31-41.
54. Cady EB, Iwata O, Bainbridge A, Wyatt JS, Robertson NJ. Phosphorus magnetic resonance spectroscopy 2 h after perinatal cerebral hypoxia-ischemia prognosticates outcome in the newborn piglet. J Neurochem. 2008;107(4):1027-35. Epub 2008/09/13.
55. Robertson NJ, Cox IJ. Magnetic resonance spectroscopy of the neonatal brain. In: Rutherford MMRI of the neonatal brainLondon: WB Saunders, 2002:295-313. 2006.
56. Penrice J, Cady EB, Lorek A, Wylezinska M, Amess PN, Aldridge RF, et al. Proton magnetic resonance spectroscopy of the brain in normal preterm and term infants, and early changes after perinatal hypoxia-ischemia. PediatrRes. 1996;40(1):6-14.
57. Penrice J, Lorek A, Cady EB, Amess PN, Wylezinska M, Cooper CE, et al. Proton magnetic resonance spectroscopy of the brain during acute hypoxia-ischemia and delayed cerebral energy failure in the newborn piglet. PediatrRes. 1997;41(6):795-802.
58. Thayyil S, Chandrasekaran M, Taylor A, Bainbridge A, Cady EB, Chong WK, et al. Cerebral magnetic resonance biomarkers in neonatal encephalopathy: a meta-analysis. Pediatrics. 2010;125(2):e382-95. Epub 2010/01/20.
59. Urenjak J, Williams SR, Gadian DG, Noble M. Specific expression of N-acetylaspartate in neurons, oligodendrocyte-type-2 astrocyte progenitors, and immature oligodendrocytes in vitro. J Neurochem. 1992;59(1):55-61. Epub 1992/07/01.
60. Mehmet H, Yue X, Penrice J, Cady E, Wyatt JC, Sarraf C, et al. Relation of impaired energy metabolism to apoptosis and necrosis following transient cerebral hypoxia-ischaemia. Cell DeathDiffer. 1998;5(4):321-9.
61. Kreis R, Ernst T, Ross BD. Development of the human brain: in vivo quantification of metabolite and water content with proton magnetic resonance spectroscopy. Magn Reson Med. 1993;30(4):424-37. Epub 1993/10/01.
62. Thornton JS, Ordidge RJ, Penrice J, Cady EB, Amess PN, Punwani S, et al. Temporal and anatomical variations of brain water apparent diffusion coefficient in perinatal cerebral hypoxic-ischemic injury: relationships to cerebral energy metabolism. Magn ResonMed. 1998;39(6):920-7.

63. Rutherford MA, Ward P, Malamatentiou C. Advanced MR techniques in the term-born neonate with perinatal brain injury. SeminFetal Neonatal Med. 2005;10(5):445-60.
64. Barkovich AJ, Miller SP, Bartha A, Newton N, Hamrick SE, Mukherjee P, et al. MR imaging, MR spectroscopy, and diffusion tensor imaging of sequential studies in neonates with encephalopathy. AJNR AmJNeuroradiol. 2006;27(3):533-47.
65. Vermeulen RJ, van Schie PE, Hendrikx L, Barkhof F, van Weissenbruch M, Knol DL, et al. Diffusion-weighted and conventional MR imaging in neonatal hypoxic ischemia: two-year follow-up study. Radiology. 2008;249(2):631-9. Epub 2008/09/18.
66. Ward P, Counsell S, Allsop J, Cowan F, Shen Y, Edwards D, et al. Reduced fractional anisotropy on diffusion tensor magnetic resonance imaging after hypoxic-ischemic encephalopathy. Pediatrics. 2006;117(4):e619-e30.
67. Steen RG, Ogg RJ, Reddick WE, Kingsley PB. Age-related changes in the pediatric brain: quantitative MR evidence of maturational changes during adolescence. AJNR AmJNeuroradiol. 1997;18(5):819-28.
68. Williams LA, Gelman N, Picot PA, Lee DS, Ewing JR, Han VK, et al. Neonatal brain: regional variability of in vivo MR imaging relaxation rates at 3.0 T--initial experience. Radiology. 2005;235(2):595-603.
69. Hagmann CF, De Vita E, Bainbridge A, Gunny R, Kapetanakis AB, Chong WK, et al. T2 at MR imaging is an objective quantitative measure of cerebral white matter signal intensity abnormality in preterm infants at term-equivalent age. Radiology. 2009;252(1):209-17. Epub 2009/06/30.
70. Shanmugalingam S, Thornton JS, Iwata O, Bainbridge A, O'Brien FE, Priest AN, et al. Comparative prognostic utilities of early quantitative magnetic resonance imaging spin-spin relaxometry and proton magnetic resonance spectroscopy in neonatal encephalopathy. Pediatrics. 2006;118(4):1467-77. Epub 2006/10/04.
71. Brown GC, Bal-Price A. Inflammatory neurodegeneration mediated by nitric oxide, glutamate, and mitochondria. MolNeurobiol. 2003;27(3):325-55.
72. Johnston MV, Trescher WH, Ishida A, Nakajima W. Neurobiology of hypoxic-ischemic injury in the developing brain. PediatrRes. 2001;49(6):735-41.
73. Northington FJ, Ferriero DM, Graham EM, Traystman RJ, Martin LJ. Early Neurodegeneration after Hypoxia-Ischemia in Neonatal Rat Is Necrosis while Delayed Neuronal Death Is Apoptosis. NeurobiolDis. 2001;8(2):207-19.
74. Orrenius S, Zhivotovsky B, Nicotera P. Regulation of cell death: the calcium-apoptosis link. NatRevMolCell Biol. 2003;4(7):552-65.
75. Taylor DL, Edwards AD, Mehmet H. Oxidative metabolism, apoptosis and perinatal brain injury. Brain Pathol. 1999;9(1):93-117.
76. Robertson NJ, Cowan FM, Cox IJ, Edwards AD. Brain alkaline intracellular pH after neonatal encephalopathy. AnnNeurol. 2002;52(6):732-42.
77. Gunn AJ, Bennet L, Gunning MI, Gluckman PD, Gunn TR. Cerebral hypothermia is not neuroprotective when started after postischemic seizures in fetal sheep. PediatrRes. 1999;46(3):274-80.
78. Cady EB, Amess P, Penrice J, Wylezinska M, Sams V, Wyatt JS. Early cerebral-metabolite quantification in perinatal hypoxic-ischaemic encephalopathy by proton and phosphorus magnetic resonance spectroscopy. Magn Reson Imaging. 1997;15(5):605-11.
79. Vannucci RC, Towfighi J, Vannucci SJ. Secondary energy failure after cerebral hypoxia-ischemia in the immature rat. JCerebBlood Flow Metab. 2004;24(10):1090-7.

80. Johnston MV, Hoon AH, Jr. Possible mechanisms in infants for selective basal ganglia damage from asphyxia, kernicterus, or mitochondrial encephalopathies. J Child Neurol. 2000;15(9):588-91. Epub 2000/10/06.
81. Myers RE. Four patterns of perinatal brain damage and their conditions of occurrence in primates. Advances in neurology. 1975;10:223-34. Epub 1975/01/01.
82. Myers RE. Two patterns of perinatal brain damage and their conditions of occurrence. Am J Obstet Gynecol. 1972;112(2):246-76. Epub 1972/01/15.
83. Barkovich AJ, Hajnal BL, Vigneron D, Sola A, Partridge JC, Allen F, et al. Prediction of neuromotor outcome in perinatal asphyxia: evaluation of MR scoring systems. AJNR AmJNeuroradiol. 1998;19(1):143-9.
84. McQuillen PS, Ferriero DM. Selective vulnerability in the developing central nervous system. PediatrNeurol. 2004;30(4):227-35.
85. Sie LT, van der Knaap MS, Oosting J, De Vries LS, Lafeber HN, Valk J. MR patterns of hypoxic-ischemic brain damage after prenatal, perinatal or postnatal asphyxia. Neuropediatrics. 2000;31(3):128-36.
86. Volpe JJ. Hypoxic-Ischemic Encephalopathy. Neurology of Newborn2008. p. 245-480.
87. Agnew DM, Koehler RC, Guerguerian AM, Shaffner DH, Traystman RJ, Martin LJ, et al. Hypothermia for 24 hours after asphyxic cardiac arrest in piglets provides striatal neuroprotection that is sustained 10 days after rewarming. PediatrRes. 2003;54(2):253-62.
88. Tooley JR, Satas S, Porter H, Silver IA, Thoresen M. Head cooling with mild systemic hypothermia in anesthetized piglets is neuroprotective. AnnNeurol. 2003;53(1):65-72.
89. Busto R, Globus MY, Dietrich WD, Martinez E, Valdes I, Ginsberg MD. Effect of mild hypothermia on ischemia-induced release of neurotransmitters and free fatty acids in rat brain. Stroke. 1989;20(7):904-10.
90. Kil HY, Zhang J, Piantadosi CA. Brain temperature alters hydroxyl radical production during cerebral ischemia/reperfusion in rats. JCerebBlood Flow Metab. 1996;16(1):100-6.
91. McCullough JN, Zhang N, Reich DL, Juvonen TS, Klein JJ, Spielvogel D, et al. Cerebral metabolic suppression during hypothermic circulatory arrest in humans. AnnThoracSurg. 1999;67(6):1895-9.
92. Zeevalk GD, Nicklas WJ. Hypothermia, metabolic stress, and NMDA-mediated excitotoxicity. JNeurochem. 1993;61(4):1445-53.
93. Simbruner G, Mittal RA, Rohlmann F, Muche R. Systemic hypothermia after neonatal encephalopathy: outcomes of neo.nEURO.network RCT. Pediatrics. 2010;126(4):e771-8. Epub 2010/09/22.
94. Zhou WH, Cheng GQ, Shao XM, Liu XZ, Shan RB, Zhuang DY, et al. Selective Head Cooling with Mild Systemic Hypothermia After Neonatal Hypoxic-Ischemic Encephalopathy: A Multicenter Randomized Controlled Trial in China. J Pediatr. 2010. Epub 2010/05/22.
95. Jacobs SE, Morley CJ, Inder TE, Stewart MJ, Smith KR, McNamara PJ, et al. Whole-body hypothermia for term and near-term newborns with hypoxic-ischemic encephalopathy: a randomized controlled trial. Arch Pediatr Adolesc Med. 2011;165(8):692-700. Epub 2011/04/06.
96. Perlman JM, Wyllie J, Kattwinkel J, Atkins DL, Chameides L, Goldsmith JP, et al. Part 11: neonatal resuscitation: 2010 International Consensus on Cardiopulmonary Resuscitation and Emergency Cardiovascular Care Science With Treatment Recommendations. Circulation. 2010;122(16 Suppl 2):S516-38.

Epub 2010/10/22.
97. Wyatt JS, Gluckman PD, Liu PY, Azzopardi D, Ballard R, Edwards AD, et al. Determinants of outcomes after head cooling for neonatal encephalopathy. Pediatrics. 2007;119(5):912-21.
98. Bona E, Hagberg H, Loberg EM, Bagenholm R, Thoresen M. Protective effects of moderate hypothermia after neonatal hypoxia-ischemia: short- and long-term outcome. PediatrRes. 1998;43(6):738-45.
99. Haaland K, Loberg EM, Steen PA, Thoresen M. Posthypoxic hypothermia in newborn piglets. PediatrRes. 1997;41(4 Pt 1):505-12.
100. Nedelcu J, Klein MA, Aguzzi A, Martin E. Resuscitative hypothermia protects the neonatal rat brain from hypoxic-ischemic injury. Brain Pathol. 2000;10(1):61-71.
101. Iwata O, Iwata S. Filling the evidence gap: how can we improve the outcome of neonatal encephalopathy in the next 10 years? Brain Dev. 2011;33(3):221-8. Epub 2010/12/28.
102. Faulkner S, Bainbridge A, Kato T, Chandrasekaran M, Kapetanakis AB, Hristova M, et al. Xenon augmented hypothermia reduces early lactate/N-acetylaspartate and cell death in perinatal asphyxia. Ann Neurol. 2011;70(1):133-50. Epub 2011/06/16.
103. Ma D, Hossain M, Chow A, Arshad M, Battson RM, Sanders RD, et al. Xenon and hypothermia combine to provide neuroprotection from neonatal asphyxia. AnnNeurol. 2005;58(2):182-93.
104. Dietrich WD, Atkins CM, Bramlett HM. Protection in animal models of brain and spinal cord injury with mild to moderate hypothermia. J Neurotrauma. 2009;26(3):301-12. Epub 2009/02/28.
105. Guan J, Gunn AJ, Sirimanne ES, Tuffin J, Gunning MI, Clark R, et al. The window of opportunity for neuronal rescue with insulin-like growth factor-1 after hypoxia-ischemia in rats is critically modulated by cerebral temperature during recovery. JCerebBlood Flow Metab. 2000;20(3):513-9.
106. Liu Y, Barks JD, Xu G, Silverstein FS. Topiramate extends the therapeutic window for hypothermia-mediated neuroprotection after stroke in neonatal rats. Stroke. 2004;35(6):1460-5.
107. Vanhamme L, van den Boogaart A, Van Huffel S. Improved method for accurate and efficient quantification of MRS data with use of prior knowledge. J Magn Reson. 1997;129(1):35-43. Epub 1998/01/04.
108. van den Boogaart A. MRUI Manual: A User's Guide to the Magnetic Resonance User Interface Software Package (Version 96.3). . Delft Technical Univ Press, Delft, The Netherlands. 1997. Epub 1997/01/04.
109. Mandel P, Edel-Harth S. Free nucleotides in the rat brain during post-natal development. J Neurochem. 1966;13(7):591-5. Epub 1966/07/01.
110. Petroff OA, Prichard JW, Behar KL, Alger JR, den Hollander JA, Shulman RG. Cerebral intracellular pH by 31P nuclear magnetic resonance spectroscopy. Neurology. 1985;35(6):781-8. Epub 1985/06/01.
111. Pettegrew JW, Withers G, Panchalingam K, Post JF. Considerations for brain pH assessment by 31P NMR. Magn Reson Imaging. 1988;6(2):135-42. Epub 1988/03/01.
112. Basser PJ, Pierpaoli C. A simplified method to measure the diffusion tensor from seven MR images. Magn Reson Med. 1998;39(6):928-34. Epub 1998/06/11.
113. Yue X, Mehmet H, Penrice J, Cooper C, Cady E, Wyatt JS, et al. Apoptosis and necrosis in the newborn piglet brain following transient cerebral hypoxia-ischaemia. NeuropatholApplNeurobiol. 1997;23(1):16-25.

114. Beilharz EJ, Williams CE, Dragunow M, Sirimanne ES, Gluckman PD. Mechanisms of delayed cell death following hypoxic-ischemic injury in the immature rat: evidence for apoptosis during selective neuronal loss. Brain ResMolBrain Res. 1995;29(1):1-14.
115. Geddes R, Vannucci RC, Vannucci SJ. Delayed cerebral atrophy following moderate hypoxia-ischemia in the immature rat. DevNeurosci. 2001;23(3):180-5.
116. Marion DW, Penrod LE, Kelsey SF, Obrist WD, Kochanek PM, Palmer AM, et al. Treatment of traumatic brain injury with moderate hypothermia. NEnglJMed. 1997;336(8):540-6.
117. Gladstone DJ, Black SE, Hakim AM. Toward wisdom from failure: lessons from neuroprotective stroke trials and new therapeutic directions. Stroke. 2002;33(8):2123-36.
118. Mehmet H, Yue X, Squier MV, Lorek A, Cady E, Penrice J, et al. Increased apoptosis in the cingulate sulcus of newborn piglets following transient hypoxia-ischaemia is related to the degree of high energy phosphate depletion during the insult. NeurosciLett. 1994;181(1-2):121-5.
119. Ackerman JJ, Grove TH, Wong GG, Gadian DG, Radda GK. Mapping of metabolites in whole animals by 31P NMR using surface coils. Nature. 1980;283(5743):167-70.
120. Black SM, Bedolli MA, Martinez S, Bristow JD, Ferriero DM, Soifer SJ. Expression of neuronal nitric oxide synthase corresponds to regions of selective vulnerability to hypoxia-ischaemia in the developing rat brain. NeurobiolDis. 1995;2(3):145-55.
121. Jensen FE. The role of glutamate receptor maturation in perinatal seizures and brain injury. IntJDevNeurosci. 2002;20(3-5):339-47.
122. Takahashi T, Shirane R, Sato S, Yoshimoto T. Developmental changes of cerebral blood flow and oxygen metabolism in children. AJNR AmJNeuroradiol. 1999;20(5):917-22.
123. Wallimann T, Dolder M, Schlattner U, Eder M, Hornemann T, O'Gorman E, et al. Some new aspects of creatine kinase (CK): compartmentation, structure, function and regulation for cellular and mitochondrial bioenergetics and physiology. Biofactors. 1998;8(3-4):229-34.
124. Bessman SP, Geiger PJ. Transport of energy in muscle: the phosphorylcreatine shuttle. Science. 1981;211(4481):448-52.
125. Saks VA, Rosenshtraukh LV, Smirnov VN, Chazov EI. Role of creatine phosphokinase in cellular function and metabolism. CanJPhysiol Pharmacol. 1978;56(5):691-706.
126. Kato H, Kogure K. Biochemical and molecular characteristics of the brain with developing cerebral infarction. Cell MolNeurobiol. 1999;19(1):93-108.
127. Kirino T, Tsujita Y, Tamura A. Induced tolerance to ischemia in gerbil hippocampal neurons. JCerebBlood Flow Metab. 1991;11(2):299-307.
128. Vannucci RC, Towfighi J, Vannucci SJ. Hypoxic preconditioning and hypoxic-ischemic brain damage in the immature rat: pathologic and metabolic correlates. JNeurochem. 1998;71(3):1215-20.
129. Glaister M. Multiple sprint work : physiological responses, mechanisms of fatigue and the influence of aerobic fitness. Sports Med. 2005;35(9):757-77.
130. Korzeniewski B, Zoladz JA. Some factors determining the PCr recovery overshoot in skeletal muscle. BiophysChem. 2005;116(2):129-36.
131. Banerjee A, Grosso MA, Brown JM, Rogers KB, Whitman GJ. Oxygen metabolite effects on creatine kinase and cardiac energetics after reperfusion. AmJPhysiol. 1991;261(2 Pt 2):H590-H7.

132. Flaherty JT, Weisfeldt ML, Bulkley BH, Gardner TJ, Gott VL, Jacobus WE. Mechanisms of ischemic myocardial cell damage assessed by phosphorus-31 nuclear magnetic resonance. Circulation. 1982;65(3):561-70.
133. Kida M, Fujiwara H, Ishida M, Kawai C, Ohura M, Miura I, et al. Ischemic preconditioning preserves creatine phosphate and intracellular pH. Circulation. 1991;84(6):2495-503.
134. Kobara M, Tatsumi T, Matoba S, Yamahara Y, Nakagawa C, Ohta B, et al. Effect of ischemic preconditioning on mitochondrial oxidative phosphorylation and high energy phosphates in rat hearts. JMolCell Cardiol. 1996;28(2):417-28.
135. Novel-Chate V, Aussedat J, Saks VA, Rossi A. Adaptation to chronic hypoxia alters cardiac metabolic response to beta stimulation: novel face of phosphocreatine overshoot phenomenon. JMolCell Cardiol. 1995;27(8):1679-87.
136. Straeter-Knowlen IM, Butterworth EJ, Buchthal SD, Hollander JA, Caulfield JB, Jennings RB, et al. PCr overshoot': a study of the duration in canine myocardium. NMR Biomed. 2002;15(1):52-9.
137. Flogel U, Godecke A, Klotz LO, Schrader J. Role of myoglobin in the antioxidant defense of the heart. FASEB J. 2004;18(10):1156-8.
138. Adcock KH, Nedelcu J, Loenneker T, Martin E, Wallimann T, Wagner BP. Neuroprotection of creatine supplementation in neonatal rats with transient cerebral hypoxia-ischemia. DevNeurosci. 2002;24(5):382-8.
139. Erecinska M, Thoresen M, Silver IA. Effects of hypothermia on energy metabolism in Mammalian central nervous system. JCerebBlood Flow Metab. 2003;23(5):513-30.
140. Wilken B, Ramirez JM, Probst I, Richter DW, Hanefeld F. Creatine protects the central respiratory network of mammals under anoxic conditions. PediatrRes. 1998;43(1):8-14.
141. Kloner RA, Jennings RB. Consequences of brief ischemia: stunning, preconditioning, and their clinical implications: part 2. Circulation. 2001;104(25):3158-67.
142. Hoffmeister HM, Stein G, Storf R, Seipel L. Phosphocreatine and adenine nucleotides in postasphyxial hearts with normal basal function and normal oxygen demand. Basic ResCardiol. 1987;82 Suppl 2:311-6.
143. Reimer KA, Hill ML, Jennings RB. Prolonged depletion of ATP and of the adenine nucleotide pool due to delayed resynthesis of adenine nucleotides following reversible myocardial ischemic injury in dogs. JMolCell Cardiol. 1981;13(2):229-39.
144. Pan JW, Takahashi K. Cerebral energetic effects of creatine supplementation in humans. AmJPhysiol RegulIntegrComp Physiol. 2007;292(4):R1745-R50.
145. Rawson ES, Clarkson PM, Price TB, Miles MP. Differential response of muscle phosphocreatine to creatine supplementation in young and old subjects. Acta Physiol Scand. 2002;174(1):57-65.
146. Buchli R, Duc CO, Martin E, Boesiger P. Assessment of absolute metabolite concentrations in human tissue by 31P MRS in vivo. Part I: Cerebrum, cerebellum, cerebral gray and white matter. Magn ResonMed. 1994;32(4):447-52.
147. Iwata O, Iwata S, Bainbridge A, De Vita E, Matsuishi T, Cady EB, et al. Supra- and sub-baseline phosphocreatine recovery in developing brain after transient hypoxia-ischaemia: relation to baseline energetics, insult severity and outcome. Brain. 2008;131(Pt 8):2220-6. Epub 2008/08/02.
148. Brierley JB, Brown AW, Meldrum BS. The nature and time course of the neuronal alterations resulting from oligaemia and hypoglycaemia in the brain of Macaca mulatta. Brain Res. 1971;25(3):483-99. Epub 1971/02/05.

149. Loberg EM, Hassel B, Fonnum F, Torvik A. Early entry of plasma proteins into damaged neurons in brain infarcts. An immunohistochemical study on experimental animals. APMIS : acta pathologica, microbiologica, et immunologica Scandinavica. 1994;102(10):771-6. Epub 1994/10/01.
150. Wyatt JS, Robertson NJ. Time for a cool head-neuroprotection becomes a reality. Early HumDev. 2005;81(1):5-11.
151. Kristian T. Metabolic stages, mitochondria and calcium in hypoxic/ischemic brain damage. Cell Calcium. 2004;36(3-4):221-33.
152. Gass A, Niendorf T, Hirsch JG. Acute and chronic changes of the apparent diffusion coefficient in neurological disorders--biophysical mechanisms and possible underlying histopathology. J Neurol Sci. 2001;186 Suppl 1:S15-23. Epub 2001/05/04.
153. Kendall GS, Kapetanakis A, Ratnavel N, Azzopardi D, Robertson NJ. Passive cooling for initiation of therapeutic hypothermia in neonatal encephalopathy. Arch Dis Child Fetal Neonatal Ed. 2010;95(6):F408-12. Epub 2010/09/28.
154. Hagberg H. Mitochondrial impairment in the developing brain after hypoxia-ischemia. JBioenergBiomembr. 2004;36(4):369-73.
155. Iwata S, Iwata O, Thornton JS, Shanmugalingam S, Bainbridge A, Peebles D, et al. Superficial brain is cooler in small piglets: neonatal hypothermia implications. Ann Neurol. 2006;60(5):578-85. Epub 2006/10/19.
156. Thoresen M, Penrice J, Lorek A, Cady EB, Wylezinska M, Kirkbride V, et al. Mild hypothermia after severe transient hypoxia-ischemia ameliorates delayed cerebral energy failure in the newborn piglet. PediatrRes. 1995;37(5):667-70.

Supplementary Material and Appendix

List of Abstracts and Presented at Meetings from this analysed data

List of Publications related to this work

List of Publications derived from this work

Appendix 1. Supplemental Tables for Chapter 4.3: “Temporal and spatial evolution of secondary energy failure and cerebral injury”

Appendix 2. "Therapeutic time window" duration decreases with increasing severity of cerebral hypoxia-ischaemia under normothermia and delayed hypothermia in newborn piglets.

Appendix 3. Supra- and sub-baseline phosphocreatine recovery in developing brain after transient hypoxia-ischaemia: relation to baseline energetics, insult severity and outcome.

List of Abstracts and Presentations at Meetings from the analysed data

- Invited Speaker at Scientific Meetings

Brain monitoring during therapeutic hypothermia.
Iwata O.
Invited lecture at the 14th Annual Meeting of the Japan Association of Brain Hypothermia, Kagoshima, Japan, July 2011.

Therapeutic hypothermia for asphyxiated newborn infants: Key factors for the promotion of standard cooling.
Iwata O.
Symposium at the 47th Annual Meeting of the Japan Society of Perinatal and Neonatal Medicine, Sapporo, Japan, July 2011.

Resuscitation and brain protection based on Consensus 2010: Practical workshop for therapeutic hypothermia.
Iwata O.
Symposium at the 56th Annual Meeting of the Japan Society for Premature and Newborn Medicine, Tokyo, Japan, November 2011.

Illusion or reality? Acute cerebral injury and advanced magnetic resonance imaging.
Iwata O.
Symposium at the 52nd Annual Meeting of the Japanese Society of Child Neurology, Fukuoka, Japan, May 2010.

Years of practice without essential knowledge: What to do next to protect developing brain?
Iwata O, Iwata S.
Invited lecture at the 10th Asian and Oceanian Congress of Child Neurology, Daegu, Korea, June 2009.

Bench to bedside, Tertiary Centers to the developing world. "Tailoring" best available neuroprotection in high and low resource settings.
Iwata O, Iwata S.
Invited lecture at Annual Malaysian Perinatal Congress, Kuala Lumpur, Malaysia, April 2008.

Mechanism of perinatal brain injury, seizure and treatments.
Iwata O.
Symposium at the 53rd Annual Meeting of the Japan Society for Premature and Newborn Medicine, Sapporo, Japan, October, 2008.

Bench to Bedside, Tertiary Centres to Developing World: "Tailoring" Best Available Neuroprotection in High and Low Resource Settings.
Iwata O, Iwata S.
Invited lecture at the 50th Annual Meeting of the Japanese Society of Child Neurology, Tokyo, Japan, May 2008.

Therapeutic intervention in Neonatal Brain Injury.
Iwata O and Iwata S.
Invited lecture at the 9th Asian and Oceania Congress of Child Neurology, Cebu, Philippines, January 2007.

Bench to Cotside: Refining Therapeutic Hypothermia in Asphyxial Newborn Infants.
Iwata O.
Young Investigator Prize Lecture at the Summer Meeting of the Neonatal Society, Portsmouth, UK, June 2007.

Therapeutic intervention for perinatal cerebral injury: Challenge against “the sea of heterogeneity”.
Iwata O and Iwata S.
Symposium “Saving the Neonatal Brain” at the 2nd Congress of Asian Society for Pediatric Research, Yokohama, Japan, December, 2006.

- Abstracts and presentations at Scientific Meetings

Determinants of regional cerebral temperature in newborn infants.
Iwata S, Unno M, Saitsu H, Tanaka S, Okada J, Hirose A, Kanda H, Maeno Y, Matsuishi T, Iwata O.
The 115th Annual Meeting of the Japan Pediatric Society, Fukuoka, Japan, April 2012.

Hypothermic Neuroprotection for Encephalopathic Infants and Children in Japan: Past, Present and Future.
Iwata O, Kawano G, Takenouchi T, Nabetani M, Iwata S, Ueta I, Shimizu M, Ibara S, Tamura M, Nagao K.
The 4th International Hypothermia Symposium, Tokyo, Japan, September 2011.

Determination factors of regional cerebral temperatures in the newborn infant.
Iwata S, Iwata O, Oya T, Matsuishi T.
The 52nd Annual Meeting of the Japanese Society of Child Neurology, Fukuoka, Japan, May 2010.

Physiological Effects of 50% Xenon Inhaled Alone or Combined with Therapeutic Hypothermia for 24 h in an Experimental Model of Perinatal Asphyxia.
Kato T, Faulkner S, Bainbridge A, Evans S, De Vita E, Kapetanakis A, Iwata O, Cady E, Scaravilli F, Robertson NJ.
Annual Meeting of Pediatric Academic Societies, Baltimore, U.S.A, May 2009.

Indirect Evidence to Support Neuroprotective Effect of Hypothermia in Acute Child Encephalopathy.
Kawano G, Iwata O, Iwata S, Kawano K, Ohbu K, Kuki I, Yamanouchi H, Rinka H, Shiomi M, Kikuchi A, Yoshikawa H, Matsuishi T.
Annual Meeting of Pediatric Academic Societies, Baltimore, U.S.A, May 2009.

Amiloride Does Not Provide Significant Neuroprotection When Administered after Resuscitation in a Newborn Piglet Model of Perinatal Asphyxia.
Kapetanakis A, Bainbridge A, Kato T, Faulkner S, Evans S, Iwata O, Cady EB, Sacravilli F, Robertson NJ.
Annual Meeting of Pediatric Academic Societies, Baltimore, U.S.A, May 2009.

Determinants of regional brain temperature in the newborn infant: Are small body weight infants at increased risks of excessive cooling?
Iwata S, Iwata O, Kato T, Wyatt JS, Cady EB, Kanda H, Maeno Y, Matsuishi T, Robertson NJ.
The 111th Annual Meeting of the Japan Pediatric Society, Tokyo, Japan, April 2008.

Development of cooling mattress using low-tech heat buffering system: Is stable whole body cooling provided safely to asphyxiated newborn infants without electronic devices?
Iwata S, Iwata O, Kato T, Kapetanakis A, Evans S, Olson L, Setterwall F, Kanda H, Maeno Y, Matsuishi T, Lagercrantz H, Wyatt JS, Cady EB, Robertson NJ
The 111th Annual Meeting of the Japan Pediatric Society, Tokyo, Japan, April 2008.

Low-tech, Low-cost cooling device for global infant population with birth asphyxia.

Iwata S, Iwata O, Olson L, Kapetanakis A, Kato T, Evans S, Araki Y, Kakuma T, Setterwall F, Matsuishi T, Lagercrantz H, Robertson NJ
Annual Meeting of Pediatric Academic Societies, Honolulu, Hawaii, USA, May 2008.

Body-size determines regional cerebral temperature at normothermia, whole body cooling and selective head cooling.
Iwata O, Iwata S, Thornton J, Bainbridge A, MatsuishiT, Wyatt JS, Cady EB, Robertson NJ.
Annual Meeting of Pediatric Academic Societies, Honolulu, Hawaii, USA, May 2008.

"PCr recovery overshoot" in developing brain after transient hypoxia-ischaemia: relation to baseline energetics, insult severity and outcome.
Iwata O, Iwata S, Bainbridge A, De Vita E, Cady EB, Robertson NJ.
6th Hershey Conference on Developmental Brain Injury, Paris, France, June 2008.

Body-size determines regional cerebral temperature at normothermia, whole body cooling and selective head cooling.
Iwata O, Iwata S, Thornton J, Bainbridge A, MatsuishiT, Wyatt JS, Cady EB, Robertson NJ.
The 3rd Congress of Asian Society for Pediatric Research, Tokyo, Japan, October 2007.

Unexpected tight relationship between regional cerebral temperature and body weight in the newborn piglet.
Iwata S, Iwata O, Kanda H, Maeno Y, Matsuishi T, Kato T, Wyatt JS, Cady EB, Robertson NJ.
The 52nd Annual Meeting of the Japan Society for Premature and Newborn Medicine, Takamatsu, Japan, November 2007.

Cerebral insult severity, therapeutic time window and regional severity of secondary energy failure in newborn piglets.
Iwata O, De Vita E, Bainbridge A, Iwata S, Priest A, West DA, Thornton JS, Cady EB, Ordidge R, Wyatt JS, Robertson NJ
Annual Meeting of Pediatric Academic Societies, Washington DC, May 2006.

Both regional brain temperature and efficiency of cap cooling depend on body weight.
Iwata O, Iwata S, De Vita E, Bainbridge A, Thornton JS, Cady EB, Wyatt JS, Robertson NJ
Annual Meeting of Pediatric Academic Societies, Washington DC, May 2006.

Relationship between ADC and regional changes in brain metabolites from proton (^{1}H) MRS imaging in the 48 hours following transient hypoxia-ischaemia.
Bainbridge A, Iwata O, De Vita E, Iwata S, Thornton JS, Cady EB, Wyatt JS, Robertson NJ
Annual Meeting of Pediatric Academic Societies, Washington DC, May 2006.

Very early phosphorus MRS markers of outcome after transient perinatal cerebral hypoxia-ischaemia.
Cady EB, Bainbridge A, Iwata O, De Vita E, Robertson NJ.
Annual Meeting of Pediatric Academic Societies, Washington DC, May 2006.

Quantitative T2 relaxometry during 48 hours after transient hypoxia-ischemia: correlation with ^{1}H MRS imaging.
De Vita E, Bainbridge A, Iwata O, Iwata S, Thornton JS, Cady EB, Wyatt JS, Robertson NJ.
Annual Meeting of Pediatric Academic Societies, Washington DC, May 2006.

Correlation between brain-water T2 relaxometry and 1H MRSI following perinatal transient cerebral hypoxia-ischemia.
De Vita E, Bainbridge A, Iwata O, Iwata S, Thornton JS, Wyatt JS, Robertson NJ, Cady EB.
12th Scientific Meeting and Exhibition of the International Society for Magnetic Resonance in Medicine, Seattle, May 2006.

Correlation between ADC and metabolic ratios with 31P chemical shift imaging in a piglet model of hypoxia-ischaemia.
Bainbridge A, Iwata O, De Vita E, Iwata S, Thornton JS, Cady EB, Wyatt JS, Robertson NJ.
12th Scientific Meeting and Exhibition of the International Society for Magnetic Resonance in Medicine, Seattle, May 2006.

Brain water ADC and ^{1}H magnetic resonance spectroscopic imaging of cerebral metabolite ratios in a piglet hypoxia-ischaemia model.
Bainbridge A, Iwata O, De Vita E, Iwata S, Thornton JS, Cady EB, Wyatt JS, Robertson NJ.
12th Scientific Meeting and Exhibition of the International Society for Magnetic Resonance in Medicine, Seattle, May 2006.

Increased inorganic phosphate is a very early marker of adverse outcome following transient perinatal hypoxia-ischaemia.
Cady EB, Bainbridge A, Iwata O, Wyatt JS, Robertson NJ.
12th Scientific Meeting and Exhibition of the International Society for Magnetic Resonance in Medicine, Seattle, May 2006.

Changes in intracellular pH after perinatal cerebral hypoxia-ischaemia using the chemical shift of α- and β-ATP, phosphoethanolamine and inorganic phosphate.
Cady EB, Bainbridge A, Iwata O, Wyatt JS, Robertson NJ.
12th Scientific Meeting and Exhibition of the International Society for Magnetic Resonance in Medicine, Seattle, May 2006.

List of publications related to this work

1. Brain temperature in newborn piglets under selective head cooling with minimal systemic hypothermia.
   Iwata O, Iwata S, Tamura M, Nakamura T, Sugiura M, Ogiso Y.
   Pediatr Int. 2003 Apr;45(2):163-8

2. Early head cooling in newborn piglets is neuroprotective even in the absence of profound systemic hypothermia.
   Iwata O, Iwata S, Tamura M, Nakamura T, Sugiura M, Ogiso Y, Takashima S.
   Pediatr Int. 2003 Oct;45(5):522-9.

3. The AP-1 transcription factor c-Jun is required for efficient axonal regeneration.
   Raivich G, Bohatschek M, Da Costa C, Iwata O, Galiano M, Hristova M, Nateri AS, Makwana M, Riera-Sans L, Wolfer DP, Lipp HP, Aguzzi A, Wagner EF, Behrens A.
   Neuron. 2004 Jul 8;43(1):57-67.

4. Depth of delayed cooling alters neuroprotection pattern after hypoxia-ischemia.
   Iwata O, Thornton JS, Sellwood MW, Iwata S, Sakata Y, Noone MA, O'Brien FE, Bainbridge A, De Vita E, Raivich G, Peebles D, Scaravilli F, Cady EB, Ordidge R, Wyatt JS, Robertson NJ.
   Ann Neurol. 2005 Jul;58(1):75-87.

5. N-methyl-isobutyl-amiloride ameliorates brain injury when commenced before hypoxia ischemia in neonatal mice.
   Kendall GS, Robertson NJ, Iwata O, Peebles D, Raivich G.
   Pediatr Res. 2006 Feb;59(2):227-31.

6. Delayed whole-body cooling to 33 or 35 degrees C and the development of impaired energy generation consequential to transient cerebral hypoxia-ischemia in the newborn piglet.
   O'Brien FE, Iwata O, Thornton JS, De Vita E, Sellwood MW, Iwata S, Sakata YS, Charman S, Ordidge R, Cady EB, Wyatt JS, Robertson NJ.
   Pediatrics. 2006 May;117(5):1549-59.

7. Comparative prognostic utilities of early quantitative magnetic resonance imaging spin-spin relaxometry and proton magnetic resonance spectroscopy in neonatal encephalopathy.
   Shanmugalingam S, Thornton JS, Iwata O, Bainbridge A, O'Brien FE, Priest AN, Ordidge RJ, Cady EB, Wyatt JS, Robertson NJ.
   Pediatrics. 2006 Oct;118(4):1467-77.

8. Superficial brain is cooler in small piglets: neonatal hypothermia implications.
   Iwata S, Iwata O, Thornton JS, Shanmugalingam S, Bainbridge A, Peebles D, Wyatt JS, Cady EB, Robertson NJ.
   Ann Neurol. 2006 Nov;60(5):578-85.

9. Abnormal white matter appearance on term FLAIR predicts neuro-developmental outcome at 6 years old following preterm birth.
   Iwata S, Iwata O, Bainbridge A, Nakamura T, Kihara H, Hizume E, Sugiura M, Tamura M, Matsuishi T.
   Int J Dev Neurosci. 2007 Dec;25(8):523-30.

10. Bench to bedside strategies for optimizing neuroprotection following perinatal hypoxia-ischaemia in high and low resource settings.
    Robertson NJ, Iwata O.
    Early Hum Dev. 2007 Dec;83(12):801-11.

11. Therapeutic hypothermia for birth asphyxia in low-resource settings: a pilot randomised controlled trial.
    Robertson NJ, Nakakeeto M, Hagmann C, Cowan FM, Acolet D, Iwata O, Allen E, Elbourne D, Costello A, Jacobs I.
    Lancet. 2008 Sep 6;372(9641):801-3.

12. Phosphorus magnetic resonance spectroscopy 2 h after perinatal cerebral hypoxia-ischemia prognosticates outcome in the newborn piglet.
    Cady EB, Iwata O, Bainbridge A, Wyatt JS, Robertson NJ.
    J Neurochem. 2008 Nov;107(4):1027-35.

13. Therapeutic hypothermia can be induced and maintained using either commercial water bottles or a "phase changing material" mattress in a newborn piglet model.
    Iwata S, Iwata O, Olson L, Kapetanakis A, Kato T, Evans S, Araki Y, Kakuma T, Matsuishi T, Setterwall F, Lagercrantz H, Robertson NJ.
    Arch Dis Child. 2009 May;94(5):387-91.

14. Subtle white matter injury is common in term-born infants with a wide range of risks.
    Iwata S, Bainbridge A, Nakamura T, Tamura M, Takashima S, Matsuishi T, Iwata O.
    Int J Dev Neurosci. 2010 Nov;28(7):573-80.

15. Determinants of outcomes following acute child encephalopathy and encephalitis: pivotal effect of early and delayed cooling.
    Kawano G, Iwata O, Iwata S, Kawano K, Obu K, Kuki I, Rinka H, Shiomi M, Yamanouchi H, Kakuma T, Takashima S, Matsuishi T; Research Network for Acute Encephalopathy in Childhood.
    Arch Dis Child. 2011 Oct;96(10):936-41.

16. Filling the evidence gap: how can we improve the outcome of neonatal encephalopathy in the next 10 years?
    Iwata O, Iwata S.
    Brain Dev. 2011 Mar;33(3):221-8.

17. Past, present and future of hypothermic neuroprotection for neonatal encephalopathy in Japan: time to say good-by to the old remedies.
    Iwata O, Takenouchi T.
    Brain Dev. 2012 Feb;34(2):163-4.

18. Hypothermia for neonatal encephalopathy: Nationwide Survey of Clinical Practice in Japan as of August 2010.
    Iwata O, Nabetani M, Takenouchi T, Iwaibara T, Iwata S, Tamura M; Working Group on Therapeutic Hypothermia for Neonatal Encephalopathy, Ministry of Health, Labor and Welfare, Japan; Japan Society for Perinatal and Neonatal Medicine.
    Acta Paediatr. 2012 May;101(5):e197-202.

19. Qualitative brain MRI at term and cognitive outcomes at 9 years after very preterm birth.
    Iwata S, Nakamura T, Hizume E, Kihara H, Takashima S, Matsuishi T, Iwata O.
    Pediatrics. 2012 May;129(5):e1138-47.

List of publications derived from this work

1. "Therapeutic time window" duration decreases with increasing severity of cerebral hypoxia-ischaemia under normothermia and delayed hypothermia in newborn piglets.
   Iwata O, Iwata S, Thornton JS, De Vita E, Bainbridge A, Herbert L, Scaravilli F, Peebles D, Wyatt JS, Cady EB, Robertson NJ.
   Brain Res. 2007 Jun 18;1154:173-80.

2. Supra- and sub-baseline phosphocreatine recovery in developing brain after transient hypoxia-ischaemia: relation to baseline energetics, insult severity and outcome.
   Iwata O, Iwata S, Bainbridge A, De Vita E, Matsuishi T, Cady EB, Robertson NJ.
   Brain. 2008 Aug;131(Pt 8):2220-6.

Appendix 1.

Supplemental Tables for Chapter 4.3: “Temporal and spatial evolution of secondary energy failure and cerebral injury”

Index of Supplemental Tables

Suppl Table 1: Temporal changes in ^{31}P MRS biomarkers after hypoxia-ischaemia……...157

Suppl Table 2: Temporal changes in regional ADC after hypoxia-ischaemia.....158

Suppl Table 3: Temporal changes in regional T2 relaxation time after hypoxia-ischaemia……162

Suppl Table 4: Influence of insult severity and survival time to magnetic resonance biomarkers and histo-pathological brain injury…….....166

A. Influence of insult severity (acute energy depletion) to temporal changes in MR biomarkers ……...166

B. Influence of insult severity (acute energy depletion) to histo-pathological brain injury ……..168

C. Influence of survival time after resuscitation to histo-pathological brain Injury ……..169

Suppl Table 5: ^{31}P MRS biomarkers and histo-pathological injury (adjusted for AED and survival time after resuscitation)……..170

A. ^{31}P MRS biomarkers 1-48 h after resuscitation and neuronal death assessed using H & E stains…….170

B. ^{31}P MRS biomarkers 1-48 h after resuscitation and TUNEL positive apoptotic cell death …….....172

C-1. ^{31}P MRS biomarkers 1-48 h after resuscitation and CD68 positive microglia in the grey matter ……...174

C-2. ^{31}P MRS biomarkers 1-48 h after resuscitation and CD68 positive microglia in the white matter…….176

D-1. ^{31}P MRS biomarkers 1-48 h after resuscitation and CD68 positive vessels in the grey matter……....177

D-2. ^{31}P MRS biomarkers 1-48 h after resuscitation and CD68 positive vessels in the white matter ……..179

E. ^{31}P MRS biomarkers 1-48 h after resuscitation and white matter injury assessed using H & E stains……..180

F. ^{31}P MRS biomarkers 1-48 h after resuscitation and white matter injury assessed using LFB/Nissl stains……181
G. ^{31}P MRS biomarkers 1-48 h after resuscitation and axonal injury assessed using β-APP immune-histochemical stain……182

Suppl Table 6: Regional ADC and histo-pathological injury in corresponding regions (adjusted for AED and survival time after resuscitation)……183
A. ADC 1 to 48 hours after resuscitation and neuronal death assessed using H & E stains ……183
B. ADC 1-48 h after resuscitation and TUNEL positive apoptotic cell death……..184
C-1. ADC 1-48 h after resuscitation and CD68 positive microglia in the grey matter ……185
C-2. ADC 1-48 h after resuscitation and CD68 positive microglia in the white matter ……185
D-1. ADC 1-48 h after resuscitation and CD68 positive vessels in the grey matter ……186
D-2. ADC 1-48 h after resuscitation and CD68 positive vessels in the white matter ……186
E. ADC 1-48 h after resuscitation and white matter injury assessed using H & E stains ……187
F. ADC 1-48 h after resuscitation and white matter injury assessed using LFB/Nissl stains ……187
G. ADC 1-48 h after resuscitation and axonal injury assessed using β-APP immune-histochemical stain……... 188

Suppl Table 7: Regional T2 relaxation time 1-48 h after resuscitation and histo-pathological injury in corresponding regions (adjusted for AED and survival time after resuscitation)..…… 189
A. T2 1-48 h after resuscitation and neuronal death assessed using H & E stains ……189
B. T2 1-48 h after resuscitation and TUNEL positive apoptotic cell death…….190
C-1. T2 1-48 h after resuscitation and CD68 positive microglia in the grey matter ……191
C-2. T2 1-48 h after resuscitation and CD68 positive microglia in the white matter ……191
D-1. T2 1-48 h after resuscitation and CD68 positive vessels in the grey matter...192

D-2. T2 1-48 h after resuscitation and CD68 positive vessels in the white matter ……192
E. T2 1-48 h after resuscitation and white matter injury assessed using H & E stains ……193
F. T2 1-48 h after resuscitation and white matter injury assessed using LFB/Nissl stains ……193
G. T2 1-48 h after resuscitation and axonal injury assessed using β-APP immune-histochemical stain……194

Suppl Table 8: Serial ^{31}P MRS biomarkers 1-48 h before termination and histo-pathological injury……195
A. ^{31}P MRS biomarkers 1-48 h before termination and neuronal death in the grey matter assessed using H & E stains……195
B. ^{31}P MRS biomarkers 1-48 h before termination and TUNEL positive apoptotic cell death in the grey matter……197
C-1. ^{31}P MRS biomarkers 1-48 h before termination and CD68 positive microglia in the grey matter……199
C-2. ^{31}P MRS biomarkers 1-48 h before termination and CD68 positive microglia in the white matter……201
D-1. ^{31}P MRS biomarkers 1-48 h before termination and CD68 positive vessels in the grey matter……202
D-2. ^{31}P MRS biomarkers 1-48 h before termination and CD68 positive vessels in the white matter……204
E. ^{31}P MRS biomarkers 1-48 h before termination and white matter injury assessed using H & E stains……205
F. ^{31}P MRS biomarkers 1-48 h before termination and white matter injury assessed using LFB/Nissl stains……206
G. ^{31}P MRS biomarkers 1-48 h before termination and white matter injury assessed using β-APP immune-histochemical stain……207

Suppl Table 9: Serial ADC 1-48 h before termination and histo-pathological injury in corresponding regions……208
A. ADC 1 to 48 hours before termination and neuronal death in the grey matter assessed using H & E stains……208
B. ADC 1-48 h before termination and TUNEL positive apoptotic cell death in the grey matter ……209

C-1. ADC 1-48 h before termination and CD68 positive microglia in the grey matter ……210
C-2. ADC 1-48 h before termination and CD68 positive microglia in the white matter ……210
D-1. ADC 1-48 h before termination and CD68 positive vessels in the grey matter ……211
D-2. ADC 1-48 h before termination and CD68 positive vessels in the white matter ……211
E. ADC 1-48 h before termination and white matter injury assessed using H & E stains ……212
F. ADC 1-48 h before termination and white matter injury assessed using LFB/Nissl stains……212
G. ADC 1-48 h before termination and white matter injury assessed using β-APP immune-histochemical stain…….. 213

Suppl Table 10: Serial T2 maps 1-48 h before termination and histo-pathological injury in corresponding regions….....214
A. T2 1-48 h before termination and neuronal death in the grey matter assessed using H & E stains……..214
B. T2 1-48 h before termination and TUNEL positive apoptotic cell death in the grey matter……..215
C-1. T2 1-48 h before termination and CD68 positive microglia in the grey matter ……216
C-2. T2 1-48 h before termination and CD68 positive microglia in the white matter ……216
D-1. T2 1-48 h before termination and CD68 positive vessels in the grey matter ……217
D-2. T2 1-48 h before termination and CD68 positive vessels in the white matter ……217
E. T2 1-48 h before termination and white matter injury assessed using H & E stains ……218
F. T2 1-48 h before termination and white matter injury assessed using LFB/Nissl stains……..218
G. T2 1-48 h before termination and white matter injury assessed using β-APP immune-histochemical stain……219

Supplemental Table 4.3-1: Temporal changes in ^{31}P MRS biomarkers after hypoxia-ischaemia

		Time after resuscitation (h)									
		Baseline	1 - < 3	3 - < 6	6 - < 12	12 - < 18	18 - < 24	24 - < 30	30 - < 36	36 - < 42	42 - < 48
	(n)	(18)	(18)	(18)	(18)	(17)	(14)	(9)	(7)	(5)	(4)
NTP/EPP	Mean	0.21	0.19	0.19	0.18	0.18	0.15	0.15	0.14	0.18	0.15
	SD	0.03	0.03	0.02	0.03	0.04	0.07	0.04	0.05	0.03	0.06
	p		0.003	0.003	<0.001	<0.001	0.004	0.002	0.005	0.043	0.111
PCr/EPP	Mean	0.23	0.21	0.21	0.18	0.17	0.14	0.13	0.13	0.13	0.12
	SD	0.02	0.04	0.03	0.05	0.05	0.06	0.06	0.04	0.03	0.05
	p		0.188	0.061	0.001	0.001	0.001	0.004	0.010	0.020	0.044
Pi/EPP	Mean	0.19	0.30	0.27	0.34	0.37	0.49	0.48	0.51	0.43	0.51
	SD	0.03	0.11	0.08	0.14	0.15	0.24	0.20	0.19	0.09	0.23
	p		<0.001	0.001	<0.001	<0.001	0.001	0.003	0.007	0.010	0.065
PCr/Pi	Mean	1.22	0.84	0.87	0.66	0.60	0.43	0.40	0.31	0.34	0.30
	SD	0.29	0.40	0.32	0.38	0.38	0.37	0.39	0.20	0.14	0.19
	p		<0.001	0.001	<0.001	<0.001	<0.001	0.001	0.002	0.007	0.006

Statistical significance was assumed with p-values < 0.01 (Dunnett test).

P-values for the periods after 24 hours are presented only for reference because of the limited number of surviving subjects.

Supplemental Table 4.3-2: Temporal changes in regional ADC after hypoxia-ischaemia

			Time after resuscitation (h)																	
			Baseline		1 - < 3		3 - < 6		6 - < 12		12 - < 18	18 - < 24	24 - < 30		30 - < 36		36 - < 42		42 - < 48	
Cortical grey matter	Sagittal top	n	18		18		18		17		16	11	9		5	b	5	b	4	
		Mean	1.114		0.950		0.832		0.778		0.742	0.685	0.653		0.595		0.562		0.650	
		SD	0.099		0.241		0.285		0.323		0.352	0.262	0.229		0.130		0.130		0.101	
		p			0.009		0.001		<0.001		0.001	0.001	<0.001		0.001		<0.001		0.001	
	Sagittal bottom	n	18		18	a	18	a	17		16	11	9		5	c	5	c	4	a
		Mean	1.087		0.858		0.771		0.713		0.680	0.570	0.552		0.546		0.499		0.480	
		SD	0.072		0.247		0.249		0.259		0.284	0.252	0.225		0.148		0.072		0.096	
		p			0.001		<0.001		<0.001		<0.001	<0.001	<0.001		0.002		<0.001		<0.001	
	Parietal top	n	18		18		18		17		16	11	9		5	a	5	a	4	
		Mean	1.124		0.950		0.832		0.789		0.766	0.738	0.625		0.625		0.621		0.564	
		SD	0.087		0.187		0.273		0.306		0.299	0.264	0.254		0.127		0.096		0.062	
		p			0.001		<0.001		<0.001		<0.001	0.001	<0.001		0.001		<0.001		0.001	
	Parietal bottom	n	18		18		18		17		16	11	9		5	d	5	d	4	
		Mean	1.121		0.915		0.819		0.746		0.706	0.616	0.554		0.567		0.543		0.538	
		SD	0.090		0.213		0.274		0.324		0.319	0.287	0.225		0.125		0.090		0.122	
		p			0.001		<0.001		<0.001		<0.001	<0.001	<0.001		<0.001		<0.001		0.001	
	Temporal	n	16		16	a	16	a	15		13	9	8		5	a	5	a	3	a
		Mean	1.162		1.082		1.040		0.967		0.915	0.827	0.849		0.936	b	0.900	b	0.697	
		SD	0.085		0.091		0.178		0.213		0.233	0.219	0.229		0.210	c	0.246	c	0.179	
		p			<0.001		0.010		0.004		0.003	0.001	0.005		0.069	d	0.071	d	0.044	
	Group mean	Mean	1.120	A	0.950		0.859		0.802		0.769	0.693	0.652		0.654		0.625		0.583	
		SD	0.70	D	0.170		0.222		0.254		0.257	0.226	0.195		0.096		0.097		0.074	
		p			0.001		<0.001		<0.001		<0.001	<0.001	<0.001		0.001		0.001		<0.001	

			Time after resuscitation (h)									
			Baseline		1 - < 3	3 - < 6	6 - < 12	12 - < 18	18 - < 24	24 - < 30	30 - < 36	36 - < 42	42 - < 48
	Hippocampus	n	8	B	8	8	7	5	3	2	2	2	2
		mean	1.139		1.063	0.952	0.997	0.889	0.809	0.848	0.832	0.688	0.705
		SD	0.059		0.153	0.192	0.234	0.240	0.166	0.031	0.010	0.261	0.197
		p			0.162	0.034	0.104	0.055	0.052	0.045	0.009	0.230	0.183
Deep grey matter	Caudate nucleus	n	15	a	15	15	14	12	9	8	5	5	3
		Mean	1.100	e	0.990	0.864	0.829	0.802	0.702	0.741	0.788	0.730	0.559
		SD	0.072		0.156	0.257	0.253	0.264	0.246	0.160	0.187	0.204	0.217
		p			0.017	0.002	0.001	0.003	0.001	0.001	0.042	0.033	0.096
	Putamen	n	15	f	15	15	14	12	9	8	5	5	3
		Mean	1.074		0.927	0.769	0.715	0.690	0.675	0.653	0.636	0.620	0.510
		SD	0.076		0.213	0.248	0.283	0.263	0.275	0.183	0.208	0.201	0.179
		p			0.006	<0.001	<0.001	<0.001	0.004	<0.001	0.010	0.009	0.037
	Anterior thalamus	n	15	g	15	15	14	12	9	8	5	5	3
		Mean	1.076		0.985	0.905	0.899	0.864	0.812	0.798	0.741	0.684	0.679
		SD	0.065		0.149	0.255	0.306	0.230	0.262	0.208	0.197	0.218	0.193
		p			0.012	0.014	0.038	0.006	0.006	0.005	0.016	0.013	0.087
	Lateral thalamus	n	15	b	15	15	14	12	9	8	5	5	3
		Mean	0.952	e	0.855	0.745	0.738	0.714	0.707	0.612	0.592	0.591	0.473
		SD	0.057	f	0.172	0.276	0.265	0.237	0.243	0.209	0.259	0.252	0.083
		p		g	0.029	0.008	0.005	0.003	0.009	0.001	0.030	0.028	0.007
	Medial thalamus	n	15	a	15	15	14	12	9	8	5	5	3
		Mean	1.030	b	1.006	0.966	0.950	0.875	0.774	0.740	0.654	0.608	0.554
		SD	0.057		0.091	0.190	0.188	0.203	0.225	0.188	0.236	0.246	0.132
		p			0.370	0.237	0.150	0.015	0.008	0.001	0.022	0.017	0.013
	Group mean	Mean	1.046	A	0.952	0.850	0.826	0.789	0.734	0.709	0.682	0.647	0.555
		SD	0.046	B	0.126	0.213	0.218	0.215	0.225	0.168	0.201	0.210	0.155
		p			0.006	0.002	0.002	0.001	0.002	<0.001	0.015	0.013	0.036

			Time after resuscitation (h)										
			Baseline		1 - < 3	3 - < 6	6 - < 12	12 - < 18	18 - < 24	24 - < 30	30 - < 36	36 - < 42	42 - < 48
Peripheral white matter	Sagittal	n	16	a	16	16	15	14	11	9	5	5	4
		Mean	1.076		0.874	0.758	0.720	0.698	0.565	0.546	0.502	0.484	0.550
		SD	0.065		0.243	0.285	0.301	0.291	0.265	0.233	0.050	0.050	0.076
		p			0.006	0.001	0.001	0.001	<0.001	<0.001	<0.001	<0.001	0.001
	Parietal	n	15	a	15	15	14	13	11	9	5	5	4
		Mean	1.159	e	0.950	0.861	0.800	0.753	0.702	0.664	0.683	0.627	0.601
		SD	0.0.67		0.242	0.289	0.336	0.311	0.280	0.242	0.185	0.097	0.146
		p			0.003	0.001	0.002	0.001	<0.001	<0.001	0.006	0.001	0.009
	Temporal	n	16	e	16	16	15	14	11	9	5	5	4
		Mean	1.008		0.894	0.786	0.749	0.700	0.677	0.641	0.632	0.570	0.601
		SD	0.124		0.226	0.280	0.310	0.273	0.289	0.307	0.264	2.18	1.75
		p			0.022	0.003	0.005	0.003	0.009	0.009	0.030	0.004	0.003
	Group mean	Mean	1.079	C	0.909	0.806	0.762	0.724	0.648	0.617	0.606	5.60	5.84
		SD	0.063	E	0.218	0.254	0.288	0.280	0.260	0.238	0.132	0.83	0.88
		p			0.005	0.001	0.001	0.001	0.001	0.001	0.003	<0.001	0.002

			Time after resuscitation (h)										
			Baseline		1 - < 3	3 - < 6	6 - < 12	12 - < 18	18 - < 24	24 - < 30	30 - < 36	36 - < 42	42 - < 48
Central whiter matter	Superior periventricular	n	15	e	15	15	14	11	9	8	5	5	4
		Mean	0.912		0.850	0.728	0.638	0.590	0.502	0.504	0.530	5.53	5.72
		SD	0.095		0.137	0.214	0.192	0.209	0.153	0.164	0.180	1.90	1.28
		p			0.036	0.003	<0.001	0.002	<0.001	0.001	0.017	0.022	0.026
	Periventricular	n	14	b	14	14	13	11	9	8	5	5	4
		Mean	0.976		0.897	0.778	0.690	0.640	0.649	0.600	0.628	0.687	0.701
		SD	0.126		0.113	0.231	0.220	0.230	0.227	0.230	0.250	0.219	0.166
		p			0.010	0.002	<0.001	0.002	0.003	0.002	0.041	0.052	0.068
	Posterior limb of internal capsule	n	12	b	12	12	11	10	8	6	4	4	3
		Mean	1.152	e	0.882	0.736	0.665	0.671	0.558	0.499	0.570	0.448	0.526
		SD	0.141		0.297	0.297	0.365	0.329	0.197	0.205	0.189	0.066	0.090
		p			0.004	0.001	0.003	0.003	0.001	0.003	0.025	0.001	0.002
Group mean		Mean	0.994	C	0.875	0.755	0.674	0.651	0.569	0.526	0.564	0.563	0.607
		SD	0.081	D	0.155	0.221	0.232	0.251	0.170	0.171	0.187	0.135	0.120
		p		E	0.004	0.001	0.001	0.001	<0.001	<0.001	0.007	0.002	0.012

ADC values shown as $10^{-3} \cdot mm^2 \cdot sec^{-1}$.

a-g: statistical significance from within group comparisons with p < 0.05 (a), p < 0.01 (b –d) and p < 0.01 (e-g)

A-E: statistical significance from between group mean comparisons with p < 0.01 (A-C) and p < 0.001 (D-E)

Statistical significance was assumed with p-values < 0.01 (Dunnett test).

P-values for the periods after 24 hours are presented only for reference because of the limited number of surviving subjects.

Supplemental Table 4.3-3: Temporal changes in regional T2 relaxation time after hypoxia-ischaemia

			Time after resuscitation (h)																						
			Baseline		1 - < 3		3 - < 6		6 - < 12		12 - < 18		18 - < 24		24 - < 30		30 - < 36		36 - < 42		42 - < 48		
Cortical grey matter	Sagittal top	n	11		11		11		10		9		8		6		3		3		2		
		Mean	66.62		71.62		75.30		78.52		78.26		85.54		98.96		91.91		92.88		100.83		
		SD	8.45		11.10		14.68		14.16		16.58		20.02		22.03		25.03		19.20		14.24		
		p			0.026		0.021		0.006		0.032		0.026		0.031		0.243		0.083		0.034		
	Sagittal bottom	n	11		11		11		10		9		8		6		3		3		2		a
		Mean	66.04		70.07		72.87		75.77		75.28		83.24		91.00		83.35		82.11		90.36		
		SD	9.71		9.98		10.81		12.82		16.19		18.22		16.29		16.78		15.77		6.29		
		p			0.002		<0.001		0.001		0.030		0.003		0.005		0.169		0.106		0.098		
	Parietal top	n	11		11		11		10		9		8		6		3		3		2		
		Mean	67.54		68.20		69.82		75.53		75.20		80.12		94.06		91.90		90.83		96.73		
		SD	11.55		11.72		9.96		14.86		17.02		16.93		18.84		22.39		23.19		7.77		
		p			0.650		0.421		0.025		0.096		0.041		0.004		0.049		0.059		0.004		
	Parietal bottom	n	11		11		11		10		9		8		6		3		3		2		
		Mean	68.77		69.65		72.16		73.68		74.73		77.88		90.77		83.23		82.48		90.74		
		SD	9.81		9.70		9.40		9.76		10.63		14.33		15.81		18.31		17.78		17.44		
		p			0.383		0.017		0.001		0.001		0.011		0.002		0.063		0.042		0.148		
	Temporal	n	11		11		11		10		7		6		4		2		2		0		a
		Mean	73.10		77.53		77.75		78.01		79.45		85.84		96.90		79.52		88.12				
		SD	11.41		12.16		14.33		11.59		16.82		17.06		24.23		20.16		27.09				
		p			0.020		0.009		0.016		0.583		0.308		0.240		0.913		0.436				
	Group mean	Mean	68.41	E	71.41	E	73.58	E	76.30	C	76.13	A	81.85	A	94.21	A	86.99	A	87.26		94.66		
		SD	9.69	F	10.43	F	10.93	F	11.98	E	14.42	C	16.48	C	17.86	C	19.42		18.59		11.43		
		p			0.005		0.002		0.001		0.017		0.012		0.010		0.145		0.074		0.026		

			Time after resuscitation (h)																					
			Baseline		1 - < 3		3 - < 6		6 - < 12		12 - < 18		18 - < 24		24 - < 30		30 - < 36		36 - < 42		42 - < 48	
Deep grey matter	Hippocampus	n	11	C	11	G	11	A	10	A	8	B	7	B	5		3		3		1	
		mean	65.19	G	69.74	H	68.77	G	71.76	D	76.37	D	81.43	D	83.59		73.48		74.82		78.80	
		SD	8.36		8.90		7.47		8.33		13.49		15.62		16.21		11.60		10.94			
		p			0.043		0.048		0.003		0.001		0.006		0.020		0.105		0.052			
	Caudate nucleus	n	11		11		11		10		8		7		5		3		3		1	
		Mean	63.93		67.11		69.69		69.88		72.77		76.30		79.51		68.84		72.10		65.70	
		SD	10.88		12.72		11.77		10.74		11.23		15.62		11.93		5.57		5.60			
		p			0.201		0.055		0.022		0.043		0.088		0.045		0.422		0.169			
	Putamen	N	11		11	a	11		10		8		7		5		3		3		1	
		Mean	62.93		65.65		68.14		68.94		71.45		80.49		80.04		70.70		75.23		67.74	
		SD	8.80		7.77		8.21		8.19		8.72		13.76		16.10		8.29		6.88			
		p			0.064		0.030		0.051		0.034		0.010		0.163		0.542		0.241			
	Anterior thalamus	n	11		11	a	11		10		8		7		5		3		3		1	
		Mean	54.73		57.86		61.72		63.22		65.24		64.52		73.73		65.64		66.20		59.37	
		SD	8.83		7.15		11.39		12.36		12.39		8.74		11.69		4.83		4.25			
		p			0.003		0.017		0.035		0.073		0.050		0.040		0.115		0.061			
	Lateral thalamus	n	11		11		11		10		8		7		5		3		3		1	
		Mean	59.16		62.93		63.58		66.35		69.10		74.61		75.28		70.20		70.22		71.68	
		SD	9.72		9.15		9.66		10.53		10.08		11.34		5.64		3.62		1.53			
		p			0.004		0.003		0.002		0.022		0.007		0.034		0.188		0.188			
	Medial thalamus	n	11		11		11		10		9		8		5		3		3		2	
		Mean	62.47		64.57		67.70		66.29		66.35		68.64		71.24		77.99		75.09		81.57	
		SD	5.68		3.62		6.80		6.70		7.54		8.15		9.68		19.33		15.37		21.74	
		p			0.210		0.096		0.266		0.254		0.118		0.117		0.304		0.304		0.572	
	Group mean	Mean	60.64	A	63.63	C	66.17	C	66.93		68.51		71.50		75.35		70.68		71.77		69.24	
		SD	7.26		6.92		7.81		8.64		8.56		10.56		8.63		7.53		4.56		4.31	
		p			0.001		0.001		0.011		0.008		0.004		0.050		0.279		0.167		0.776	

			Time after resuscitation (h)																					
			Baseline		1 - < 3		3 - < 6		6 - < 12		12 - < 18		18 - < 24		24 - < 30		30 - < 36		36 - < 42		42 - < 48	
Peripheral white matter	Sagittal	n	9	c	9	e	9	a	8	e	7		7		4		3		3	c	2	
		Mean	58.73		57.16		58.72	e	62.94		56.90		59.72		66.55		69.20		69.25		75.87	
		SD	9.51		6.90		6.76	f	7.88		9.76		10.89		18.25		21.68		14.76		19.36	
		p			0.588		0.999		0.444		0.549		0.952		0.921		0.517		0.334		0.603	
	Parietal	n	11	e	11	f	11	a	10	f	9	c	8	c	5	a	3	a	3	d	2	a
		Mean	56.19		60.75		64.28		64.72		64.22		67.66		71.81		78.64		77.90		87.33	
		SD	3.24		5.28		5.36		6.04		7.70		7.65		12.08		19.17		12.48		16.29	
		p			0.005		<0.001		0.001		0.006		0.002		0.019		0.127		0.052		0.229	
	Temporal	n	11	c	11	e	11	e	10	e	8	c	7	c	5	a	3	a	3	c	2	a
		Mean	46.41	e	46.75	f	50.17	f	50.84	f	54.43		55.07		55.22		49.85		48.29	d	48.51	
		SD	3.50		3.11		5.69		6.45		6.35		9.20		11.62		7.35		6.18		8.70	
		p			0.566		0.120		0.139		0.032		0.042		0.187		0.626		0.776		0.781	
	Group mean	Mean	53.54	C	54.92	E	57.64	A	59.14	A	58.81	A	61.21	A	64.79	A	65.90		65.15		70.57	
		SD	3.33	E	3.74	G	5.39	E	6.12	C	6.65	B	7.42	B	11.93		15.78		10.83		14.79	
		p			0.258		0.082		0.033		0.069		0.014		0.131		0.302		0.192		0.425	

			Time after resuscitation (h)																					
			Baseline		1 - < 3		3 - < 6		6 - < 12		12 - < 18		18 - < 24		24 - < 30		30 - < 36		36 - < 42		42 - < 48	
Central whiter matter	Superior periventricular	n	11	e	11	e	11	e	10	e	8	e	7	c	4		3		3		2	a
		Mean	49.86		49.22		50.51		52.39		52.92		54.71		54.27		50.21		49.91		48.01	b
		SD	7.56		6.27		5.37		6.07		5.64		6.93		8.35		6.45		4.93		7.42	
		p			0.495		0.765		0.234		0.044		0.046		0.266		0.773		0.758		0.738	
	Periventricular	n	3	e	3	e	3	e	3	e	3	e	3	c	2		1		1		1	a
		Mean	67.91	f	70.63	f	70.44	f	71.30	f	76.84	f	78.91	d	80.64		81.90		79.03		83.82	
		SD	3.18		1.05		2.77		7.41		2.99		5.72		1.28							
		p			0.310		0.357		0.537		0.074		0.114		0.120							
	Posterior limb of internal capsule	n	11	f	11	f	11	f	10	f	9	f	8	d	5		3		3		2	b
		Mean	48.56		50.23		53.31		56.00		55.20		57.26		63.23		62.14		61.81		64.26	
		SD	3.67		4.95		7.06		7.77		9.43		10.49		14.87		23.09		10.25		6.44	
		p			0.044		0.049		0.019		0.058		0.016		0.054		0.334		0.065		0.042	
	Group mean	Mean	51.08	A	51.86	C	53.53	C	55.66	D	55.55	C	57.97	C	61.74	C	57.30	A	57.73		59.93	
		SD	4.43	F	4.07	F	6.06	F	7.05	E	8.63	D	9.21	D	10.96		15.46		8.79		12.30	
		p		G	0.170	H	0.223	G	0.069		0.142		0.036		0.036		0.399		0.117		0.222	

T2 relaxation times are shown as milliseconds.

a-f: statistical significance from within group comparisons with p < 0.05 (a-b), p < 0.01 (c–d) and p < 0.001 (e-f)

A-H: statistical significance from between group comparisons with p < 0.05 (A-B), p < 0.01 (C-D) and p < 0.001 (E-H)

Statistical significance was assumed with p-values < 0.01 (Dunnett test).

P-values for the periods after 24 hours are presented only for reference because of the limited number of surviving subjects.

Supplemental Table 4.3-4: Influence of insult severity and survival time to magnetic resonance biomarkers and histo-pathological brain injury

A. Influence of insult severity (acute energy depletion) to temporal changes in MR biomarkers

		Time after resuscitation (h)																	
		1 - < 3		3 - < 6		6 - < 12		12 - < 18		18 - < 24		24 - < 30		30 - < 36		36 - < 42		42 - < 48	
		r	p	r	p	r	p	r	p	r	p	r	p	r	p	r	p	r	p
	NTP/EPP	-0.40	0.103	-0.34	0.163	-0.34	0.172	-0.19	0.462	-0.41	0.142	-0.73	0.027	-0.73	0.061	-0.86	0.065	-0.50	0.498
	PCr/EPP	-0.34	0.172	-0.44	0.070	-0.29	0.236	-0.31	0.219	-0.53	0.049	-0.69	0.038	-0.83	0.021	-0.96	0.011	-0.91	0.092
	Pi/EPP	0.33	0.178	0.50	0.035	0.33	0.185	0.23	0.376	0.45	0.106	0.67	0.046	0.79	0.033	0.84	0.076	0.60	0.397
	PCr/Pi	-0.35	0.151	0.00	0.060	-0.42	0.081	-0.37	0.148	-0.46	0.099	-0.56	0.119	-0.77	0.042	-0.87	0.056	-0.83	0.167
ADC	Sagittal CTX-top	-0.62	0.006	-0.46	0.056	-0.27	0.304	-0.11	0.692	-0.33	0.328	-0.59	0.092	-0.73	0.159	-0.26	0.672	-0.80	0.205
ADC	Sagittal CTX-bottom	-0.75	0.000	-0.65	0.004	-0.50	0.041	-0.37	0.164	-0.32	0.335	-0.51	0.159	-0.77	0.130	-0.70	0.189	-0.78	0.219
ADC	Parietal CTX-top	-0.27	0.288	-0.42	0.080	-0.26	0.306	-0.14	0.619	0.13	0.704	0.04	0.924	0.66	0.225	0.28	0.644	0.45	0.548
ADC	Parietal CTX-bottom	-0.56	0.015	-0.59	0.010	-0.52	0.033	-0.38	0.142	-0.20	0.549	-0.50	0.171	-0.96	0.010	-0.95	0.013	-0.99	0.008
ADC	Temporal CTX	0.01	0.973	-0.29	0.275	-0.15	0.598	-0.10	0.747	-0.38	0.312	-0.70	0.052	-0.79	0.052	-0.89	0.044	-1.00	0.055
ADC	Hippocampus	-0.70	0.054	-0.57	0.139	-0.20	0.674	-0.14	0.829	0.69	0.512								
ADC	Caudate nucleus	-0.40	0.139	-0.32	0.239	0.02	0.953	0.08	0.805	-0.62	0.074	-0.82	0.013	-0.94	0.018	-0.80	0.105	-0.76	0.450
ADC	Putamen	-0.50	0.059	-0.54	0.036	-0.48	0.083	-0.54	0.069	-0.56	0.121	-0.39	0.345	-0.45	0.444	-0.45	0.443	-1.00	0.051
ADC	Anterior thalamus	-0.33	0.230	-0.43	0.115	-0.33	0.243	-0.39	0.209	-0.60	0.086	-0.89	0.003	-0.40	0.509	-0.60	0.289	-0.90	0.283
ADC	Lateral thalamus	-0.59	0.021	-0.54	0.040	-0.53	0.052	-0.54	0.072	-0.85	0.004	-0.59	0.126	-0.66	0.229	-0.62	0.270	-0.98	0.129
ADC	Medial thalamus	-0.62	0.013	-0.51	0.051	-0.39	0.167	-0.39	0.207	-0.74	0.023	-0.73	0.039	-0.40	0.501	-0.37	0.540	-0.68	0.521
ADC	Sagittal WM	-0.53	0.035	-0.61	0.013	-0.49	0.063	-0.36	0.205	-0.44	0.181	-0.35	0.359	-0.23	0.711	-0.10	0.878	-0.75	0.246
ADC	Parietal WM	-0.43	0.042	-0.47	0.075	-0.32	0.264	-0.19	0.527	-0.29	0.384	-0.38	0.312	-0.58	0.302	-0.82	0.087	-0.54	0.462
ADC	Temporal WM	-0.34	0.200	-0.34	0.200	-0.22	0.432	-0.23	0.432	-0.07	0.828	-0.09	0.826	0.17	0.787	0.36	0.555	0.34	0.657
ADC	Superior periventricular WM	-0.57	0.025	-0.59	0.021	-0.50	0.071	-0.51	0.106	-0.23	0.548	-0.18	0.663	-0.30	0.623	-0.34	0.574	-0.58	0.419
ADC	Periventricular WM	-0.25	0.391	-0.31	0.285	-0.08	0.786	-0.31	0.353	-0.29	0.447	-0.19	0.655	-0.52	0.368	-0.56	0.330	-0.37	0.629
ADC	PLIC	-0.55	0.062	-0.48	0.114	-0.34	0.306	-0.35	0.323	-31.0	0.455	-0.21	0.687	-0.66	0.344	0.51	0.491	-0.87	0.327

		Time after resuscitation (h)																	
		1 - < 3		3 - < 6		6 - < 12		12 - < 18		18 - < 24		24 - < 30		30 - < 36		36 - < 42		42 - < 48	
		r	p	r	p	r	p	r	p	r	p	r	p	r	p	r	p	r	p
T_2	Sagittal CTX-top	-0.13	0.694	0.21	0.564	0.21	0.564	0.23	0.551	0.01	0.984	0.16	0.763	0.41	0.728	-0.11	0.931		
	Sagittal CTX-bottom	-0.03	0.942	-0.02	0.946	0.19	0.595	0.30	0.428	0.01	0.989	0.17	0.741	0.75	0.459	0.49	0.673		
	Parietal CTX-top	-0.10	0.776	0.29	0.394	0.13	0.720	0.25	0.519	-0.12	0.780	0.14	0.796	0.41	0.733	0.33	0.783		
	Parietal CTX-bottom	-0.08	0.806	-0.05	0.874	-0.08	0.837	0.07	0.865	-0.02	0.687	-0.01	0.981	0.24	0.846	0.04	0.976		
	Temporal CTX	-0.26	0.443	-0.44	0.181	-0.17	0.633	0.09	0.850	0.29	0.580	0.46	0.541						
	Hippocampus	0.11	0.752	-0.16	0.630	0.11	0.773	0.29	0.488	0.21	0.654	0.24	0.697	0.88	0.316	0.69	0.520		
	Caudate nucleus	-0.27	0.429	-0.37	0.261	0.02	0.957	0.25	0.549	0.16	0.737	0.40	0.506	0.61	0.582	0.01	0.991		
	Putamen	-0.36	0.282	-0.13	0.706	0.24	0.500	0.56	0.147	0.69	0.087	0.07	0.908	1.00	0.015	0.97	0.163		
	Anterior thalamus	-0.23	0.500	0.14	0.684	0.32	0.374	0.75	0.032	0.59	0.166	-0.03	0.962	0.60	0.592	-0.60	0.588		
	Lateral thalamus	-0.30	0.377	-0.31	0.349	-0.01	0.987	0.51	0.195	0.40	0.380	0.33	0.587	0.59	0.596	0.02	0.990		
	Medial thalamus	0.59	0.058	0.81	0.003	0.79	0.007	0.63	0.068	0.38	0.349	0.93	0.020	1.00	0.018	1.00	0.022		
	Sagittal WM	0.20	0.607	0.67	0.046	0.65	0.083	0.57	0.178	0.08	0.873	0.93	0.066	0.96	0.192	0.95	0.207		
	Parietal WM	0.52	0.102	0.75	0.009	0.60	0.066	0.44	0.239	0.67	0.067	0.96	0.009	0.98	0.138	0.98	0.135		
	Temporal WM	-0.24	0.472	0.50	0.119	0.33	0.349	0.43	0.283	0.15	0.750	0.45	0.448	0.97	0.163	0.95	0.204		
	Superior periventricular WM	0.05	0.880	0.40	0.227	0.31	0.388	0.06	0.892	-0.10	0.835	-0.17	0.827	0.60	0.593	0.42	0.724		
	Periventricular WM	0.60	0.588	0.27	0.827	0.45	0.703	0.53	0.646	0.64	0.559								
	PLIC	0.37	0.263	0.51	0.112	0.49	0.146	0.35	0.360	0.23	0.577	0.94	0.020	1.00	0.058	0.89	0.304		

Statistical significance was assumed with p-values < 0.01 (Dunnett test).

P-values for the periods after 24 hours are presented only for reference because of the limited number of surviving subjects.

Abbreviations: CTX, cerebral cortex; WM, white matter; PCIC, posterior limb of the internal capsule.

B. Influence of insult severity (acute energy depletion) to histo-pathological brain injury

	Brain damage in the grey matter							
	Neuronal death (H&E)		TUNEL (+) apoptosis		CD68 (+) microglia		CD68(+) vessel	
	r	p	r	p	r	p	r	p
Sagittal top	0.39	0.110	-0.13	0.600	0.05	0.859	0.03	0.909
Sagittal bottom	0.39	0.110	-0.16	0.536	0.41	0.095	0.29	0.242
Parietal top	0.30	0.227	-0.09	0.721	0.11	0.663	-0.04	0.874
Parietal bottom	0.44	0.068	-0.14	0.588	-0.16	0.520	-0.19	0.462
Temporal	0.44	0.068	-0.14	0.588	-0.16	0.520	-0.19	0.462
Hippocampus	-0.01	0.986	-0.30	0.432	0.48	0.195	0.68	0.046
Caudate nucleus	0.29	0.316	-0.33	0.247	0.73	0.002	0.74	0.002
Putamen	0.20	0.502	-0.13	0.651	0.63	0.011	0.40	0.136
Anterior thalamus	0.44	0.113	-0.36	0.210	0.67	0.006	0.74	0.002
Lateral thalamus	0.01	0.982	-0.26	0.341	0.82	<0.001	0.82	<0.001
Medial thalamus	0.07	0.792	-0.13	0.659	0.59	0.025	0.84	<0.001

	Brain damage in the white matter									
	H & E		LFB		CD68 (+) microglia		CD68 (+) vessel		β-APP	
	r	p	r	p	r	p	r	p	r	p
Sagittal	0.54	0.024	-0.73	0.001	-0.01	0.965	0.39	0.125	0.06	0.830
Parietal	0.40	0.125	-0.75	0.001	0.21	0.430	0.36	0.169	0.18	0.494
Temporal	0.33	0.206	-0.63	0.009	0.11	0.698	0.46	0.076	0.02	0.950
Superior Periventricular	0.37	0.146	-0.05	0.846	0.66	0.004	0.64	0.006	0.30	0.246
Periventricular	0.45	0.079	-0.03	0.918	0.58	0.018	0.43	0.097	0.28	0.302
PLIC	0.36	0.251	0.03	0.931	0.00	0.994	0.22	0.549	0.18	0.623
Sagittal	0.54	0.024	-0.73	0.001	-0.01	0.965	0.39	0.125	0.06	0.830

Abbreviation: PCIC, posterior limb of the internal capsule.

C. Influence of survival time after resuscitation to histo-pathological brain injury

	Brain damage in the grey matter							
	Neuronal death (H&E)		TUNEL (+) apoptosis		CD68 (+) microglia		CD68(+) vessel	
	r	p	r	p	r	p	r	p
Sagittal top	0.08	0.740	0.20	0.423	-0.16	0.535	-0.24	0.335
Sagittal bottom	0.23	0.352	0.45	0.063	-0.54	0.021	-0.41	0.089
Parietal top	0.23	0.365	0.26	0.294	-0.42	0.083	-0.42	0.087
Parietal bottom	0.20	0.420	0.30	0.227	-0.19	0.449	-0.21	0.400
Temporal	0.04	0.876	0.40	0.126	-0.33	0.207	-0.33	0.214
Hippocampus	0.24	0.533	0.17	0.672	-0.47	0.208	-0.48	0.196
Caudate nucleus	-0.19	0.519	0.47	0.092	-0.32	0.246	-0.30	0.278
Putamen	-0.32	0.259	0.36	0.207	-0.44	0.098	-0.11	0.703
Anterior thalamus	0.04	0.900	0.48	0.086	-0.25	0.370	-0.28	0.307
Lateral thalamus	0.06	0.829	-0.07	0.792	-0.44	0.099	-0.46	0.085
Medial thalamus	0.17	0.553	0.14	0.626	-0.53	0.054	-0.38	0.177

	Brain damage in the white matter									
	H & E		LFB		CD68 (+) microglia		CD68 (+) vessel		β-APP	
	r	p	r	p	r	p	r	p	r	p
Sagittal	0.06	0.830	0.34	0.179	-0.18	0.486	-0.29	0.255	0.20	0.437
Parietal	0.18	0.510	0.22	0.404	-0.23	0.386	-0.58	0.018	-0.07	0.792
Temporal	0.16	0.566	0.37	0.159	-0.34	0.192	-0.32	0.233	-0.22	0.414
Superior Periventricular	0.16	0.545	0.08	0.768	-0.35	0.165	-0.22	0.399	0.07	0.783
Periventricular	0.19	0.492	0.11	0.676	-0.47	0.067	-0.22	0.420	0.13	0.629
PLIC	0.10	0.757	0.03	0.931	-0.03	0.940	-0.09	0.803	0.63	0.049
Sagittal	0.06	0.830	0.34	0.179	-0.18	0.486	-0.29	0.255	0.20	0.437

P values are presented without correction for multiple comparisons.

Abbreviation: PCIC, posterior limb of the internal capsule.

Supplemental Table 4.3-5: ^{31}P MRS biomarkers and histo-pathological injury

(adjusted for AED and survival time after resuscitation)

A. ^{31}P MRS biomarkers 1-48 h after resuscitation and neuronal death assessed using H & E stains

		Time after resuscitation (h)																	
		1 - < 3		3 - < 6		6 - < 12		12 - < 18		18 - < 24		24 - < 30		30 - < 36		36 - < 42		42 - < 48	
		F	p	F	p	F	p	F	p	F	p	F	p	F	p	F	p	F	p
NTP/EPP	Sagittal top	0.03	0.874	1.18	0.296	5.86	0.030	6.93	0.021	8.37	0.016	3.06	0.141	0.22	0.672	0.89	0.519	0.21	0.726
	Sagittal bottom	0.03	0.867	0.47	0.503	0.83	0.379	1.14	0.305	1.65	0.228	3.73	0.111	0.24	0.657	0.47	0.618	0.08	0.824
	Parietal top	0.08	0.783	1.65	0.219	1.40	0.257	1.79	0.204	2.07	0.181	2.00	0.216	0.10	0.773	0.12	0.787	0.00	0.994
	Parietal bottom	0.07	0.799	1.42	0.254	0.69	0.421	1.46	0.249	1.89	0.200	1.08	0.346	0.06	0.821	4.55	0.279	76.27	0.073
	Temporal	0.41	0.536	0.12	0.732	4.38	0.058	5.28	0.042	6.05	0.036	2.04	0.226	1.14	0.363	1.16	0.476	0.30	0.683
	Hippocampus	0.07	0.806	0.56	0.488	8.20	0.035	14.29	0.019	4.53	0.123								
	Caudate nucleus	0.27	0.615	0.73	0.413	5.54	0.040	7.21	0.025	5.53	0.047	1.13	0.366	3.68	0.195	1.29	0.459	0.34	0.666
	Putamen	0.05	0.821	0.57	0.466	2.80	0.125	2.72	0.130	1.46	0.258	1.54	0.283	0.99	0.393	1.25	0.465	0.32	0.672
	Anterior thalamus	2.51	0.144	4.95	0.050	5.67	0.039	6.30	0.031	7.60	0.022	4.76	0.095	0.84	0.427	2.88	0.339	0.75	0.546
	Lateral thalamus	0.33	0.580	0.54	0.479	3.21	0.101	0.94	0.354	1.23	0.296	0.29	0.618	0.10	0.773	1.56	0.429	0.41	0.636
	Medial thalamus	0.04	0.852	0.01	0.915	12.57	0.005	7.21	0.023	8.26	0.018	1.76	0.256	0.22	0.668	1.33	0.455	0.35	0.661
PCr/EPP	Sagittal top	1.11	0.311	1.25	0.283	11.78	0.004	21.56	<0.00	23.81	0.001	4.31	0.093	15.25	0.030	0.89	0.518	0.01	0.925
	Sagittal bottom	1.02	0.329	1.36	0.263	5.23	0.038	5.00	0.044	6.22	0.032	29.56	0.003	1.22	0.349	0.47	0.617	0.00	0.976
	Parietal top	0.91	0.357	0.68	0.424	5.09	0.041	7.44	0.017	7.00	0.025	6.18	0.055	7.47	0.072	0.12	0.786	0.10	0.807
	Parietal bottom	1.89	0.191	1.62	0.223	5.03	0.042	6.29	0.026	6.50	0.029	4.31	0.093	5.71	0.097	4.50	0.280	24.53	0.127
	Temporal	0.09	0.773	0.01	0.936	3.15	0.101	3.78	0.078	5.51	0.043	0.53	0.506	0.33	0.608	1.17	0.475	0.03	0.882
	Hippocampus	2.56	0.171	4.09	0.099	16.79	0.009	11.67	0.027	9.86	0.052								
	Caudate nucleus	0.88	0.372	0.30	0.593	8.06	0.018	16.22	0.003	7.46	0.026	0.32	0.611	35.87	0.027	1.30	0.458	0.05	0.865
	Putamen	0.33	0.580	0.16	0.699	1.50	0.249	3.41	0.095	1.14	0.313	0.36	0.583	1.21	0.352	1.26	0.464	0.04	0.871
	Anterior thalamus	8.57	0.015	4.03	0.072	9.18	0.013	13.59	0.004	11.21	0.009	11.49	0.028	0.49	0.533	2.90	0.338	0.18	0.745
	Lateral thalamus	0.00	0.982	0.07	0.794	1.68	0.221	2.88	0.120	2.62	0.140	0.32	0.603	9.81	0.052	1.58	0.428	0.07	0.835
	Medial thalamus	0.13	0.729	0.15	0.705	3.71	0.080	5.20	0.046	9.32	0.014	1.12	0.349	1.49	0.310	1.34	0.454	0.05	0.861

		Time after resuscitation (h)																	
		1 - < 3		3 - < 6		6 - < 12		12 - < 18		18 - < 24		24 - < 30		30 - < 36		36 - < 42		42 - < 48	
		F	p	F	p	F	p	F	p	F	p	F	p	F	p	F	p	F	p
Pi/EPP	Sagittal top	2.01	0.178	2.08	0.171	10.87	0.005	14.21	0.002	17.16	0.002	5.26	0.070	0.46	0.544	3.55	0.311	0.14	0.772
	Sagittal bottom	0.74	0.403	1.88	0.192	4.68	0.048	3.59	0.081	4.56	0.058	8.65	0.032	0.10	0.775	1.78	0.410	0.04	0.871
	Parietal top	1.67	0.217	1.72	0.211	4.69	0.048	5.48	0.036	5.66	0.039	5.88	0.060	0.42	0.562	0.61	0.579	0.00	0.960
	Parietal bottom	2.72	0.121	2.96	0.107	3.80	0.072	4.37	0.057	5.20	0.046	3.81	0.108	0.35	0.597	1.08	0.487	587.6	0.026
	Temporal	0.13	0.729	0.49	0.496	3.50	0.086	5.31	0.042	6.66	0.030	0.90	0.397	0.49	0.535	4.98	0.268	0.20	0.729
	Hippocampus	2.31	0.189	1.79	0.239	7.81	0.038	6.63	0.062	6.16	0.089								
	Caudate nucleus	2.12	0.176	0.77	0.401	5.15	0.047	10.86	0.009	7.08	0.029	2.12	0.242	8.20	0.103	5.77	0.251	0.24	0.712
	Putamen	1.68	0.224	0.29	0.605	1.42	0.262	3.26	0.101	1.40	0.267	0.83	0.415	0.55	0.513	5.49	0.257	0.23	0.718
	Anterior thalamus	7.03	0.024	6.01	0.034	7.00	0.025	13.35	0.004	9.44	0.013	2.70	0.176	0.35	0.597	23.02	0.131	0.56	0.592
	Lateral thalamus	0.26	0.620	0.00	0.949	2.80	0.122	2.59	0.139	2.39	0.157	0.73	0.440	0.35	0.597	7.62	0.221	0.30	0.682
	Medial thalamus	0.28	0.605	0.06	0.815	6.30	0.029	6.11	0.033	9.42	0.013	0.81	0.418	0.12	0.748	6.01	0.247	0.24	0.708
PCr/Pi	Sagittal top	2.13	0.166	2.56	0.132	21.56	0.000	31.99	0.000	51.20	0.000	6.50	0.051	13.59	0.035	7.49	0.223	0.76	0.543
	Sagittal bottom	1.81	0.199	3.84	0.070	10.23	0.006	6.90	0.021	19.77	0.001	56.40	0.001	1.50	0.308	3.26	0.322	0.40	0.642
	Parietal top	2.33	0.149	2.88	0.112	11.23	0.005	10.88	0.006	22.33	0.001	9.40	0.028	3.29	0.168	1.06	0.491	0.09	0.811
	Parietal bottom	3.97	0.066	4.62	0.050	11.30	0.005	10.00	0.007	18.50	0.002	7.37	0.042	2.44	0.216	0.62	0.575	5.57	0.255
	Temporal	0.15	0.706	0.45	0.515	7.12	0.020	8.25	0.015	9.59	0.013	4.72	0.096	1.16	0.361	11.78	0.181	1.00	0.501
	Hippocampus	4.77	0.081	3.00	0.144	22.28	0.005	26.82	0.007	3.98	0.140								
	Caudate nucleus	2.68	0.133	0.51	0.493	13.50	0.004	35.49	0.000	10.78	0.011	4.70	0.119	237.9	0.004	14.52	0.163	1.11	0.483
	Putamen	1.69	0.223	0.03	0.859	3.22	0.103	6.80	0.026	2.40	0.155	6.35	0.065	3.55	0.156	13.51	0.169	1.07	0.489
	Anterior thalamus	7.67	0.020	5.41	0.042	9.80	0.011	9.09	0.013	9.68	0.012	1.08	0.357	0.36	0.591	217.2	0.043	2.43	0.363
	Lateral thalamus	0.00	0.987	0.06	0.806	3.10	0.106	3.33	0.098	7.11	0.026	1.26	0.325	5.96	0.092	22.07	0.134	1.34	0.454
	Medial thalamus	0.36	0.562	0.04	0.849	6.52	0.027	7.84	0.019	12.26	0.007	12.74	0.023	4.47	0.125	15.39	0.159	1.14	0.479

B. ^{31}P MRS biomarkers 1-48 h after resuscitation and TUNEL positive apoptotic cell death

		Time after resuscitation (h)																	
		1 - < 3		3 - < 6		6 - < 12		12 - < 18		18 - < 24		24 - < 30		30 - < 36		36 - < 42		42 - < 48	
		F	p	F	p	F	p	F	p	F	p	F	p	F	p	F	p	F	p
NTP/EPP	Sagittal top	0.05	0.820	0.20	0.664	2.56	0.132	0.94	0.350	1.12	0.316	1.93	0.224	0.00	0.990	0.00	0.975	0.14	0.769
	Sagittal bottom	0.06	0.817	0.15	0.700	9.28	0.009	3.60	0.080	1.47	0.253	4.96	0.076	0.47	0.541	1.32	0.456	0.34	0.663
	Parietal top	0.05	0.822	0.08	0.781	5.89	0.029	1.67	0.219	0.62	0.450	3.22	0.133	0.00	0.968	0.00	0.993	0.12	0.786
	Parietal bottom	0.01	0.919	0.40	0.538	6.07	0.027	3.19	0.097	1.07	0.326	5.49	0.066	0.09	0.780	10.84	0.188	1142.	0.019
	Temporal	0.28	0.607	0.29	0.600	1.78	0.206	0.53	0.483	0.53	0.484	0.05	0.833	0.27	0.638	0.88	0.520	0.21	0.726
	Hippocampus	4.54	0.086	0.07	0.796	0.53	0.500	3.97	0.117	7.39	0.073								
	Caudate nucleus	0.03	0.871	0.00	0.959	1.21	0.297	0.40	0.543	0.82	0.393	0.01	0.921	0.17	0.717	0.03	0.885	0.02	0.908
	Putamen	0.00	0.965	0.07	0.798	13.43	0.004	2.47	0.147	1.69	0.226	2.55	0.186	0.06	0.828	0.49	0.612	1.83	0.406
	Anterior thalamus	0.15	0.710	0.95	0.353	0.04	0.844	0.11	0.752	0.05	0.830	0.83	0.414	0.40	0.570	0.00	0.984	0.13	0.778
	Lateral thalamus	0.06	0.815	0.03	0.862	2.56	0.138	1.51	0.247	4.26	0.069	0.11	0.755	0.00	0.999	0.37	0.651	1.42	0.445
	Medial thalamus	0.01	0.941	0.09	0.764	4.47	0.061	2.52	0.147	4.22	0.074	0.01	0.915	1.56	0.339				
PCr/EPP	Sagittal top	0.36	0.558	1.10	0.311	2.60	0.129	1.34	0.267	2.03	0.184	4.48	0.088	0.12	0.751	0.00	0.977	0.64	0.569
	Sagittal bottom	0.98	0.339	2.34	0.148	8.15	0.013	5.09	0.042	3.44	0.093	6.04	0.057	1.84	0.268	1.33	0.455	0.05	0.862
	Parietal top	0.21	0.655	0.82	0.380	4.51	0.052	3.00	0.107	2.17	0.172	5.22	0.071	0.24	0.659	0.00	0.994	0.57	0.587
	Parietal bottom	0.27	0.611	0.85	0.372	6.28	0.025	4.56	0.052	2.98	0.115	8.21	0.035	1.38	0.324	10.69	0.189	7.85	0.218
	Temporal	0.03	0.860	1.45	0.251	2.47	0.142	1.09	0.319	1.29	0.286	0.73	0.442	0.04	0.860	0.89	0.518	0.01	0.926
	Hippocampus	0.14	0.724	0.68	0.446	1.18	0.327	1.78	0.253	2.87	0.189								
	Caudate nucleus	0.11	0.749	0.88	0.371	0.70	0.421	0.30	0.595	0.97	0.353	0.19	0.690	0.01	0.940	0.03	0.884	0.24	0.709
	Putamen	0.00	0.977	0.20	0.663	5.53	0.041	4.55	0.059	2.48	0.150	7.35	0.053	0.03	0.875	0.48	0.613	8.88	0.206
	Anterior thalamus	0.86	0.376	0.14	0.712	0.11	0.747	0.04	0.838	0.14	0.717	0.58	0.487	0.10	0.777	0.00	0.985	0.61	0.578
	Lateral thalamus	0.48	0.501	0.56	0.469	1.06	0.325	1.31	0.279	4.91	0.054	0.34	0.594	0.01	0.921	0.37	0.652	6.09	0.245
	Medial thalamus	0.00	0.995	0.37	0.558	2.58	0.139	3.48	0.095	5.74	0.043	0.16	0.718	0.03	0.873				

		Time after resuscitation (h)																	
		1 - < 3		3 - < 6		6 - < 12		12 - < 18		18 - < 24		24 - < 30		30 - < 36		36 - < 42		42 - < 48	
		F	p	F	p	F	p	F	p	F	p	F	p	F	p	F	p	F	p
Pi/EPP	Sagittal top	0.00	0.974	0.13	0.720	4.09	0.063	1.34	0.267	1.92	0.196	3.62	0.115	0.07	0.815	0.09	0.816	0.22	0.723
	Sagittal bottom	0.18	0.682	0.75	0.400	15.05	0.002	4.77	0.048	2.71	0.131	7.39	0.042	1.32	0.334	5.93	0.248	0.24	0.709
	Parietal top	0.05	0.826	0.08	0.786	6.98	0.019	2.13	0.168	1.45	0.257	4.47	0.088	0.11	0.758	0.11	0.799	0.19	0.740
	Parietal bottom	0.00	0.970	0.07	0.800	8.71	0.011	4.03	0.066	2.14	0.174	7.02	0.045	0.44	0.556	1.95	0.396	94.80	0.065
	Temporal	0.42	0.529	0.00	0.991	3.60	0.082	0.82	0.386	0.84	0.384	0.22	0.665	0.02	0.886	3.53	0.311	0.14	0.772
	Hippocampus	0.26	0.632	0.09	0.774	0.68	0.448	4.60	0.098	4.21	0.132								
	Caudate nucleus	0.00	0.952	0.16	0.694	1.29	0.282	0.44	0.523	1.04	0.337	0.13	0.740	0.01	0.917	0.31	0.677	0.05	0.862
	Putamen	0.00	0.950	0.00	0.999	10.22	0.010	3.28	0.100	1.93	0.198	1.67	0.266	0.08	0.791	0.08	0.820	2.50	0.359
	Anterior thalamus	0.14	0.720	0.35	0.566	0.01	0.942	0.11	0.748	0.10	0.765	0.75	0.435	0.22	0.672	0.10	0.807	0.20	0.731
	Lateral thalamus	1.06	0.325	0.81	0.387	1.84	0.202	1.58	0.237	5.15	0.049	0.18	0.696	0.00	0.992	0.05	0.859	1.92	0.398
	Medial thalamus	0.01	0.940	0.03	0.877	3.02	0.113	2.42	0.154	4.39	0.070	0.00	0.980	0.59	0.522				
PCr/Pi	Sagittal top	0.55	0.470	0.96	0.343	3.07	0.101	1.42	0.254	2.36	0.156	3.03	0.142	0.01	0.930	0.21	0.729	0.01	0.951
	Sagittal bottom	0.75	0.401	1.87	0.193	5.84	0.030	3.87	0.071	3.21	0.104	3.42	0.124	0.49	0.536	15.11	0.160	1.13	0.480
	Parietal top	0.35	0.562	0.63	0.442	3.63	0.078	2.37	0.147	2.17	0.171	2.91	0.149	0.04	0.856	0.24	0.711	0.00	0.969
	Parietal bottom	0.30	0.591	0.83	0.379	4.83	0.045	3.60	0.080	3.44	0.093	4.37	0.091	0.33	0.605	1.11	0.484	14.46	0.164
	Temporal	0.06	0.808	0.21	0.652	0.99	0.339	0.31	0.589	0.81	0.393	0.00	0.968	0.05	0.840	7.45	0.224	0.76	0.544
	Hippocampus	0.01	0.931	0.45	0.534	0.87	0.394	1.22	0.331	1.27	0.342								
	Caudate nucleus	0.03	0.874	0.52	0.485	0.63	0.447	0.12	0.736	0.31	0.591	0.08	0.798	0.02	0.911	0.57	0.589	0.02	0.909
	Putamen	0.01	0.927	0.15	0.709	4.32	0.064	2.84	0.123	2.15	0.176	1.23	0.330	0.06	0.818	0.02	0.908	0.57	0.588
	Anterior thalamus	0.30	0.598	0.35	0.568	0.02	0.881	0.06	0.810	0.09	0.772	0.99	0.376	0.14	0.737	0.22	0.720	0.00	0.960
	Lateral thalamus	1.16	0.305	0.58	0.462	2.54	0.139	1.96	0.191	5.19	0.049	0.14	0.729	0.00	0.986	0.01	0.947	0.44	0.627
	Medial thalamus	0.02	0.890	0.00	0.978	2.92	0.118	2.56	0.144	3.91	0.083	0.00	0.974	0.00	0.985				

C-1. ^{31}P MRS biomarkers 1-48 h after resuscitation and CD68 positive microglia in the grey matter

		Time after resuscitation (h)																	
		1 - < 3		3 - < 6		6 - < 12		12 - < 18		18 - < 24		24 - < 30		30 - < 36		36 - < 42		42 - < 48	
		F	p	F	p	F	p	F	p	F	p	F	p	F	p	F	p	F	p
NTP/EPP	Sagittal top	0.84	0.375	0.39	0.544	1.48	0.244	2.06	0.175	1.34	0.274	4.09	0.099	0.41	0.567	0.24	0.708	0.99	0.501
	Sagittal bottom	0.18	0.674	0.87	0.367	5.84	0.030	4.48	0.054	8.35	0.016	4.87	0.078	0.66	0.475	0.27	0.696	0.02	0.903
	Parietal top	2.89	0.111	2.09	0.170	2.88	0.112	2.64	0.128	3.82	0.079	4.10	0.099	0.68	0.471	0.57	0.587	2.16	0.381
	Parietal bottom	0.31	0.584	0.59	0.455	0.49	0.496	1.26	0.283	0.53	0.483	4.02	0.101	1.17	0.359	0.03	0.900	0.27	0.693
	Temporal	1.66	0.222	1.27	0.281	0.18	0.680	0.21	0.656	0.00	0.961	0.71	0.448	0.08	0.801	1.70	0.416	8.55	0.210
	Hippocampus	0.67	0.452	2.42	0.180	1.90	0.226	0.06	0.822	0.17	0.705								
	Caudate nucleus	2.20	0.166	0.39	0.545	2.78	0.124	0.29	0.603	0.39	0.547	0.03	0.861	1.30	0.337	0.41	0.639	1.54	0.432
	Putamen	0.01	0.905	3.54	0.087	0.07	0.793	0.03	0.856	0.00	0.968	0.42	0.550	0.60	0.494	4.67	0.276	1.12	0.482
	Anterior thalamus	1.54	0.240	0.36	0.562	1.88	0.197	0.02	0.882	0.30	0.595	0.10	0.769	1.01	0.389	0.57	0.587	2.16	0.381
	Lateral thalamus	2.91	0.116	0.21	0.656	1.46	0.252	0.03	0.873	0.00	0.954	0.10	0.769	1.01	0.389	0.57	0.587	2.16	0.381
	Medial thalamus	0.05	0.820	2.50	0.145	0.18	0.677	0.00	0.971	0.01	0.928	0.62	0.488	0.18	0.713				
PCr/EPP	Sagittal top	0.80	0.386	0.59	0.454	1.55	0.234	2.63	0.129	4.46	0.061	40.03	0.001	0.07	0.813	0.24	0.709	3.79	0.302
	Sagittal bottom	1.84	0.197	2.69	0.123	8.41	0.012	5.95	0.030	15.41	0.003	15.95	0.010	0.11	0.761	0.27	0.695	0.03	0.898
	Parietal top	5.57	0.033	3.09	0.100	3.43	0.085	3.49	0.084	13.79	0.004	30.25	0.003	0.03	0.867	0.57	0.588	11.68	0.181
	Parietal bottom	1.23	0.286	0.99	0.337	2.53	0.134	3.18	0.098	2.41	0.151	35.93	0.002	0.05	0.832	0.02	0.901	1.04	0.494
	Temporal	1.90	0.194	0.47	0.507	0.19	0.672	0.14	0.717	0.01	0.915	0.52	0.511	0.01	0.930	1.69	0.418	3780.	0.010
	Hippocampus	2.49	0.175	2.37	0.184	0.54	0.495	0.02	0.897	0.00	0.998								
	Caudate nucleus	0.02	0.884	0.23	0.639	0.12	0.736	0.16	0.695	0.72	0.417	0.06	0.822	0.47	0.542	0.40	0.640	6.82	0.233
	Putamen	1.11	0.316	1.46	0.252	0.09	0.772	0.04	0.845	0.29	0.605	1.37	0.307	0.03	0.864	4.72	0.275	0.30	0.682
	Anterior thalamus	0.03	0.856	0.05	0.821	0.06	0.805	0.02	0.883	0.57	0.470	0.01	0.922	0.04	0.852	0.57	0.588	11.68	0.181
	Lateral thalamus	0.26	0.621	1.14	0.309	0.03	0.870	0.01	0.928	0.00	0.951	0.01	0.922	0.04	0.852	0.57	0.588	11.68	0.181
	Medial thalamus	1.89	0.199	2.49	0.145	0.14	0.713	0.00	0.970	0.32	0.587	1.18	0.357	0.01	0.929				

		Time after resuscitation (h)																	
		1 - < 3		3 - < 6		6 - < 12		12 - < 18		18 - < 24		24 - < 30		30 - < 36		36 - < 42		42 - < 48	
		F	p	F	p	F	p	F	p	F	p	F	p	F	p	F	p	F	p
Pi/EPP	Sagittal top	2.58	0.130	2.05	0.174	3.04	0.103	2.34	0.150	3.35	0.097	9.57	0.027	0.43	0.557	0.02	0.916	1.33	0.455
	Sagittal bottom	0.93	0.351	1.58	0.230	8.07	0.013	6.36	0.026	14.21	0.004	12.24	0.017	0.73	0.455	1.08	0.488	0.01	0.949
	Parietal top	5.76	0.031	4.72	0.048	5.22	0.038	4.18	0.062	10.51	0.009	10.64	0.022	0.79	0.439	0.11	0.795	2.98	0.334
	Parietal bottom	2.01	0.178	2.19	0.161	2.59	0.130	2.31	0.152	1.80	0.209	10.34	0.024	1.19	0.355	0.03	0.892	0.38	0.647
	Temporal	0.99	0.339	0.35	0.567	0.19	0.671	0.31	0.587	0.05	0.834	0.24	0.651	0.04	0.860	0.45	0.625	14.51	0.163
	Hippocampus	1.62	0.259	1.39	0.291	1.96	0.221	0.01	0.910	0.01	0.923								
	Caudate nucleus	0.14	0.719	0.00	0.970	1.28	0.283	0.63	0.446	0.98	0.347	0.43	0.547	2.22	0.233	0.06	0.847	2.08	0.386
	Putamen	0.52	0.486	0.27	0.613	0.08	0.777	0.02	0.884	0.30	0.595	0.00	0.963	1.03	0.385	87.84	0.068	0.83	0.529
	Anterior thalamus	0.34	0.570	0.54	0.478	1.39	0.263	0.42	0.532	0.95	0.356	0.29	0.616	1.20	0.353	0.11	0.795	2.98	0.334
	Lateral thalamus	0.01	0.905	0.24	0.632	0.24	0.631	0.16	0.696	0.04	0.853	0.29	0.616	1.20	0.353	0.11	0.795	2.98	0.334
	Medial thalamus	0.93	0.359	1.12	0.314	0.46	0.513	0.14	0.716	0.34	0.577	0.07	0.810	0.38	0.599				
PCr/Pi	Sagittal top	6.13	0.027	3.32	0.090	3.84	0.070	3.75	0.075	10.87	0.008	59.63	0.001	0.00	0.981	0.00	0.996	0.29	0.684
	Sagittal bottom	0.93	0.352	2.46	0.139	12.44	0.003	7.80	0.015	13.28	0.005	9.69	0.026	0.45	0.551	1.89	0.401	0.22	0.721
	Parietal top	10.27	0.006	4.49	0.052	3.84	0.070	3.20	0.097	46.23	0.000	44.17	0.001	0.02	0.893	0.03	0.883	0.67	0.563
	Parietal bottom	6.03	0.028	5.49	0.034	6.01	0.028	4.99	0.044	6.41	0.030	54.05	0.001	0.26	0.647	0.10	0.804	0.04	0.876
	Temporal	2.91	0.114	0.30	0.594	0.01	0.922	0.02	0.903	0.16	0.701	0.66	0.461	0.14	0.736	0.24	0.712	1.99	0.392
	Hippocampus	2.27	0.192	1.08	0.345	0.44	0.538	0.00	0.996	0.28	0.633								
	Caudate nucleus	0.07	0.802	0.07	0.790	0.69	0.424	0.32	0.582	1.93	0.198	0.08	0.796	0.18	0.700	0.01	0.935	0.48	0.615
	Putamen	1.65	0.226	0.27	0.615	0.02	0.887	0.00	0.992	1.29	0.285	1.75	0.257	0.06	0.828	1009.	0.020	3.85	0.300
	Anterior thalamus	0.00	0.996	0.16	0.698	0.54	0.478	0.08	0.779	1.61	0.236	0.05	0.834	0.01	0.911	0.03	0.883	0.67	0.563
	Lateral thalamus	0.33	0.580	0.74	0.408	0.02	0.881	0.01	0.919	0.15	0.703	0.05	0.834	0.01	0.911	0.03	0.883	0.67	0.563
	Medial thalamus	1.73	0.217	0.86	0.375	0.12	0.740	0.03	0.875	1.34	0.280	1.36	0.329	0.06	0.829				

C-2. ^{31}P MRS biomarkers 1-48 h after resuscitation and CD68 positive microglia in the white matter

		Time after resuscitation (h)																	
		1 - < 3		3 - < 6		6 - < 12		12 - < 18		18 - < 24		24 - < 30		30 - < 36		36 - < 42		42 - < 48	
		F	p	F	p	F	p	F	p	F	p	F	p	F	p	F	p	F	p
NTP/EPP	Sagittal	0.63	0.442	0.64	0.439	1.26	0.282	2.92	0.113	1.46	0.254	3.11	0.138	0.00	0.995	2.13	0.383	12.43	0.176
	Parietal	0.89	0.365	0.62	0.445	1.65	0.223	2.33	0.155	1.89	0.203	3.71	0.112	1.36	0.328	0.18	0.745	0.79	0.538
	Temporal	0.03	0.867	0.33	0.577	0.47	0.508	1.73	0.215	2.05	0.186	0.43	0.550	0.20	0.683	6.78	0.233	559.6	0.027
	Superior Periventricular	0.34	0.572	0.24	0.632	3.23	0.096	3.86	0.073	2.35	0.156	0.08	0.789	1.28	0.340	0.08	0.824	0.47	0.617
	Periventricular	0.24	0.636	1.82	0.202	0.81	0.386	1.28	0.282	4.25	0.066	0.22	0.655	0.08	0.793	1.42	0.445	6.48	0.238
	PLIC	0.31	0.597	0.94	0.370	1.46	0.272	2.84	0.153	2.95	0.161								
PCr/EPP	Sagittal	2.83	0.117	2.48	0.140	3.60	0.080	4.25	0.062	4.52	0.059	23.82	0.005	0.00	0.987	2.11	0.384	737.9	0.023
	Parietal	0.65	0.435	0.42	0.527	1.45	0.251	2.45	0.146	7.12	0.026	28.07	0.003	0.06	0.827	0.18	0.746	2.88	0.339
	Temporal	14.26	0.003	21.84	0.001	7.57	0.018	4.33	0.062	3.57	0.091	0.86	0.405	0.56	0.508	6.70	0.235	12.96	0.173
	Superior Periventricular	6.46	0.025	8.61	0.012	4.43	0.055	2.37	0.150	2.18	0.171	0.18	0.689	0.06	0.829	0.08	0.825	1.69	0.418
	Periventricular	2.17	0.166	2.51	0.139	0.89	0.363	1.20	0.296	1.26	0.288	0.00	0.985	0.00	0.963	1.41	0.446	268.4	0.039
	PLIC	2.74	0.149	6.30	0.046	4.26	0.085	1.51	0.273	7.87	0.049								
Pi/EPP	Sagittal	3.86	0.071	3.64	0.079	4.03	0.066	3.53	0.085	3.46	0.092	8.49	0.033	0.01	0.921	0.56	0.591	23.45	0.130
	Parietal	2.20	0.164	1.72	0.214	2.96	0.111	2.60	0.135	5.49	0.044	10.05	0.025	2.00	0.252	0.01	0.953	1.05	0.492
	Temporal	4.05	0.067	10.38	0.007	3.95	0.070	3.23	0.100	2.87	0.125	0.00	0.972	0.58	0.503	1.45	0.442	1072.	0.019
	Superior Periventricular	4.10	0.064	3.99	0.067	3.54	0.083	2.40	0.147	2.25	0.165	0.63	0.464	1.97	0.255	0.00	0.968	0.64	0.571
	Periventricular	0.77	0.396	1.63	0.225	0.99	0.339	1.41	0.261	1.81	0.208	0.00	0.949	0.04	0.847	0.37	0.653	10.35	0.192
	PLIC	1.07	0.341	2.77	0.147	3.91	0.095	2.08	0.209	6.67	0.061								
PCr/Pi	Sagittal	13.32	0.003	7.48	0.017	7.55	0.017	6.49	0.026	8.82	0.014	35.60	0.002	0.10	0.767	0.31	0.678	2.51	0.358
	Parietal	5.81	0.033	3.03	0.107	4.12	0.065	3.94	0.073	24.03	0.001	42.01	0.001	0.00	0.966	0.00	0.959	0.22	0.721
	Temporal	10.77	0.007	15.53	0.002	5.79	0.033	4.20	0.065	1.89	0.203	0.71	0.447	0.06	0.823	0.83	0.529	8.58	0.209
	Superior Periventricular	5.06	0.042	4.42	0.056	4.03	0.066	3.04	0.107	0.50	0.495	0.21	0.664	0.01	0.934	0.04	0.880	0.11	0.800
	Periventricular	2.01	0.182	1.65	0.224	0.84	0.376	0.78	0.395	0.37	0.558	0.01	0.925	0.09	0.782	0.19	0.741	1.65	0.421
	PLIC	1.66	0.246	4.53	0.077	3.95	0.094	2.03	0.214	8.31	0.045								

D-1. ^{31}P MRS biomarkers 1-48 h after resuscitation and CD68 positive vessels in the grey matter

		Time after resuscitation (h)																	
		1 - < 3		3 - < 6		6 - < 12		12 - < 18		18 - < 24		24 - < 30		30 - < 36		36 - < 42		42 - < 48	
		F	p	F	p	F	p	F	p	F	p	F	p	F	p	F	p	F	p
NTP/EPP	Sagittal top	0.47	0.506	0.61	0.450	1.80	0.201	4.37	0.057	3.51	0.090	3.97	0.103	1.23	0.348	0.57	0.587	2.16	0.381
	Sagittal bottom	0.05	0.830	0.89	0.361	3.65	0.077	3.64	0.079	7.21	0.023	3.19	0.134	1.01	0.388	1.42	0.445	6.48	0.238
	Parietal top	1.14	0.304	1.81	0.200	3.26	0.093	3.67	0.078	5.14	0.047	4.10	0.099	0.43	0.558	0.57	0.587	2.16	0.381
	Parietal bottom	0.34	0.567	0.87	0.366	1.01	0.332	2.14	0.167	1.36	0.271	4.09	0.099	0.24	0.656	1.42	0.445	6.48	0.238
	Temporal	2.14	0.169	0.88	0.366	0.33	0.578	0.21	0.657	0.01	0.943	0.85	0.408	0.08	0.793	1.42	0.445	6.48	0.238
	Hippocampus	1.32	0.303	0.74	0.429	1.95	0.221	0.24	0.651	0.61	0.492								
	Caudate nucleus	2.73	0.127	0.00	0.972	2.58	0.137	0.39	0.547	0.09	0.767								
	Putamen	0.26	0.621	1.10	0.316	1.30	0.278	1.34	0.274	0.79	0.396	0.12	0.749	1.19	0.354	0.03	0.900	0.27	0.693
	Anterior thalamus	3.06	0.108	0.02	0.892	2.31	0.157	0.03	0.871	0.07	0.798	0.10	0.769	1.01	0.389	0.57	0.587	2.16	0.381
	Lateral thalamus	3.28	0.097	0.16	0.700	1.69	0.220	0.01	0.940	0.03	0.861	0.10	0.769	1.01	0.389	0.57	0.587	2.16	0.381
	Medial thalamus	1.00	0.340	0.92	0.360	0.24	0.632	0.00	0.994	0.01	0.913	0.62	0.488	0.18	0.713				
PCr/EPP	Sagittal top	2.26	0.155	2.18	0.162	2.64	0.127	3.95	0.068	8.65	0.015	39.08	0.002	0.03	0.880	0.57	0.588	11.68	0.181
	Sagittal bottom	0.14	0.710	0.56	0.467	2.56	0.132	3.27	0.094	17.86	0.002	27.86	0.003	0.20	0.686	1.41	0.446	268.4	0.039
	Parietal top	9.05	0.009	7.31	0.017	6.97	0.019	5.78	0.032	16.07	0.002	18.51	0.008	0.03	0.884	0.57	0.588	11.68	0.181
	Parietal bottom	1.43	0.252	1.35	0.264	3.44	0.085	4.47	0.054	4.97	0.050	37.76	0.002	0.17	0.706	1.41	0.446	268.4	0.039
	Temporal	1.85	0.198	0.43	0.524	0.15	0.707	0.10	0.762	0.03	0.862	0.72	0.445	0.00	0.963	1.41	0.446	268.4	0.039
	Hippocampus	6.19	0.055	5.37	0.068	1.45	0.282	1.17	0.339	0.84	0.426								
	Caudate nucleus	0.04	0.851	0.22	0.646	0.01	0.911	0.05	0.834	0.06	0.806								
	Putamen	0.96	0.348	1.03	0.332	0.81	0.387	2.45	0.149	0.53	0.485	0.77	0.429	0.05	0.832	0.02	0.901	1.04	0.494
	Anterior thalamus	0.02	0.904	0.10	0.761	0.01	0.923	0.01	0.941	0.11	0.743	0.01	0.922	0.04	0.852	0.57	0.588	11.68	0.181
	Lateral thalamus	0.00	0.970	0.30	0.593	0.00	0.966	0.05	0.827	0.05	0.823	0.01	0.922	0.04	0.852	0.57	0.588	11.68	0.181
	Medial thalamus	2.05	0.183	3.91	0.076	0.61	0.454	0.26	0.621	0.03	0.871	1.18	0.357	0.01	0.929				

		Time after resuscitation (h)																	
		1 - < 3		3 - < 6		6 - < 12		12 - < 18		18 - < 24		24 - < 30		30 - < 36		36 - < 42		42 - < 48	
		F	p	F	p	F	p	F	p	F	p	F	p	F	p	F	p	F	p
Pi/EPP	Sagittal top	4.18	0.060	3.01	0.105	3.09	0.101	3.20	0.097	5.85	0.036	8.26	0.035	1.46	0.313	0.11	0.795	2.98	0.334
	Sagittal bottom	0.55	0.472	1.13	0.305	4.05	0.064	3.65	0.078	13.19	0.005	7.08	0.045	1.06	0.379	0.37	0.653	10.35	0.192
	Parietal top	7.00	0.019	8.57	0.011	7.96	0.014	5.85	0.031	11.63	0.007	9.67	0.027	0.50	0.529	0.11	0.795	2.98	0.334
	Parietal bottom	2.46	0.139	3.23	0.094	4.06	0.063	3.60	0.080	3.73	0.082	10.51	0.023	0.21	0.678	0.37	0.653	10.35	0.192
	Temporal	1.06	0.323	0.29	0.599	0.25	0.629	0.28	0.609	0.00	0.978	0.32	0.600	0.04	0.847	0.37	0.653	10.35	0.192
	Hippocampus	3.82	0.108	3.48	0.121	3.52	0.119	0.53	0.509	0.58	0.503								
	Caudate nucleus	0.14	0.711	0.15	0.702	0.56	0.469	0.22	0.652	0.13	0.726								
	Putamen	0.76	0.401	0.24	0.633	1.18	0.302	1.26	0.289	0.33	0.580	0.03	0.864	1.87	0.265	0.03	0.892	0.38	0.647
	Anterior thalamus	0.35	0.569	0.08	0.781	1.07	0.323	0.26	0.619	0.28	0.612	0.29	0.616	1.20	0.353	0.11	0.795	2.98	0.334
	Lateral thalamus	0.26	0.620	0.03	0.866	0.70	0.420	0.35	0.569	0.15	0.711	0.29	0.616	1.20	0.353	0.11	0.795	2.98	0.334
	Medial thalamus	0.44	0.521	1.45	0.256	0.07	0.795	0.00	0.991	0.00	0.959	0.07	0.810	0.38	0.599				
PCr/Pi	Sagittal top	10.49	0.006	3.95	0.067	3.61	0.078	4.39	0.056	10.95	0.008	61.58	0.001	0.02	0.887	0.03	0.883	0.67	0.563
	Sagittal bottom	0.17	0.690	0.80	0.386	4.03	0.064	3.92	0.069	17.23	0.002	29.78	0.003	0.27	0.642	0.19	0.741	1.65	0.421
	Parietal top	11.98	0.004	8.26	0.012	6.91	0.020	5.39	0.037	22.53	0.001	22.13	0.005	0.03	0.878	0.03	0.883	0.67	0.563
	Parietal bottom	6.26	0.025	6.70	0.021	8.04	0.013	6.74	0.022	12.65	0.005	53.68	0.001	0.49	0.535	0.19	0.741	1.65	0.421
	Temporal	2.85	0.117	0.21	0.654	0.01	0.931	0.01	0.938	0.00	0.995	0.64	0.467	0.09	0.782	0.19	0.741	1.65	0.421
	Hippocampus	4.65	0.084	2.63	0.165	1.12	0.339	0.65	0.464	0.27	0.639								
	Caudate nucleus	0.01	0.941	0.44	0.521	0.24	0.632	0.14	0.715	0.18	0.679								
	Putamen	1.05	0.328	0.12	0.736	0.90	0.362	1.71	0.220	0.50	0.496	1.08	0.356	0.01	0.913	0.10	0.804	0.04	0.876
	Anterior thalamus	0.00	0.979	0.01	0.918	0.26	0.619	0.03	0.873	0.59	0.463	0.05	0.834	0.01	0.911	0.03	0.883	0.67	0.563
	Lateral thalamus	0.03	0.865	0.06	0.810	0.11	0.751	0.02	0.884	0.39	0.549	0.05	0.834	0.01	0.911	0.03	0.883	0.67	0.563
	Medial thalamus	1.95	0.193	1.96	0.192	0.16	0.697	0.10	0.764	0.01	0.938	1.36	0.329	0.06	0.829				

D-2. ^{31}P MRS biomarkers 1-48 h after resuscitation and CD68 positive vessels in the white matter

		Time after resuscitation (h)																	
		1 - < 3		3 - < 6		6 - < 12		12 - < 18		18 - < 24		24 - < 30		30 - < 36		36 - < 42		42 - < 48	
		F	p	F	p	F	p	F	p	F	p	F	p	F	p	F	p	F	p
NTP/EPP	Sagittal	0.47	0.504	0.95	0.347	1.42	0.255	5.06	0.044	2.21	0.168	1.40	0.290	0.08	0.793	1.42	0.445	6.48	0.238
	Parietal	1.81	0.204	0.46	0.511	5.94	0.031	4.99	0.047	3.39	0.099	3.85	0.107						
	Temporal	0.26	0.617	0.20	0.666	0.81	0.385	0.75	0.406	4.48	0.063	0.42	0.550	0.60	0.494	4.67	0.276	1.12	0.482
	Superior Periventricular	0.27	0.610	0.73	0.410	0.55	0.471	0.18	0.679	0.81	0.389	0.03	0.875	0.03	0.871	3.15	0.327	27.38	0.120
	Periventricular	0.03	0.865	2.59	0.133	0.22	0.644	0.34	0.570	0.27	0.616	0.05	0.828	0.08	0.793	1.42	0.445	6.48	0.238
	PLIC	0.30	0.602	0.09	0.777	5.06	0.066	9.55	0.027	6.92	0.058								
PCr/EPP	Sagittal	3.06	0.104	3.40	0.088	4.35	0.057	4.75	0.050	5.12	0.047	8.30	0.035	0.00	0.963	1.41	0.446	268.4	0.039
	Parietal	9.78	0.009	8.27	0.014	12.58	0.004	10.68	0.007	13.07	0.006	34.09	0.002						
	Temporal	8.57	0.013	9.13	0.011	1.89	0.195	1.60	0.233	4.07	0.075	1.37	0.307	0.03	0.864	4.72	0.275	0.30	0.682
	Superior Periventricular	1.68	0.217	1.79	0.203	0.18	0.681	0.01	0.927	0.11	0.749	0.63	0.463	0.00	0.955	3.12	0.328	63.96	0.079
	Periventricular	0.03	0.859	0.00	0.983	0.10	0.755	0.26	0.620	1.31	0.280	0.95	0.375	0.00	0.963	1.41	0.446	268.4	0.039
	PLIC	3.42	0.114	7.16	0.037	5.26	0.062	2.53	0.172	7.48	0.052								
Pi/EPP	Sagittal	2.85	0.115	2.36	0.149	3.40	0.088	4.11	0.065	3.96	0.075	4.11	0.099	0.04	0.847	0.37	0.653	10.35	0.192
	Parietal	7.04	0.021	4.57	0.054	12.01	0.005	7.74	0.018	8.25	0.018	9.73	0.026						
	Temporal	4.83	0.048	8.91	0.011	2.44	0.144	1.60	0.232	4.06	0.075	0.00	0.963	1.03	0.385	87.84	0.068	0.83	0.529
	Superior Periventricular	0.28	0.606	1.10	0.313	0.06	0.818	0.01	0.942	0.15	0.707	0.64	0.459	0.10	0.772	0.80	0.535	73.58	0.074
	Periventricular	0.19	0.672	0.00	0.954	0.01	0.941	0.48	0.501	1.02	0.337	0.55	0.490	0.04	0.847	0.37	0.653	10.35	0.192
	PLIC	2.15	0.193	2.10	0.197	4.72	0.073	2.80	0.155	8.56	0.043								
PCr/Pi	Sagittal	10.08	0.007	5.66	0.033	7.43	0.017	7.30	0.019	6.16	0.032	10.65	0.022	0.09	0.782	0.19	0.741	1.65	0.421
	Parietal	12.51	0.004	6.98	0.022	19.05	0.001	14.67	0.003	19.55	0.002	55.29	0.001						
	Temporal	6.61	0.025	6.27	0.028	1.22	0.290	0.90	0.364	1.18	0.306	1.75	0.257	0.06	0.828	1009.	0.020	3.85	0.300
	Superior Periventricular	0.61	0.447	1.72	0.213	0.11	0.748	0.00	0.972	0.01	0.915	0.82	0.408	0.10	0.768	0.45	0.623	3.77	0.303
	Periventricular	0.01	0.917	0.16	0.695	0.21	0.656	0.46	0.513	2.25	0.164	1.19	0.324	0.09	0.782	0.19	0.741	1.65	0.421
	PLIC	5.25	0.062	3.69	0.103	4.67	0.074	4.17	0.097	3.13	0.152								

E. ^{31}P MRS biomarkers 1-48 h after resuscitation and white matter injury assessed using H & E stains

		Time after resuscitation (h)																	
		1 - < 3		3 - < 6		6 - < 12		12 - < 18		18 - < 24		24 - < 30		30 - < 36		36 - < 42		42 - < 48	
		F	p	F	p	F	p	F	p	F	p	F	p	F	p	F	p	F	p
NTP/EPP	Sagittal	0.25	0.628	0.94	0.349	5.36	0.038	7.02	0.021	6.02	0.034	1.39	0.291	0.23	0.664	0.88	0.521	0.21	0.728
	Parietal	0.08	0.785	1.21	0.292	3.28	0.095	5.69	0.036	4.55	0.062	1.39	0.291	0.23	0.664	0.88	0.521	0.21	0.728
	Temporal	0.19	0.674	0.47	0.504	4.83	0.048	3.40	0.092	3.34	0.101	0.01	0.926	0.00	0.986	0.00	0.993	0.11	0.800
	Superior Periventricular	0.00	0.984	0.02	0.891	3.27	0.094	3.64	0.080	4.67	0.056	0.66	0.454	0.00	0.983	0.00	1.000		
	Periventricular	0.07	0.799	0.15	0.701	14.52	0.002	8.97	0.012	9.87	0.010	2.02	0.214	0.00	0.999	0.88	0.521	0.21	0.728
	PLIC	0.06	0.816	0.24	0.638	15.19	0.005	10.59	0.014	19.60	0.004	0.30	0.637	1.61	0.425				
PCr/EPP	Sagittal	3.12	0.101	4.05	0.065	12.06	0.004	19.83	0.001	20.30	0.001	6.60	0.050	0.86	0.421	0.88	0.520	0.01	0.927
	Parietal	3.18	0.100	3.65	0.080	12.73	0.004	20.71	0.001	17.78	0.002	6.60	0.050	0.86	0.421	0.88	0.520	0.01	0.927
	Temporal	6.05	0.030	8.40	0.013	12.76	0.004	11.75	0.006	9.71	0.012	0.00	0.977	0.83	0.430	0.00	0.992	0.52	0.601
	Superior Periventricular	4.54	0.053	5.25	0.039	8.90	0.011	15.01	0.002	11.16	0.007	2.08	0.209	4.01	0.139	0.00	1.000		
	Periventricular	1.84	0.200	4.02	0.068	8.05	0.015	9.75	0.010	12.55	0.005	6.12	0.056	1.15	0.362	0.88	0.520	0.01	0.927
	PLIC	0.62	0.454	1.35	0.279	6.44	0.035	4.98	0.061	16.69	0.006	0.17	0.719	1.28	0.461				
Pi/EPP	Sagittal	4.51	0.054	3.26	0.094	11.12	0.005	11.27	0.006	12.05	0.006	3.75	0.111	0.02	0.906	3.49	0.313	0.14	0.774
	Parietal	3.23	0.098	2.25	0.160	7.94	0.016	10.66	0.008	9.74	0.012	3.75	0.111	0.02	0.906	3.49	0.313	0.14	0.774
	Temporal	5.65	0.035	5.50	0.037	11.73	0.005	6.71	0.025	6.22	0.034	0.07	0.801	0.09	0.781	0.12	0.785	0.17	0.754
	Superior Periventricular	4.76	0.048	4.56	0.052	9.00	0.010	8.62	0.012	8.19	0.017	1.90	0.227	0.07	0.814				
	Periventricular	0.84	0.377	1.42	0.256	15.71	0.002	11.42	0.006	12.15	0.006	5.23	0.071	0.14	0.735	3.49	0.313	0.14	0.774
	PLIC	0.27	0.620	0.83	0.389	8.12	0.021	7.94	0.026	25.27	0.002	2.37	0.264	60.52	0.081				
PCr/Pi	Sagittal	7.98	0.014	4.95	0.044	17.70	0.001	20.44	0.001	24.71	0.001	7.09	0.045	0.37	0.586	7.34	0.225	0.75	0.545
	Parietal	7.97	0.015	4.73	0.050	17.65	0.001	21.60	0.001	23.81	0.001	7.09	0.045	0.37	0.586	7.34	0.225	0.75	0.545
	Temporal	6.86	0.022	5.86	0.032	13.45	0.003	11.14	0.007	9.70	0.012	0.01	0.938	0.34	0.598	0.27	0.697	0.00	0.983
	Superior Periventricular	6.37	0.025	4.22	0.061	10.81	0.006	15.32	0.002	14.29	0.004	3.32	0.128	2.60	0.205	0.00	1.000		
	Periventricular	1.67	0.221	2.00	0.182	7.58	0.018	7.60	0.019	7.28	0.022	4.98	0.076	0.31	0.617	7.34	0.225	0.75	0.545
	PLIC	0.90	0.370	1.98	0.197	8.84	0.018	5.98	0.044	8.78	0.025	0.03	0.880	12.83	0.173				

F. ^{31}P MRS biomarkers 1-48 h after resuscitation and white matter injury assessed using LFB/Nissl stains

		Time after resuscitation (h)																	
		1 - < 3		3 - < 6		6 - < 12		12 - < 18		18 - < 24		24 - < 30		30 - < 36		36 - < 42		42 - < 48	
		F	p	F	p	F	p	F	p	F	p	F	p	F	p	F	p	F	p
NTP/EPP	Sagittal	0.66	0.431	0.23	0.638	1.36	0.264	3.50	0.086	5.71	0.038	0.02	0.899	1.87	0.265				
	Parietal	0.18	0.678	0.36	0.560	3.51	0.085	3.30	0.097	8.13	0.019	0.34	0.585	2.01	0.251	1.42	0.445	6.48	0.238
	Temporal	0.69	0.423	0.19	0.667	1.71	0.215	2.43	0.147	4.37	0.066	0.85	0.408	0.08	0.793	1.42	0.445	6.48	0.238
	Superior Periventricular	1.08	0.318	0.02	0.886	0.92	0.356	4.73	0.050	12.23	0.006								
	Periventricular	0.98	0.341	0.01	0.915	0.78	0.395	4.13	0.067	12.23	0.006								
	PLIC	0.52	0.491	0.42	0.534	4.43	0.069	2.71	0.144	4.38	0.081	0.02	0.895	4.70	0.275				
PCr/EPP	Sagittal	0.01	0.914	0.22	0.644	0.07	0.800	0.04	0.849	1.25	0.289	0.01	0.920	0.04	0.854				
	Parietal	0.02	0.896	0.00	0.951	0.06	0.813	0.13	0.721	1.87	0.204	0.00	0.947	0.04	0.852	1.41	0.446	268.4	0.039
	Temporal	0.04	0.836	0.07	0.795	0.89	0.363	1.31	0.277	1.86	0.205	0.72	0.445	0.00	0.963	1.41	0.446	268.4	0.039
	Superior Periventricular	0.58	0.460	0.75	0.404	1.64	0.223	3.02	0.108	4.45	0.061								
	Periventricular	0.23	0.640	0.36	0.559	1.11	0.312	2.33	0.155	4.45	0.061								
	PLIC	2.76	0.135	3.65	0.093	3.08	0.117	1.50	0.261	6.42	0.044	0.06	0.829	0.49	0.610				
Pi/EPP	Sagittal	0.36	0.558	0.02	0.901	0.31	0.586	1.08	0.319	2.83	0.124	0.30	0.605	2.29	0.228				
	Parietal	0.07	0.792	0.00	0.996	0.53	0.482	1.27	0.284	4.21	0.070	0.29	0.614	1.89	0.263	0.37	0.653	10.35	0.192
	Temporal	0.03	0.858	0.03	0.872	0.69	0.422	1.56	0.238	2.42	0.154	0.32	0.600	0.04	0.847	0.37	0.653	10.35	0.192
	Superior Periventricular	0.00	0.987	0.47	0.504	0.92	0.354	5.48	0.037	6.47	0.029								
	Periventricular	0.01	0.911	0.27	0.613	0.60	0.452	4.51	0.057	6.47	0.029								
	PLIC	2.00	0.195	4.11	0.077	4.74	0.061	2.53	0.156	8.23	0.028	0.31	0.633	86.29	0.068				
PCr/Pi	Sagittal	0.00	0.986	0.15	0.702	0.17	0.688	0.16	0.695	0.12	0.740	0.02	0.888	0.01	0.916				
	Parietal	0.01	0.910	0.02	0.890	0.26	0.618	0.30	0.596	0.38	0.555	0.00	0.977	0.04	0.857	0.19	0.741	1.65	0.421
	Temporal	0.54	0.478	0.19	0.671	1.59	0.232	1.62	0.230	1.02	0.339	0.64	0.467	0.09	0.782	0.19	0.741	1.65	0.421
	Superior Periventricular	0.56	0.469	1.07	0.320	1.84	0.198	2.44	0.144	2.15	0.174								
	Periventricular	0.28	0.609	0.65	0.435	1.29	0.278	1.82	0.204	2.15	0.174								
	PLIC	2.95	0.124	6.16	0.038	4.81	0.060	2.33	0.171	6.87	0.040	0.11	0.769	722.6	0.024				

G. ^{31}P MRS biomarkers 1-48 h after resuscitation and axonal injury assessed using β-APP immune-histochemical stain

		Time after resuscitation (h)																	
		1 - < 3		3 - < 6		6 - < 12		12 - < 18		18 - < 24		24 - < 30		30 - < 36		36 - < 42		42 - < 48	
		F	p	F	p	F	p	F	p	F	p	F	p	F	p	F	p	F	p
NTP/EPP	Sagittal	0.00	0.997	0.09	0.772	2.31	0.153	1.08	0.319	0.95	0.353	6.72	0.049	0.71	0.462	0.57	0.587	2.16	0.381
	Parietal	0.06	0.813	0.19	0.671	4.05	0.067	3.56	0.086	3.44	0.096	4.22	0.095	0.04	0.846	0.00	0.993	0.11	0.800
	Temporal	0.00	0.950	0.28	0.605	3.88	0.072	1.41	0.260	0.62	0.451	2.44	0.193	0.71	0.462	0.57	0.587	2.16	0.381
	Superior Periventricular	0.49	0.497	2.25	0.158	6.51	0.024	4.88	0.047	2.84	0.123	8.52	0.033	1.88	0.264	0.57	0.587	2.16	0.381
	Periventricular	0.01	0.940	0.22	0.649	5.19	0.042	4.02	0.070	4.40	0.062	3.47	0.122	0.05	0.833	0.07	0.838	0.43	0.631
	PLIC	1.32	0.294	3.05	0.131	3.07	0.130	3.37	0.126	0.88	0.401								
PCr/EPP	Sagittal	0.03	0.871	0.04	0.850	0.80	0.387	0.95	0.349	3.38	0.096	16.37	0.010	2.36	0.222	0.57	0.588	11.68	0.181
	Parietal	0.02	0.882	0.11	0.749	1.19	0.296	1.48	0.249	8.72	0.016	8.55	0.033	0.01	0.913	0.00	0.992	0.52	0.601
	Temporal	2.03	0.179	3.44	0.089	8.33	0.014	4.94	0.048	2.67	0.137	4.68	0.097	2.36	0.222	0.57	0.588	11.68	0.181
	Superior Periventricular	6.54	0.024	8.01	0.014	18.32	0.001	12.05	0.005	9.93	0.010	17.34	0.009	1.53	0.304	0.57	0.588	11.68	0.181
	Periventricular	1.34	0.270	2.90	0.114	7.24	0.020	5.41	0.040	10.87	0.008	12.07	0.018	0.04	0.860	0.07	0.839	1.54	0.432
	PLIC	0.21	0.665	0.02	0.905	0.88	0.384	1.08	0.347	1.08	0.357								
Pi/EPP	Sagittal	0.18	0.681	0.21	0.654	2.35	0.149	0.74	0.408	2.40	0.152	17.50	0.009	1.56	0.300	0.11	0.795	2.98	0.334
	Parietal	0.04	0.847	0.01	0.925	2.33	0.153	1.41	0.259	5.96	0.037	6.57	0.050	0.17	0.705	0.12	0.785	0.17	0.754
	Temporal	1.22	0.291	2.12	0.171	9.90	0.008	2.79	0.123	1.61	0.237	3.65	0.129	1.56	0.300	0.11	0.795	2.98	0.334
	Superior Periventricular	5.49	0.036	7.89	0.015	19.86	0.001	8.38	0.013	6.78	0.026	25.98	0.004	3.99	0.140	0.11	0.795	2.98	0.334
	Periventricular	1.25	0.285	2.15	0.169	8.72	0.012	4.53	0.057	8.24	0.017	7.72	0.039	0.18	0.698	0.01	0.954	0.58	0.585
	PLIC	0.95	0.367	0.18	0.684	0.74	0.423	1.09	0.345	1.14	0.345								
PCr/Pi	Sagittal	0.19	0.670	0.24	0.631	1.09	0.316	1.26	0.284	4.00	0.073	13.14	0.015	1.25	0.346	0.03	0.883	0.67	0.563
	Parietal	0.35	0.566	0.30	0.593	1.44	0.253	1.63	0.227	5.18	0.049	4.20	0.096	0.18	0.698	0.27	0.697	0.00	0.983
	Temporal	1.68	0.219	3.03	0.107	6.41	0.026	4.36	0.061	3.26	0.104	1.28	0.322	1.25	0.346	0.03	0.883	0.67	0.563
	Superior Periventricular	7.51	0.017	10.60	0.006	18.40	0.001	12.66	0.004	10.40	0.009	11.18	0.020	0.59	0.500	0.03	0.883	0.67	0.563
	Periventricular	2.83	0.118	3.95	0.070	8.95	0.011	6.09	0.031	9.38	0.012	9.31	0.028	0.00	0.987	0.05	0.866	0.09	0.814
	PLIC	0.99	0.359	0.24	0.641	1.51	0.265	2.23	0.196	0.66	0.462								

P-values presented without correction for multiple comparisons. P-values for the periods after 24 hours are presented only for reference because of the limited number of surviving subjects. Abbreviation: PCIC, posterior limb of the internal capsule.

Supplemental Table 4.3-6: Regional ADC 1-48 h after resuscitation and histo-pathological injury in corresponding regions (adjusted for AED and survival time after resuscitation)

A. ADC 1 to 48 hours after resuscitation and neuronal death assessed using H & E stains

	Time after resuscitation (h)																	
	1 - < 3		3 - < 6		6 - < 12		12 - < 18		18 - < 24		24 - < 30		30 - < 36		36 - < 42		42 - < 48	
	F	p	F	p	F	p	F	p	F	p	F	p	F	p	F	p	F	p
Sagittal top	3.32	0.090	9.93	0.007	54.45	0.000	43.40	0.000	58.25	0.000	6.70	0.049	0.37	0.653	0.70	0.556	0.98	0.503
Sagittal bottom	1.04	0.325	2.98	0.106	4.52	0.053	3.39	0.091	4.81	0.064	18.90	0.007	30.96	0.113	52.20	0.088	4.89	0.270
Parietal top	0.84	0.375	4.29	0.057	6.01	0.029	7.83	0.016	10.18	0.015	3.39	0.125	0.16	0.759	0.49	0.611	0.17	0.754
Parietal bottom	3.90	0.068	4.17	0.060	4.11	0.064	3.56	0.084	5.84	0.046	20.36	0.006	1.38	0.449	0.74	0.549	1.43	0.443
Temporal	0.75	0.403	3.78	0.076	4.59	0.055	6.26	0.034	0.05	0.830	0.71	0.446	5.34	0.260	1.74	0.413		
Hippocampus	0.03	0.862	0.06	0.826	0.15	0.725	3.67	0.306	.	.								
Caudate nucleus	0.90	0.366	2.49	0.146	4.60	0.061	5.80	0.053	1.18	0.357	3.12	0.175	0.38	0.649	0.17	0.750	.	.
Putamen	0.01	0.931	1.09	0.321	2.20	0.169	2.38	0.161	4.95	0.077	1.21	0.332	19.06	0.143	71.11	0.075	.	.
Anterior thalamus	4.60	0.058	5.41	0.042	4.82	0.053	6.76	0.035	0.51	0.517	10.59	0.031	5.35	0.260	11.76	0.181	.	.
Lateral thalamus	4.46	0.058	4.77	0.051	4.71	0.055	10.12	0.013	0.79	0.414	0.00	0.997	27.61	0.120	26.41	0.122	.	.
Medial thalamus	4.96	0.048	1.56	0.238	1.89	0.200	10.70	0.011	1.61	0.261	0.86	0.407	28.41	0.118	13.32	0.170		

B. ADC 1-48 h after resuscitation and TUNEL positive apoptotic cell death

	Time after resuscitation (h)																	
	1 - < 3		3 - < 6		6 - < 12		12 - < 18		18 - < 24		24 - < 30		30 - < 36		36 - < 42		42 - < 48	
	F	p	F	p	F	p	F	p	F	p	F	p	F	p	F	p	F	p
Sagittal top	0.31	0.587	0.79	0.388	1.98	0.183	4.89	0.047	3.94	0.088	4.00	0.102	0.07	0.841	0.01	0.938	0.00	0.992
Sagittal bottom	0.04	0.839	0.23	0.639	4.22	0.061	4.16	0.064	2.33	0.170	4.86	0.079	4.72	0.275	73.42	0.074	1.54	0.432
Parietal top	0.15	0.701	4.28	0.058	6.32	0.026	5.97	0.031	4.41	0.074	1.99	0.217	0.78	0.539	2.01	0.391	0.00	0.974
Parietal bottom	0.04	0.853	0.06	0.813	2.60	0.131	2.33	0.153	1.86	0.215	6.75	0.048	2.53	0.357	0.40	0.640	2.64	0.351
Temporal	2.21	0.163	0.03	0.858	0.01	0.931	0.01	0.928	0.30	0.607	0.37	0.575	3.76	0.303	1.32	0.456		
Hippocampus	0.36	0.582	0.01	0.914	1.16	0.360	0.74	0.547										
Caudate nucleus	3.20	0.104	3.61	0.087	1.11	0.319	0.16	0.708	0.66	0.477	1.00	0.391	0.01	0.925	0.08	0.824	.	.
Putamen	0.76	0.405	1.44	0.257	3.01	0.113	1.11	0.324	0.12	0.745	0.58	0.487	0.01	0.934	0.00	0.998	.	.
Anterior thalamus	1.21	0.296	0.60	0.456	0.11	0.745	0.21	0.658	0.08	0.792	0.52	0.510	0.01	0.936	0.05	0.857	.	.
Lateral thalamus	10.42	0.008	5.37	0.041	4.30	0.065	1.58	0.245	0.00	0.950	0.29	0.618	0.00	0.961	0.00	0.958	.	.
Medial thalamus	0.49	0.500	0.06	0.808	0.05	0.836	2.16	0.185	0.00	0.979	2.60	0.205						

C-1. ADC 1-48 h after resuscitation and CD68 positive microglia in the grey matter

	Time after resuscitation (h)																	
	1 - < 3		3 - < 6		6 - < 12		12 - < 18		18 - < 24		24 - < 30		30 - < 36		36 - < 42		42 - < 48	
	F	p	F	p	F	p	F	p	F	p	F	p	F	p	F	p	F	p
Sagittal top	1.46	0.246	3.27	0.092	6.24	0.027	2.92	0.113	4.82	0.064	15.48	0.011	0.63	0.574	0.32	0.671	0.21	0.724
Sagittal bottom	3.60	0.079	7.49	0.016	9.10	0.010	4.11	0.065	3.71	0.095	2.23	0.196	340.2	0.034	14.00	0.166	10.36	0.192
Parietal top	4.32	0.057	5.46	0.035	3.60	0.080	4.86	0.048	7.85	0.026	27.60	0.003	22.21	0.133	1888.	0.015	0.46	0.620
Parietal bottom	0.41	0.531	0.83	0.379	1.59	0.230	1.20	0.295	2.10	0.191	15.96	0.010	0.01	0.931	77.74	0.072	0.01	0.936
Temporal	4.35	0.059	1.40	0.260	0.23	0.645	0.01	0.932	0.11	0.759	0.69	0.452	0.42	0.633	1.14	0.480		
Hippocampus	7.78	0.049	155.3	0.000	0.25	0.651	0.08	0.829										
Caudate nucleus	5.68	0.036	5.47	0.039	5.93	0.035	9.87	0.016	0.38	0.569	0.86	0.407	1.38	0.449	2.70	0.348	.	.
Putamen	0.13	0.727	0.02	0.902	0.00	0.953	0.61	0.458	0.12	0.748	0.64	0.470	192.7	0.046	30.54	0.114	.	.
Anterior thalamus	3.67	0.082	3.95	0.072	3.45	0.093	2.73	0.142	1.67	0.266	0.16	0.707	0.33	0.666	0.18	0.746	.	.
Lateral thalamus	4.43	0.059	6.24	0.030	3.52	0.090	11.74	0.009	0.11	0.759	0.05	0.840	0.03	0.897	0.03	0.894	.	.
Medial thalamus	10.38	0.009	12.00	0.006	1.37	0.273	3.29	0.113	0.19	0.682	0.33	0.608						

C-2. ADC 1-48 h after resuscitation and CD68 positive microglia in the white matter

	Time after resuscitation (h)																	
	1 - < 3		3- < 6		6 - < 12		12 - < 18		18 - < 24		24 - < 30		30 - < 36		36 - < 42		42 - < 48	
	F	p	F	p	F	p	F	p	F	p	F	p	F	p	F	p	F	p
Sagittal	2.74	0.124	3.51	0.085	4.35	0.061	5.48	0.041	9.46	0.018	24.63	0.004	15.09	0.160	6.34	0.241	1.76	0.412
Parietal	1.11	0.315	1.95	0.190	2.28	0.162	1.58	0.240	3.56	0.101	5.70	0.063	0.83	0.529	0.03	0.892	0.01	0.928
Temporal	1.43	0.256	0.29	0.598	1.37	0.269	2.76	0.131	1.05	0.345	0.03	0.864	16.25	0.155	4.65	0.276	3.02	0.333
Superior Periventricular	0.58	0.463	0.75	0.406	2.05	0.182	0.37	0.561	0.00	0.991	0.38	0.573	0.00	0.966	0.00	0.972	0.01	0.930
Periventricular	0.40	0.541	1.49	0.250	0.56	0.473	0.07	0.799	0.00	0.994	1.76	0.255	0.36	0.656	0.41	0.637	1.90	0.400
PLIC	5.14	0.064	3.36	0.117	2.42	0.181	3.35	0.141	0.17	0.723								

D-1. ADC 1-48 h after resuscitation and CD68 positive vessels in the grey matter

	Time after resuscitation (h)																	
	1 - < 3		3 - < 6		6 - < 12		12 - < 18		18 - < 24		24 - < 30		30 - < 36		36 - < 42		42 - < 48	
	F	p	F	p	F	p	F	p	F	p	F	p	F	p	F	p	F	p
Sagittal top	5.35	0.036	6.50	0.023	7.38	0.018	5.34	0.039	13.05	0.009	24.28	0.004	1.34	0.453	0.73	0.550	0.52	0.603
Sagittal bottom	6.47	0.023	8.32	0.012	9.32	0.009	5.71	0.034	7.24	0.031	8.09	0.036	0.08	0.824	0.00	0.975	0.33	0.667
Parietal top	11.15	0.005	14.19	0.002	10.46	0.007	17.06	0.001	9.26	0.019	32.33	0.002	22.21	0.133	1888.	0.015	0.46	0.620
Parietal bottom	1.42	0.254	2.02	0.177	3.18	0.098	2.49	0.141	2.67	0.146	16.01	0.010	0.48	0.614	2.12	0.383	0.50	0.609
Temporal	3.95	0.070	1.42	0.256	0.21	0.653	0.02	0.902	0.04	0.856	0.88	0.401	0.35	0.661	0.95	0.508		
Hippocampus	8.36	0.045	90.38	0.001	0.31	0.615	0.29	0.684										
Caudate nucleus	6.45	0.028	6.34	0.029	6.00	0.034	4.18	0.080										
Putamen	0.00	0.968	0.27	0.615	1.31	0.279	0.30	0.597	0.07	0.802	0.44	0.542	0.13	0.778	0.24	0.710	.	.
Anterior thalamus	4.91	0.049	7.53	0.019	5.17	0.046	23.96	0.002	1.67	0.266	0.16	0.707	0.33	0.666	0.18	0.746		
Lateral thalamus	4.66	0.054	2.30	0.160	2.30	0.160	13.99	0.006	0.11	0.759	0.05	0.840	0.03	0.897	0.03	0.894	.	.
Medial thalamus	0.02	0.895	0.10	0.758	1.80	0.213	11.79	0.011	0.17	0.699	0.33	0.608						

D-2. ADC 1-48 h after resuscitation and CD68 positive vessels in the white matter

	Time after resuscitation (h)																	
	1 - < 3		3 - < 6		6 - < 12		12 - < 18		18 - < 24		24 - < 30		30 - < 36		36 - < 42		42 - < 48	
	F	p	F	p	F	p	F	p	F	p	F	p	F	p	F	p	F	p
Sagittal	2.43	0.145	4.19	0.063	4.58	0.056	6.25	0.031	6.42	0.039	7.88	0.038	7.52	0.223	12.07	0.178	2.68	0.349
Parietal	7.11	0.022	6.67	0.025	12.74	0.005	10.26	0.011	6.59	0.037	6.27	0.054						
Temporal	0.05	0.835	0.03	0.873	0.07	0.790	1.84	0.208	1.46	0.273	0.00	0.950	0.34	0.664	0.12	0.786	0.06	0.842
Superior Periventricular	1.48	0.250	7.31	0.021	0.97	0.348	0.04	0.850	0.04	0.854	1.21	0.333	0.79	0.537	1.17	0.475	1.53	0.432
Periventricular	0.28	0.609	0.05	0.820	0.10	0.755	0.28	0.613	0.64	0.461	1.76	0.255	0.36	0.656	0.41	0.637	1.90	0.400
PLIC	5.13	0.064	3.79	0.099	4.91	0.078	7.92	0.048	0.58	0.525								

E. ADC 1-48 h after resuscitation and white matter injury assessed using H & E stains

	Time after resuscitation (h)																	
	1 - < 3		3 - < 6		6 - < 12		12 - < 18		18 - < 24		24 - < 30		30 - < 36		36 - < 42		42 - < 48	
	F	p	F	p	F	p	F	p	F	p	F	p	F	p	F	p	F	p
Sagittal	5.38	0.039	15.13	0.002	25.07	0.000	51.68	0.000	21.80	0.002	18.24	0.008	0.18	0.743	0.05	0.856	0.29	0.685
Parietal	2.89	0.117	9.92	0.009	13.82	0.004	11.45	0.008	17.47	0.004	22.97	0.005	9.01	0.205	15.61	0.158	10.17	0.193
Temporal	3.29	0.097	1.68	0.221	5.49	0.041	7.42	0.023	3.86	0.097	1.36	0.309	0.47	0.619	1.02	0.497	1.45	0.441
Superior Periventricular	0.01	0.906	0.73	0.411	4.89	0.051	10.18	0.015	4.66	0.083	3.06	0.155						
Periventricular	0.96	0.351	0.30	0.593	2.67	0.137	1.20	0.309	1.68	0.251	0.72	0.443	3.56	0.310	3.10	0.329	0.66	0.566
PLIC	0.92	0.365	6.65	0.033	6.16	0.042	5.34	0.060	4.32	0.106	1.09	0.406						

F. ADC 1-48 h after resuscitation and white matter injury assessed using LFB/Nissl stains

	Time after resuscitation (h)																	
	1 - < 3		3 - < 6		6 - < 12		12 - < 18		18 - < 24		24 - < 30		30 - < 36		36 - < 42		42 - < 48	
	F	p	F	p	F	p	F	p	F	p	F	p	F	p	F	p	F	p
Sagittal	0.29	0.603	0.28	0.604	0.32	0.581	0.12	0.737	0.54	0.486	0.02	0.882						
Parietal	0.09	0.767	0.10	0.758	0.02	0.903	0.00	0.962	0.43	0.535	0.29	0.614	0.08	0.829	0.10	0.808	0.14	0.772
Temporal	2.34	0.154	12.24	0.005	5.86	0.036	1.09	0.325	1.07	0.342	3.40	0.139	126.2	0.057	95.31	0.065	26.92	0.121
Superior Periventricular	0.75	0.405	8.73	0.013	3.93	0.075	0.14	0.719	0.30	0.609								
Periventricular	0.06	0.815	1.14	0.311	1.43	0.263	0.01	0.941	0.34	0.583								
PLIC	5.24	0.051	6.82	0.031	2.54	0.155	3.00	0.134	0.43	0.549	0.00	0.989						

G. ADC 1-48 h after resuscitation and axonal injury assessed using β-APP immune-histochemical stain

		Time after resuscitation (h)																	
		1 - < 3		3 - < 6		6 - < 12		12 - < 18		18 - < 24		24 - < 30		30 - < 36		36 - < 42		42 - < 48	
		F	p	F	p	F	p	F	p	F	p	F	p	F	p	F	p	F	p
ADC	Sagittal	2.06	0.177	1.06	0.324	3.77	0.078	3.70	0.083	7.14	0.032	27.79	0.003	2.40	0.365	311.8	0.036	8.81	0.207
	Parietal	0.11	0.751	0.75	0.406	1.59	0.236	0.70	0.424	2.56	0.153	2.39	0.183	5.02	0.267	0.43	0.630	0.34	0.665
	Temporal	1.07	0.324	0.17	0.686	2.98	0.115	4.65	0.060	2.59	0.158	1.24	0.329	9.58	0.199	66.89	0.077	899.3	0.021
	Superior Periventricular	0.03	0.862	0.10	0.763	6.18	0.032	3.60	0.100	0.47	0.524	0.23	0.659	0.11	0.797	0.19	0.736	0.27	0.693
	Periventricular	4.72	0.055	1.90	0.198	5.74	0.040	1.31	0.290	0.92	0.381	0.54	0.505	0.01	0.951	0.00	0.970	0.11	0.792
	PLIC	2.33	0.178	1.52	0.264	2.61	0.167	2.92	0.163	0.01	0.945								

P-values presented without correction for multiple comparisons.

P-values for the periods after 24 hours are presented only for reference because of the limited number of surviving subjects.

Supplemental Table 4.3-7: Regional T2 relaxation time 1-48 h after resuscitation and histo-pathological injury in corresponding regions (adjusted for AED and survival time after resuscitation)

A. T2 1-48 h after resuscitation and neuronal death assessed using H & E stains

		Time after resuscitation (h)																	
		1 - < 3		3 - < 6		6 - < 12		12 - < 18		18 - < 24		24 - < 30		30 - < 36		36 - < 42		42 - < 48	
		F	p	F	p	F	p	F	p	F	p	F	p	F	p	F	p	F	p
T2	Sagittal top	1.74	0.229	3.27	0.114	2.66	0.154	2.40	0.182	1.95	0.235	4.80	0.160						
	Sagittal bottom	0.22	0.653	0.91	0.373	0.15	0.710	0.06	0.820	0.01	0.947	3.42	0.205						
	Parietal top	2.95	0.129	3.09	0.122	2.82	0.144	3.70	0.112	4.47	0.102	7.64	0.110						
	Parietal bottom	2.02	0.198	3.01	0.127	3.02	0.133	1.67	0.253	0.30	0.613	2.67	0.244						
	Temporal	0.08	0.783	0.16	0.699	0.14	0.724	0.12	0.750	0.15	0.732								
	Hippocampus	0.83	0.458	0.54	0.540	0.03	0.889												
	Caudate nucleus	0.58	0.475	1.30	0.298	9.30	0.028	5.68	0.097	98.22	0.010								
	Putamen	0.04	0.852	0.47	0.518	1.33	0.292	0.23	0.659	0.26	0.645	0.23	0.718						
	Anterior thalamus	0.00	0.988	0.78	0.412	1.62	0.250	0.14	0.729	1.36	0.327	1.02	0.497						
	Lateral thalamus	2.19	0.183	4.94	0.062	2.14	0.194	1.40	0.303	0.97	0.398	547.2	0.027						
	Medial thalamus	2.40	0.165	26.18	0.001	6.04	0.049	15.58	0.011	25.36	0.007	19.72	0.141						

B. T2 1-48 h after resuscitation and TUNEL positive apoptotic cell death

		Time after resuscitation (h)																	
		1 - < 3		3 - < 6		6 - < 12		12 - < 18		18 - < 24		24 - < 30		30 - < 36		36 - < 42		42 - < 48	
		F	p	F	p	F	p	F	p	F	p	F	p	F	p	F	p	F	p
T2	Sagittal top	0.92	0.369	0.95	0.362	0.48	0.513	1.05	0.353	2.81	0.169	104.4	0.009						
	Sagittal bottom	5.93	0.045	9.79	0.017	6.12	0.048	9.19	0.029	9.03	0.040	2.56	0.251						
	Parietal top	2.75	0.141	1.05	0.340	2.82	0.144	3.65	0.114	10.43	0.032	3.69	0.195						
	Parietal bottom	1.56	0.252	4.77	0.065	3.68	0.103	7.19	0.044	6.66	0.061	1.02	0.419						
	Temporal	1.60	0.247	11.69	0.011	8.58	0.026	27.63	0.013	4.74	0.161								
	Hippocampus	0.06	0.828	10.17	0.086	1.65	0.422												
	Caudate nucleus	0.21	0.661	2.23	0.186	0.49	0.515	0.18	0.698	0.01	0.927								
	Putamen	1.11	0.333	0.09	0.774	1.01	0.354	2.21	0.211	0.41	0.570	42.16	0.097						
	Anterior thalamus	0.22	0.657	0.02	0.888	0.00	0.986	0.11	0.757	0.00	0.959	1.81	0.407						
	Lateral thalamus	0.00	0.964	0.72	0.426	0.09	0.776	0.07	0.799	2.43	0.217	0.01	0.947						
	Medial thalamus	2.44	0.162	1.26	0.299	0.17	0.693	7.00	0.046	2.30	0.204	7.79	0.219						

C-1. T2 1-48 h after resuscitation and CD68 positive microglia in the grey matter

		Time after resuscitation (h)																	
		1 - < 3		3 - < 6		6 - < 12		12 - < 18		18 - < 24		24 - < 30		30 - < 36		36 - < 42		42 - < 48	
		F	p	F	p	F	p	F	p	F	p	F	p	F	p	F	p	F	p
T2	Sagittal top	0.11	0.748	0.13	0.730	0.23	0.647	0.40	0.557	0.17	0.699	1.01	0.420						
	Sagittal bottom	0.73	0.420	2.37	0.168	1.38	0.284	0.83	0.403	0.75	0.435	0.00	0.997						
	Parietal top	0.67	0.441	1.47	0.265	0.83	0.397	0.98	0.368	0.31	0.607	0.11	0.770						
	Parietal bottom	0.04	0.849	0.95	0.362	1.22	0.312	2.89	0.150	1.44	0.297	0.04	0.860						
	Temporal	0.52	0.496	0.37	0.561	1.53	0.262	0.18	0.699	0.04	0.854								
	Hippocampus	1.58	0.336	0.61	0.518	5.81	0.250												
	Caudate nucleus	0.19	0.680	0.92	0.369	1.18	0.318	1.25	0.327	0.91	0.410	14.96	0.161						
	Putamen	1.30	0.292	1.12	0.326	0.18	0.689	2.53	0.187	3.59	0.154	4.76	0.274						
	Anterior thalamus	0.25	0.633	0.07	0.792	0.08	0.783	0.37	0.575										
	Lateral thalamus	0.00	0.983	0.00	0.956	0.01	0.923	0.45	0.541										
	Medial thalamus	0.00	0.970	0.01	0.937	0.00	0.992	0.16	0.703	1.12	0.349	0.27	0.693						

C-2. T2 1-48 h after resuscitation and CD68 positive microglia in the white matter

		Time after resuscitation (h)																	
		1 - < 3		3 - < 6		6 - < 12		12 - < 18		18 - < 24		24 - < 30		30 - < 36		36 - < 42		42 - < 48	
		F	p	F	p	F	p	F	p	F	p	F	p	F	p	F	p	F	p
T2	Sagittal	0.08	0.787	0.96	0.373	3.71	0.127	0.04	0.863	0.14	0.733								
	Parietal	0.39	0.554	10.68	0.017	10.96	0.021	1.91	0.239	3.02	0.157	1.04	0.493						
	Temporal	2.38	0.167	0.25	0.634	1.52	0.264	0.23	0.657	0.00	0.994	0.18	0.744						
	Superior Periventricular	4.89	0.063	0.38	0.557	0.11	0.751	0.13	0.736	0.04	0.859								
	Periventricular																		
	PLIC	4.18	0.096	0.00	0.998	0.32	0.602	0.17	0.709	0.32	0.631								

D-1. T2 1-48 h after resuscitation and CD68 positive vessels in the grey matter

		Time after resuscitation (h)																	
		1 - < 3		3 - < 6		6 - < 12		12 - < 18		18 - < 24		24 - < 30		30 - < 36		36 - < 42		42 - < 48	
		F	p	F	p	F	p	F	p	F	p	F	p	F	p	F	p	F	p
T2	Sagittal top	0.22	0.653	0.28	0.612	0.62	0.460	1.02	0.359	0.47	0.533	0.59	0.522						
	Sagittal bottom	0.84	0.391	2.26	0.176	1.25	0.307	0.71	0.439	0.85	0.410	0.18	0.711						
	Parietal top	0.78	0.407	1.81	0.221	0.96	0.365	1.39	0.292	0.38	0.570	0.11	0.770						
	Parietal bottom	0.35	0.575	1.16	0.317	1.11	0.332	0.91	0.384	0.11	0.761	0.04	0.860						
	Temporal	0.76	0.413	0.42	0.536	1.36	0.288												
	Hippocampus	1.53	0.342	0.90	0.444														
	Caudate nucleus	0.63	0.452	0.52	0.495	2.37	0.175												
	Putamen	0.68	0.437	0.47	0.513	0.01	0.919	0.28	0.628	3.11	0.176	4.76	0.274						
	Anterior thalamus	0.28	0.611	0.08	0.779	0.16	0.701	0.37	0.575										
	Lateral thalamus	0.02	0.891	0.03	0.861	0.01	0.909	0.45	0.541										
	Medial thalamus	0.08	0.785	0.00	0.969	0.01	0.944	1.11	0.341	1.06	0.361	0.27	0.693						

D-2. T2 1-48 h after resuscitation and CD68 positive vessels in the white matter

		Time after resuscitation (h)																	
		1 - < 3		3 - < 6		6 - < 12		12 - < 18		18 - < 24		24 - < 30		30 - < 36		36 - < 42		42 - < 48	
		F	p	F	p	F	p	F	p	F	p	F	p	F	p	F	p	F	p
T2	Sagittal	0.03	0.871	0.32	0.598	1.93	0.237	0.03	0.883	0.00	0.954								
	Parietal	1.46	0.273	10.26	0.019	5.61	0.064	1.43	0.297	3.19	0.149								
	Temporal	0.05	0.838	0.11	0.751	3.13	0.127	1.81	0.249	0.44	0.553	0.58	0.585						
	Superior Periventricular	0.22	0.657	0.03	0.869	2.06	0.201	0.14	0.727	0.11	0.758								
	Periventricular																		
	PLIC	0.05	0.825	0.70	0.442	3.22	0.147	0.71	0.460	0.01	0.921								

E. T2 1-48 h after resuscitation and white matter injury assessed using H & E stains

		Time after resuscitation (h)																	
		1 - < 3		3 - < 6		6 - < 12		12 - < 18		18 - < 24		24 - < 30		30 - < 36		36 - < 42		42 - < 48	
		F	p	F	p	F	p	F	p	F	p	F	p	F	p	F	p	F	p
T_2	Sagittal	1.90	0.227	0.69	0.445	8.58	0.043	1.72	0.281	3.77	0.147								
	Parietal	3.46	0.112	4.23	0.085	7.19	0.044	3.33	0.142	10.46	0.032	8.47	0.211						
	Temporal	2.42	0.164	0.08	0.782	1.39	0.284	0.36	0.583	2.30	0.226	0.04	0.868						
	Superior Periventricular	2.47	0.160	0.73	0.421	0.12	0.737	1.41	0.300	0.07	0.809								
	Periventricular																		
	PLIC	0.13	0.734	4.83	0.070	11.22	0.020	3.66	0.128	1.48	0.311								

F. T2 1-48 h after resuscitation and white matter injury assessed using LFB/Nissl stains

		Time after resuscitation (h)																	
		1 - < 3		3 - < 6		6 - < 12		12 - < 18		18 - < 24		24 - < 30		30 - < 36		36 - < 42		42 - < 48	
		F	p	F	p	F	p	F	p	F	p	F	p	F	p	F	p	F	p
T_2	Sagittal	0.22	0.659	1.01	0.362	1.03	0.368	0.00	0.968	0.00	0.969								
	Parietal	0.39	0.557	9.90	0.020	16.86	0.009	7.97	0.048	3.62	0.130	1.04	0.493						
	Temporal	0.04	0.845	1.49	0.261	1.92	0.215	0.22	0.665	0.03	0.883	0.58	0.585						
	Superior Periventricular	0.06	0.809	0.30	0.602	1.96	0.211	1.06	0.361	1.06	0.378								
	Periventricular																		
	PLIC	0.85	0.393	0.42	0.539	4.51	0.087	0.84	0.412	0.40	0.573								

G. T2 1-48 h after resuscitation and axonal injury assessed using β-APP immune-histochemical stain

		Time after resuscitation (h)																	
		1 - < 3		3 - < 6		6 - < 12		12 - < 18		18 - < 24		24 - < 30		30 - < 36		36 - < 42		42 - < 48	
		F	p	F	p	F	p	F	p	F	p	F	p	F	p	F	p	F	p
T_2	Sagittal	2.15	0.202	0.00	0.995	2.18	0.214	0.31	0.617	1.24	0.347								
	Parietal	0.10	0.765	1.55	0.260	2.99	0.145	1.32	0.315	2.04	0.226	1.06	0.491						
	Temporal	2.45	0.162	0.64	0.448	0.20	0.672	0.45	0.541	1.01	0.389	0.78	0.540						
	Superior Periventricular	15.07	0.006	3.54	0.102	1.17	0.321	0.13	0.736	3.08	0.178								
	Periventricular																		
	PLIC	0.01	0.925	1.69	0.250	1.58	0.277	0.33	0.606	0.02	0.893								

P-values presented without correction for multiple comparisons.

P-values for the periods after 24 hours are presented only for reference because of the limited number of surviving subjects.

Abbreviation: PLIC, posterior limb of the internal capsule.

Supplemental Table 4.3-8: Serial ^{31}P MRS biomarkers 1-48 h before termination and histo-pathological injury

A. ^{31}P MRS biomarkers 1-48 h before termination and neuronal death in the grey matter assessed using H & E stains

		Time before termination (h)																	
		1 - < 3		3 - < 6		6 - < 12		12 - < 18		18 - < 24		24 - < 30		30 - < 36		36 - < 42		42 - < 48	
		r	p	r	p	r	p	r	p	r	p	r	p	r	p	r	p	r	p
NTP/EPP	Sagittal top	-0.59	0.011	-0.55	0.019	-0.57	0.013	-0.48	0.054	-0.35	0.219	-0.49	0.184	-0.38	0.403	0.11	0.856	-0.23	0.768
	Sagittal bottom	-0.37	0.134	-0.24	0.330	-0.38	0.123	-0.25	0.335	-0.21	0.475	-0.26	0.495	0.38	0.408	0.42	0.484	-0.50	0.501
	Parietal top	-0.38	0.121	-0.33	0.175	-0.45	0.062	-0.33	0.192	-0.38	0.175	-0.42	0.256	-0.27	0.560	0.45	0.444	-0.07	0.929
	Parietal bottom	-0.40	0.097	-0.29	0.251	-0.42	0.081	-0.26	0.323	-0.38	0.180	-0.42	0.257	-0.23	0.622	0.50	0.388	0.43	0.568
	Temporal	-0.57	0.021	-0.46	0.071	-0.56	0.024	-0.41	0.129	-0.28	0.350	-0.57	0.144	-0.44	0.319	-0.85	0.072	0.01	0.987
	Hippocampus	-0.59	0.093	-0.84	0.005	-0.74	0.024	-0.56	0.146	-0.24	0.607								
	Caudate nucleus	-0.62	0.019	-0.55	0.041	-0.66	0.011	-0.55	0.052	-0.34	0.277	-0.50	0.259	-0.42	0.411	-0.20	0.743	-0.02	0.978
	Putamen	-0.43	0.122	-0.39	0.172	-0.49	0.076	-0.45	0.109	-0.55	0.053	-0.56	0.146	-0.47	0.290	-0.68	0.209	-0.08	0.924
	Anterior thalamus	-0.66	0.011	-0.54	0.045	-0.61	0.021	-0.68	0.008	-0.56	0.045	-0.81	0.016	-0.85	0.015	0.01	0.983	-0.80	0.202
	Lateral thalamus	-0.20	0.475	-0.24	0.398	-0.44	0.102	-0.50	0.068	-0.32	0.294	-0.43	0.293	-0.35	0.436	0.31	0.607	-0.50	0.505
	Medial thalamus	-0.47	0.079	-0.58	0.023	-0.71	0.003	-0.55	0.044	-0.19	0.530	-0.52	0.189	-0.57	0.187	-0.34	0.580	-0.45	0.552
PCr/EPP	Sagittal top	-0.71	0.001	-0.78	<0.00	-0.63	0.005	-0.50	0.041	-0.74	0.002	-0.57	0.106	-0.31	0.493	0.76	0.140	-0.29	0.708
	Sagittal bottom	-0.65	0.003	-0.62	0.006	-0.55	0.017	-0.44	0.075	-0.44	0.115	-0.54	0.133	0.15	0.752	0.62	0.265	0.04	0.965
	Parietal top	-0.62	0.006	-0.68	0.002	-0.58	0.012	-0.44	0.078	-0.60	0.024	-0.58	0.103	-0.27	0.557	0.59	0.298	-0.36	0.643
	Parietal bottom	-0.66	0.003	-0.67	0.002	-0.59	0.010	-0.44	0.075	-0.62	0.018	-0.56	0.115	-0.23	0.620	0.52	0.367	-0.02	0.984
	Temporal	-0.48	0.059	-0.49	0.057	-0.41	0.115	-0.28	0.320	-0.40	0.175	-0.41	0.318	-0.38	0.398	0.55	0.338	-0.54	0.463
	Hippocampus	-0.58	0.100	-0.86	0.003	-0.73	0.026	-0.60	0.120	-0.90	0.006								
	Caudate nucleus	-0.56	0.036	-0.71	0.005	-0.53	0.049	-0.43	0.139	-0.69	0.012	-0.43	0.330	-0.31	0.554	0.85	0.072	-0.51	0.491
	Putamen	-0.32	0.269	-0.35	0.223	-0.26	0.373	-0.16	0.598	-0.36	0.233	-0.41	0.314	-0.35	0.445	0.70	0.191	-0.46	0.541
	Anterior thalamus	-0.80	0.001	-0.68	0.008	-0.67	0.009	-0.56	0.036	-0.72	0.005	-0.79	0.019	-0.82	0.024	0.46	0.435	0.43	0.566
	Lateral thalamus	-0.19	0.489	-0.46	0.082	-0.33	0.237	-0.27	0.344	-0.47	0.109	-0.45	0.268	-0.34	0.452	0.69	0.194	-0.01	0.987
	Medial thalamus	-0.36	0.187	-0.66	0.008	-0.56	0.031	-0.52	0.056	-0.54	0.057	-0.45	0.269	-0.39	0.393	0.69	0.196	-0.07	0.935

		Time before termination (h)																	
		1 - < 3		3 - < 6		6 - < 12		12 - < 18		18 - < 24		24 - < 30		30 - < 36		36 - < 42		42 - < 48	
		r	p	r	p	r	p	r	p	r	p	r	p	r	p	r	p	r	p
Pi/EPP	Sagittal top	0.68	0.002	0.72	0.001	0.63	0.005	0.58	0.015	0.63	0.015	0.64	0.062	0.43	0.330	-0.49	0.404	0.68	0.319
	Sagittal bottom	0.53	0.022	0.51	0.031	0.45	0.060	0.43	0.084	0.38	0.187	0.52	0.156	-0.43	0.330	-0.65	0.240	0.58	0.421
	Parietal top	0.55	0.019	0.60	0.009	0.53	0.024	0.48	0.052	0.56	0.036	0.63	0.068	0.29	0.536	-0.64	0.247	0.41	0.592
	Parietal bottom	0.57	0.014	0.56	0.016	0.51	0.033	0.44	0.081	0.60	0.024	0.63	0.070	0.25	0.593	-0.67	0.218	-0.95	0.047
	Temporal	0.53	0.035	0.52	0.037	0.49	0.056	0.42	0.119	0.37	0.211	0.56	0.150	0.56	0.192	0.43	0.469	0.70	0.297
	Hippocampus	0.57	0.110	0.80	0.010	0.68	0.044	0.58	0.130	0.79	0.035								
	Caudate nucleus	0.62	0.017	0.69	0.006	0.62	0.019	0.53	0.060	0.65	0.022	0.56	0.188	0.63	0.182	-0.20	0.746	0.72	0.277
	Putamen	0.41	0.149	0.42	0.131	0.37	0.196	0.33	0.249	0.51	0.078	0.58	0.134	0.59	0.165	0.21	0.733	0.72	0.276
	Anterior thalamus	0.77	0.001	0.65	0.013	0.67	0.009	0.61	0.021	0.69	0.009	0.74	0.035	0.74	0.055	-0.50	0.391	0.50	0.500
	Lateral thalamus	0.26	0.343	0.43	0.114	0.42	0.117	0.40	0.162	0.37	0.218	0.50	0.203	0.36	0.427	-0.60	0.283	0.70	0.299
	Medial thalamus	0.42	0.119	0.63	0.012	0.61	0.015	0.57	0.032	0.35	0.239	0.52	0.191	0.62	0.137	-0.19	0.758	0.70	0.301
PCr/Pi	Sagittal top	-0.81	0.000	-0.84	0.000	-0.70	0.001	-0.58	0.015	-0.73	0.003	-0.67	0.050	-0.42	0.346	0.77	0.132	-0.77	0.231
	Sagittal bottom	-0.87	0.000	-0.77	0.000	-0.67	0.002	-0.56	0.020	-0.49	0.075	-0.70	0.035	0.23	0.618	0.85	0.069	-0.59	0.415
	Parietal top	-0.82	0.000	-0.78	0.000	-0.66	0.003	-0.57	0.018	-0.65	0.012	-0.73	0.026	-0.26	0.568	0.83	0.085	-0.55	0.446
	Parietal bottom	-0.85	0.000	-0.81	0.000	-0.69	0.002	-0.58	0.014	-0.70	0.005	-0.72	0.029	-0.21	0.655	0.83	0.084	0.84	0.161
	Temporal	-0.64	0.007	-0.59	0.017	-0.47	0.069	-0.29	0.288	-0.39	0.188	-0.51	0.197	-0.63	0.127	-0.17	0.789	-0.85	0.149
	Hippocampus	-0.64	0.065	-0.92	0.000	-0.73	0.025	-0.69	0.056	-0.93	0.002								
	Caudate nucleus	-0.61	0.020	-0.76	0.002	-0.56	0.038	-0.56	0.045	-0.74	0.006	-0.47	0.291	-0.53	0.284	0.53	0.358	-0.86	0.139
	Putamen	-0.11	0.717	-0.26	0.376	-0.23	0.428	-0.28	0.361	-0.19	0.553	0.08	0.871	0.18	0.740	0.23	0.707	0.44	0.557
	Anterior thalamus	-0.71	0.004	-0.61	0.021	-0.64	0.015	-0.64	0.015	-0.67	0.013	-0.76	0.027	-0.82	0.025	0.69	0.197	-0.38	0.618
	Lateral thalamus	-0.44	0.104	-0.46	0.086	-0.35	0.199	-0.32	0.267	-0.33	0.279	-0.43	0.291	-0.38	0.406	0.84	0.073	-0.70	0.298
	Medial thalamus	-0.55	0.036	-0.69	0.005	-0.56	0.031	-0.52	0.056	-0.44	0.137	-0.45	0.263	-0.60	0.152	0.48	0.409	-0.72	0.283

B. ^{31}P MRS biomarkers 1-48 h before termination and TUNEL positive apoptotic cell death in the grey matter

		Time before termination (h)																	
		1 - < 3		3 - < 6		6 - < 12		12 - < 18		18 - < 24		24 - < 30		30 - < 36		36 - < 42		42 - < 48	
		r	p	r	p	r	p	r	p	r	p	r	p	r	p	r	p	r	p
NTP/EPP	Sagittal top	-0.19	0.460	-0.20	0.430	-0.26	0.291	-0.10	0.705	0.40	0.152	0.47	0.200	0.41	0.367	0.71	0.176	0.15	0.850
	Sagittal bottom	-0.22	0.389	-0.44	0.071	-0.54	0.022	-0.53	0.028	0.05	0.861	-0.01	0.982	-0.23	0.615	0.64	0.241	0.62	0.376
	Parietal top	-0.21	0.393	-0.42	0.083	-0.40	0.104	-0.46	0.061	0.10	0.740	0.24	0.540	-0.10	0.825	0.89	0.044	-0.26	0.742
	Parietal bottom	-0.17	0.496	-0.45	0.065	-0.44	0.067	-0.53	0.030	0.05	0.861	0.02	0.961	-0.22	0.640	0.55	0.337	0.58	0.424
	Temporal	-0.03	0.917	-0.25	0.356	-0.16	0.568	-0.17	0.544	0.49	0.086	0.55	0.157	0.44	0.321	0.86	0.065	0.20	0.796
	Hippocampus	-0.56	0.119	-0.71	0.031	-0.27	0.475	0.14	0.749	0.57	0.184								
	Caudate nucleus	-0.10	0.723	-0.14	0.644	-0.14	0.624	-0.10	0.753	0.32	0.319	0.22	0.629	-0.04	0.942	0.89	0.043	-0.02	0.982
	Putamen	-0.34	0.238	-0.42	0.131	-0.56	0.036	-0.63	0.016	0.01	0.982	0.02	0.965	-0.45	0.316	0.46	0.439	-0.75	0.252
	Anterior thalamus	-0.05	0.860	-0.07	0.807	0.02	0.942	0.17	0.568	0.35	0.244	0.66	0.078	0.38	0.399	0.75	0.148	-0.34	0.658
	Lateral thalamus	-0.37	0.170	-0.29	0.303	-0.22	0.432	0.05	0.866	0.18	0.551	0.58	0.128	0.22	0.640	0.29	0.642	-0.26	0.742
	Medial thalamus	-0.34	0.241	-0.42	0.133	-0.32	0.265	-0.28	0.348	0.22	0.502	0.18	0.700	-0.02	0.970	0.92	0.078	-0.82	0.392
PCr/EPP	Sagittal top	-0.21	0.404	-0.37	0.135	-0.29	0.250	-0.31	0.231	0.03	0.927	0.19	0.617	0.51	0.246	0.01	0.993	0.17	0.828
	Sagittal bottom	-0.33	0.181	-0.58	0.011	-0.57	0.013	-0.66	0.004	-0.32	0.268	-0.16	0.684	-0.36	0.427	0.25	0.689	-0.16	0.836
	Parietal top	-0.31	0.219	-0.50	0.033	-0.41	0.090	-0.53	0.031	-0.24	0.402	0.03	0.946	0.13	0.777	0.27	0.662	0.50	0.496
	Parietal bottom	-0.30	0.222	-0.50	0.033	-0.45	0.063	-0.56	0.020	-0.22	0.447	-0.15	0.711	-0.41	0.358	0.10	0.873	-0.08	0.919
	Temporal	-0.12	0.647	-0.35	0.182	-0.31	0.238	-0.44	0.098	-0.02	0.943	0.38	0.350	0.35	0.439	-0.28	0.649	0.32	0.680
	Hippocampus	-0.47	0.205	-0.44	0.239	-0.36	0.346	-0.16	0.697	-0.10	0.835								
	Caudate nucleus	-0.06	0.831	-0.27	0.360	-0.24	0.415	-0.29	0.340	-0.25	0.438	0.07	0.876	-0.06	0.916	0.04	0.947	0.39	0.611
	Putamen	-0.37	0.189	-0.57	0.032	-0.52	0.060	-0.73	0.003	-0.38	0.197	-0.22	0.596	-0.32	0.487	0.71	0.183	0.49	0.511
	Anterior thalamus	-0.04	0.901	-0.17	0.554	-0.11	0.700	-0.15	0.615	-0.05	0.870	0.47	0.237	0.65	0.118	-0.02	0.970	0.56	0.442
	Lateral thalamus	-0.21	0.464	-0.31	0.257	-0.21	0.447	-0.01	0.963	-0.14	0.648	0.54	0.172	0.62	0.135	0.21	0.740	0.23	0.766
	Medial thalamus	-0.28	0.341	-0.52	0.059	-0.32	0.261	-0.38	0.197	-0.50	0.098	-0.15	0.755	0.05	0.930	0.27	0.728	1.00	0.027

		Time before termination (h)																	
		1 - < 3		3 - < 6		6 - < 12		12 - < 18		18 - < 24		24 - < 30		30 - < 36		36 - < 42		42 - < 48	
		r	p	r	p	r	p	r	p	r	p	r	p	r	p	r	p	r	p
Pi/EPP	Sagittal top	0.21	0.415	0.32	0.200	0.23	0.368	0.26	0.319	-0.21	0.482	-0.24	0.537	-0.42	0.344	0.03	0.962	-0.18	0.817
	Sagittal bottom	0.29	0.236	0.56	0.016	0.58	0.013	0.70	0.002	0.13	0.671	0.11	0.769	0.21	0.644	-0.48	0.413	-0.63	0.374
	Parietal top	0.27	0.280	0.46	0.055	0.41	0.089	0.57	0.018	0.07	0.816	-0.09	0.811	0.06	0.906	-0.34	0.578	-0.02	0.984
	Parietal bottom	0.24	0.331	0.51	0.033	0.45	0.063	0.62	0.008	0.05	0.872	0.07	0.866	0.20	0.676	-0.71	0.180	-.976	0.024
	Temporal	0.06	0.816	0.29	0.273	0.24	0.367	0.36	0.188	-0.28	0.361	-0.52	0.183	-0.51	0.242	-0.43	0.472	-0.68	0.319
	Hippocampus	0.48	0.189	0.67	0.048	0.31	0.415	0.04	0.932	-0.17	0.718								
	Caudate nucleus	0.11	0.705	0.20	0.496	0.21	0.470	0.22	0.467	0.02	0.951	-0.13	0.779	-0.16	0.757	-0.29	0.642	-0.27	0.728
	Putamen	0.39	0.169	0.50	0.070	0.54	0.049	0.73	0.003	0.15	0.623	0.07	0.876	0.30	0.514	-0.17	0.783	0.75	0.253
	Anterior thalamus	0.03	0.930	0.05	0.863	0.05	0.860	-0.01	0.970	-0.13	0.666	-0.52	0.184	-0.44	0.327	0.00	0.995	0.04	0.963
	Lateral thalamus	0.31	0.262	0.30	0.271	0.18	0.516	-0.02	0.945	0.08	0.804	-0.45	0.262	-0.17	0.709	0.49	0.400	0.46	0.538
	Medial thalamus	0.31	0.276	0.42	0.140	0.30	0.304	0.30	0.315	0.14	0.659	-0.07	0.890	-0.12	0.822	-0.93	0.069	-0.15	0.902
PCr/Pi	Sagittal top	-0.37	0.130	-0.42	0.085	-0.33	0.179	-0.34	0.188	0.01	0.963	0.04	0.917	0.57	0.184	-0.09	0.887	0.30	0.697
	Sagittal bottom	-0.39	0.109	-0.50	0.036	-0.52	0.026	-0.62	0.008	-0.28	0.330	-0.28	0.464	-0.20	0.669	0.52	0.371	0.58	0.418
	Parietal top	-0.36	0.140	-0.45	0.063	-0.38	0.121	-0.50	0.042	-0.21	0.478	-0.07	0.850	0.16	0.735	0.37	0.535	0.24	0.757
	Parietal bottom	-0.38	0.122	-0.44	0.070	-0.40	0.100	-0.54	0.025	-0.19	0.506	-0.25	0.523	-0.22	0.636	0.70	0.185	0.87	0.132
	Temporal	-0.17	0.523	-0.29	0.272	-0.31	0.244	-0.39	0.154	0.07	0.813	0.43	0.286	0.58	0.177	0.26	0.675	0.78	0.223
	Hippocampus	-0.35	0.363	-0.40	0.286	-0.35	0.350	-0.19	0.645	-0.06	0.894								
	Caudate nucleus	-0.11	0.717	-0.26	0.376	-0.23	0.428	-0.28	0.361	-0.19	0.553	0.08	0.871	0.18	0.740	0.23	0.707	0.44	0.557
	Putamen	-0.38	0.179	-0.49	0.078	-0.48	0.084	-0.62	0.018	-0.27	0.368	-0.15	0.720	-0.34	0.457	0.41	0.493	-0.50	0.498
	Anterior thalamus	-0.15	0.609	-0.25	0.392	-0.20	0.495	-0.10	0.742	0.03	0.924	0.57	0.139	0.63	0.130	-0.06	0.927	0.21	0.792
	Lateral thalamus	-0.38	0.167	-0.45	0.093	-0.32	0.245	-0.08	0.798	-0.13	0.669	0.53	0.175	0.43	0.340	-0.44	0.458	-0.28	0.723
	Medial thalamus	-0.37	0.198	-0.55	0.041	-0.36	0.212	-0.34	0.259	-0.34	0.276	0.05	0.913	0.16	0.756	0.98	0.018	0.46	0.699

C-1. ^{31}P MRS biomarkers 1-48 h before termination and CD68 positive microglia in the grey matter

		Time before termination (h)																	
		1 - < 3		3 - < 6		6 - < 12		12 - < 18		18 - < 24		24 - < 30		30 - < 36		36 - < 42		42 - < 48	
		r	p	r	p	r	p	r	p	r	p	r	p	r	p	r	p	r	p
NTP/EPP	Sagittal top	0.23	0.367	0.30	0.222	0.43	0.076	0.25	0.342	0.21	0.462	0.19	0.616	-0.67	0.097	-0.36	0.548	0.01	0.986
	Sagittal bottom	0.20	0.430	0.37	0.127	0.34	0.168	0.21	0.418	0.00	0.993	-0.11	0.780	-0.36	0.433	-0.05	0.938	-0.73	0.272
	Parietal top	0.36	0.141	0.33	0.179	0.55	0.017	0.43	0.089	0.20	0.497	0.18	0.637	-0.17	0.717	-0.21	0.741	-0.19	0.813
	Parietal bottom	0.24	0.340	0.28	0.260	0.39	0.115	0.19	0.466	0.30	0.301	0.27	0.487	0.20	0.667	-0.08	0.893	-0.65	0.348
	Temporal	0.09	0.736	0.12	0.672	0.26	0.337	0.26	0.343	-0.07	0.817	-0.44	0.276	-0.55	0.202	0.14	0.822	-0.77	0.234
	Hippocampus	-0.12	0.754	0.19	0.618	-0.31	0.410	0.34	0.406	0.51	0.242								
	Caudate nucleus	-0.13	0.647	0.12	0.671	0.18	0.533	0.07	0.801	0.03	0.927	-0.52	0.185	-0.08	0.870	-0.31	0.611	-0.38	0.618
	Putamen	-0.14	0.629	0.16	0.580	-0.13	0.645	-0.07	0.813	-0.09	0.767	-0.61	0.108	-0.35	0.445	-0.03	0.968	-0.77	0.234
	Anterior thalamus	0.00	0.997	0.08	0.788	0.15	0.589	0.00	0.997	-0.05	0.865	-0.50	0.206	-0.03	0.951	-0.21	0.741	-0.19	0.813
	Lateral thalamus	-0.24	0.397	0.07	0.807	0.10	0.724	0.05	0.863	0.07	0.823	-0.50	0.206	-0.03	0.951	-0.21	0.741	-0.19	0.813
	Medial thalamus	-0.09	0.770	0.19	0.521	-0.15	0.599	0.02	0.949	0.00	0.989	-0.43	0.333	-0.43	0.394	0.13	0.871	-0.82	0.388
PCr/EPP	Sagittal top	0.39	0.113	0.40	0.098	0.44	0.068	0.29	0.262	0.42	0.138	0.46	0.214	-0.62	0.141	-0.08	0.893	-0.12	0.876
	Sagittal bottom	0.26	0.304	0.51	0.032	0.48	0.046	0.42	0.095	0.31	0.288	0.08	0.835	-0.18	0.706	0.48	0.418	0.35	0.653
	Parietal top	0.49	0.038	0.56	0.016	0.65	0.003	0.59	0.013	0.46	0.096	0.41	0.273	-0.46	0.304	-0.10	0.873	0.10	0.904
	Parietal bottom	0.53	0.025	0.51	0.030	0.51	0.031	0.37	0.141	0.38	0.180	0.49	0.180	0.32	0.479	0.38	0.528	0.31	0.688
	Temporal	0.16	0.559	0.21	0.431	0.34	0.192	0.41	0.134	-0.16	0.603	-0.60	0.114	-0.36	0.425	0.76	0.140	0.36	0.642
	Hippocampus	0.01	0.973	-0.06	0.880	-0.16	0.679	-0.07	0.864	0.16	0.725								
	Caudate nucleus	-0.24	0.398	0.11	0.688	0.13	0.645	0.02	0.953	-0.02	0.954	-0.68	0.065	-0.38	0.405	-0.06	0.925	0.19	0.813
	Putamen	-0.08	0.772	0.02	0.958	-0.01	0.974	-0.14	0.632	-0.22	0.466	-0.85	0.007	-0.48	0.281	0.53	0.357	0.36	0.636
	Anterior thalamus	-0.12	0.660	0.10	0.731	0.12	0.660	-0.04	0.886	-0.16	0.609	-0.60	0.116	-0.36	0.431	-0.10	0.873	0.10	0.904
	Lateral thalamus	-0.29	0.300	0.04	0.894	0.10	0.712	0.07	0.811	-0.04	0.902	-0.60	0.116	-0.36	0.431	-0.10	0.873	0.10	0.904
	Medial thalamus	-0.01	0.967	0.01	0.977	-0.03	0.925	0.00	0.995	-0.11	0.744	-0.76	0.048	-0.34	0.505	0.75	0.247	0.38	0.752

		Time before termination (h)																	
		1 - < 3		3 - < 6		6 - < 12		12 - < 18		18 - < 24		24 - < 30		30 - < 36		36 - < 42		42 - < 48	
		r	p	r	p	r	p	r	p	r	p	r	p	r	p	r	p	r	p
Pi/EPP	Sagittal top	-0.35	0.159	-0.42	0.084	-0.39	0.113	-0.39	0.123	-0.41	0.146	-0.44	0.234	0.73	0.063	-0.48	0.417	-0.23	0.773
	Sagittal bottom	-0.22	0.380	-0.46	0.056	-0.42	0.080	-0.34	0.187	-0.17	0.562	-0.07	0.850	0.35	0.445	-0.49	0.397	0.49	0.511
	Parietal top	-0.45	0.058	-0.53	0.025	-0.57	0.013	-0.55	0.021	-0.40	0.153	-0.43	0.252	0.10	0.832	-0.62	0.269	-0.23	0.772
	Parietal bottom	-0.41	0.088	-0.47	0.050	-0.41	0.092	-0.41	0.100	-0.43	0.124	-0.49	0.179	-0.17	0.715	-0.55	0.341	0.36	0.640
	Temporal	-0.12	0.659	-0.20	0.452	-0.25	0.344	-0.30	0.286	0.17	0.570	0.56	0.146	0.44	0.323	-0.05	0.931	0.88	0.121
	Hippocampus	0.10	0.796	0.00	0.992	0.16	0.676	-0.04	0.920	-0.22	0.643								
	Caudate nucleus	0.14	0.615	-0.19	0.509	-0.19	0.510	-0.06	0.829	0.02	0.942	0.46	0.249	-0.04	0.929	-0.48	0.414	-0.01	0.992
	Putamen	0.13	0.641	-0.10	0.727	-0.01	0.968	0.05	0.857	0.17	0.581	0.67	0.070	0.20	0.676	-0.45	0.442	0.57	0.434
	Anterior thalamus	0.00	0.995	-0.20	0.486	-0.19	0.495	-0.03	0.921	0.10	0.739	0.42	0.297	-0.05	0.911	-0.62	0.269	-0.23	0.772
	Lateral thalamus	0.24	0.400	-0.11	0.705	-0.14	0.614	-0.07	0.818	0.04	0.903	0.42	0.297	-0.05	0.911	-0.62	0.269	-0.23	0.772
	Medial thalamus	0.09	0.770	-0.08	0.781	0.02	0.956	-0.04	0.899	0.10	0.769	0.57	0.179	0.30	0.564	-0.12	0.876	0.88	0.319
PCr/Pi	Sagittal top	0.57	0.013	0.51	0.032	0.50	0.034	0.46	0.065	0.60	0.024	0.66	0.054	-0.65	0.117	0.48	0.412	0.09	0.914
	Sagittal bottom	0.39	0.112	0.52	0.027	0.49	0.040	0.39	0.123	0.18	0.534	0.33	0.388	-0.33	0.475	0.69	0.194	-0.40	0.596
	Parietal top	0.57	0.013	0.54	0.020	0.67	0.003	0.71	0.001	0.51	0.062	0.64	0.063	-0.33	0.474	0.61	0.278	0.15	0.847
	Parietal bottom	0.72	0.001	0.66	0.003	0.57	0.013	0.54	0.027	0.61	0.022	0.70	0.036	0.18	0.700	0.71	0.177	-0.31	0.695
	Temporal	0.13	0.636	0.11	0.682	0.30	0.261	0.53	0.043	-0.23	0.442	-0.52	0.184	-0.48	0.275	0.34	0.580	-0.69	0.310
	Hippocampus	-0.07	0.850	-0.12	0.761	-0.22	0.570	-0.07	0.863	-0.01	0.983								
	Caudate nucleus	-0.05	0.855	0.08	0.791	0.09	0.742	-0.01	0.979	-0.10	0.747	-0.50	0.210	-0.26	0.576	0.50	0.395	-0.02	0.980
	Putamen	-0.02	0.956	-0.03	0.930	-0.05	0.852	-0.08	0.774	-0.27	0.377	-0.67	0.070	-0.45	0.317	0.67	0.214	-0.46	0.538
	Anterior thalamus	0.06	0.840	0.07	0.809	0.12	0.669	-0.03	0.917	-0.20	0.507	-0.45	0.269	-0.22	0.643	0.61	0.278	0.15	0.847
	Lateral thalamus	-0.21	0.444	-0.06	0.847	0.03	0.923	-0.01	0.979	-0.12	0.692	-0.45	0.269	-0.22	0.643	0.61	0.278	0.15	0.847
	Medial thalamus	-0.07	0.818	-0.06	0.848	-0.10	0.747	0.00	1.000	-0.19	0.550	-0.56	0.194	-0.41	0.419	0.48	0.522	-0.68	0.522

C-2. ^{31}P MRS biomarkers 1-48 h before termination and CD68 positive microglia in the white matter

		Time before termination (h)																	
		1 - < 3		3 - < 6		6 - < 12		12 - < 18		18 - < 24		24 - < 30		30 - < 36		36 - < 42		42 - < 48	
		r	p	r	p	r	p	r	p	r	p	r	p	r	p	r	p	r	p
NTP/EPP	Sagittal	0.27	0.296	0.39	0.123	0.46	0.064	0.18	0.501	0.21	0.479	0.20	0.599	-0.43	0.337	0.11	0.862	-0.81	0.194
	Parietal	0.19	0.475	0.38	0.153	0.43	0.100	0.20	0.484	0.20	0.507	0.20	0.613	-0.23	0.621	-0.12	0.850	-0.56	0.440
	Temporal	0.35	0.188	0.40	0.127	0.29	0.284	-0.01	0.985	-0.24	0.439	-0.50	0.208	-0.34	0.463	-0.13	0.832	-0.82	0.178
	Superior Periventricular	0.08	0.765	0.35	0.170	0.15	0.555	-0.07	0.799	-0.19	0.508	-0.64	0.064	-0.26	0.572	-0.10	0.876	-0.62	0.382
	Periventricular	-0.48	0.061	-0.04	0.883	-0.24	0.379	-0.03	0.922	0.08	0.782	-0.32	0.403	-0.42	0.349	0.17	0.780	-0.70	0.303
	PLIC	0.37	0.298	0.51	0.136	0.29	0.413	0.07	0.856	-0.11	0.794	-0.46	0.543	-0.34	0.658	-0.02	0.987		
PCr/EPP	Sagittal	0.49	0.047	0.55	0.024	0.57	0.016	0.40	0.125	0.41	0.141	0.40	0.282	-0.38	0.406	0.74	0.154	0.38	0.622
	Parietal	0.33	0.213	0.41	0.115	0.44	0.088	0.26	0.355	0.38	0.197	0.41	0.278	-0.47	0.291	0.28	0.654	0.27	0.730
	Temporal	0.54	0.029	0.64	0.008	0.69	0.003	0.58	0.024	0.26	0.388	-0.76	0.030	-0.39	0.387	0.51	0.381	0.39	0.611
	Superior Periventricular	-0.02	0.927	0.26	0.319	0.28	0.269	0.24	0.365	0.12	0.688	-0.80	0.009	-0.48	0.281	0.34	0.575	0.30	0.703
	Periventricular	-0.37	0.158	-0.17	0.533	-0.15	0.572	-0.12	0.670	-0.17	0.552	-0.51	0.164	-0.26	0.579	0.75	0.144	0.33	0.675
	PLIC	0.42	0.232	0.52	0.122	0.48	0.158	0.19	0.632	0.38	0.356	-0.92	0.082	-0.34	0.663	1.00	0.048		
Pi/EPP	Sagittal	-0.40	0.110	-0.53	0.030	-0.46	0.063	-0.42	0.102	-0.43	0.128	-0.42	0.263	0.29	0.533	-0.15	0.809	0.85	0.146
	Parietal	-0.30	0.265	-0.46	0.074	-0.41	0.119	-0.37	0.180	-0.38	0.196	-0.43	0.252	0.10	0.839	-0.59	0.299	0.22	0.778
	Temporal	-0.43	0.101	-0.55	0.028	-0.51	0.046	-0.38	0.157	-0.18	0.563	0.57	0.141	0.17	0.713	-0.14	0.821	0.73	0.271
	Superior Periventricular	0.00	0.991	-0.26	0.316	-0.23	0.374	-0.12	0.654	-0.06	0.829	0.64	0.066	0.12	0.797	-0.56	0.323	0.31	0.693
	Periventricular	0.46	0.072	0.15	0.582	0.13	0.641	0.08	0.779	0.13	0.667	0.45	0.221	0.30	0.507	0.06	0.925	0.88	0.119
	PLIC	-0.35	0.328	-0.46	0.177	-0.34	0.331	-0.13	0.734	-0.25	0.546	0.69	0.309	0.23	0.768	0.00	0.998		
PCr/Pi	Sagittal	0.68	0.003	0.67	0.003	0.62	0.007	0.60	0.014	0.63	0.015	0.64	0.066	-0.43	0.334	0.43	0.469	-0.68	0.325
	Parietal	0.55	0.029	0.51	0.046	0.48	0.060	0.44	0.104	0.56	0.048	0.64	0.063	-0.38	0.402	0.72	0.175	-0.20	0.801
	Temporal	0.56	0.026	0.69	0.003	0.72	0.002	0.66	0.007	0.39	0.193	-0.58	0.129	-0.40	0.373	0.36	0.554	-0.59	0.415
	Superior Periventricular	-0.05	0.859	0.23	0.379	0.23	0.365	0.20	0.464	0.13	0.664	-0.58	0.101	-0.40	0.374	0.72	0.174	-0.26	0.736
	Periventricular	-0.30	0.268	-0.23	0.385	-0.23	0.383	-0.17	0.539	-0.24	0.402	-0.39	0.296	-0.36	0.429	0.22	0.727	-0.69	0.313
	PLIC	0.62	0.058	0.67	0.033	0.57	0.086	0.36	0.339	0.37	0.366	-0.71	0.290	-0.40	0.600	0.45	0.702		

D-1. ^{31}P MRS biomarkers 1-48 h before termination and CD68 positive vessels in the grey matter

		Time before termination (h)																	
		1 - < 3		3 - < 6		6 - < 12		12 - < 18		18 - < 24		24 - < 30		30 - < 36		36 - < 42		42 - < 48	
		r	p	r	p	r	p	r	p	r	p	r	p	r	p	r	p	r	p
NTP/EPP	Sagittal top	0.38	0.120	0.42	0.082	0.46	0.054	0.31	0.222	0.12	0.696	0.16	0.690	-0.78	0.041	-0.21	0.741	-0.19	0.813
	Sagittal bottom	0.25	0.315	0.42	0.079	0.32	0.197	0.27	0.294	0.05	0.869	0.14	0.728	-0.76	0.050	0.17	0.780	-0.70	0.303
	Parietal top	0.51	0.032	0.39	0.107	0.56	0.017	0.40	0.108	0.08	0.782	-0.02	0.970	-0.28	0.540	-0.21	0.741	-0.19	0.813
	Parietal bottom	0.32	0.199	0.35	0.158	0.45	0.063	0.25	0.336	0.29	0.311	0.28	0.462	0.24	0.608	0.17	0.780	-0.70	0.303
	Temporal	0.05	0.841	0.10	0.708	0.28	0.291	0.26	0.357	-0.03	0.935	-0.30	0.472	-0.42	0.349	0.17	0.780	-0.70	0.303
	Hippocampus	-0.16	0.684	0.18	0.639	-0.25	0.510	0.13	0.766	0.27	0.564								
	Caudate nucleus	-0.24	0.396	0.09	0.764	0.17	0.550	0.06	0.835	0.07	0.827								
	Putamen	-0.12	0.676	0.03	0.908	-0.36	0.184	-0.48	0.081	-0.35	0.240	-0.63	0.097	-0.28	0.544	-0.08	0.893	-0.65	0.348
	Anterior thalamus	-0.17	0.552	0.03	0.922	0.17	0.552	0.03	0.927	0.02	0.942	-0.50	0.206	-0.03	0.951	-0.21	0.741	-0.19	0.813
	Lateral thalamus	-0.19	0.505	0.06	0.826	0.13	0.649	0.04	0.882	0.05	0.872	-0.50	0.206	-0.03	0.951	-0.21	0.741	-0.19	0.813
	Medial thalamus	-0.28	0.338	0.09	0.754	-0.05	0.871	-0.06	0.839	-0.02	0.964	-0.43	0.333	-0.43	0.394	0.13	0.871	-0.82	0.388
PCr/EPP	Sagittal top	0.49	0.038	0.49	0.039	0.54	0.020	0.46	0.061	0.59	0.027	0.45	0.221	-0.58	0.170	-0.10	0.873	0.10	0.904
	Sagittal bottom	0.27	0.279	0.41	0.091	0.39	0.110	0.27	0.292	0.47	0.089	0.41	0.279	-0.30	0.512	0.75	0.144	0.33	0.675
	Parietal top	0.64	0.004	0.68	0.002	0.73	0.001	0.67	0.003	0.51	0.063	0.23	0.560	-0.53	0.226	-0.10	0.873	0.10	0.904
	Parietal bottom	0.59	0.010	0.57	0.014	0.57	0.014	0.40	0.112	0.46	0.097	0.50	0.166	0.61	0.147	0.75	0.144	0.33	0.675
	Temporal	0.09	0.736	0.20	0.462	0.34	0.201	0.39	0.151	-0.13	0.673	-0.52	0.192	-0.26	0.579	0.75	0.144	0.33	0.675
	Hippocampus	-0.11	0.772	-0.11	0.786	-0.18	0.642	-0.08	0.847	0.01	0.981								
	Caudate nucleus	-0.37	0.177	0.04	0.876	0.09	0.758	0.04	0.888	0.03	0.922								
	Putamen	-0.13	0.640	-0.23	0.415	-0.28	0.317	-0.56	0.037	-0.63	0.021	-0.84	0.009	-0.48	0.278	0.38	0.528	0.31	0.688
	Anterior thalamus	-0.29	0.304	0.05	0.856	0.12	0.678	0.01	0.965	-0.09	0.761	-0.60	0.116	-0.36	0.431	-0.10	0.873	0.10	0.904
	Lateral thalamus	-0.22	0.441	0.08	0.770	0.18	0.528	0.12	0.684	-0.06	0.850	-0.60	0.116	-0.36	0.431	-0.10	0.873	0.10	0.904
	Medial thalamus	-0.36	0.205	-0.08	0.788	-0.07	0.808	-0.13	0.662	-0.17	0.591	-0.76	0.048	-0.34	0.505	0.75	0.247	0.38	0.752

		Time before termination (h)																	
		1 - < 3		3 - < 6		6 - < 12		12 - < 18		18 - < 24		24 - < 30		30 - < 36		36 - < 42		42 - < 48	
		r	p	r	p	r	p	r	p	r	p	r	p	r	p	r	p	r	p
Pi/EPP	Sagittal top	-0.44	0.067	-0.46	0.054	-0.43	0.072	-0.47	0.056	-0.50	0.071	-0.41	0.268	0.83	0.021	-0.62	0.269	-0.23	0.772
	Sagittal bottom	-0.26	0.293	-0.42	0.085	-0.40	0.104	-0.32	0.208	-0.31	0.283	-0.35	0.355	0.78	0.039	0.06	0.925	0.88	0.119
	Parietal top	-0.59	0.010	-0.59	0.009	-0.62	0.006	-0.59	0.013	-0.41	0.144	-0.26	0.500	0.22	0.630	-0.62	0.269	-0.23	0.772
	Parietal bottom	-0.49	0.039	-0.54	0.022	-0.48	0.044	-0.46	0.062	-0.47	0.087	-0.50	0.169	-0.15	0.755	0.06	0.925	0.88	0.119
	Temporal	-0.07	0.784	-0.20	0.469	-0.26	0.331	-0.29	0.304	0.14	0.640	0.45	0.260	0.30	0.507	0.06	0.925	0.88	0.119
	Hippocampus	0.17	0.663	0.02	0.964	0.16	0.678	0.05	0.914	-0.04	0.930								
	Caudate nucleus	0.28	0.321	-0.10	0.734	-0.13	0.655	-0.04	0.880	-0.01	0.972								
	Putamen	0.16	0.578	0.10	0.715	0.25	0.371	0.45	0.109	0.43	0.146	0.65	0.083	0.14	0.772	-0.55	0.341	0.36	0.640
	Anterior thalamus	0.17	0.544	-0.13	0.648	-0.17	0.537	-0.04	0.886	0.07	0.822	0.42	0.297	-0.05	0.911	-0.62	0.269	-0.23	0.772
	Lateral thalamus	0.16	0.563	-0.15	0.594	-0.21	0.463	-0.11	0.720	0.05	0.874	0.42	0.297	-0.05	0.911	-0.62	0.269	-0.23	0.772
	Medial thalamus	0.32	0.271	-0.03	0.911	0.02	0.946	0.10	0.758	0.14	0.672	0.57	0.179	0.30	0.564	-0.12	0.876	0.88	0.319
PCr/Pi	Sagittal top	0.55	0.019	0.55	0.017	0.59	0.010	0.61	0.009	0.74	0.002	0.63	0.068	-0.64	0.120	0.61	0.278	0.15	0.847
	Sagittal bottom	0.37	0.126	0.42	0.085	0.43	0.076	0.28	0.277	0.36	0.203	0.59	0.094	-0.54	0.212	0.22	0.727	-0.69	0.313
	Parietal top	0.70	0.001	0.69	0.001	0.78	0.000	0.78	0.000	0.54	0.048	0.48	0.194	-0.41	0.358	0.61	0.278	0.15	0.847
	Parietal bottom	0.79	0.000	0.71	0.001	0.65	0.004	0.57	0.017	0.65	0.012	0.71	0.032	0.35	0.442	0.22	0.727	-0.69	0.313
	Temporal	0.08	0.779	0.09	0.735	0.28	0.287	0.49	0.062	-0.20	0.504	-0.43	0.287	-0.36	0.429	0.22	0.727	-0.69	0.313
	Hippocampus	-0.23	0.551	-0.19	0.627	-0.27	0.486	-0.19	0.661	-0.10	0.837								
	Caudate nucleus	-0.25	0.377	-0.01	0.986	0.02	0.952	-0.04	0.905	-0.04	0.895								
	Putamen	-0.23	0.419	-0.26	0.350	-0.33	0.232	-0.47	0.089	-0.48	0.099	-0.65	0.079	-0.41	0.359	0.71	0.177	-0.31	0.695
	Anterior thalamus	-0.13	0.646	-0.01	0.977	0.08	0.787	-0.04	0.903	-0.16	0.592	-0.45	0.269	-0.22	0.643	0.61	0.278	0.15	0.847
	Lateral thalamus	-0.14	0.613	-0.02	0.955	0.12	0.683	0.05	0.858	-0.14	0.652	-0.45	0.269	-0.22	0.643	0.61	0.278	0.15	0.847
	Medial thalamus	-0.31	0.274	-0.16	0.595	-0.16	0.575	-0.20	0.519	-0.22	0.488	-0.56	0.194	-0.41	0.419	0.48	0.522	-0.68	0.522

D-2. ^{31}P MRS biomarkers 1-48 h before termination and CD68 positive vessels in the white matter

		Time before termination (h)																	
		1 - < 3		3 - < 6		6 - < 12		12 - < 18		18 - < 24		24 - < 30		30 - < 36		36 - < 42		42 - < 48	
		r	p	r	p	r	p	r	p	r	p	r	p	r	p	r	p	r	p
NTP/EPP	Sagittal	0.10	0.705	0.45	0.072	0.31	0.220	0.05	0.844	0.05	0.864	0.10	0.793	-0.42	0.349	0.17	0.780	-0.70	0.303
	Parietal	0.13	0.619	0.35	0.185	0.48	0.062	0.25	0.361	0.18	0.567	0.27	0.486						
	Temporal	0.12	0.658	0.19	0.478	0.25	0.344	-0.05	0.854	-0.20	0.520	-0.61	0.108	-0.35	0.445	-0.03	0.968	-0.77	0.234
	Superior Periventricular	-0.37	0.140	-0.02	0.938	-0.20	0.450	-0.35	0.189	-0.23	0.438	-0.49	0.185	-0.42	0.352	0.07	0.909	-0.83	0.174
	Periventricular	-0.14	0.602	0.22	0.407	-0.13	0.631	-0.18	0.522	-0.16	0.580	-0.17	0.653	-0.42	0.349	0.17	0.780	-0.70	0.303
	PLIC	0.38	0.278	0.60	0.070	0.36	0.309	0.07	0.855	-0.09	0.833	-0.46	0.543	-0.34	0.658	-0.02	0.987		
PCr/EPP	Sagittal	0.24	0.358	0.43	0.083	0.45	0.068	0.32	0.227	0.32	0.259	0.23	0.558	-0.26	0.579	0.75	0.144	0.33	0.675
	Parietal	0.32	0.233	0.64	0.008	0.68	0.004	0.64	0.010	0.44	0.137	0.49	0.177						
	Temporal	0.17	0.530	0.31	0.237	0.48	0.057	0.38	0.160	0.19	0.544	-0.85	0.007	-0.48	0.281	0.53	0.357	0.36	0.636
	Superior Periventricular	-0.26	0.321	-0.06	0.827	0.02	0.955	-0.07	0.797	-0.39	0.164	-0.64	0.062	-0.42	0.350	0.70	0.187	0.39	0.611
	Periventricular	0.00	0.995	0.06	0.818	0.04	0.875	-0.16	0.576	-0.13	0.660	-0.25	0.526	-0.26	0.579	0.75	0.144	0.33	0.675
	PLIC	0.32	0.365	0.54	0.110	0.52	0.128	0.39	0.294	0.55	0.154	-0.92	0.082	-0.34	0.663	1.00	0.048		
Pi/EPP	Sagittal	-0.15	0.565	-0.44	0.076	-0.34	0.184	-0.28	0.291	-0.29	0.312	-0.25	0.514	0.30	0.507	0.06	0.925	0.88	0.119
	Parietal	-0.23	0.400	-0.52	0.040	-0.56	0.023	-0.50	0.059	-0.35	0.237	-0.49	0.177						
	Temporal	-0.17	0.535	-0.32	0.229	-0.41	0.115	-0.26	0.350	-0.12	0.705	0.67	0.070	0.20	0.676	-0.45	0.442	0.57	0.434
	Superior Periventricular	0.34	0.184	0.02	0.951	0.05	0.865	0.15	0.585	0.29	0.323	0.52	0.152	0.27	0.563	-0.25	0.687	0.80	0.199
	Periventricular	0.12	0.672	-0.15	0.578	0.01	0.965	0.10	0.715	0.13	0.661	0.19	0.616	0.30	0.507	0.06	0.925	0.88	0.119
	PLIC	-0.30	0.408	-0.44	0.203	-0.34	0.330	-0.23	0.554	-0.40	0.324	0.69	0.309	0.23	0.768	0.00	0.998		
PCr/Pi	Sagittal	0.38	0.135	0.51	0.035	0.45	0.070	0.45	0.081	0.48	0.079	0.47	0.197	-0.36	0.429	0.22	0.727	-0.69	0.313
	Parietal	0.48	0.062	0.67	0.005	0.68	0.004	0.64	0.010	0.42	0.154	0.70	0.036						
	Temporal	0.10	0.717	0.25	0.343	0.47	0.068	0.35	0.198	0.28	0.360	-0.67	0.070	-0.45	0.317	0.67	0.214	-0.46	0.538
	Superior Periventricular	-0.17	0.519	-0.07	0.804	-0.03	0.914	-0.04	0.899	-0.27	0.345	-0.40	0.285	-0.45	0.313	0.52	0.369	-0.64	0.362
	Periventricular	0.12	0.655	0.10	0.712	0.04	0.878	0.02	0.953	-0.04	0.882	-0.04	0.918	-0.36	0.429	0.22	0.727	-0.69	0.313
	PLIC	0.32	0.376	0.67	0.035	0.54	0.110	0.46	0.208	0.64	0.091	-0.71	0.290	-0.40	0.600	0.45	0.702		

E. ^{31}P MRS biomarkers 1-48 h before termination and white matter injury assessed using H & E stains

		Time before termination (h)																	
		1 - < 3		3 - < 6		6 - < 12		12 - < 18		18 - < 24		24 - < 30		30 - < 36		36 - < 42		42 - < 48	
		r	p	r	p	r	p	r	p	r	p	r	p	r	p	r	p	r	p
NTP/EPP	Sagittal	-0.67	0.003	-0.71	0.002	-0.66	0.004	-0.43	0.101	-0.12	0.693	-0.15	0.703	-0.18	0.702	0.89	0.041	-0.78	0.225
	Parietal	-0.57	0.021	-0.73	0.001	-0.53	0.035	-0.38	0.166	-0.14	0.653	-0.15	0.703	-0.18	0.702	0.89	0.041	-0.78	0.225
	Temporal	-0.61	0.012	-0.44	0.090	-0.52	0.040	-0.34	0.210	-0.01	0.969	0.32	0.446	-0.06	0.899	0.95	0.014	-0.45	0.553
	Superior Periventricular	-0.62	0.008	-0.43	0.082	-0.59	0.013	-0.24	0.362	-0.01	0.972	0.12	0.759	0.27	0.562	0.71	0.182		
	Periventricular	-0.65	0.007	-0.65	0.007	-0.72	0.002	-0.40	0.143	0.08	0.784	-0.20	0.602	-0.43	0.331	0.89	0.041	-0.78	0.225
	PLIC	-0.87	0.000	-0.76	0.004	-0.68	0.015	-0.51	0.111	0.11	0.753	0.12	0.816	-0.63	0.252	0.74	0.262	-0.50	0.667
PCr/EPP	Sagittal	-0.77	0.000	-0.80	0.000	-0.70	0.002	-0.66	0.005	-0.71	0.004	-0.39	0.305	-0.18	0.702	0.45	0.450	0.78	0.225
	Parietal	-0.75	0.001	-0.78	0.000	-0.65	0.006	-0.64	0.010	-0.64	0.019	-0.39	0.305	-0.18	0.702	0.45	0.450	0.78	0.225
	Temporal	-0.67	0.004	-0.72	0.002	-0.65	0.007	-0.74	0.002	-0.54	0.056	0.28	0.510	0.06	0.899	0.53	0.361	0.89	0.106
	Superior Periventricular	-0.65	0.005	-0.72	0.001	-0.66	0.004	-0.73	0.001	-0.61	0.020	-0.19	0.626	0.27	0.562	0.71	0.182		
	Periventricular	-0.57	0.020	-0.74	0.001	-0.68	0.004	-0.72	0.002	-0.50	0.068	-0.32	0.407	-0.43	0.331	0.45	0.450	0.78	0.225
	PLIC	-0.68	0.015	-0.74	0.006	-0.53	0.078	-0.50	0.116	-0.44	0.205	-0.09	0.862	-0.32	0.604	0.63	0.368	0.50	0.667
Pi/EPP	Sagittal	0.76	0.000	0.81	0.000	0.72	0.001	0.72	0.002	0.62	0.019	0.39	0.305	0.05	0.924	-0.89	0.041	-0.26	0.742
	Parietal	0.67	0.004	0.77	0.001	0.61	0.012	0.67	0.007	0.65	0.016	0.39	0.305	0.05	0.924	-0.89	0.041	-0.26	0.742
	Temporal	0.66	0.006	0.68	0.004	0.66	0.005	0.72	0.003	0.42	0.155	-0.18	0.672	0.06	0.899	-0.53	0.361	0.00	1.000
	Superior Periventricular	0.69	0.002	0.72	0.001	0.72	0.001	0.75	0.001	0.48	0.080	0.19	0.626	-0.13	0.775	-0.71	0.182		
	Periventricular	0.65	0.007	0.76	0.001	0.78	0.000	0.72	0.002	0.32	0.260	0.32	0.407	0.34	0.463	-0.89	0.041	-0.26	0.742
	PLIC	0.75	0.005	0.77	0.004	0.63	0.029	0.63	0.037	0.38	0.277	0.31	0.552	0.63	0.252	0.11	0.895	0.50	0.667
PCr/Pi	Sagittal	-0.76	0.000	-0.81	0.000	-0.72	0.001	-0.71	0.002	-0.69	0.007	-0.39	0.305	-0.18	0.702	0.89	0.041	0.26	0.742
	Parietal	-0.73	0.001	-0.79	0.000	-0.65	0.006	-0.67	0.007	-0.65	0.016	-0.39	0.305	-0.18	0.702	0.89	0.041	0.26	0.742
	Temporal	-0.66	0.005	-0.68	0.004	-0.64	0.007	-0.70	0.004	-0.46	0.113	0.28	0.510	-0.06	0.899	0.53	0.361	0.00	1.000
	Superior Periventricular	-0.67	0.003	-0.70	0.002	-0.69	0.002	-0.73	0.001	-0.55	0.041	-0.19	0.626	0.27	0.562	0.71	0.182		
	Periventricular	-0.55	0.028	-0.73	0.001	-0.73	0.001	-0.72	0.002	-0.45	0.105	-0.32	0.407	-0.43	0.331	0.89	0.041	0.26	0.742
	PLIC	-0.70	0.011	-0.77	0.004	-0.63	0.027	-0.58	0.059	-0.53	0.117	-0.09	0.862	-0.63	0.252	-0.11	0.895	-0.50	0.667

F. ^{31}P MRS biomarkers 1-48 h before termination and white matter injury assessed using LFB/Nissl stains

		Time before termination (h)																	
		1 - < 3		3 - < 6		6 - < 12		12 - < 18		18 - < 24		24 - < 30		30 - < 36		36 - < 42		42 - < 48	
		r	p	r	p	r	p	r	p	r	p	r	p	r	p	r	p	r	p
NTP/EPP	Sagittal	0.58	0.015	0.33	0.201	0.33	0.192	0.09	0.749	-0.22	0.458	0.41	0.272	0.61	0.144				
	Parietal	0.70	0.002	0.34	0.205	0.47	0.067	0.26	0.358	-0.02	0.951	0.52	0.154	0.79	0.034	-0.35	0.559	0.78	0.225
	Temporal	0.60	0.014	0.16	0.552	0.34	0.203	0.21	0.454	-0.10	0.751	0.25	0.555	0.41	0.363	-0.35	0.559	0.78	0.225
	Superior Periventricular	0.41	0.104	0.31	0.232	0.15	0.557	-0.14	0.605	-0.38	0.182								
	Periventricular	0.42	0.105	0.31	0.246	0.14	0.605	-0.12	0.660	-0.38	0.182								
	PLIC	0.70	0.012	0.42	0.176	0.42	0.176	0.19	0.568	-0.11	0.754	-0.66	0.158	0.00	1.000	-0.26	0.742	0.00	1.000
PCr/EPP	Sagittal	0.34	0.184	0.20	0.432	0.12	0.656	0.02	0.952	-0.01	0.970	0.14	0.725	0.61	0.144				
	Parietal	0.45	0.079	0.31	0.243	0.24	0.365	0.17	0.537	0.15	0.618	0.41	0.268	0.63	0.127	-0.71	0.182	-0.26	0.742
	Temporal	0.42	0.102	0.19	0.481	0.10	0.706	0.07	0.805	0.20	0.523	0.41	0.310	0.20	0.661	-0.71	0.182	-0.26	0.742
	Superior Periventricular	0.36	0.159	0.26	0.323	0.15	0.557	-0.08	0.757	-0.10	0.726								
	Periventricular	0.36	0.166	0.25	0.346	0.14	0.605	-0.12	0.660	-0.10	0.726								
	PLIC	0.47	0.120	0.47	0.120	0.36	0.247	0.32	0.333	0.19	0.599	-0.66	0.158	-0.35	0.559	0.26	0.742	-0.87	0.333
Pi/EPP	Sagittal	-0.46	0.066	-0.25	0.331	-0.20	0.445	-0.05	0.842	-0.04	0.903	-0.14	0.725	-0.61	0.144				
	Parietal	-0.58	0.019	-0.34	0.205	-0.30	0.257	-0.19	0.498	-0.21	0.490	-0.52	0.154	-0.79	0.034	0.00	1.000	-0.78	0.225
	Temporal	-0.51	0.043	-0.22	0.414	-0.16	0.552	-0.11	0.710	-0.29	0.332	-0.58	0.134	-0.41	0.363	0.00	1.000	-0.78	0.225
	Superior Periventricular	-0.41	0.104	-0.31	0.232	-0.15	0.557	-0.03	0.918	-0.03	0.907								
	Periventricular	-0.42	0.105	-0.31	0.246	-0.14	0.605	0.00	1.000	-0.03	0.907								
	PLIC	-0.53	0.077	-0.47	0.120	-0.42	0.176	-0.45	0.163	-0.27	0.458	0.39	0.441	0.00	1.000	-0.78	0.225	0.00	1.000
PCr/Pi	Sagittal	0.34	0.176	0.25	0.331	0.16	0.546	0.08	0.780	0.06	0.836	0.14	0.725	0.61	0.144				
	Parietal	0.46	0.073	0.34	0.205	0.26	0.332	0.21	0.452	0.27	0.376	0.41	0.268	0.79	0.034	0.00	1.000	0.78	0.225
	Temporal	0.45	0.078	0.22	0.414	0.13	0.627	0.14	0.620	0.34	0.253	0.41	0.310	0.41	0.363	0.00	1.000	0.78	0.225
	Superior Periventricular	0.41	0.104	0.31	0.232	0.20	0.432	0.03	0.918	0.03	0.907								
	Periventricular	0.42	0.105	0.31	0.246	0.20	0.467	0.00	1.000	0.03	0.907								
	PLIC	0.53	0.077	0.47	0.120	0.42	0.176	0.39	0.239	0.27	0.458	-0.66	0.158	0.00	1.000	0.78	0.225	0.00	1.000

G. ^{31}P MRS biomarkers 1-48 h before termination and white matter injury assessed using β-APP immune-histochemical stain

		Time before termination (h)																	
		1 - < 3		3 - < 6		6 - < 12		12 - < 18		18 - < 24		24 - < 30		30 - < 36		36 - < 42		42 - < 48	
		r	p	r	p	r	p	r	p	r	p	r	p	r	p	r	p	r	p
NTP/EPP	Sagittal	-0.38	0.129	-0.44	0.078	-0.39	0.121	-0.40	0.121	-0.04	0.887	0.13	0.742	0.00	1.000	0.58	0.308	0.26	0.742
	Parietal	-0.37	0.156	-0.54	0.033	-0.39	0.133	-0.47	0.080	-0.05	0.879	-0.12	0.768	-0.43	0.332	0.87	0.058	-0.45	0.553
	Temporal	-0.42	0.104	-0.35	0.187	-0.43	0.099	-0.41	0.129	-0.03	0.930	0.41	0.310	0.00	1.000	0.58	0.308	0.26	0.742
	Superior Periventricular	-0.64	0.005	-0.52	0.032	-0.62	0.008	-0.51	0.042	-0.22	0.453	-0.02	0.964	-0.30	0.515	0.58	0.308	0.26	0.742
	Periventricular	-0.63	0.008	-0.63	0.009	-0.46	0.076	-0.32	0.240	0.11	0.721	0.22	0.572	0.06	0.899	0.63	0.252	-0.21	0.789
	PLIC	-0.33	0.353	-0.54	0.107	-0.40	0.259	-0.44	0.240	-0.13	0.762	-0.89	0.106	-0.89	0.106	0.00	1.000		
PCr/EPP	Sagittal	-0.27	0.289	-0.38	0.136	-0.31	0.229	-0.50	0.047	-0.51	0.066	-0.17	0.654	0.16	0.735	0.58	0.308	0.26	0.742
	Parietal	-0.28	0.294	-0.32	0.222	-0.26	0.338	-0.36	0.183	-0.49	0.086	-0.30	0.430	-0.29	0.530	0.29	0.638	0.89	0.106
	Temporal	-0.50	0.050	-0.61	0.012	-0.59	0.016	-0.78	0.001	-0.48	0.098	0.23	0.578	0.16	0.735	0.58	0.308	0.26	0.742
	Superior Periventricular	-0.66	0.004	-0.72	0.001	-0.69	0.002	-0.72	0.002	-0.61	0.021	-0.20	0.604	-0.18	0.701	0.58	0.308	0.26	0.742
	Periventricular	-0.56	0.024	-0.60	0.014	-0.46	0.075	-0.58	0.025	-0.42	0.139	-0.02	0.964	0.24	0.606	0.21	0.734	0.74	0.262
	PLIC	-0.28	0.440	-0.45	0.195	-0.40	0.259	-0.62	0.073	-0.49	0.219	-0.89	0.106	-0.89	0.106	0.87	0.333		
Pi/EPP	Sagittal	0.28	0.280	0.36	0.155	0.34	0.189	0.52	0.041	0.31	0.285	0.24	0.537	0.16	0.735	0.00	1.000	0.26	0.742
	Parietal	0.28	0.288	0.33	0.212	0.24	0.376	0.37	0.180	0.45	0.123	0.36	0.336	0.29	0.530	-0.29	0.638	0.00	1.000
	Temporal	0.44	0.089	0.55	0.028	0.57	0.022	0.75	0.001	0.30	0.317	-0.14	0.745	0.16	0.735	0.00	1.000	0.26	0.742
	Superior Periventricular	0.68	0.003	0.70	0.002	0.68	0.003	0.77	0.001	0.53	0.049	0.25	0.510	0.42	0.350	0.00	1.000	0.26	0.742
	Periventricular	0.54	0.031	0.57	0.022	0.49	0.054	0.58	0.023	0.28	0.335	0.10	0.806	0.00	1.000	0.11	0.866	0.11	0.895
	PLIC	0.22	0.534	0.36	0.304	0.45	0.195	0.56	0.116	0.21	0.625	0.89	0.106	0.89	0.106	0.00	1.000		
PCr/Pi	Sagittal	-0.30	0.235	-0.35	0.168	-0.32	0.204	-0.49	0.056	-0.40	0.159	-0.17	0.654	0.00	1.000	0.00	1.000	-0.26	0.742
	Parietal	-0.29	0.283	-0.32	0.234	-0.24	0.376	-0.35	0.200	-0.45	0.123	-0.30	0.430	-0.43	0.332	0.29	0.638	0.00	1.000
	Temporal	-0.50	0.047	-0.57	0.023	-0.57	0.020	-0.73	0.002	-0.36	0.234	0.23	0.578	0.00	1.000	0.00	1.000	-0.26	0.742
	Superior Periventricular	-0.68	0.002	-0.71	0.001	-0.68	0.003	-0.74	0.001	-0.54	0.047	-0.20	0.604	-0.30	0.515	0.00	1.000	-0.26	0.742
	Periventricular	-0.56	0.024	-0.58	0.018	-0.49	0.054	-0.57	0.026	-0.35	0.217	-0.02	0.964	0.06	0.899	-0.11	0.866	-0.11	0.895
	PLIC	-0.28	0.440	-0.36	0.304	-0.45	0.195	-0.56	0.116	-0.41	0.311	-0.89	0.106	-0.89	0.106	0.00	1.000		

P-values presented without correction for multiple comparisons. R and p values for the periods after 24 hours are presented only for reference because of the limited number of surviving subjects. Abbreviation: PLIC, posterior limb of the internal capsule.

Supplemental Table 4.3-9: Serial ADC 1-48 h before termination and histo-pathological injury in corresponding regions

A. ADC 1 to 48 hours before termination and neuronal death in the grey matter assessed using H & E stains

	Time before termination (h)																	
	1 - < 3		3 - < 6		6 - < 12		12 - < 18		18 - < 24		24 - < 30		30 - < 36		36 - < 42		42 - < 48	
	r	p	r	p	r	p	r	p	r	p	r	p	r	p	r	p	r	p
Sagittal top	-0.75	0.000	-0.80	0.000	-0.82	0.000	-0.85	0.000	-0.57	0.052	-0.35	0.362	-0.20	0.669	-0.74	0.156	-0.58	0.423
Sagittal bottom	-0.82	0.000	-0.73	0.001	-0.70	0.002	-0.62	0.011	-0.38	0.224	-0.46	0.210	-0.64	0.125	-0.64	0.245	-0.85	0.146
Parietal top	-0.72	0.001	-0.60	0.008	-0.50	0.043	-0.60	0.015	-0.38	0.221	-0.32	0.399	0.05	0.908	0.25	0.681	0.43	0.575
Parietal bottom	-0.74	0.000	-0.74	0.000	-0.63	0.007	-0.63	0.008	-0.46	0.135	-0.43	0.248	-0.12	0.792	-0.35	0.564	-0.15	0.848
Temporal	-0.64	0.007	-0.51	0.042	-0.58	0.024	-0.51	0.078	-0.82	0.004	-0.50	0.209	-0.66	0.104	0.53	0.363	-0.34	0.781
Hippocampus	-0.46	0.252	-0.53	0.175	-0.48	0.276	-0.66	0.222										
Caudate nucleus	-0.49	0.074	-0.54	0.048	-0.56	0.047	-0.46	0.151	-0.29	0.449	-0.49	0.266	-0.48	0.333	-0.78	0.121	0.50	0.668
Putamen	-0.33	0.249	-0.40	0.161	-0.29	0.322	-0.47	0.121	-0.34	0.334	-0.25	0.554	-0.15	0.746	-0.75	0.145	-0.84	0.371
Anterior thalamus	-0.63	0.017	-0.53	0.050	-0.58	0.031	-0.69	0.013	-0.67	0.035	-0.77	0.025	-0.65	0.112	-0.80	0.102	-0.36	0.763
Lateral thalamus	-0.37	0.169	-0.35	0.197	-0.39	0.165	-0.53	0.077	-0.45	0.198	-0.54	0.165	-0.44	0.328	-0.65	0.237	-0.94	0.222
Medial thalamus	-0.61	0.015	-0.60	0.019	-0.56	0.038	-0.54	0.071	-0.47	0.176	-0.47	0.236	-0.46	0.294	-0.60	0.281	-0.97	0.148

B. ADC 1-48 h before termination and TUNEL positive apoptotic cell death in the grey matter

	Time before termination (h)																	
	1 - < 3		3 - < 6		6 - < 12		12 - < 18		18 - < 24		24 - < 30		30 - < 36		36 - < 42		42 - < 48	
	r	p	r	p	r	p	r	p	r	p	r	p	r	p	r	p	r	p
Sagittal top	-0.50	0.035	-0.47	0.052	-0.45	0.069	-0.35	0.184	-0.10	0.761	-0.06	0.884	0.27	0.556	0.23	0.714	0.10	0.901
Sagittal bottom	-0.45	0.060	-0.47	0.048	-0.48	0.050	-0.49	0.056	-0.34	0.275	-0.03	0.946	-0.14	0.771	-0.09	0.889	0.93	0.075
Parietal top	-0.55	0.019	-0.45	0.064	-0.41	0.099	-0.62	0.011	-0.57	0.051	-0.29	0.446	-0.20	0.669	-0.29	0.638	-0.40	0.603
Parietal bottom	-0.35	0.153	-0.33	0.183	-0.42	0.095	-0.48	0.061	-0.15	0.641	-0.02	0.958	-0.03	0.944	-0.02	0.969	0.11	0.892
Temporal	-0.04	0.871	-0.03	0.917	-0.02	0.956	-0.06	0.855	0.24	0.512	-0.18	0.670	0.55	0.198	-0.50	0.397	0.85	0.348
Hippocampus	-0.25	0.543	-0.45	0.267	-0.73	0.064	0.30	0.627	0.91	0.277								
Caudate nucleus	-0.29	0.309	-0.37	0.192	-0.39	0.194	-0.35	0.289	-0.21	0.588	-0.10	0.838	-0.19	0.725	-0.21	0.740	-0.87	0.334
Putamen	-0.33	0.256	-0.29	0.317	-0.34	0.232	-0.37	0.241	-0.32	0.362	-0.17	0.689	-0.50	0.257	-0.61	0.271	-0.90	0.289
Anterior thalamus	-0.15	0.602	-0.13	0.655	-0.20	0.496	0.06	0.859	0.02	0.962	0.16	0.707	-0.17	0.713	-0.20	0.750	-0.97	0.170
Lateral thalamus	-0.24	0.386	-0.28	0.308	-0.23	0.427	-0.10	0.765	0.23	0.517	0.30	0.467	0.31	0.503	0.19	0.758	-0.29	0.811
Medial thalamus	-0.15	0.607	-0.15	0.599	-0.10	0.751	-0.10	0.776	-0.02	0.951	-0.22	0.640	-0.01	0.987	0.92	0.083		

C-1. ADC 1-48 h before termination and CD68 positive microglia in the grey matter

	Time before termination (h)																	
	1 - < 3		3 - < 6		6 - < 12		12 - < 18		18 - < 24		24 - < 30		30 - < 36		36 - < 42		42 - < 48	
	r	p	r	p	r	p	r	p	r	p	r	p	r	p	r	p	r	p
Sagittal top	0.55	0.018	0.53	0.024	0.53	0.028	0.56	0.024	0.38	0.226	0.42	0.259	0.30	0.520	-0.08	0.905	0.30	0.701
Sagittal bottom	0.46	0.053	0.46	0.055	0.45	0.068	0.28	0.294	0.33	0.292	0.05	0.897	-0.23	0.615	-0.79	0.112	-0.95	0.047
Parietal top	0.64	0.005	0.50	0.034	0.59	0.013	0.59	0.017	0.52	0.085	0.32	0.397	0.48	0.282	0.92	0.029	0.86	0.140
Parietal bottom	0.55	0.018	0.51	0.031	0.46	0.066	0.45	0.084	0.30	0.348	0.25	0.518	-0.32	0.483	-0.91	0.034	-0.78	0.218
Temporal	-0.07	0.797	-0.09	0.751	-0.15	0.606	0.02	0.957	-0.47	0.176	-0.54	0.167	-0.54	0.209	0.47	0.429	-0.82	0.390
Hippocampus	-0.52	0.188	-0.17	0.693	-0.27	0.559	0.19	0.760	-0.31	0.802								
Caudate nucleus	0.43	0.106	0.45	0.094	0.34	0.241	0.37	0.241	-0.45	0.193	-0.53	0.179	-0.59	0.160	-0.01	0.994	1.00	0.043
Putamen	-0.18	0.522	0.08	0.782	-0.15	0.613	-0.16	0.616	-0.63	0.052	-0.67	0.072	-0.78	0.041	-0.89	0.045	-0.84	0.371
Anterior thalamus	0.10	0.715	0.17	0.543	0.28	0.337	0.13	0.683	0.01	0.977	-0.55	0.154	-0.22	0.644	-0.07	0.916	0.59	0.598
Lateral thalamus	-0.15	0.600	-0.16	0.566	0.13	0.652	0.11	0.730	-0.35	0.324	-0.51	0.192	-0.59	0.160	-0.54	0.347	-0.18	0.888
Medial thalamus	-0.32	0.270	0.02	0.947	0.15	0.616	-0.01	0.981	-0.65	0.058	-0.92	0.003	-0.82	0.044	0.15	0.855		

C-2. ADC 1-48 h before termination and CD68 positive microglia in the white matter

	Time before termination (h)																	
	1 - < 3		3 - < 6		6 - < 12		12 - < 18		18 - < 24		24 - < 30		30 - < 36		36 - < 42		42 - < 48	
	r	p	r	p	r	p	r	p	r	p	r	p	r	p	r	p	r	p
Sagittal	0.69	0.003	0.75	0.001	0.73	0.002	0.64	0.013	0.45	0.141	0.35	0.357	-0.76	0.046	-0.84	0.079	-0.72	0.276
Parietal	0.67	0.007	0.58	0.022	0.53	0.053	0.51	0.075	0.34	0.274	0.27	0.483	-0.86	0.012	-0.98	0.003	-0.95	0.055
Temporal	0.53	0.042	0.48	0.068	0.45	0.105	0.34	0.262	-0.07	0.831	-0.54	0.168	-0.44	0.327	-0.48	0.416	0.02	0.979
Superior Periventricular	0.14	0.627	0.32	0.239	0.32	0.261	-0.20	0.543	-0.50	0.137	-0.59	0.166	-0.71	0.073	-0.41	0.491	0.49	0.506
Periventricular	-0.27	0.349	0.01	0.963	-0.39	0.193	-0.38	0.247	-0.19	0.607	-0.40	0.328	-0.50	0.256	-0.22	0.728	-0.25	0.752
PLIC	0.74	0.014	0.72	0.019	0.72	0.028	0.61	0.106	-0.10	0.836	-0.94	0.059	-0.98	0.025	-1.00	0.006		

D-1. ADC 1-48 h before termination and CD68 positive vessels in the grey matter

	Time before termination (h)																	
	1 - < 3		3 - < 6		6 - < 12		12 - < 18		18 - < 24		24 - < 30		30 - < 36		36 - < 42		42 - < 48	
	r	p	r	p	r	p	r	p	r	p	r	p	r	p	r	p	r	p
Sagittal top	0.56	0.016	0.65	0.004	0.69	0.002	0.70	0.003	0.44	0.157	0.40	0.289	0.46	0.304	-0.05	0.943	0.24	0.756
Sagittal bottom	0.51	0.032	0.54	0.020	0.54	0.026	0.41	0.112	0.39	0.210	0.33	0.392	0.12	0.797	-0.87	0.056	-0.71	0.294
Parietal top	0.81	0.000	0.72	0.001	0.80	0.000	0.64	0.007	0.53	0.076	0.41	0.269	0.52	0.237	0.92	0.029	0.86	0.140
Parietal bottom	0.67	0.002	0.62	0.006	0.57	0.017	0.55	0.028	0.33	0.292	0.26	0.493	0.15	0.753	-0.63	0.257	-0.15	0.848
Temporal	-0.05	0.851	-0.08	0.758	-0.14	0.613	0.06	0.848	-0.22	0.541	-0.55	0.157	-0.55	0.200	0.30	0.624	-0.71	0.499
Hippocampus	-0.51	0.198	-0.17	0.680	-0.17	0.718	-0.31	0.606										
Caudate nucleus	0.43	0.114	0.42	0.119	0.32	0.262	0.28	0.377										
Putamen	-0.32	0.239	-0.03	0.927	-0.37	0.192	-0.46	0.136	-0.59	0.072	-0.64	0.085	-0.75	0.052	-0.83	0.079	-0.61	0.583
Anterior thalamus	0.15	0.597	0.18	0.511	0.27	0.358	0.16	0.614	0.01	0.977	-0.55	0.154	-0.22	0.644	-0.07	0.916	0.59	0.598
Lateral thalamus	-0.16	0.564	-0.19	0.493	0.13	0.657	0.10	0.754	-0.35	0.324	-0.51	0.192	-0.59	0.160	-0.54	0.347	-0.18	0.888
Medial thalamus	-0.14	0.625	0.05	0.856	0.07	0.829	-0.02	0.958	-0.73	0.025	-0.92	0.003	-0.82	0.044	0.15	0.855		

D-2. ADC 1-48 h before termination and CD68 positive vessels in the white matter

	Time before termination (h)																	
	1 - < 3		3 - < 6		6 - < 12		12 - < 18		18 - < 24		24 - < 30		30 - < 36		36 - < 42		42 - < 48	
	r	p	r	p	r	p	r	p	r	p	r	p	r	p	r	p	r	p
Sagittal	0.45	0.079	0.63	0.009	0.66	0.007	0.55	0.044	0.36	0.254	0.20	0.613	-0.59	0.162	-0.65	0.234	-0.88	0.121
Parietal	0.76	0.001	0.74	0.002	0.71	0.004	0.58	0.038	0.41	0.186	0.34	0.375						
Temporal	0.10	0.735	0.10	0.718	0.15	0.622	0.27	0.376	0.04	0.919	-0.55	0.160	-0.15	0.753	-0.14	0.823	0.24	0.757
Superior Periventricular	-0.34	0.216	-0.19	0.505	-0.21	0.470	-0.43	0.168	-0.52	0.128	-0.59	0.166	-0.80	0.032	-0.91	0.033	-0.21	0.792
Periventricular	-0.23	0.436	0.02	0.939	-0.17	0.589	-0.23	0.494	-0.56	0.092	-0.40	0.328	-0.50	0.256	-0.22	0.728	-0.25	0.752
PLIC	0.35	0.329	0.62	0.055	0.62	0.076	0.50	0.209	0.23	0.623	-0.94	0.059	-0.98	0.025	-1.00	0.006		

E. ADC 1-48 h before termination and white matter injury assessed using H & E stains

	Time before termination (h)																	
	1 - < 3		3 - < 6		6 - < 12		12 - < 18		18 - < 24		24 - < 30		30 - < 36		36 - < 42		42 - < 48	
	r	p	r	p	r	p	r	p	r	p	r	p	r	p	r	p	r	p
Sagittal	-0.65	0.006	-0.84	0.000	-0.77	0.001	-0.76	0.002	-0.48	0.118	-0.55	0.130	-0.22	0.631	-0.67	0.215	0.26	0.742
Parietal	-0.76	0.001	-0.72	0.002	-0.73	0.003	-0.72	0.005	-0.40	0.197	-0.48	0.196	0.27	0.562	-0.45	0.450	-0.78	0.225
Temporal	-0.80	0.000	-0.76	0.001	-0.61	0.020	-0.40	0.171	-0.14	0.681	0.28	0.510	0.24	0.606	-0.05	0.933	-0.89	0.106
Superior Periventricular	-0.81	0.000	-0.68	0.005	-0.76	0.002	-0.26	0.413	0.08	0.831	0.13	0.775	0.13	0.775	0.00	1.000		
Periventricular	-0.58	0.029	-0.36	0.204	-0.68	0.010	-0.47	0.146	-0.05	0.886	0.32	0.441	0.02	0.967	0.11	0.858	0.78	0.225
PLIC	-0.56	0.060	-0.71	0.009	-0.94	0.000	-0.86	0.001	-0.50	0.174	0.15	0.770	0.32	0.604	-0.32	0.684	-0.50	0.667

F. ADC 1-48 h before termination and white matter injury assessed using LFB/Nissl stains

	Time before termination (h)																	
	1 - < 3		3 - < 6		6 - < 12		12 - < 18		18 - < 24		24 - < 30		30 - < 36		36 - < 42		42 - < 48	
	r	p	r	p	r	p	r	p	r	p	r	p	r	p	r	p	r	p
Sagittal	0.33	0.219	0.52	0.041	0.61	0.016	0.34	0.239	0.31	0.329	0.14	0.725	-0.20	0.661				
Parietal	0.06	0.838	0.17	0.537	0.09	0.750	0.21	0.492	0.51	0.091	0.31	0.416	0.00	1.000	0.35	0.559	0.26	0.742
Temporal	0.31	0.254	0.42	0.120	0.54	0.046	0.57	0.042	0.52	0.100	0.41	0.310	0.61	0.144	0.71	0.182	0.26	0.742
Superior Periventricular	0.12	0.660	0.00	1.000	0.24	0.407	0.31	0.334	-0.06	0.873								
Periventricular	-0.10	0.726	0.03	0.907	0.31	0.305	0.30	0.370	-0.06	0.873								
PLIC	0.64	0.025	0.70	0.012	0.71	0.014	0.65	0.044	0.00	1.000	-0.66	0.158	-0.71	0.182	-0.26	0.742	0.00	1.000

G. ADC 1-48 h before termination and white matter injury assessed using β-APP immune-histochemical stain

	Time before termination (h)																	
	1 - < 3		3 - < 6		6 - < 12		12 - < 18		18 - < 24		24 - < 30		30 - < 36		36 - < 42		42 - < 48	
	r	p	r	p	r	p	r	p	r	p	r	p	r	p	r	p	r	p
Sagittal	-0.52	0.041	-0.69	0.003	-0.54	0.040	-0.63	0.016	-0.53	0.076	-0.22	0.569	0.00	1.000	-0.29	0.638	-0.78	0.225
Parietal	-0.44	0.104	-0.38	0.166	-0.19	0.515	-0.45	0.126	-0.41	0.184	-0.20	0.615	0.29	0.530	0.00	1.000	0.00	1.000
Temporal	-0.69	0.004	-0.73	0.002	-0.53	0.050	-0.41	0.169	-0.19	0.567	0.04	0.923	0.00	1.000	-0.29	0.638	-0.78	0.225
Superior Periventricular	-0.56	0.031	-0.65	0.009	0.60	0.024	-0.17	0.607	0.34	0.341	0.43	0.335	0.10	0.832	0.29	0.638	-0.78	0.225
Periventricular	-0.65	0.012	-0.62	0.018	-0.46	0.114	-0.27	0.419	0.19	0.604	0.66	0.073	0.30	0.515	-0.53	0.361	-0.32	0.684
PLIC	-0.24	0.510	-0.36	0.314	-0.60	0.090	-0.41	0.311	-0.78	0.041	-0.89	0.106	-0.45	0.553	-0.87	0.333		

P-values presented without correction for multiple comparisons..

R and p values for the periods after 24 hours are presented only for reference because of the limited number of surviving subjects.

Abbreviation: PLIC, posterior limb of the internal capsule.

Supplemental Table 4.3-10: Serial T2 maps 1-48 h before termination and histo-pathological injury in corresponding regions

A. T2 1-48 h before termination and neuronal death in the grey matter assessed using H & E stains

	Time before termination (h)																	
	1 - < 3		3 - < 6		6 - < 12		12 - < 18		18 - < 24		24 - < 30		30 - < 36		36 - < 42		42 - < 48	
	r	p	r	p	r	p	r	p	r	p	r	p	r	p	r	p	r	p
Sagittal top	0.43	0.187	0.43	0.191	0.41	0.210	0.68	0.044	0.58	0.102	0.66	0.110	0.42	0.404	0.13	0.918	-0.14	0.912
Sagittal bottom	0.36	0.283	0.28	0.400	0.27	0.420	0.39	0.294	0.42	0.259	0.06	0.899	0.63	0.184	0.68	0.521	0.66	0.546
Parietal top	0.54	0.087	0.43	0.183	0.51	0.113	0.69	0.042	0.66	0.054	0.78	0.041	0.80	0.054	0.99	0.102	0.84	0.371
Parietal bottom	0.30	0.376	0.36	0.278	0.37	0.262	0.67	0.049	0.60	0.090	0.67	0.101	0.59	0.222	0.90	0.292	0.77	0.444
Temporal	0.01	0.972	-0.04	0.903	-0.01	0.988	0.23	0.589	0.00	0.995	-0.38	0.533	-0.69	0.309				
Hippocampus	0.25	0.633	0.46	0.363	0.58	0.229	0.77	0.227	0.85	0.356								
Caudate nucleus	0.25	0.481	0.33	0.348	0.38	0.274	0.77	0.025	0.38	0.406	0.70	0.186	-0.10	0.899	-0.10	0.937		
Putamen	-0.02	0.965	0.34	0.337	0.30	0.406	0.10	0.795	0.32	0.441	0.45	0.369	-0.04	0.946	-0.51	0.658		
Anterior thalamus	0.00	0.993	0.24	0.505	0.53	0.116	0.52	0.156	0.38	0.354	0.45	0.374	0.62	0.260	0.64	0.559		
Lateral thalamus	0.09	0.803	0.10	0.769	0.13	0.710	0.41	0.278	0.65	0.080	0.95	0.004	0.92	0.028	0.78	0.427		
Medial thalamus	0.74	0.009	0.68	0.021	0.38	0.256	0.56	0.118	0.59	0.094	0.50	0.257	0.62	0.264	0.99	0.084	0.93	0.234

B. T2 1-48 h before termination and TUNEL positive apoptotic cell death in the grey matter

	Time before termination (h)																	
	1 - < 3		3 - < 6		6 - < 12		12 - < 18		18 - < 24		24 - < 30		30 - < 36		36 - < 42		42 - < 48	
	r	p	r	p	r	p	r	p	r	p	r	p	r	p	r	p	r	p
Sagittal top	0.57	0.067	0.52	0.103	0.33	0.321	0.42	0.265	0.59	0.097	0.43	0.335	0.36	0.484	0.97	0.162	0.87	0.332
Sagittal bottom	0.87	0.000	0.84	0.001	0.72	0.013	0.68	0.042	0.74	0.024	0.60	0.154	0.55	0.259	0.98	0.130	0.97	0.155
Parietal top	0.79	0.004	0.76	0.007	0.54	0.085	0.65	0.058	0.56	0.117	0.55	0.201	0.52	0.293	1.00	0.059	0.95	0.209
Parietal bottom	0.67	0.024	0.68	0.023	0.50	0.115	0.55	0.128	0.65	0.058	0.37	0.414	0.52	0.291	1.00	0.059	0.99	0.092
Temporal	0.81	0.002	0.85	0.001	0.80	0.003	0.66	0.073	0.83	0.020	0.08	0.894	0.70	0.296				
Hippocampus	0.16	0.761	0.32	0.531	0.10	0.851	0.20	0.805	-0.04	0.977								
Caudate nucleus	0.24	0.509	0.31	0.379	0.36	0.301	0.18	0.669	0.25	0.589	0.45	0.445	0.99	0.012	0.97	0.150		
Putamen	0.68	0.030	0.55	0.096	0.70	0.025	0.58	0.102	0.50	0.212	0.61	0.202	0.54	0.344	0.41	0.732		
Anterior thalamus	0.29	0.411	0.43	0.219	0.26	0.465	0.32	0.409	0.12	0.783	0.04	0.934	0.26	0.674	0.87	0.329		
Lateral thalamus	0.16	0.643	0.05	0.891	0.13	0.715	0.44	0.234	0.19	0.647	-0.05	0.924	-0.13	0.836	-0.03	0.984		
Medial thalamus	0.56	0.072	0.56	0.075	0.39	0.236	0.50	0.176	0.62	0.076	0.37	0.417	0.04	0.953	0.29	0.811	0.51	0.661

C-1. T2 1-48 h before termination and CD68 positive microglia in the grey matter

	Time before termination (h)																	
	1 - < 3		3 - < 6		6 - < 12		12 - < 18		18 - < 24		24 - < 30		30 - < 36		36 - < 42		42 - < 48	
	r	p	r	p	r	p	r	p	r	p	r	p	r	p	r	p	r	p
Sagittal top	-0.43	0.189	-0.33	0.315	-0.29	0.383	-0.36	0.336	-0.35	0.362	-0.31	0.495	0.23	0.656	-0.58	0.606	-0.35	0.775
Sagittal bottom	-0.56	0.072	-0.53	0.091	-0.55	0.079	-0.54	0.138	-0.50	0.171	-0.65	0.117	0.12	0.819	-0.17	0.889	-0.21	0.864
Parietal top	-0.62	0.044	-0.57	0.068	-0.50	0.117	-0.53	0.140	-0.43	0.246	-0.38	0.404	0.04	0.947				
Parietal bottom	-0.48	0.132	-0.49	0.126	-0.52	0.101	-0.60	0.088	-0.58	0.103	-0.36	0.425	0.24	0.647	0.01	0.996	-0.23	0.852
Temporal	-0.37	0.267	-0.35	0.289	-0.44	0.174	-0.10	0.809	-0.48	0.276	0.59	0.297	0.03	0.966				
Hippocampus	-0.08	0.874	-0.07	0.903	-0.58	0.225	-0.19	0.806	-0.85	0.356								
Caudate nucleus	-0.50	0.117	-0.53	0.092	-0.33	0.328	-0.26	0.493	-0.46	0.249	-0.64	0.169	-0.70	0.184	-0.97	0.167		
Putamen	-0.43	0.185	-0.43	0.185	-0.50	0.114	-0.08	0.844	-0.30	0.474	0.35	0.494	0.32	0.594	0.07	0.955		
Anterior thalamus	-0.37	0.265	-0.42	0.203	-0.56	0.072	-0.32	0.407	-0.41	0.317								
Lateral thalamus	-0.51	0.111	-0.45	0.170	-0.51	0.106	-0.32	0.408	-0.52	0.182								
Medial thalamus	0.24	0.480	-0.12	0.737	-0.34	0.306	0.22	0.573	0.20	0.599	0.90	0.005	0.91	0.031	1.00	0.066	0.99	0.084

C-2. T2 1-48 h before termination and CD68 positive microglia in the white matter

	Time before termination (h)																	
	1 - < 3		3 - < 6		6 - < 12		12 - < 18		18 - < 24		24 - < 30		30 - < 36		36 - < 42		42 - < 48	
	r	p	r	p	r	p	r	p	r	p	r	p	r	p	r	p	r	p
Sagittal	-0.17	0.668	0.00	0.999	0.14	0.720	0.13	0.781	0.17	0.723	-0.11	0.831	0.31	0.694	1.00	0.023	0.98	0.116
Parietal	-0.10	0.789	-0.21	0.570	-0.23	0.524	-0.08	0.855	-0.03	0.936	-0.09	0.854	0.94	0.017	0.81	0.396	0.56	0.620
Temporal	-0.28	0.397	-0.32	0.337	-0.36	0.273	0.09	0.815	0.92	0.001	0.90	0.015	0.76	0.134	1.00	0.020	0.20	0.874
Superior Periventricular	0.01	0.988	0.05	0.887	0.24	0.484	0.84	0.005	0.66	0.074	0.89	0.019	0.98	0.023	-0.02	0.989	-0.28	0.819
Periventricular	0.94	0.219	0.94	0.221	0.88	0.321	0.99	0.088	1.00	0.043	0.95	0.212						
PLIC	-0.09	0.816	-0.13	0.732	0.18	0.649	0.16	0.726	0.45	0.312	0.41	0.490	0.96	0.180	0.94	0.220	0.99	0.109

D-1. T2 1-48 h before termination and CD68 positive vessels in the grey matter

	Time before termination (h)																	
	1 - < 3		3 - < 6		6 - < 12		12 - < 18		18 - < 24		24 - < 30		30 - < 36		36 - < 42		42 - < 48	
	r	p	r	p	r	p	r	p	r	p	r	p	r	p	r	p	r	p
Sagittal top	-0.43	0.189	-0.33	0.315	-0.29	0.383	-0.36	0.336	-0.35	0.362	-0.31	0.495	0.23	0.656	-0.58	0.606	-0.35	0.775
Sagittal bottom	-0.56	0.072	-0.53	0.091	-0.55	0.079	-0.54	0.138	-0.50	0.171	-0.65	0.117	0.12	0.819	-0.17	0.889	-0.21	0.864
Parietal top	-0.62	0.044	-0.57	0.068	-0.50	0.117	-0.53	0.140	-0.43	0.246	-0.38	0.404	0.04	0.947				
Parietal bottom	-0.48	0.132	-0.49	0.126	-0.52	0.101	-0.60	0.088	-0.58	0.103	-0.36	0.425	0.24	0.647	0.01	0.996	-0.23	0.852
Temporal	-0.37	0.267	-0.35	0.289	-0.44	0.174	-0.10	0.809	-0.48	0.276	0.59	0.297	0.03	0.966				
Hippocampus	-0.08	0.874	-0.07	0.903	-0.58	0.225	-0.19	0.806	-0.85	0.356								
Caudate nucleus	-0.50	0.117	-0.53	0.092	-0.33	0.328	-0.26	0.493	-0.46	0.249	-0.64	0.169	-0.70	0.184	-0.97	0.167		
Putamen	-0.43	0.185	-0.43	0.185	-0.50	0.114	-0.08	0.844	-0.30	0.474	0.35	0.494	0.32	0.594	0.07	0.955		
Anterior thalamus	-0.37	0.265	-0.42	0.203	-0.56	0.072	-0.32	0.407	-0.41	0.317								
Lateral thalamus	-0.51	0.111	-0.45	0.170	-0.51	0.106	-0.32	0.408	-0.52	0.182								
Medial thalamus	0.24	0.480	-0.12	0.737	-0.34	0.306	0.22	0.573	0.20	0.599	0.90	0.005	0.91	0.031	1.00	0.066	0.99	0.084

D-2. T2 1-48 h before termination and CD68 positive vessels in the white matter

	Time before termination (h)																	
	1 - < 3		3 - < 6		6 - < 12		12 - < 18		18 - < 24		24 - < 30		30 - < 36		36 - < 42		42 - < 48	
	r	p	r	p	r	p	r	p	r	p	r	p	r	p	r	p	r	p
Sagittal	0.03	0.934	0.15	0.709	0.21	0.595	0.32	0.485	0.35	0.446	0.07	0.901	0.31	0.694	1.00	0.023	0.98	0.116
Parietal	-0.41	0.237	-0.45	0.192	-0.35	0.319	-0.29	0.494	-0.26	0.542	-0.27	0.555						
Temporal	-0.13	0.694	-0.10	0.782	-0.32	0.344	-0.09	0.820	0.72	0.043	0.97	0.001	0.83	0.081	0.93	0.232	-0.14	0.914
Superior Periventricular	-0.03	0.933	-0.10	0.773	0.12	0.728	0.22	0.574	0.53	0.179	0.89	0.019	0.98	0.023	-0.02	0.989	-0.28	0.819
Periventricular	0.94	0.219	0.94	0.221	0.88	0.321	0.99	0.088	1.00	0.043	0.95	0.212						
PLIC	-0.21	0.592	-0.31	0.421	-0.08	0.834	-0.14	0.760	0.11	0.813	-0.08	0.902	0.96	0.180	0.94	0.220	0.99	0.109

E. T2 1-48 h before termination and white matter injury assessed using H & E stains

	Time before termination (h)																	
	1 - < 3		3 - < 6		6 - < 12		12 - < 18		18 - < 24		24 - < 30		30 - < 36		36 - < 42		42 - < 48	
	r	p	r	p	r	p	r	p	r	p	r	p	r	p	r	p	r	p
Sagittal	0.73	0.027	0.73	0.027	0.52	0.154	0.79	0.034	0.79	0.034	0.62	0.188	0.78	0.225	0.00	1.000	0.00	1.000
Parietal	0.49	0.153	0.51	0.133	0.76	0.010	0.76	0.030	0.76	0.030	0.32	0.490	0.00	1.000	0.87	0.333	0.87	0.333
Temporal	0.40	0.218	0.29	0.380	0.33	0.316	0.28	0.458	-0.38	0.351	0.13	0.805	0.00	1.000	0.00	1.000	-0.87	0.333
Superior Periventricular	-0.03	0.921	-0.22	0.512	-0.24	0.475	-0.56	0.118	-0.43	0.292	-0.17	0.749	0.26	0.742	-0.87	0.333	-0.87	0.333
Periventricular	-0.87	0.333	-0.87	0.333	-0.87	0.333	-0.87	0.333	-0.87	0.333	-0.87	0.333						
PLIC	0.59	0.075	0.76	0.012	0.72	0.018	0.79	0.019	0.03	0.952	0.09	0.864	0.95	0.051				

F. T2 1-48 h before termination and white matter injury assessed using LFB/Nissl stains

	Time before termination (h)																	
	1 - < 3		3 - < 6		6 - < 12		12 - < 18		18 - < 24		24 - < 30		30 - < 36		36 - < 42		42 - < 48	
	r	p	r	p	r	p	r	p	r	p	r	p	r	p	r	p	r	p
Sagittal	-0.09	0.825	0.17	0.656	0.00	1.000	0.00	1.000	0.00	1.000	-0.13	0.805						
Parietal	-0.38	0.275	-0.59	0.071	-0.31	0.378	-0.62	0.101	-0.39	0.334	0.00	1.000	-0.71	0.182	-0.87	0.333	-0.87	0.333
Temporal	-0.30	0.372	-0.12	0.726	-0.12	0.726	-0.62	0.074	-0.25	0.547	-0.66	0.158	-0.71	0.182	-0.87	0.333	0.00	1.000
Superior Periventricular	0.10	0.770	0.10	0.770	-0.50	0.117	-0.27	0.476	-0.08	0.846								
Periventricular																		
PLIC	-0.35	0.324	-0.52	0.122	-0.35	0.324	-0.38	0.356	0.25	0.547	-0.39	0.441						

G. T2 1-48 h before termination and white matter injury assessed using β-APP immune-histochemical stain

	Time before termination (h)																	
	1 - < 3		3 - < 6		6 - < 12		12 - < 18		18 - < 24		24 - < 30		30 - < 36		36 - < 42		42 - < 48	
	r	p	r	p	r	p	r	p	r	p	r	p	r	p	r	p	r	p
Sagittal	0.63	0.068	0.74	0.023	0.28	0.464	0.36	0.434	0.36	0.434	0.70	0.123	0.95	0.051	0.00	1.000	0.00	1.000
Parietal	0.61	0.061	0.45	0.198	0.55	0.102	0.50	0.206	0.35	0.395	0.04	0.937	0.26	0.668	0.87	0.333	0.87	0.333
Temporal	0.40	0.219	0.41	0.213	0.29	0.380	0.10	0.803	-0.36	0.385	0.17	0.749	-0.22	0.718	0.00	1.000	-0.87	0.333
Superior Periventricular	0.00	1.000	-0.05	0.889	-0.43	0.191	-0.70	0.035	-0.72	0.042	-0.58	0.231	0.32	0.684	-0.87	0.333	-0.87	0.333
Periventricular	0.00	1.000	-0.87	0.333	0.00	1.000	-0.87	0.333	-0.87	0.333	0.00	1.000						
PLIC	0.17	0.663	0.60	0.090	0.39	0.297	0.30	0.510	0.15	0.746	0.53	0.361	0.87	0.333	0.87	0.333	0.87	0.333

P-values are presented without correction for multiple comparisons.

R and p values for the periods after 24 hours are presented only for reference because of the limited number of surviving subjects.

Abbreviation: PLIC, posterior limb of the internal capsule.

Appendix 2.

"Therapeutic time window" duration decreases with increasing severity of cerebral hypoxia-ischaemia under normothermia and delayed hypothermia in newborn piglets.

Iwata O, Iwata S, Thornton JS, De Vita E, Bainbridge A, Herbert L, Scaravilli F, Peebles D, Wyatt JS, Cady EB, Robertson NJ.

Brain Res. 2007 Jun 18;1154:173-80.